NOTICE

The quality of this microform is heavily dependent upon the quality of the original thesis submitted for microfilming. Every effort has been made to ensure the highest quality of reproduction possible.

If pages are missing, contact the university which granted the degree.

Some pages may have indistinct print especially if the original pages were typed with a poor typewriter ribbon or if the university sent us an inferior photocopy.

Reproduction in full or in part of this microform is governed by the Canadian Copyright Act, R.S.C. 1970, c. C-30, and subsequent amendments.

AVIS

La qualité de cette microforme dépend grandement de la qualité de la thèse soumise au microfilmage. Nous avons tout fait pour assurer une qualité supérieure de reproduction.

S'il manque des pages, veuillez communiquer avec l'université qui a conféré le grade.

La qualité d'impression de certaines pages peut laisser à désirer, surtout si les pages originales ont été dactylographiées à l'aide d'un ruban usé ou si l'université nous a fait parvenir une photocopie de qualité inférieure.

La reproduction, même partielle, de cette microforme est soumise à la Loi canadienne sur le droit d'auteur, SRC 1970, c. C-30, et ses amendements subséquents.

Canada

TRANSPORT STUDIES IN PERVAPORATION

By

Rajesh Kumar Tyagi

A THESIS SUBMITTED TO
THE SCHOOL OF GRADUATE STUDIES AND RESEARCH
IN PARTIAL FULFILLMENT OF THE REQUIREMENTS
FOR THE DEGREE OF
DOCTOR OF PHILOSOPHY
IN THE DEPARTMENT OF CHEMICAL ENGINEERING
UNIVERSITY OF OTTAWA

Ottawa, Ontario,
August 1993

ISBN 0-315-89712-0

Canada

UNIVERSITÉ D'OTTAWA
UNIVERSITY OF OTTAWA

Abstract

In the theoretical part of this work, mathematical equations were derived for describing steady state pervaporation transport considering the chemical potential gradient as the driving force for the flow of penetrant. The membrane is split perpendicular to the penetrant flow direction into small segments in which an imaginary liquid (or vapor) phase is in thermodynamic equilibrium with each membrane segment. The mathematical equations obtained for pure penetrant permeation are the same as derived by the pore flow model. Based on the analysis of binary mixture system, the possibility of concentration polarization phenomena occurring inside the membrane was pointed out. In the analysis of binary mixture system, coupling was considered in the liquid-filled region of the membrane but no coupling was considered in the vapor-filled region of the membrane. The theoretical prediction of concentration polarization occurring inside the membrane was substantiated by experimental data.

In the experimental part of the work separation of acetic acid/water mixture by pervaporation in the entire composition range was investigated using symmetric and dense aromatic polyamide membrane. Aromatic polyamide is a highly hydrophilic material. The effect of downstream pressure on the pure component permeation was studied at 25°C. First, the penetrant concentration profiles of pure water inside the membrane were established at different downstream pressures by performing steady state pervaporation experiments. Secondly, the profiles of the binary penetrant mixture (acetic acid/water) inside the membrane were established. The process variables studied were; feed temperature (25°C, 35°C and 40°C), downstream pressure (467 Pa, 1200 Pa and 2666 Pa) and feed composition covering the complete range of the binary mixture composition. These experiments were performed by using a stack of

identical membranes during steady state pervaporation, stopping the pervaporation experiment, dividing the stack into substacks, desorbing and analyzing the penetrants sorbed from each substack.

Sorption experiments were performed from liquid phase and vapor phase for the binary mixture of acetic acid-water. The sorption experiments from the liquid phase were performed at 25°C, 35°C and 40°C for the entire binary mixture composition range. Vapor sorption isotherms were also established at these temperatures.

The value obtained for the amount of penetrant in the membrane during steady state pervaporation in some cases was higher than the corresponding equilibrium sorption value. This seems impossible from the thermodynamic point of view. It was concluded that there are two different equilibria. The first one is the static equilibrium achieved during sorption experiments and the second one is the dynamic equilibrium achieved during pervaporation experiments. The structure of the polymeric membrane is different under these two circumstances. Based on the experimental data a novel design for the pervaporation membrane has been proposed.

State of permeant (penetrant) study for acetic acid-water-polyamide system was performed using differential scanning calorimetry technique. Acetic acid present in the membrane did not show any response in the thermogram corresponding to the phase change. It was concluded that acetic acid present in the membrane was in non-freezable bound state. Some spectroscopic studies were also undertaken using FTIR-ATR (Attenuated Total Reflection) technique to study the penetrant interaction with the polymeric membrane.

Penetrant concentration profiles predicted from the newly developed transport model were compared with the experimental penetrant profiles.

Acknowledgements

I wish to express my sincere appreciation and gratitude to my supervisor Professor T. Matsuura for his invaluable guidance, constructive criticism and continued encouragement throughout the course of this study and in the preparation of the thesis.

My sincere thanks are due to Dr. A. E. Fouda and Dr. P. Handa of the Institute for Environmental Chemistry for helpful suggestions and for their help in the computer programming and differential scanning calorimetry studies, respectively. I would also like to thank other staff of the Institute for Environmental Chemistry (IEC) of the National Research Council of Canada. The equipment and the technical support provided by the IEC of the National Research Council are also deeply appreciated.

I also would like to thank other individuals who have helped me directly or indirectly in the course of this study.

Finally, the financial support provided by the Government of India, Ministry of Human Resources Development is gratefully acknowledged.

I dedicate this thesis to my parents.

Nomenclature

a = activity of pure penetrant, mol/m^3

a_i, a_j = activity of penetrant i and j, respectively, mol/m^3

a_2, a_3 = activity of pure penetrant at upstream and downstream, respectively, mol/m^3

A = parameter defined by equation 3.15 for a pure component system, $mol/sec\text{-}m^2\text{-}Pa$

A_{mixt} = a proportionality constant for the liquid mixture, $mol/sec\text{-}m^2\text{-}Pa$

b = affinity constant, Pa^{-1}

B = parameter defined by equation 3.15 for a pure component system, $mol/sec\text{-}m^2\text{-}Pa^2$

$B_{i,25}$ = parameter B for component i at 25°C, $mol/sec\text{-}m^2\text{-}Pa^2$

$B_{i,35}$ = parameter B for component j at 35°C, $mol/sec\text{-}m^2\text{-}Pa^2$

c = concentration of the penetrant, mol/m^3

c_2 = concentration of penetrant at the upstream face of the membrane, mol/m^3

c_3 = concentration of penetrant at the downstream face of the membrane, mol/m^3

c_i^l = concentration of penetrant i in liquid phase, mol/m^3

c_i^v = concentration of penetrant i in vapor phase, mol/m^3

c_j^l = concentration of penetrant j in liquid phase, mol/m^3

c_j^v = concentration of penetrant j in vapor phase, mol/m^3

c_s = saturated concentration of sorbed species in the polymer, mol/m^3

C_0 = concentration of penetrant at feed-membrane interface, mol/m^3

D = diffusion coefficient of the penetrant molecule, m^2/sec (cm^2/sec)

D_0 = diffusion coefficient at zero penetrant concentration, m^2/sec (cm^2/sec)

D_c = concentration dependent diffusion coefficient, m^2/sec (cm^2/sec)

$\overline{D}$ = concentration average diffusion coefficient, m^2/sec (cm^2/sec)

E_P = apparent total activation energy, kJ/mol

E_T = Dimroth's solvent polarity parameter, kJ/mol

f_i^l = constant for component i in liquid part

f_i^v = constant for component i in vapor part

J = permeation rate, mol/sec-m^2 (kg/m^2-hr)

J_{liq} = permeation rate when phase is liquid, mol/sec-m^2 (kg/m^2-hr)

J_{vap} = permeation rate when phase is vapor, mol/sec-m^2 (kg/m^2-hr)

J_0 = pre-exponential factor in equation 2.37 at 0°C, mol/sec-m^2 (kg/m^2-hr)

J_i, J_j = permeation rate for component i and j, respectively, mol/sec-m^2 (kg/m^2-hr)

$J_{i,25}$ = permeation rate for component i at 25°C, mol/sec-m^2 (kg/m^2-hr)

$J_{i,35}$ = permeation rate for component i at 35°C, mol/sec-m^2 (kg/m^2-hr)

k = mass transfer coefficient, m/s

k_H = Henry's law coefficient, mol/kg-Pa

k'_H = (unit weight of Polymer/volume of adsorbed gas molecules).k_H, mol/m^3-Pa

l = thickness of the membrane, m

M = molecular weight

M_i, M_j = molecular weights of component i and j, respectively

N_i = total number of pores per effective membrane area, dimensionless

P_2, P_*, P_3 = pressure at the pore inlet (upstream), saturation vapor pressure, and pressure at the pore outlet (downstream), respectively, Pa (mm Hg)

$P_{i,*}$, $P_{j,*}$ = partial vapor pressure of component i and j, respectively at the phase boundary, Pa (mm Hg)

$P_{i,3}$, $P_{j,3}$ = partial vapor pressure of component i and j, respectively in downstream vapor, Pa (mm Hg)

$P_{i,l}$, $P_{j,l}$ = partial vapor pressure of component i and j, respectively at a distance l in the membrane, Pa (mm Hg)

R = gas constant, 8.314 J/(mol-K)

R_b = pore radius, m

T = temperature, K

t = thickness of the adsorbed monolayer, m

T_g = glass transition temperature of the polymer, K

v = penetrant velocity, m/sec

V = molar volume, m^3/mol

w_i = weight fraction of component i in feed stream

w_j = weight fraction of component j in feed stream

w_i' = weight fraction of component i in the permeate stream

w_j' = weight fraction of component j in the permeate stream

x = amount of gas adsorbed in a unit mass of membrane material, mol/kg

X_i = mole fraction of component i as function of distance

$X_{i,l}$ = mole fraction of component i at a distance l

$X_{i,2}$ and $X_{i,*}$ = mole fraction of component i (acetic acid) in liquid feed mixture and at the phase boundary, respectively, dimensionless

$Y_{i,3}$ = mole fraction of component i (acetic acid) in the downstream, dimensionless

subscripts = subscript i and j refer to acetic acid and water, respectively
subscript 2, $*$ and 3 refer to the upstream, phase boundary and downstream, respectively
subscript 25 and 35 refer to the temperature of the feed mixture in degree °C
subscript l refers to the quantities concerned (e. g. partial pressure) at a distance l
superscript l and v refer to liquid and vapor phases, respectively

Greek Letters

$\alpha_{i,j}$ = separation factor for pervaporation

β = enrichment factor for pervaporation

δ = total membrane thickness, m

δ_{sp} = solubility parameter, $(J - m^3)^{1/2}$

$\frac{\delta_a}{\delta}$ = relative liquid-filled portion of membrane, dimensionless

$\frac{\delta_b}{\delta}$ = relative vapor-filled portion of membrane, dimensionless

$\delta_{b,25}$ = vapor-filled region at 25°C

η_l = viscosity of liquid, Pa-sec

η_v = surface viscosity of the adsorption layer of vapor, Pa-sec

ρ = density, kg/m^3 (g/cc)

ρ_i, ρ_j = density of component i and j, respectively, kg/m^3 (g/cc)

μ = chemical potential, kJ/kg-mol

μ^0 = standard chemical potential, kJ/kg-mol

μ_i = chemical potential of component i, kJ/kg-mol

μ_2 = chemical potential at the upstream side, kJ/kg-mol

μ_3 = chemical potential at the downstream side, kJ/kg-mol

ω = plasticization constant

Abbreviations

CA = cellulose acetate

DSC = differential scanning calorimetry

PA = polyamide (polymer used in the present study)

PAA = poly(acrylic acid)

PAN = poly(acrylonitrile)

PDMS or SR = poly(dimethylsiloxane) or silicone rubber

PE = poly(ethylene)

PEBA =poly(ether-block-polyamide)

PEI = poly(etherimide)

PSF = poly(sulphone)

PTFE = poly(tetra-fluoroethylene)

PTMSP =poly(1-[trimethylsilyl]-1-propyne)

PVA = poly(vinylalcohol)

PVDF = poly(vinylidene fluoride)

SEM = scanning electron microscope

Contents

Abstract ii

Acknowledgements iv

Nomenclature v

Abbreviations x

1 Introduction 1

1.1 Pervaporation 1

1.2 Objectives of the Thesis 7

2 Background 9

2.1 Polymeric Membrane Materials for Pervaporation 12

2.2 Pervaporation Membrane Development 13

2.2.1 Polymer Selection for Pervaporation Membranes 14

2.2.2 Design and Preparation of Pervaporation Membranes 16

2.3 Characterization of Pervaporation Membranes 20

2.4 Transport in and Through Pervaporation Membranes 22

2.4.1 Pore Flow Model 24

2.4.2 Solution-Diffusion Model 30

2.4.3 Free Volume Model 37

2.5 Sorption Measurements for Polymeric Membranes 40

2.6 Penetrant Concentration Profile Inside the Membrane 42

2.7 State of Permeant (Penetrant) Studies Using Calorimetry 45
2.8 Microscopic and Spectroscopic Studies for Polymer Films 46
2.8.1 Microscopic Studies 46
2.8.2 Spectroscopic Studies 47
2.9 Process Parameters Affecting Pervaporation 48
2.9.1 Effect of Feed Temperature 48
2.9.2 Effect of Feed Composition 49
2.9.3 Effect of Charge Pressure 49

3 Theoretical Development **51**
3.1 Single Component System 52
3.2 Binary Component System 57
3.3 Strategy for Plotting Theoretical Concentration Profiles Inside the Membrane for Binary Mixture Systems 60
3.3.1 Calculation of Phase Boundary in the Imaginary Phase at 25°C 61
3.3.2 Calculation of Mass Transfer Coefficient 62
3.3.3 Calculation of Phase Boundary and Mass Transfer Coefficient at Different Temperatures 63
3.3.4 Penetrant Profile in the Imaginary Phase 64
3.3.5 Penetrant Profile in the Membrane Phase 65

4 Experimental Aspects **67**
4.1 Membrane Preparation 67
4.2 Pervaporation Experiments 68
4.3 Liquid Sorption Studies 71
4.4 Vapor Sorption Studies 72
4.5 State of Permeant Studies Using Calorimetry 74
4.6 Microscopic and Spectroscopic Studies 75
4.6.1 Microscopic Studies 75
4.6.2 Spectroscopic Studies 75

5 Results and Discussion 76

5.1 Microscopic Studies for Polyamide Membrane 76

5.2 Pervaporation of Acetic Acid-Water Binary Mixture 78

5.3 Pure Component Pervaporation 80

5.3.1 Calculations Using the Newly Developed Transport Model . . 83

5.4 Liquid Sorption Studies from Binary Mixture of Acetic Acid and Water 85

5.5 Vapor Sorption Studies for Polyamide-Acetic Acid-Water 91

5.6 Pure Penetrant Concentration Profile Inside the Membrane During Steady State Pervaporation 95

5.6.1 Calculations Using the Solution-Diffusion Model 98

5.7 Effect of Process Variables on Penetrant Concentration Profiles . . . 99

5.8 Testing the Transport Models 108

5.8.1 Effect of Process Variables on the Phase Boundary 108

5.9 Calorimetric Studies for the State of Permeant 122

5.10 Spectroscopic Studies 127

5.11 Implications of the Experimental Data for the Membrane Design . . . 128

6 Conclusions 132

7 Recommendations and Future Directions 134

A Some Azeotropic Distillation Processes 151

B Membranes Used in Pervaporation Processes 153

C BET Approximation 157

D Concentration Polarization 159

D.1 A General Concept of Concentration Polarization 159

D.2 Concentration Polarization Defined Inside the Membrane 159

E Vapor-Liquid Equilibrium Data 162

F Derivation of Fick's First Law Equation 166

G Pervaporation Data for Binary Mixture 168

H Pervaporation Data for Pure Component 170

I Calibration Curve Used for the Analysis 173

J Liquid Sorption Data 175

K Vapor Sorption Data 179

L Pure Penetrant Profile Data 183

M Binary Penetrant Profile Data 189

N Calculations Using Solution-Diffusion Model 199

O Results of FTIR-ATR Study 201

P Calculation Results Using the Model 204

Q Computer Program and Sample Output 217

List of Figures

1.1 Schematic Diagram of Pervaporation Process 2
2.1 A Schematic Diagram of Membrane Cross-sections (Mulder, 1991) . . 18
2.2 A Conceptual Diagram of Pore Flow Model 26
2.3 Calculated Concentration Profiles with Concentration Dependent Diffusion Coefficients Using Solution-Diffusion Model (Mulder and Smolders, 1984); 1, water; 2, ethanol; and 3, mixture 36
3.1 A Conceptual Diagram of the Model 53
4.1 Experimental Set-Up of Pervaporation System Used 69
4.2 A Schematic Diagram of Vapor Sorption Apparatus 73
5.1 Scanning Electron Micrographs of the Symmetric Polyamide Membrane 77
5.2 Pervaporation Data for Acetic Acid/Water System for Aromatic Polyamide Membrane 79
5.3 Effect of Downstream Pressure on the Pure Acetic Acid Permeation Rate at 25°C 81
5.4 Effect of Downstream Pressure on the Pure Water Permeation Rate at 25°C 82
5.5 Liquid Sorption Data for Acetic Acid/Water System for Aromatic Polyamide Membrane 86
5.6 Liquid Sorption Data for Acetic Acid/Water System for Aromatic Polyamide Membrane 87
5.7 Liquid Sorption Data for Acetic Acid/Water System for Aromatic Polyamide Membrane 88

5.8 Vapor Sorption Data for Acetic Acid/Water System for Aromatic Polyamide Membrane 92
5.9 Vapor Sorption Data for Acetic Acid/Water System for Aromatic Polyamide Membrane 93
5.10 Vapor Sorption Data for Acetic Acid/Water System for Aromatic Polyamide Membrane 94
5.11 Effect of Downstream Pressure on the Pure Water Concentration Profile Inside the Membrane at 25°C 96
5.12 Effect of Downstream Pressure on Penetrant Profile Across the Membrane for Acetic Acid/Water at 25°C 100
5.13 Effect of Feed Temperature on Penetrant Profile Across the Membrane for Acetic Acid/Water Mixture 104
5.14 Effect of Feed Composition on Penetrant Profile Across the Membrane for Acetic Acid/Water Mixture at 25°C 105
5.15 Calculated Penetrant Profile Compared with the Experimental Data . 114
5.16 Calculated Penetrant Profile Compared with the Experimental Data . 115
5.17 Calculated Penetrant Profile Compared with the Experimental Data . 116
5.18 Calculated Penetrant Profile Compared with the Experimental Data . 118
5.19 Calculated Penetrant Profile Compared with the Experimental Data . 119
5.20 Calculated Penetrant Profile Compared with the Experimental Data . 120
5.21 Calorimetric Analysis of Polyamide Membrane 123
5.22 Calorimetric Analysis of Polyamide-Acetic Acid System 124
5.23 Calorimetric Analysis of Polyamide-Water System 126
I.1 Calibration Curve for the Gas Chromatographic Analysis of Acetic Acid-Water Mixture 174
O.1 Infrared Spectra of Dry Polyamide Membrane 202
O.2 Infrared Spectra of Polyamide Membrane Soaked in Acetic Acid . . . 203
P.1 Calculated Penetrant Concentration Profile Compared with the Experimental Profiles 205
P.2 Calculated Penetrant Concentration Profile Compared with the Experimental Profiles 206

P.3 Calculated Penetrant Concentration Profile Compared with the Experimental Profiles 207
P.4 Calculated Penetrant Concentration Profile Compared with the Experimental Profiles 208
P.5 Calculated Penetrant Concentration Profile Compared with the Experimental Profiles 209
P.6 Calculated Penetrant Concentration Profile Compared with the Experimental Profiles 210
P.7 Calculated Penetrant Concentration Profile Compared with the Experimental Profiles 211
P.8 Calculated Penetrant Concentration Profile Compared with the Experimental Profiles 212
P.9 Calculated Penetrant Concentration Profile Compared with the Experimental Profiles 213
P.10 Calculated Penetrant Concentration Profile Compared with the Experimental Profiles 214
P.11 Calculated Penetrant Concentration Profile Compared with the Experimental Profiles 215
P.12 Calculated Penetrant Concentration Profile Compared with the Experimental Profiles 216

List of Tables

2.1 Separation of Acetic Acid/Water Mixture by Pervaporation 11

5.1 Pervaporation Data for Single Polyamide Membrane at 25°C and at the Downstream Pressure of 467 Pa 80

5.2 Comparison of Pervaporation Selectivity to the Liquid Sorption Selectivity 90

5.3 Liquid Sorption Data at Different Temperatures 90

5.4 Results of the Calculations Based on the Solution-Diffusion Model for Pure Water Permeation at Different Downstream Pressures for Polyamide Membrane at 25°C 98

5.5 Effect of Downstream Pressure on Permeation Characteristics at 25°C and at 0.50 Acetic Acid Mole Fraction in the Feed 106

5.6 Effect of Feed Temperature on Permeation Characteristics at the Downstream Pressure of 467 Pa (3.5 mm Hg) and at 0.50 Acetic Acid Mole Fraction in the Feed 107

5.7 Effect of Feed Composition on Permeation Characteristics at 25°C and at the Downstream Pressure of 467 Pa (3.5 mm Hg) 107

5.8 Effect of Downstream Pressure on the Phase Boundary 109

5.9 Effect of Feed Composition on the Phase Boundary 110

5.10 Effect of Temperature on the Phase Boundary 111

5.11 Summary of Calculation Data Showing Acid Mole Fraction in the Membrane Phase at Different Positions 112

A.1 Some Azeotropic Distillation Processes 152

B.1 Polymeric Materials Used in Pervaporation 154

B.2 Polymeric Materials Used in Pervaporation 155
B.3 Polymeric Materials Used in Pervaporation 156
C.1 Comparison of Function $1-(\frac{P_3}{P_2})^2$ and $F_2(\frac{P_3}{P_2})$ 158
E.1 Vapor-Liquid Equilibrium Data for Acetic Acid/Water System at 25°C Source: Gmehling et al. (1981) pp 89-109 163
E.2 Vapor-Liquid Equilibrium Data for Acetic Acid/Water System at 35°C Source: Gmehling et al. (1981) pp 89-109 164
E.3 Vapor-Liquid Equilibrium Data for Acetic Acid/Water System at 40°C Source: Gmehling et al. (1981) pp 89-109 165
G.1 Pervaporation Data for a Single Polyamide Membrane at 25°C and at the Downstream Pressure of 467 Pa (3.5 mm Hg) for Binary Mixture of Acetic Acid/Water 169
H.1 Pervaporation Data for Pure Water with a Single Polyamide Membrane at 25°C and at Different Downstream Pressures 171
H.2 Pervaporation Data for Pure Acetic Acid with a Single Polyamide Membrane at 25°C and at Different Downstream Pressures 172
J.1 Liquid Sorption Data for Polyamide-Acetic Acid/Water System at 25°C 176
J.2 Liquid Sorption Data for Polyamide-Acetic Acid/Water System at 35°C 177
J.3 Liquid Sorption Data for Polyamide-Acetic Acid/Water System at 40°C 178
K.1 Vapor Sorption Data for Polyamide-Acetic Acid/Water System at 25°C 180
K.2 Vapor Sorption Data for Polyamide-Acetic Acid/Water System at 35°C 181
K.3 Vapor Sorption Data for Polyamide-Acetic Acid/Water System at 40°C 182
L.1 Data for the Profile of Pure Water Content and Permeation Rate at Downstream Pressure of 467 Pa 184
L.2 Data for the Profile of Pure Water Content and Permeation Rate at Downstream Pressure of 1466 Pa 185
L.3 Data for the Profile of Pure Water Content and Permeation Rate Downstream Pressure of 2666 Pa 186
L.4 Data for Permeation Rate at Downstream Pressure of 4000 Pa 187
L.5 Data for the Profile of Pure Water Content and Permeation Rate at Downstream Pressure of 13332 Pa 188

M.1 Data for the Concentration Profile and Pervaporation of Binary Mixture at 25°C and at the Downstream Pressure of 467 Pa 190
M.2 Data for the Concentration Profile and Pervaporation of Binary Mixture at 25°C and at the Downstream Pressure of 467 Pa 191
M.3 Data for the Concentration Profile and Pervaporation of Binary Mixture at 25°C and at the Downstream Pressure of 467 Pa 192
M.4 Data for the Concentration Profile and Pervaporation of Binary Mixture at 25°C and at the Downstream Pressure of 467 Pa 193
M.5 Data for the Concentration Profile and Pervaporation of Binary Mixture at 25°C and at the Downstream Pressure of 467 Pa 194
M.6 Data for the Concentration Profile and Pervaporation of Binary Mixture at 35°C and at the Downstream Pressure of 467 Pa 195
M.7 Data for the Concentration Profile and Pervaporation of Binary Mixture at 40°C and at the Downstream Pressure of 467 Pa 196
M.8 Data for the Concentration Profile and Pervaporation of Binary Mixture at the Downstream Pressure of 1200 Pa and 25°C 197
M.9 Data for the Concentration Profile and Pervaporation of Binary Mixture at the Downstream Pressure of 2666 Pa and 25°C 198

Chapter 1

Introduction

1.1 Pervaporation

In pervaporation the component to be separated from a liquid feed mixture is "evaporated through a membrane". Mass transport across the membrane in pervaporation is achieved by lowering the activity of the permeating components on the downstream side. A schematic diagram of pervaporation process is shown in figure 1.1. Pervaporation membrane process most often competes with distillation for separation (Rautenbach and Albrecht, 1989; Neel, 1991; Flemming and Slater, 1992; and Osada and Nakagawa, 1992). For example, a study (Pearce, 1991) concludes that energy savings by pervaporation can be up to 60 %, with savings of 30 % on overall production costs for alcohol dehydration.

Low activity or low partial pressure at the downstream side in pervaporation can be achieved by one of the following methods:

1. By using an inert gas for continuously sweeping the downstream side of the membrane (sweep gas pervaporation).

2. By applying vacuum to the downstream side of the membrane and by continuously pumping off the permeating vapors (vacuum pervaporation).

3. By applying a temperature gradient across the membrane. This requires a

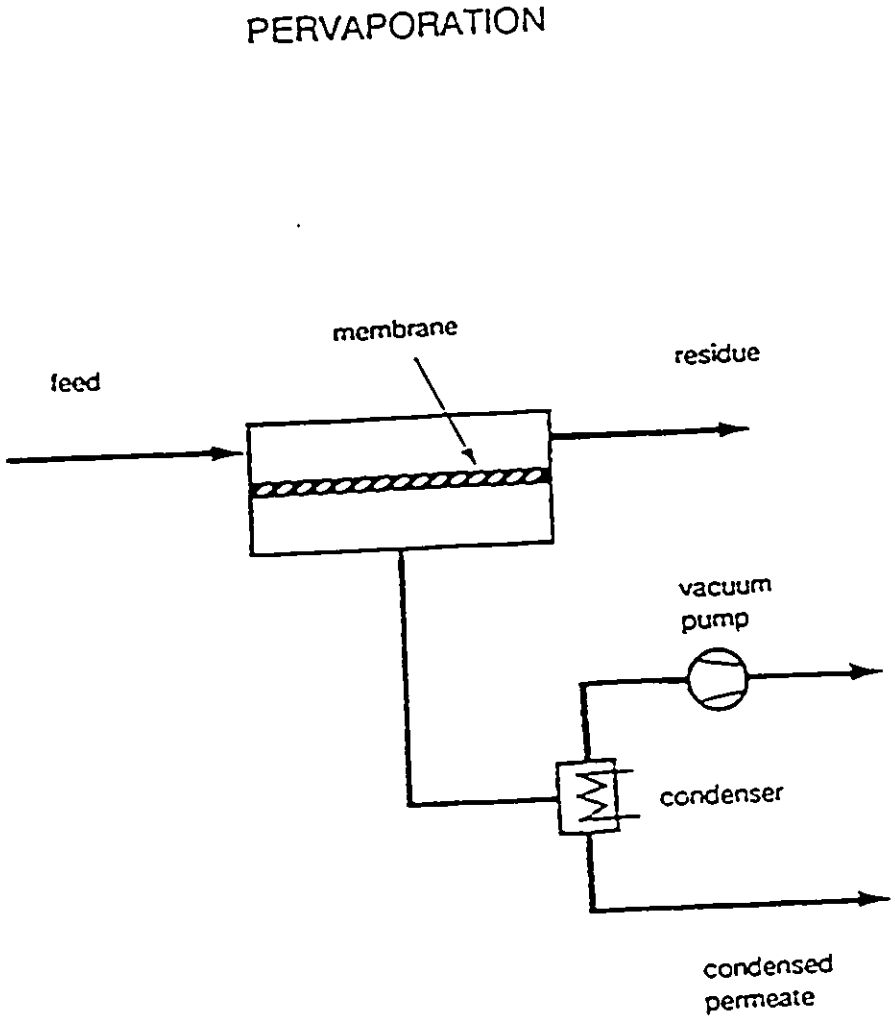

Figure 1.1: Schematic Diagram of Pervaporation Process

preheater for increasing the temperature of the feed mixture. A condenser is also necessary on the downstream side to remove the condensed vapors (permeated through the membrane) from the inert sweep gas. This method is sometimes termed as "thermopervaporation" (Aptel et al., 1976). However, according to Böddeker (Böddeker, 1990 A), the terms "thermopervaporation" should be discouraged and instead "vacuum pervaporation" should be used for this variant of pervaporation.

4. By applying an inert liquid (Cabasso et al., 1974 A) on the downstream side. Permeating components are diluted at the downstream side by an inert liquid. This process is called "perstraction" or "osmotic distillation".

In method "1" the sweeping gas should be recycled requiring condensation of the permeating vapors by cooling and preheating, whereas in method "2" the mechanical compression of the vapors in the vacuum pump requires high power consumption. For economical reasons, only methods "2" and "3" are applicable in large installations (Brüschke, 1988). In contrast with conventional vacuum pervaporation, method "4," i. e. perstraction, does not involve any phase-change of the penetrant(s) during its transport through the membrane, nevertheless, some of the drawbacks of perstraction are:

- A slower desorption step at the downstream surface of the membrane leading to lower permeation rates as compared to conventional pervaporation.
- The permeating component is obtained in a diluted state, and its recovery necessitates an additional rectification or regeneration step.

While discussing pervaporation and its variants, a brief discussion on vapor permeation is also necessary as they are closely related to each other. Pervaporation and vapor permeation differ only in so far that the feed is in a vapor phase in vapor permeation and in liquid phase in pervaporation. In both cases the driving force for the material transport through the membrane is the difference in the chemical potential of permeating components between feed and downstream side. Compared to pervaporation, vapor permeation has the advantage that no phase change occurs while

going from the feed to the downstream side. Therefore, the problem of supplying the enthalpy of evaporation in the pervaporation process is avoided. Vapor permeation is suitable especially for the purification/treatment of the top vapor stream of fractionation columns which can directly be used as a feed stream.

A wide variety of streams may be processed using pervaporation. But for pervaporation to be economically viable in the separation, the following requirements should be fulfilled:

- Selectivity of pervaporation should be much higher than that of an ordinary evaporation process, i. e. higher than the thermodynamic enrichment.
- Good pervaporation membranes should exhibit strong interaction with the desired component of the feed stream. The strong interaction of desired component will lead to high permeation rates.

The most important and promising category of separation problem solved by pervaporation is the separation of azeotropic mixtures and/or mixtures with small differences in boiling characteristics. Table A in appendix A shows some conventional azeotropic distillation processes. All of the azeotropic distillation processes are high energy intensive processes. Sometimes, even to choose the best entrainer is a difficult problem. Additionally, these entrainers have disposal problems. The separation of these mixtures is difficult using other conventional membrane processes such as reverse osmosis. Generally in reverse osmosis the problem of osmotic pressure is encountered. As an examples, in the reverse osmosis separation process of ethanol-water mixture, the built-up of osmotic pressure counteracting the applied driving-force has limited its applicability to below 20 wt % of ethanol in ethanol-water mixture. Pervaporation can be used for this separation as osmotic pressure will not be a limiting factor for the separation. Pervaporation is different from distillation because selectivity in pervaporation does not depend upon relative volatilities of components. Therefore, azeotropic distillation process can be replaced by pervaporation at lower investment cost and with drastically reduced environmental problems.

Pervaporation can be used and is rather advantageous for treating heat sensitive chemical mixtures. Pervaporation can be used in applications such as esterification

reactions where the equilibrium could be shifted toward the product by removal of water. Pervaporation process is also attractive for treating waste streams which are too concentrated for carbon adsorption and too dilute for incineration processes. A list of various separations attempted by pervaporation using different polymeric membranes is given in the table B.1, table B.2 and table B.3 in appendix B.

The potential of pervaporation has been proven for the following problems of separation:

- Azeotropic mixture separation.
- Aqueous-organic mixture separation; the separation of water or organic component from the aqueous-organic mixture depending upon the requirement.
- Membrane stripping, selective removal of small or relatively small amount of an organic component from an aqueous-organic stream.
- Organic/organic liquid mixture separation.

Among the applications mentioned above, the separation of organic/organic mixtures represents the least developed and the largest potential commercial application. Although organic/organic mixture separation was widely investigated in the beginning of an extensive pervaporation research effort (Binning et al., 1961) about 30 years ago, yet this type of separation by pervaporation membrane has not been developed to an industrial scale. The only successful technical development effort for separating azeotropic organic-organic mixture was reported in the literature (Chen et al., 1989).

Aqueous-organic mixture separation using pervaporation is at the threshold of commercialization and represents a potential application. Acetic acid and water mixture fractionation by pervaporation is one example of this category of separation. Acetic acid and water do not form an azeotrope. However, it is not easy to recover acetic acid by the use of simple distillation process because the relative volatility of acetic acid with respect to water is low. Therefore, the following techniques are used for acetic acid recovery from its various impurities and water:

- Azeotropic distillation,
- Liquid-liquid extraction,
- Extraction distillation, and
- Adsorption.

All of these processes are energy intensive processes. It is desirable to develop a new separation process for saving energy. Pervaporation membrane separation is a potential candidate for this purpose.

1.2 Objectives of the Thesis

In membrane separation processes it is desirable to have a polymer film which combines the characteristics of high permeation rate through polymer films with good selectivity. In order to obtain good permeation rates and high selectivity for a liquid mixture, it is essential to choose the right membrane as well as the optimum operating conditions. Therefore, the design of an efficient membrane for a specific application is very important.

However, to design a pervaporation membrane for a specific application one should have a good understanding of the transport mechanism involved. In this work some relevant transport studies were planned and performed to have a better understanding of the pervaporation transport mechanism. These transport studies will help to design more efficient pervaporation membranes.

A review of the available literature (Neel, 1991) on pervaporation asserts that there are already numerous transport studies. Nonetheless, few simple questions concerning pervaporation transport still can not be answered. The main reason is that almost all of these studies (Binning et al., 1961; Aptel et al., 1974 A; Greenlaw et al., 1977 A; and Mulder and Smolders, 1984) are based on an approach which considers the membrane as a black-box. A few of the specific questions that should be answered are:

- Where does the phase change (from liquid to vapor) take place during pervaporation ?
- Where does the membrane selectivity take place ?
- How does the position of phase boundary affect membrane selectivity ?

The major objective of the present work is to obtain indicators and guidelines for the design of pervaporation membranes. Other objectives are as follows:

1. To test experimentally the theoretical prediction of the newly developed transport model. One task is to confirm the presence of concentration polarization occurring inside the polymeric membrane during steady state pervaporation.

2. To compare the experimental results with the results obtained by the mathematical equations (simulated equations).

3. To obtain a better understanding of the state of permeant (penetrant) inside the polymeric membrane.

4. To obtain a better understanding of the transport mechanism of the pervaporation process which will lead to a better membrane design.

The following chapter contains the background of the pervaporation process in general. The chapter also contains a critical review of the transport studies available in the literature.

Chapter 2

Background

The early history of development in pervaporation has been sporadic with little continuity. Kober (1917) described an observation that "a liquid in a collodion bag, suspended in air, evaporated, although the bag was tightly closed". Subsequently, Kober coined the term "pervaporation" in 1917. Kober described the experiments for water selective permeation from an albumin/toluene solution through a collodion bag (cellulose nitrate). Farber (1935) discussed applications of pervaporation. Heisler et al. (1956) published their findings on dehydration of aqueous ethanol solutions through regenerated cellulosic membranes.

The commercial potential of pervaporation for separating azeotropic mixtures and for the separation of organic mixtures was recognized by Binning et al. (1961). Pervaporation was proposed as an industrial separation process. Their studies were focused on separating organic mixtures commonly found in petrochemical processing with cellulosic and poly(ethylene) membranes. Despite the intensive investigations by Binning and coworkers, their attempts to introduce pervaporation as an industrial process were not successful. The main reasons for this failure were insufficient permeation rate and/or selectivity for commercial applications. Other reasons for a long incubation time of the process were:

- Relatively high energy consumption compared to other membrane processes such as microfiltration, ultrafiltration or reverse osmosis because a phase change

occurs and the heat of vaporization has to be supplied.

- Difficult process design involving a temperature drop and pressure losses.
- Insufficient selectivity, permeation rate and stability of the membranes.

Nevertheless, from 1960's onwards, the practical feasibility of pervaporation was admitted, and this process began to be mentioned in review papers dealing with membrane separation techniques, such as the book published by Hwang and Kammermeyer (1975).

The earliest mention of an operating pervaporation pilot-plant dates back to 1982 (Ballweg et al., 1982). The information revealed was about a small demonstration unit installed in Brazil by a German Company called G. F. T. (Gesellschaft Für Trenntechnik, Homburg/Saar, Germany). The unit was used to dehydrate a water-ethanol mixture. The membrane used for the separation was a composite membrane consisting of three layers. An ultrafiltration poly(acrylonitrile) membrane was supported on a non-woven fabric. A very thin layer of crosslinked poly(vinylalcohol) was applied on the top of the poly(acrylonitrile) membrane.

Since then, a number of composite membranes have been developed by GFT company (Brüschke, 1988), each exhibiting good selectivity (10 to 1000) for a specific separation. Some of the commercial GFT membranes are:

1. Poly(vinylalcohol) composite membrane.
2. Silicone rubber composite membrane.
3. Modified cellulose esters membrane.

At present, most pervaporation research is concentrated on the separation of alcohol-water mixture and little has been reported on water/acetic acid mixture system. Acetic acid ranks among the top 20 organic intermediates in the chemical industries (King, 1980). Acetic acid is used in vinyl acetate, terephthalic acid, cellulose acetate and esters productions. In these industrial processes, an extensive demand for recovering acetic acid from aqueous streams exists. Acetic acid dehydration in

Table 2.1: Separation of Acetic Acid/Water Mixture by Pervaporation

Membrane used	Feed wt % Water	Total Permeation Rate kg/m^2-hr	$\alpha_{i,j}$ (water selective) -	Tempe-rature - °C	Reference - - -
PAA-co-PAN	10	0.0005	80	15	Yoshikawa et al., 1985
PAA-co-PS	10	0.0005	41	15	Yoshikawa et al., 1985
PAA-Nylon-6	24.5	0.045	69.5	15	Xu and Huang, 1988
Nylon-6/PAA	8.7	0.005	82.3	15	Huang et al., 1987
PVA/PVP	10	0.80	2.8	25	Nguyen et al., 1987 B
PVA/PAA	10	0.30	17.5	25	Nguyen et al., 1987 B
PVA/PEI	10	0.40	2.0	25	Nguyen et al., 1987 B
PSF(SO_3^-)-H^+	10	0.016	9.4	-	Nguyen et al., 1987 B
Poly(parabanic-acid)	20 -	0.5	200	70 -	Maeda et al., 1991

terephthalic acid industry was studied as a model system by Maeda et al. (1991) in which 80-85 wt % of acetic acid is dehydrated to 98 wt % and recycled to the reactor. Another potential application of pervaporation is in vinegar production by fermentation. The resulting stream has an acetic acid content of 10 wt%. Often it is advantageous to have a higher concentration of acetic acid in the vinegar such as for the production of pickled vegetables.

The pervaporation separation of acetic acid-water mixture has been studied using various polymeric membranes. A list of various polymeric membranes with their typical separation factor and permeation rate obtained is given in table 2.1.

2.1 Polymeric Membrane Materials for Pervaporation

Most polymers can be divided into two classes: glassy polymers and rubbery polymers or elastomers. This distinction is made on the basis of the state of the polymer at room temperature. Polymers with a glass transition temperature below room temperature are in the rubbery state and are, therefore, classified as rubbers or elastomers. Polymers having a glass transition temperature above room temperature are classified as glassy polymers. Within the group of glassy polymers in fact three types of polymers can be distinguished: crystalline, semi-crystalline and amorphous polymers.

Three types of membrane polymers can be identified for the pervaporation of aqueous-organic or organic-organic mixtures. These include:

1. Glassy (amorphous) polymers which interact preferentially with water.
2. Elastomeric polymers (elastomers) which interact preferentially with the organic component of the mixture.
3. Ion exchange polymers which may be viewed as crosslinked electrolytes and usually interact preferentially with water.

Glassy polymers are generally used for the dehydration of aqueous-organic mixtures. A modified PVA or poly(vinylalcohol) membrane is commercially produced by GFT company (Germany) for the dehydration of aqueous streams. Glassy polymeric membranes can also be used for the separation of an organic component from an organic-organic mixture or from an aqueous-organic mixture. For example, poly(ethylene) membranes were used for separating organic mixtures (Michaels et al., 1962; Siegel et al., 1970; Fels and Huang, 1970; and Huang and Lin, 1968). A novel glassy polymer namely, Poly(1-[trimethylsilyl]-1-propyne) or PTMSP was investigated (Hickey et al., 1992) for the separation of alcohol-water mixture. The polymer PTMSP was reported to be more alcohol selective than a rubbery polymer of poly(dimethylsiloxane). However, a decrease in both permeation rate and selectivity was observed for PTMSP membranes with time (Inaba et al., 1990).

Organic components permeate preferentially with respect to water through elastomeric polymers. The absence of polar groups in the flexible chains of elastomeric polymerics makes these polymers preferentially permeable to organic components. Polymers with these properties are excellent candidates as membrane materials for the removal of organics from aqueous-organic mixtures. Poly(esters), poly(vinylchlorides), and especially poly(dimethylsiloxane) (PDMS) are some of the polymers used (Neel, 1991) for the removal of organics from aqueous-organic mixtures by pervaporation.

Ion exchange membranes are generally water selective membranes. These membranes have been utilized for the separation of water/isopropyl alcohol and water/ethanol mixtures (Cabasso and Liu, 1985; and Böddeker and Wenzlaff, 1986). Polyion Complex or Symplex membranes formed by a simultaneous interfacial reaction of a synthetic polycation and a cellulose based polyanion were also used for the dehydration (Schwarz et al., 1991 A and Schwarz et al., 1991 B) of alcohol-water mixtures.

2.2 Pervaporation Membrane Development

Two different routes in the development of pervaporation membranes can be distinguished:

- Film membranes: films may be in an integral and unmodified form or in a modified film form. These membranes need a mechanical support. The surface of the film is sometimes modified by grafting.

- Thin-film composite membranes: a porous support substructure having a low flow resistance and stability is chosen for this purpose. A thin film of a second polymer is deposited on the top of porous support. The top layer (active layer) and porous substructure are chemically bonded together. The active layer can be deposited either from a solution or from the gas phase and cross-linked by heat treatment or by radiation.

Grafting is a polymer modification technique where a functional group is attached as a side branch irregularly to the polymer main chain. Generally, the effects of grafting are confined to the surface of substrates. One can also obtain homogeneously modified grafts (Huang et al., 1987).

2.2.1 Polymer Selection for Pervaporation Membranes

One way of selecting a polymer as a membrane material for a certain liquid mixture separation, would be to try out all the polymers available and pick the polymer with the best properties. This procedure, however, is a very time consuming process.

The first question one should be asking concerning the separation of liquid mixtures should be, which component should be separated preferentially from the mixture and whether this component is water or an organic component ? Hydrophilic polymers (glassy polymers) have to be chosen for further investigation for the removal of water from aqueous-organic mixtures, whereas hydrophobic elastomers are the most suitable polymers for the removal of an organic component from aqueous-organic mixtures. When aqueous-organic mixtures are to be treated, hydrophilicity or hydrophobicity of a polymer can be used as a guideline in membrane screening and development. However, for organic-organic mixtures such an easy concept does not exist. Therefore, screening of polymers in this case should be done based on other concepts, such as the concept of solubility parameter.

When all polymers chosen are investigated for pervaporation performance and compared, two groups can be distinguished:

- polymers with relatively high selectivity and low permeation rate, and
- polymers with relatively low selectivity and high permeation rate.

Polymers with high selectivity are preferable for further investigation because it is easier to increase permeation rate than selectivity. How to increase the permeation rate and/or selectivity is touched briefly in the discussion of asymmetric membranes and is answered in more detail in section 5.11. There are many ways of improving

the separation properties of a membrane. One way is by changing the membrane morphology and the other is by modification of the membrane material.

A semi-quantitative approach for choosing a polymeric material includes the quantification of the interaction between the polymer and mixture components (penetrants). The interaction between the polymer and mixture components can be described by means of the solubility parameter theory (Hansen, 1969; and Lee et al., 1987). For a system consisting of a polymer and a penetrant molecule this theory is a convenient tool as a first estimate of the interaction phenomena. It was shown by Hansen (1969) that the solubility parameter δ_{sp} $((J-m^3)^{1/2})$ can be divided into three parts:

$$\delta_{sp}^2 = \delta_d^2 + \delta_p^2 + \delta_H^2 \tag{2.1}$$

where δ_d represents the part of δ_{sp} due to dispersion forces, δ_p is the part due to dipolar forces, and δ_H is the contribution of hydrogen bonding (H-bonds) effects and other donor-acceptor interactions.

It should be emphasized that there are some restrictions in using the solubility parameter theory. The parameter that describes the miscibility, the free energy of mixing contains two contributions, the enthalpy of mixing and the entropy of mixing. In the solubility parameter approach only the enthalpy term is considered. The theory predicts the mixing of polymer and penetrant(s) from the properties of the pure component, therefore, specific interactions between polymer and penetrants involved upon mixing are not included.

Another possible approach is the comparison of the membrane polarity in terms of Dimroth's solvent polarity parameter value (E_T at $25°C$) (Yoshikawa et al., 1986 A), since membrane polarity influences separation behavior. The separation factor for water-ethanol mixtures tends to increase as the E_T value at $25°C$ of the alcohol deviates from that of the membrane. Separation factor tends to decrease as the value of the parameter for the membrane deviates from that of water in the pervaporation of the water-ethanol mixture. As no knowledge of the precise polymer structure is required, in particular for a newly synthesized membrane, the E_T value is one of the promising parameters for use in the development of membranes for separation of the

water-ethanol mixture.

Polyamides are reaction products of primary or secondary diamines and dibasic acids. The most important structural feature of polyamides is the -CONH- group or amide link. This functional group has a strong capacity for hydrogen bonding. Polyamides of three classes are commercially available: fully aliphatic (both diacid and diamine monomers are aliphatic); aromatic-aliphatic (the diacid monomer is aromatic and the diamine is aliphatic) and fully aromatic (both the diacid and the diamine are aromatic). All three classes of polyamides can be used for membrane making. An excellent review on polyamide membranes by Blais (1977) is available in the literature. Two kinds of aromatic polyamide materials are of special interest in reverse osmosis/ultrafiltration membrane development. One of them is essentially a random copolymer consisting of two repeat units in a molar ratio of 0.7 to 0.3. The synthesis and characterization of this material (indicated as PA) are described in detail by Gan et al. (1975). The same polymer (aromatic polyamide) has been used in the present study. The chemical structure of the polymer is presented in section 4.1.

Aromatic polyamide is an excellent membrane material because of its outstanding mechanical, thermal, chemical and hydrolytic stability as well as its permselective properties in pervaporation. Aliphatic polyamides also show good chemical stability and may be used in microfiltration/ultrafiltration/reverse osmosis application. However, aromatic polyamides are to be preferred in pervaporation (Nguyen et al., 1987 A). The properties of the aromatic polyamides are determined by the aromatic group(s) in the main chain which considerably reduce the chain flexibility. As a result, aromatic polyamides have glass transition temperature of 280°C and higher, compared to value of less than 100°C for the aliphatic polyamide.

2.2.2 Design and Preparation of Pervaporation Membranes

One can broadly classify membranes into symmetric and asymmetric membranes from the standpoint of the symmetricity of membrane (Kesting, 1985). When a membrane structure shows symmetry perpendicular to the membrane surface, the

membrane is said to be symmetric. The so-called "homogeneous" membrane is also a symmetric membrane. If the membrane shows an asymmetric structure perpendicular to the membrane surface, it is called an asymmetric membrane. Such membranes with a dense skin on a porous membrane are widely used for reverse osmosis and ultrafiltration processes. An asymmetric membrane can be formed in an integral form or in a composite form. A composite membrane usually has a porous membrane as a support. A tnin and dense layer, often of another polymer type, is applied on top of the support membrane. The top dense layer is often selected based on its high selectivity.

A schematic diagram showing symmetric, asymmetric and composite membrane is shown in figure 2.1. GFT's commercial PVA membrane is one example of composite membrane.

Integral polymeric asymmetric membranes are usually made by the phase-inversion method. The film consists of a thin dense skin layer (0.1-1.0 μm thickness, containing very small pores) on top of a porous sublayer. The phase-inversion process, which is widely used for producing an asymmetric reverse-osmosis membrane, is unsuitable for manufacturing pervaporation membranes. The reason is that this process does not provide the means to adjust, at will, the structure of the porous sublayer and the top layer. In other words, membrane design is much more restricted. Thus, a composite membrane is the best choice to obtain the suitable pervaporation membrane. However, in the present study the penetrant profile studies should be performed with symmetric membranes.

The pervaporation characteristics of an asymmetric and a symmetric membrane were compared by Rautenbach and Albrecht (1984). The permeation rate obtained by asymmetric membranes was higher than that obtained with a symmetric dense film under steady-state conditions. The permeation characteristics of asymmetric membranes depended on their orientation with respect to the permeation flow rate. The configuration having the dense skin of the membrane facing the feed was reported to have higher selectivity. On the other hand, by reversing the membrane disposition the membrane gave higher permeation rate.

A commercially available pervaporation membrane for dehydration of organic

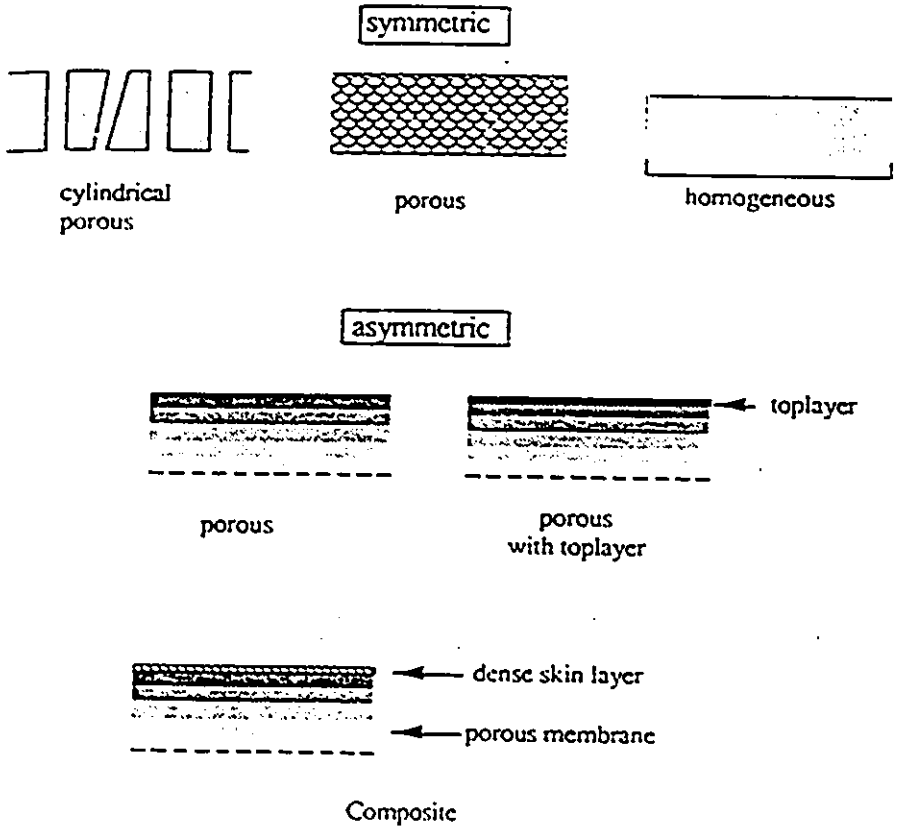

Figure 2.1: A Schematic Diagram of Membrane Cross-sections (Mulder, 1991)

aqueous mixtures is a composite membrane developed by a German company named GFT. The membrane consists of an asymmetric poly(acrylonitrile) or PAN porous support (on a non-woven fabric), with a very thin top layer of crosslinked (with maleic acid) poly(vinylalcohol) or PVA. The function of the PAN support is thought to ensure mechanical strength, while the top layer of PVA is assumed to be responsible for the separation. The selectivity is attributed to the effect of the pendant hydroxyl group that attracts water preferentially from aqueous mixtures by hydrogen bonding. The separation factor of dense poly(vinylalcohol) membranes never exceeds 200-300 (Spitzen et al., 1987) and depends on the membrane thickness. Therefore, the question arises, why are GFT membranes much more selective than PVA membranes ? On the other hand, dense PAN membranes exhibit a high separation factor ($\alpha_{i,j}$ = 1000). In this case the bottom layer of the membrane also contributes to selectivity. However, one should not neglect the crosslinked structures of GFT's PVA membranes.

There are studies in the literature indicating the importance of the support layer. For example, a systematic investigation reported by Blackadder and Keniry (1972) concerned the pervaporation transport of pure p-xylene at 30 °C through a dense film of poly(ethylene) (75 μm-thick) membrane mounted over five different supports. The experimental permeation rate values ranged from 26 to 61 g/hr-m^2.

Mochizuki et al. (1984) also demonstrated the importance of the bottom layer of the membrane and showed that it also contributes to the selectivity of the membrane. In the study by Mochizuki et al. the pervaporation performance of PDMS (polydimethylsiloxane) and PVA/PVP (polyvinylalcohol and polyvinylpyrrolidone) blend membranes was studied to separate benzene/methanol mixtures. Bilayer membrane consisted of two layers of two different materials. Both membranes were dense and symmetric. When the membranes were used individually PDMS membrane was benzene selective, whereas PVA/PVP blend membrane was methanol selective. The bilayer membrane having PDMS membrane in contact with the feed mixture was methanol selective. On the other hand, when PVA/PVP membrane faced the feed, the membrane became benzene selective. Two points should be made from this data. First the selectivity was governed by the membrane not in direct contact with the feed mixture but in contact with the downstream vapor. The second one is that

the selectivity of the membrane was reversed when the membrane was turned upside down.

Deng et al. (1990) also reported similar results. In their study poly(dimethylsiloxane) or PDMS and aromatic polyamide (PA) membranes were used. An asymmetric PA membrane was used in this case. The poly(dimethylsiloxane) membrane was laminated on the top of asymmetric PA membrane. The lamination of poly(dimethylsiloxane) on the top of an asymmetric aromatic polyamide membrane was reported to intensify the water selectivity of the aromatic polyamide membrane. Some of the conclusions were:

- Both membrane components contribute to the overall selectivity of the bilayer (two layer) membrane.
- When the PDMS membrane faced the feed liquid, the water selectivity of asymmetric polyamide membrane was intensified. The reason is that the densest and the least porous section of the asymmetric membrane is kept dry and contributes most effectively to the selectivity of the bilayer membrane.

2.3 Characterization of Pervaporation Membranes

The characterization of pervaporation membranes can be broadly classified in the following categories:

- Physical and chemical properties of the polymer. For example, glass transition temperature and degree of crystallinity of the polymer.
- The interaction between the polymer and the penetrants.
- Surface analysis or morphology of the membrane. The morphology of the membrane is generally characterized by the pore size and pore size distribution on the active surface layer of the membrane.
- Permeation rate and selectivity of the membrane under pervaporation conditions.

The most effective and the simplest method of characterizing a pervaporation membrane is by measuring permeation rate and selectivity under actual pervaporation conditions. The permeation rate is usually defined as mass (or moles) permeating through 1 m^2 of the membrane per unit time (mol/s-m^2 or kg/s-m^2). The separation factor for a binary mixture of i and j components ($\alpha_{i,j}$) is defined as:

$$\alpha_{i,j} = (\frac{W_j'}{W_i'})/(\frac{W_j}{W_i}) \tag{2.2}$$

where subscripts i and j represent respective components of the mixture. Here W and W' refer to the weight fractions of a component in the feed mixture (upstream) and downstream (permeate stream), respectively. This definition of $\alpha_{i,j}$ is valid for a system in which component j is preferentially permeated through the membrane. The separation factor $\alpha_{i,j}$ is patterned after the relative volatility of the component of binary liquid mixtures. The separation factor $\alpha_{i,j}$ is independent of concentration units used, as being the ratio of ratios.

The selectivity (enrichment factor) of a membrane for a binary mixture is expressed in terms of a β parameter. This parameter is defined in the following manner:

$$\beta = \frac{W_j'}{W_j} \tag{2.3}$$

The enrichment factor β is simply the ratio of concentrations of the preferentially permeating species in downstream and upstream. The numerical value of the enrichment factor depends on the concentration units used. Since enrichment is an engineering term, mass units seem appropriate, e.g. (w/w) when using mass fractions. Undoubtedly, $\alpha_{i,j}$ is more significant than β from the physicochemical point of view, since it increases to infinity as the membrane material approaches perfect semi-permeability. On the other hand, use of the parameter β facilitates the formulation of the mathematical equations governing the performance of a pervaporation membrane.

Sometimes, the overall performance of the membrane is evaluated by the parametric value of $J.\alpha_{i,j}$, where J is the permeation rate and $\alpha_{i,j}$ is selectivity (Yoshikawa et al., 1988). The above value of $J.\alpha_{i,j}$ was named as pervaporation separation index

(PSI) by Huang and Yeom (1991). This index is a relative measure of the separation ability of a membrane. This index could be used as a relative guideline for the design of pervaporation membrane separation processes and also to select a membrane with an optimum combination of permeation rate and selectivity. Nguyen et al. (1987 B) defined $J.(\beta - 1)$ as the overall membrane performance criteria.

2.4 Transport in and Through Pervaporation Membranes

Pervaporation literature is rich in studies on transport mechanisms (Binning et al., 1961; Aptel et al., 1974 A; Greenlaw et al., 1977 A; Mulder and Smolders, 1984; Yoshikawa et al., 1986 A; Huang et al., 1988; and Okada and Matsuura, 1991). The majority of transport studies are based on the conventional solution-diffusion (sorption-diffusion) model (Greenlaw et al., 1977 A; Long, 1965; Lee, 1975; Mulder and Smolders, 1986; Rautenbach and Albrecht, 1985; and Brun et al., 1985). According to the solution-diffusion mechanism, penetrant molecules are sorbed from the feed liquid phase into the polymeric membrane, diffuse through the membrane, and are desorbed on the downstream side. A summary of the available transport studies is presented in this section.

Binning et al. (1961) classified pervaporation membranes as nonporous films. They argued that these membranes do not contain discrete holes or pores, and these membranes neither function by a molecular-sieving action nor by a Graham-type diffusion through holes. Instead, permeation requires solubility (sorption) of penetrant in the polymer and movement of the penetrant through the membrane. Binning et al. (1961) suggested a qualitative model for the pervaporation process by assuming the existence of two zones in the polymer film under pervaporation conditions. The upstream zone ("solution zone") occupies the major portion of the membrane. This zone of the membrane may be visualized as a highly swollen state of the polymer in which there is a high concentration of penetrant liquid in the polymer structure. The downstream zone ("vapor phase zone"), in which the evaporation of liquid occurs,

may be considered as a region in which penetrant molecules are much more dispersed and polymer structure corresponds nearly to the dry polymer film. The existence of two completely different phases within the film seems quite reasonable because the opposite surfaces of the film are subjected to such different conditions. It was proposed that little selectivity occurs at the liquid-membrane interface, but most of the selectivity occurs at the interface between the "solution phase" and the "vapor phase". The diffusion in the latter zone was believed to be the rate-controlling step in the process.

Sweeny and Rose (1965) suggested that not only the chemical effects (hydrogen bonding) play a major role but the dimensions, shape, and spacing of the polymer molecules are also important. These authors put forward a hypothesis that a substance more soluble (sorbed) in a polymer film is also permeated through the film more selectively. The hypothesis was supported with the help of pervaporation and solubility (sorption) data for different polymeric membranes and penetrants. Tock et al. (1974) attempted to predict selectivities for water-dioxane mixtures from permeation rates of the pure components using solution-diffusion model with a concentration dependent diffusion coefficient. Their results show that it would hardly be possible to predict selectivities for non-ideal mixtures from single component permeation data alone. Cabasso and Liu (1985) suggested that transport during pervaporation through ionic membranes occurs through discrete paths (channels) and not by a random molecular sorption and diffusion through the amorphous polymer.

Yoshikawa et al. (1986 A and 1986 B) explained that specific and selective separation of penetrants through membranes can be realized by incorporating a group into membranes that causes a strong interaction such as hydrogen-bonding interaction. Differences in strength of the hydrogen-bonding interaction lead to selective separation of the desired component through a membrane. It was reported that not only the characteristics of the functional group, which interacts preferentially with water in the membrane, but also the environment (membrane polarity) around the functional group influenced the separation characteristics. In particular, for ethanol/water mixture the permeation mechanism of water through poly(acrylic acid-co-acrylonitrile) membranes was discussed.

Transport models for pervaporation can be subdivided into three sections:

- Pore-Flow Model
- Solution-Diffusion Model
- Free Volume Model

There are no quantitative transport models based on the irreversible thermodynamics approach.

A detailed description of these transport model is given in following sections.

2.4.1 Pore Flow Model

While the solution-diffusion mechanism is being considered valid by the majority in the membrane research community, an approach based on the preferential sorption-capillary flow mechanism has been pursued by Matsuura, Sourirajan and coworkers (Sourirajan and Matsuura, 1985). According to this mechanism a sharp concentration gradient of the liquid composition is present at the membrane polymer-fluid mixture interface. The separation of the fluid mixture components is ensured by letting the interfacial fluid flow through small membrane pores. This approach has been extended to the membrane transport by pervaporation. According to the approach, pervaporation process is considered as a combination of liquid transport (reverse osmosis) and vapor transport (membrane vapor permeation) in a series. Following the above approach a pervaporation transport theory on the basis of the pore flow mechanism has been proposed (Sourirajan et al., 1987). According to the mechanism, feed liquid enters a pore from the feed side, evaporates in the pore into a vapor phase and comes out of the pore into vacuum from the downstream side of the membrane. While no phase change inside the membrane occurs in the solution-diffusion model, according to the pore flow model, a clear boundary of liquid and vapor phases exists inside the membrane at a certain distance from the surface that is in contact with liquid feed.

The transport theory on the basis of the pore flow model starts from the assumptions that there are a bundle of straight cylindrical pores of length δ (membrane

thickness) penetrating across the active surface layer of the membrane and that all pores are in an isothermal condition. Both phases (liquid and vapor) flow through the pore by the pressure difference between both ends of the pores as the driving force. This is in contrast with the solution-diffusion mechanism, where the sorbed penetrant is considered to be driven by the concentration gradient.

The main distinction between the "pore model" and homogeneous membrane concept used in solution-diffusion approach lies in the physical meaning of the pores. On a molecular scale nothing is homogeneous. In the pore model case, a system of pores and channels limited by irregularly coiled macromolecules of the membranes can be assumed. The geometry of the polymer network sets the upper limit for the size or cross section of such pores or channels. The question arises whether it is justified to consider the interstices between the individual molecules in a polymer membrane to be pores. In other words, when does the structure stop being heterogeneous and becomes a homogeneous phase (of membrane and permeating fluid) ? This distinction is important while attempting to understand and to model the mechanism for mass transport in these systems. In the pore model of a membrane, more-or-less fixed pores are assumed. The principles that apply to macroscopic phenomena, such as Poiseuille's law, are also assumed to apply to the submicroscopic or molecular level phenomena. It can be argued that flow in small pores is unlikely to be described satisfactorily by Poiseuille's law. At the level of molecular dimensions, assuming an assembly of linear cylindrical pores running in the direction of flow is also quite unrealistic. Nonetheless, it is acceptable to characterize a pore system by calculating the number and diameter of identical cylindrical pores which would have the same total volume and flow properties as the real pore system. This simple artifice should not be objectionable provided its significance is clearly recognized.

A schematic of pore-flow model is shown in figure 2.2. The figure 2.2 shows that the pore is partially filled with liquid from the pore inlet to a distance δ_a along the cylindrical axis. The rest of the pore length δ_b is filled with vapor phase. Evaporation takes place at the liquid-vapor boundary (Sourirajan et al., 1987 and Okada and Matsuura, 1988). The pressures of upstream (feed liquid side) and downstream side are given as P_2 and P_3, respectively, and at the phase boundary the pressure must be

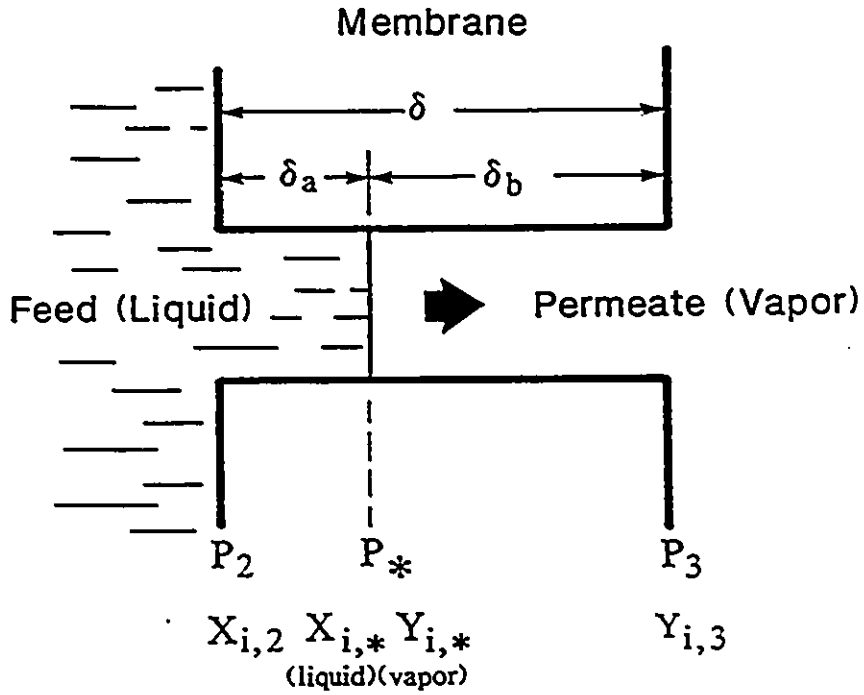

Figure 2.2: A Conceptual Diagram of Pore Flow Model

the saturation vapor pressure of feed component which is denoted by P_s. The above picture can be valid only when $P_s > P_3$. When $P_3 \geq P_s$ the entire pore is filled with liquid.

It seems rather misleading to say that the pore is filled with "liquid" and with "vapor" and there is a clear boundary separating liquid and vapor phases in the membrane. The liquid-filled portion of the pore was defined as the portion of the pore where the penetrant flows by liquid transport, while the vapor-filled portion of the pore means the portion of the pore where the penetrant flows by vapor phase transport.

First let us consider a single component system. Let us also assume that $P_s > P_3$. The transport in the liquid-filled portion of the cylindrical pore can be expressed by Poiseuille's equation and can be written as follows:

$$J_{liq} = \frac{(\kappa)(\rho)N_t}{(\eta_l)M(\delta_a)}(P_2 - P_s) \tag{2.4}$$

Defining a proportionality constant, A, as follows:

$$A = \frac{(\kappa)(\rho)N_t}{(\eta_l)M} \tag{2.5}$$

The definitions of symbols used is given in nomenclature.

The pressure of the vapor phase changes from P_s to P_3 in the vapor-filled portion of the pore. The size of the pore is assumed to be so small that it is almost filled with an adsorption layer of vapor molecules on the pore wall, the flow of which is the primary contribution to the vapor transport. The above assumption sets the upper limit to the pore sizes for which the model development is meaningful. When the pore size is within the limit, surface flow model can be used. The surface flow model was originally defined by Gilliland et al. (1958) for the vapor transport without superimposition of any other gas flow mechanism. According to the surface flow model the vapor flow is represented by the following equation:

$$J_{vap} \propto \int_{P_3}^{P_s} \frac{x^2}{P} dP \tag{2.6}$$

Assuming that for the vapor adsorption Henry's law is valid:

$$x = k_H P \tag{2.7}$$

Using equation 2.7 the equation 2.6 can be rewritten as following:

$$J_{vap} \propto k_H^2 \int_{P_3}^{P_\bullet} P dP \tag{2.8}$$

After integrating the above equation, we obtain:

$$J_{vap} \propto k_H^2 (\frac{P_\bullet + P_3}{2})(P_\bullet - P_3) \tag{2.9}$$

The main feature of equation 2.9 is that the vapor permeation rate is proportional to the average vapor pressure $((P_\bullet + P_3)/2)$ in the pore, which represents the population of vapor molecules in the pore, times the pressure differential $(P_\bullet - P_3)$, which represents the driving force applied for the movement of the vapor molecules.

Equations 2.4 and 2.9 can be combined to yield the following equation:

$$J = \frac{A}{\delta}(P_2 - P_\bullet) + \frac{B}{\delta}((P_\bullet^2) - (P_3^2)) \tag{2.10}$$

where the first term of the right hand side of the equation refers to the liquid transport, while the second term refers to the vapor transport. Parameter B in above equation is given by the following expression:

$$B = \frac{(\pi)(2R_b t - t^2)^2 t N_t R T}{(8R_b)(\eta_v)}(k_H')^2 \tag{2.11}$$

where R_b and k_H' are the pore radius and a proportionality constant involved in the gas adsorption. More precise definitions of other symbols used are given in nomenclature.

When $P_3 \geq P_\bullet$ the permeation rate is given by the following equation:

$$J = \frac{A}{\delta}(P_2 - P_3) \tag{2.12}$$

The following two equations show the relative vapor-filled region and the relative liquid-filled region in the membrane (Okada et al., 1991):

$$\frac{\delta_b}{\delta} = \frac{B(P_\bullet^2 - P_3^2)}{A(P_2 - P_\bullet) + B(P_\bullet^2 - P_3^2)} \tag{2.13}$$

and

$$\frac{\delta_a}{\delta} = \frac{A(P_2 - P_\bullet)}{A(P_2 - P_\bullet) + B(P_\bullet^2 - P_3^2)} \tag{2.14}$$

These relationships define the liquid-vapor phase boundary inside the membrane. The term $\frac{\delta_a}{\delta}$ shows the liquid part, whereas $\frac{\delta_b}{\delta}$ represents the vapor-filled region. The above two equations indicate that the ratio $\frac{\delta_a}{\delta}$ decreases, approaching a minimum value (but not zero) when P_3 (downstream pressure) approaches zero, while the above ratio approaches unity as P_3 approaches P_s (saturation vapor pressure). In other words, the pore is least filled with liquid when a high vacuum is applied on the downstream side of the membrane. The liquid-filled portion of the pore should move towards the feed-membrane interface when the downstream pressure is lowered. When the downstream pressure is sufficiently high and even greater than the saturation vapor pressure of the component there should be only liquid phase inside the membrane and the process will resemble reverse osmosis.

For the binary mixture system an assumption was made in the pore flow model that evaporation takes place at the inlet of the pore (Okada et al., 1991). In other words it is assumed that the pore is filled only with vapor. This assumption is considered valid when the pore radius is sufficiently small, the downstream pressure is sufficiently low and the swelling of the membrane with feed liquid is not too strong. The transport model for pervaporation based on the pore flow mechanism was tested by examining the main features observed in pervaporation experiments (Okada and Matsuura, 1991 and Okada et al., 1991). The pervaporation systems tested were mixtures of ethanol/n-heptane, methanol/n-heptane, methanol/ethanol, 2-propanol/water and cyclohexane/benzene. Polymeric membrane materials such as cellulose, cellulose diacetate-triacetate blend, polyamide, poly(ethylene) and poly(γ-methyl-L-glutamate) were also included in the study. Membranes were either asymmetric or symmetric but not of composite nature.

Using the pore flow model, Deng et al. (1990) calculated the composition of the penetrant mixture at the liquid-vapor phase boundary. The position of the phase boundary in the membrane pore was calculated from the transport rate in the liquid phase relative to that in the vapor phase. It was assumed that the separation of the liquid mixture occurs primarily at the phase boundary and through the vapor region. It was shown that the above assumption could explain most of the fundamental features observed experimentally for the separation of acetic acid/water mixtures.

It should be pointed out that experimental results obtained from GFT's poly-(vinylalcohol) membrane (particularly the curve correlating the water mole fraction in the downstream to that in the feed) cannot be reproduced by using the above equations. Presumably, the unique shape observed in the above correlation is either due to the composite nature of the PVA membrane prepared by GFT company (Brüschke, 1988) or due to the membrane swelling occurring at high penetrant (ethanol) concentration.

2.4.2 Solution-Diffusion Model

According to solution-diffusion model the transport of the penetrant(s) through dense membrane can be described by Fick's first law in terms of solubility and diffusivity. According to this approach, transport process consists of three successive steps:

1. Sorption of the penetrant molecules into the polymeric membrane.
2. Diffusion of the penetrant molecules through the film.
3. Desorption of the penetrant molecules, taking place at the downstream surface of the membrane.

For the single component permeation, the permeation rate is described by Fick's first law:

$$J = -D\frac{dc}{dl} \tag{2.15}$$

where J is the permeation rate, D is the diffusivity, and dc/dl is the concentration gradient of the penetrant across the membrane. Several expressions have been proposed to relate diffusivity to the penetrant concentration in the polymer. Commonly used relationships are:

$$D = D_0 exp(\omega c) \tag{2.16}$$

where c is the penetrant concentration, D_0 the diffusion coefficient of penetrant in the membrane at zero penetrant concentration and ω is a plasticizing constant expressing the influence of the plasticizing action of the penetrant on the segmental

motion. Rautenbach and Albrecht (1989) indicated that the following simplified form is sufficient for basic design calculations in pervaporation process:

$$D = D_0(1 + \omega c) \tag{2.17}$$

Choo (1962) defined a "concentration average diffusivity," $\overline{D}$, as follows:

$$\overline{D} \equiv (\int_{c_3}^{c_2} D dc)/(c_2 - c_3) \tag{2.18}$$

where c_2 and c_3 are the penetrant concentrations in the film at the upstream and downstream faces, respectively. It is evident from equation 2.18 that $\overline{D}$ will equal D if the diffusivity is not a function of penetrant concentration.

The most common assumptions made in the solution-diffusion model are as follows:

1. Permeation is the result of diffusion across the membrane through the amorphous regions of the polymer.
2. Fick's law is applicable.
3. The diffusivity is dependent on the penetrant concentration in the polymeric membrane.
4. At each membrane face, the penetrant in contact with the membrane is in thermodynamic equilibrium with the penetrant dissolved in the polymeric membrane.
5. The pressure within the membrane is constant at a value equal to the upstream pressure.

It is of interest to note that different versions of solution-diffusion (SD) model exist in the literature. These models differ in their assumptions involved. The SD model by Lee (1975) and Greenlaw et al. (1977 A) assumes that the pressure inside the membrane is a constant value, whereas the concentration of the penetrant changes across the membrane. On the other hand, the SD model by Kataoka et al. (1991) assumes that the pressure varies across the membrane but the concentration of the

penetrant across the membrane has a constant value. In the literature on solution-diffusion model no distinction is made between solution and sorption terms. These terms are used interchangeably without any repercussion.

According to the solution-diffusion approach, it appears that the permeation rate of the various components in the rubbery polymer is determined mainly by their solubility (Bell et al., 1988) in the polymer phase. In a glassy polymer, however, the permeation rate of the components is controlled by their diffusivity in the polymer matrix.

Two distinct drawbacks of the solution-diffusion model should be pointed out. The first one is related to the phase change. The solution-diffusion model does not consider phase boundary inside the membrane, while the pore-flow model does. As far back as in 1961, Binning et al. (1961) considered this phase change occurring inside the membrane, though qualitatively. The second drawback is related to the gradient of the pressure inside the membrane. The solution-diffusion model considers the pressure inside the membrane as a constant value and equal to the upstream pressure value, while in the pore-flow model there is a pressure gradient inside the membrane. There is, however, one exception to this statement, i.e. the modified solution-diffusion model by Kataoka et al. (1991) does consider the pressure profile inside the membrane, but the penetrant concentration inside the membrane has a constant value.

Greenlaw and coworkers (1977 A and 1977 B) have presented a detailed version of solution-diffusion model and substantiated their model by pervaporation experiments for single as well as multicomponent systems. The model was applied to describe the behavior of a two-component system: hexane/heptane mixture permeating through poly(ethylene) membrane.

The following equation was proposed to describe the concentration dependence of the diffusion coefficient of hexane in poly(ethylene) membrane:

$$D = D_0(1 + \omega c^n) \tag{2.19}$$

where D_0, ω and n are constants.

For equilibrium sorption, the following equation was proposed for hexane sorption in

poly(ethylene) membrane:

$$c = S_1(P/P_0) + S_2(P/P_0)^m \tag{2.20}$$

where S_1, S_2, and m are constants. Here P is the partial pressure and P_0 is the saturation vapor pressure of hexane in mm Hg. If hexane is assumed to be a perfect gas, the ratio P/P_0 should be equal to the activity, a, of hexane dissolved in the polymer, and the above equation can be rewritten as follows:

$$c = S_1.a + S_2.a^m \tag{2.21}$$

Thermodynamic equilibrium at the membrane interface was also assumed. Therefore, the chemical potential of the dissolved penetrant and the contacting fluid should be equal. This can help to correlate penetrant concentrations in the polymer to the upstream feed pressure and downstream pressure. The relevant equations for chemical potential (denoted by μ) are the following:

1. For the pure liquid in contact with the upstream face at pressure P_2, assuming constant molar volume V:

$$\mu_2 = \mu^0 + V(P_2 - P_0) \tag{2.22}$$

   where μ^0 is the chemical potential of the pure liquid at its saturation pressure.

2. Assuming the partial molar volume of hexane equal to the molar volume of pure hexane:

$$\mu_2 = \mu^0 + V(P_2 - P_0) + RTlna_2 \tag{2.23}$$

3. For the dissolved liquid at the downstream face (recall that the pressure in the membrane is assumed constant at P_2):

$$\mu_3 = \mu^0 + V(P_2 - P_0) + RTlna_3 \tag{2.24}$$

4. For pure liquid in contact with the downstream face:

$$\mu_3 = \mu^0 + V(P_3 - P_0) \tag{2.25}$$

5. For pure vapor in contact with the downstream face, assuming perfect gas behavior:

$$\mu_3 = \mu^0 + RTln(P_3/P_0) \tag{2.26}$$

Equating equation 2.22 and equation 2.23, we find that the upstream activity must be unity, i.e. $a_2 = 1$

Equating equation 2.24 and equation 2.25 we obtain the following relationship for the downstream activity, a_3, applicable when liquid phase is present at the downstream face:

$$a_3 = exp[-\frac{V}{RT}(P_2 - P_3)] \tag{2.27}$$

Equating equation 2.24 and equation 2.26 we obtain the following relationship for a_3, applicable when vapor phase is obtained at the downstream face:

$$a_3 = \frac{P_3}{P_0}exp[-\frac{V}{RT}(P_2 - P_3)] \tag{2.28}$$

The applicability of the model described above is somewhat limited by the fact that there are six experimental constants (D_0, ω, n, S_1, S_2 and m) to be determined. A simplification was made (Greenlaw et al., 1977 A) to obtain a simplified model characterized by a single empirical constant. The value of this single empirical constant can be obtained experimentally by a pervaporation experiment in which a very low downstream pressure is maintained so that a_3 is essentially zero. The pervaporation transport model involving only one constant is too simplistic and the model involving six parameters is too complicated to be useful as a simple tool.

The applicability of Fick's first law is somewhat limited for multicomponent systems in its original form. When gradients in chemical potential occur for several species, several forces act simultaneously. In these cases, the permeation rate of a given species depends not only on the gradient of its own driving force but also on the gradient or force acting on all other species. This phenomenon is called coupling. For this case, the modified Stefan-Maxwell equation has been proposed to take the above mentioned coupling effect into account by Bitter (1990). These equations have desirable properties but are quite complex in nature. These equations simplify to the Fick's first law form when coupling is not important.

Coupling phenomena are difficult to measure quantitatively, and it is difficult to estimate beforehand their extent in relation to the separation properties. However, it is possible to get indirect information from pervaporation experiments and from experimental determination of the concentration of a liquid mixture inside a polymeric film. Two phenomena have to be considered for the liquid mixtures, namely, kinetic (flow) coupling and thermodynamic coupling.

Huang and Yeom (1991) contend that the change in the permeation activation energy with the feed composition can provide some clues on the coupling behaviors in pervaporation. Activation energy was reported (Huang and Yeom, 1991) to be the function of feed composition. When the activation energy was high, the interaction was also reported to be high. The pre-exponential factor (J_0) versus feed composition curve was explained in terms of the plasticization action of the penetrants on the polymeric membrane.

Mulder and Smolders (1984 and 1986) treated the transport of ethanol and water through cellulose acetate membrane based on the Flory-Huggins thermodynamics for the description of the solution (sorption) part. The interaction parameter involved in Flory-Huggings theory accounts for the excess free energy of mixing of solvent (penetrant) with polymer. Mulder and Smolders (1986) described the kinetic part by using a penetrant concentration dependent diffusion coefficient. A preferential sorption versus preferential permeation approach to pervaporation transport was also proposed. It was reported that for many mixture systems the component preferentially sorbed by the membrane was also the component preferentially permeating through the membrane. Diffusivity was thought to be a contributing factor in determining the magnitude of selectivity. They also calculated concentration profiles of water and ethanol in cellulose acetate membranes using:

- apparent concentration independent diffusion coefficients, and
- diffusion coefficients with exponential concentration dependent and two adjustable parameters. Calculated concentration profiles with concentration dependent diffusion coefficients is shown in figure 2.3.

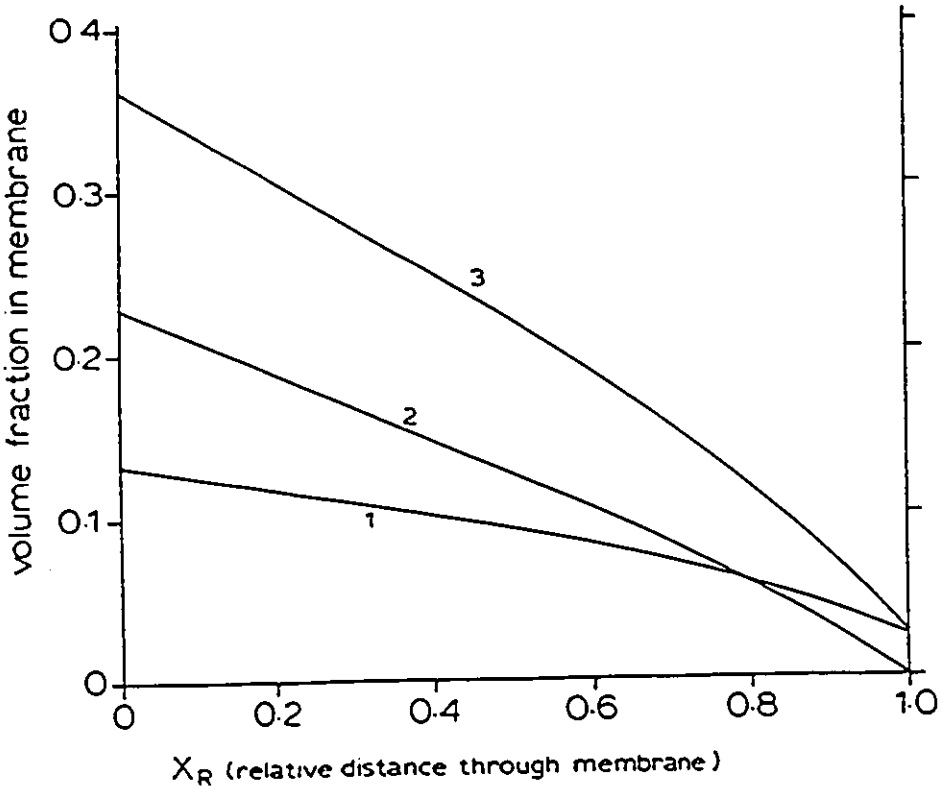

Figure 2.3: Calculated Concentration Profiles with Concentration Dependent Diffusion Coefficients Using Solution-Diffusion Model (Mulder and Smolders, 1984); 1, water; 2, ethanol; and 3, mixture

Generally, sorption to polymeric membrane is related to the interaction between the polymeric membrane and the penetrant (small molecules). Therefore, sorption is strongly dependent on the physicochemical properties of polymer chains. These properties include the structure and segmental motion of polymer chains and the physicochemical properties of small penetrant molecules. These properties of polymers and small molecules are approximately estimated by the interaction parameter, the solubility parameter, and the cohesive energy density. The diffusivity of a penetrant through a polymer is a strong function of the size and shape of the penetrant. The range of diffusivity is intrinsically limited.

While different versions of the solution-diffusion model can correlate pervaporation data well, several empirical parameters must be fitted to pure component and binary mixture data. Because of the large number of empirical parameters, the determination of the significance of a particular parameter or use of these models for predicting separations becomes suspect. Some of this empiricism must be removed if pervaporation models are to be of any use in the development and improvement of membrane or in the design of equipment from minimal amount of data.

2.4.3 Free Volume Model

The free volume approach is based on the theoretical framework proposed by Cohen and Turnbull (1959), who considered molecular transport in a liquid and related the self-diffusion coefficient to the free volume of the system. The basic concept is that a molecule can only diffuse from one place to another place if there is sufficient space or free volume available. Broadly speaking, there are two adaptations of the above mentioned framework, the first one is due to Fujita (1961) and the second one is due to Vrentas and Duda (1979).

A systematic attempt to develop a free volume theory for pervaporation of binary mixtures was made by Huang and coworkers (Fels and Huang, 1970; Fels and Huang, 1971; Rhim and Huang, 1992 and Yeom and Huang, 1992 A). The concentration dependence of the diffusion coefficients of vapors in polymers was chosen as the starting point. In this case, the free volume is a function of the temperature

and the penetrant concentration. They modified the equation of Fujita (1961) to include contributions from both penetrants to the total free volume. They used the simplified Flory-Huggins thermodynamic theory to explain the interaction between penetrant and membrane material but they did not consider the mutual interactions of the individual penetrants in the membrane. Rhim and Huang (1989) modified Fels and Huang's model by introducing the Flory-Huggins interaction parameters, which are functions of the concentration of the individual components in a membrane and feed temperature.

In Fujita's study (Fujita, 1961), the free volume was defined as the volume within the cage of a molecule minus the volume of the molecule itself. Thus the free volume is analogous to the 'hole' which is opened up by thermal fluctuations of the polymer chains. The thermodynamic diffusion coefficient D_T of a pure penetrant is given by the following equation:

$$D_T = RTA_d exp(-B_d/f(v,T)) \tag{2.29}$$

Where A_d and B_d are positive constants and $f(v,T)$ is free volume fraction. According to above relationship the probability of finding a hole whose size exceeds a critical value is proportional to $exp(-B_d/f(v,T))$. The free volume fraction of the system $f(v,T)$ is a function of the temperature and the concentration of the diffusing species and is given by:

$$f(v,T) = f(0,T) + \beta_T v_i \tag{2.30}$$

where $f(0,T)$ is the free volume fraction of the polymer itself and β_T is a proportionality constant and v_i is the volumetric concentration of the diffusing species i. If $f(0,T)$, β_T and the free volume parameters, A_d and B_d, are known, the permeation rate under pervaporation condition can be calculated (Yeom and Huang, 1992 A).

The basic free volume parameters needed were obtained (Fels and Huang, 1971) to test this theory from kinetic sorption and desorption experiments carried out with each penetrant in the polymer. The work was carried out with mixtures of aromatic and aliphatic compounds in poly(ethylene) membranes. In this method diffusion coefficients were determined experimentally by a desorption method.

Huang and coworkers (Huang et al, 1992; Rhim and Huang, 1992 and Huang and Rhim, 1992) further modified Fels and Huang (1970) model to predict the pure component permeabilities for different binary mixtures. The mixtures studied included pentane-methanol and ethanol-water. In studies of Rhim and Huang and Fels and Huang, the free volume parameters and the diffusion coefficients at zero concentration were determined from the unsteady-state desorption experiment which is highly complicated. These experimental results are very sensitive to the accuracy of the measurements and are of limited practical value for application to the steady-state pervaporation process.

Yeom and Huang (1992 A and 1992 B) recently reported a new technique for the determination of the diffusion coefficient and free volume parameter of a penetrant through a membrane from the steady-state pervaporation experiments of single components. Their treatment is based on the extension of Fujita's free volume theory and Flory-Huggins thermodynamics for describing the penetrant interaction with the polymeric membrane. The coupling parameters were also introduced to explain the coupling behavior and plasticization actions of the penetrants. The calculation of permeabilities values requires the availability of the following data:

- Equilibrium sorption data.
- Binary interaction parameters.
- Concentration dependent diffusion coefficient.
- Concentration profile.

The concentration profile of penetrant(s) was not obtained experimentally but was calculated based on the assumption that both components diffuse independently. Experimental sorption data was used to determine the upstream boundary condition only and zero concentration at the downstream side was assumed. The method consists of fitting a numerical solution of the diffusion equation to experimental pervaporation data. The introduction of the plasticization coefficient to the model equation allowed to explain the plasticization action and the coupling fluxes.

2.5 Sorption Measurements for Polymeric Membranes

Sorption experiments give system-specific information on the sorption behavior of a particular penetrant (liquid or vapor phase) in a polymeric material. This information is needed for describing the transport behavior of a penetrant through a membrane. In pervaporation process, the membrane on the feed side is in contact with the liquid phase and the same membrane is in contact with the vapor phase on the downstream side. In order to describe feed side liquid sorption behavior, either liquid phase sorption data or saturated vapor sorption data should be available. Unfortunately, measurements with saturated vapors are very difficult to perform due to condensation problems. The extrapolation from non-saturated to saturated conditions of the vapor may also lead to wrong results. Therefore, sorption data for both liquid phase and vapor phase are necessary for the description of pervaporation transport.

The term sorption is a characteristic of polymer materials. The term is a compound word that includes adsorption and absorption. Polymer materials have both crystalline and amorphous phases, but the sorption to polymeric membranes is mainly sorption to the amorphous phase of polymer materials. Generally, the equilibrium sorption properties of a polymeric material are determined by measuring the equilibrium sorption amount at a constant temperature. Then, the sorbed amount at equilibrium is plotted against the activity of the sorbed species at a constant temperature. The plot is called the sorption isotherm. Various types of sorption isotherms are known, depending on the sorption mechanism, e.g., Henry's law type, Langmuir type, Freundlich type and dual-mode type.

According to Henry's law sorption behavior, the concentration x of sorbed species in the polymer is proportional to the partial pressure:

$$x = k_H.P \tag{2.31}$$

where k_H is the solubility (sorption) coefficient or Henry's law constant. This equation, called Henry's law, is the simplest sorption equation. The linearity of x versus

p (partial pressure) is evident from the equation. Henry's law is applied to sorption of gases into rubbery polymers.

The equation for the Langmuir mode sorption is expressed as follows in terms of sorption and desorption equilibrium:

$$c = \frac{c_s b P}{1 + bP} \tag{2.32}$$

where c_s is saturated concentration of sorbed species in the polymer and b is an affinity constant. The Langmuir mode sorption parameters c_s and b are measures of the number of specific functional sites and the affinity of the penetrant for the polymeric material, respectively.

The dual-mode sorption is a combination of Henry's law mode and Langmuir mode sorptions. This sorption model has been applied for glassy polymers. In this model, Henry's law and Langmuir mode sorptions are assumed to operate in the polymer matrix phase and in microvoids of glassy polymers, respectively.

Brunauer, Emmett and Teller (1938) have proposed a theoretical equation based on a multilayer sorption. The BET (Brunauer, Emmett and Teller) equation is based on the view of a localized multilayer sorption. The BET sorption equation, expands the Langmuir sorption equation to a multimolecular-layer sorption, assuming the same heat of sorption for more than the second-layer sorption, which is equal to the heat of liquefaction. The equation is:

$$c = \frac{c_m \frac{P}{P_s}}{(\frac{1}{C_k} + \frac{C_k - 1}{C_k}\frac{P}{P_s})(1 - \frac{P}{P_s})} \tag{2.33}$$

where C_k is a constant and c_m is the concentration corresponding to monolayer coverage.

The sorption behavior of various penetrants has been studied by various authors. Measurements of vapor sorption in cellulose acetate and poly(hexamethylene adipamide) polymeric membranes were performed with a quartz crystal microbalance by Laatikainen and Lindstrom (1986). A computer-aided experimental setup for studying sorption kinetics was used by Harrison and Asfour (1992). The sorption of water vapor by an amorphous polyamide polymer was examined by Hernandez et al. (1992).

Sorption of water vapor into thin polymeric film was measured by means of a quartz crystal microbalance apparatus by Best and Moylan (1992). Sorption behavior of water vapor into a polyelectrolyte complex (polyacrylic acid and poly4-vinylpyridine) was evaluated by Hirai and Nakajima (1989) on the basis of three theories, i.e., BET equation, Flory- Huggins interaction parameter theory (χ), and cluster function theory.

The preferential sorption characteristics for isopropyl alcohol-water-cellulose acetate system from both liquid and vapor phases have been studied by Deng et al. (1990). Liquid and gas chromatographic methods were used for the study. It was found that isopropyl alcohol was preferentially adsorbed from the liquid phase while water was preferentially adsorbed from the vapor phase.

The kinetics (diffusion) and equilibrium sorption can be strongly affected by the presence of the first penetrant in the polymeric matrices. Sequential sorption of the second vapor was studied by Bontoux and Soane (1989) in the presence of first vapor while maintaining the partial vapor pressure of the first vapor to ensure that diffusion into the preswollen polymer approximated transport in a pseudobinary system. Both the rate of diffusion and equilibrium sorption of the second vapor were reported to depend on the prevailing composition of the preswollen polymer for all penetrant pairs studied. This study provides a brief glimpse of the complexity of the behavior of polymers in contact with multiple penetrants.

2.6 Penetrant Concentration Profile Inside the Membrane

A review of the available literature on the penetrant concentration profile inside the membrane shows that most of the penetrant concentration profile studies have been performed for the pure penetrant in the membrane. A summary of techniques used is presented in this section.

A micro-radiographic technique was used for the determination of the concentration gradient of vapors in polymers (Richman and Long, 1960). For the method to

be applicable for the diffusion in polymers, it is necessary to have a penetrant whose X-ray mass absorption coefficient is markedly different from that of the polymer. In this technique, the polymer film is exposed to the vapor for the desired time, removed and microtomed to provide a thin cross-sectional slice of the original film. The film is mounted on a fine grained photographic plate and exposed to a monochromatic X-ray beam. The exposed photographic plate is developed under standard conditions and then scanned with a microdensitometer. With suitable calibration, the light transmission of the plate gives a measure of the concentration of penetrant vapor.

Long (1965) calculated the concentration profile for n-heptane through poly(propylene) film by using the exponential concentration dependence of diffusion coefficient. The concentration decreased slowly with distance through the film to 90 % of its upstream value at a distance 75 % of the way through the film. From there on to the downstream side of the film, the concentration dropped rapidly to a value depending on the downstream pressure. At higher temperatures the concentration profiles were similar but dropped a little faster with distance through the film. It was concluded that all the resistance to permeation occurred near the downstream side of the film and the concentration profile resembled the two-zone process model proposed by Binning et al. (1961).

Actual concentration profiles of pure penetrants in the membrane during steady state pervaporation were reported for different polymeric films (Kim and Kammermeyer, 1970). A stacked film technique was developed which permitted peeling off films and measuring the concentration of penetrant in the membrane in different sections. The membrane-penetrant systems studied were: nylon 6-water, nylon 6-dioxane, cellulose acetate-water, poly(ethylene)-dioxane, poly(ethylene)-n-hexane and poly(ethylene)-benzene. A difference between equilibrium sorption values and penetrant concentrations just inside the membrane was also reported in some cases. Aptel et al. (1974 B) have also determined the penetrant concentration profile inside the membrane for pure penetrant using a similar technique. Concentration profiles were also reported by Paul and Ebra-Lima (1971) for pure cyclohexane inside the polymeric membrane.

Experimental concentration profiles for ethanol-water binary mixture in cellulose

acetate membranes were reported under steady-state pervaporation conditions by Mulder et al. (1985). Experimental value for the equilibrium sorption value and the penetrant concentration just inside the membrane for water-cellulose acetate system were quite close. The difference between the equilibrium sorption value and the concentration just inside the membrane at the liquid/polymer interface was considerable for the ethanol-cellulose acetate system.

A new method was proposed by Iwatsubo et al. (1988). The method can generate concentration profiles of single penetrant in the membrane under pervaporation conditions. In this method, two individual experimental data are required. The first one is the relationship between the downstream pressure and the steady-state permeation rate, and the other is the adsorption isotherm of the penetrant with the polymeric membrane. The following assumptions were made:

- Equilibrium condition is satisfied at the interfaces.
- The steady-state permeation rate is inversely proportional to the membrane thickness.

The procedure is as follows. At first, for a membrane having thickness l, the relationship between the steady-state permeation rate J and the downstream pressure ($J \quad f(P_3)$) can be measured by controlling the downstream pressure. Then, the relationship between the steady-state permeation rate J' and the downstream pressure P_3 for a membrane having a thickness of l' can be calculated from experimental data as follows:

$$J' = f(P_3)/(l'/l) \tag{2.34}$$

The steady-state permeation rate corresponding to the downstream pressure of P_3 and thickness l is denoted by J_1. Using the relationship of J' obtained for a thickness l', the downstream pressure P_3' which yields the same value as J_1 should be obtained. This pressure can be considered to be the vapor pressure of penetrant at point l' in the membrane having thickness l (l' is lower than l). Similarly, the vapor pressure can be obtained at different positions inside the membrane. Thus, pressure profiles can be constructed this way. The concentration profile can be obtained by using the sorption data of the penetrant for the polymeric membrane concerned.

An alternative technique was used on a small scale by Neel et al. (1987). This micro-device utilizes a razor-blade. A narrow sliver (approximately $300\mu m$ wide) was cut out of the membrane and inserted between two glass microscopic slides, which were subsequently sealed with a suitable plastic cement. One of the two flat compartments (say C1) was connected to a vacuum-pump by a flexible tubing. The end of tubing was tightly encased in the sealing cement which closes the fourth side of compartment (C1). This system was designed to evacuate, by pumping, the little half-cell C1, held between the two glass slides. The opposite compartment (C2) was closed on three sides only. This micro-device was placed under a microscope, the magnification of which was chosen to permit the observation of a 1 mm long segment of the sliver in the field of the apparatus. Using this device an experimental profile for pure water was generated.

The water concentration profile through a perfluorinated ionomer (NAFION^R) membrane was examined for different upstream conditions by Thomas et al. (1989). Small-angle neutron scattering technique was used to obtain the penetrant profile inside the membrane during steady-state conditions. Scattering curves corresponding to different water concentrations in the membrane were used as reference curves. The basic concept used in that study was that large changes in the small-angle neutron scattering curves occur when water concentration in the membrane changes. In these membranes, the scattering curve showed a peak, "the ionomer peak," whose position and intensity depended on the water content inside the membrane. The penetrant profiles inside the membrane were obtained in-situ.

2.7 State of Permeant (Penetrant) Studies Using Calorimetry

A typical calorimetric analysis involves monitoring the heating and cooling curves of a given sample under controlled thermal conditions. The resulting thermogram typically can be used to identify the melting and/or freezing points for the given sample. This technique can be used for state of permeant (penetrant) studies in membrane

transport studies. The 'state of permeant' refers to the bulk-like or bound-state of the penetrant molecules in the polymer. Generally, a melting/freezing diagram of a penetrant contained in a polymeric membrane is monitored in a differential scanning calorimeter (DSC) for performing the state of permeant studies. These studies are important to achieve a better understanding of the transport mechanism involved. These studies also give an indication of the degree of polymer-penetrant interaction.

A systematic investigation was carried out by Yoshikawa et al. (1990) involving a poly(dimethylsiloxane) or PDMS membrane and various penetrants. An anomalous behavior of ethanol penetrant in PDMS membrane was observed. The state of water was also studied but anomalous behavior was not observed for this penetrant-polymer system. It should be recalled that PDMS membranes are alcohol selective membranes.

2.8 Microscopic and Spectroscopic Studies for Polymer Films

2.8.1 Microscopic Studies

The scanning electron microscope, SEM, is the most useful instrument for performing morphological studies on polymer films. One of the attractive features of the SEM is the ease of sample preparation. The SEM system consists of a cathode in an evacuated tube that produces the electrons that are accelerated through the anode. A series of electromagnetic lenses produce a spot, a reduced image of the cathode, on the specimen. This spot is scanned over the specimen in a rectangular pattern while the signals are continually observed at each point and electronically processed to create an image on a cathode ray screen. A choice of sources of signal may be used to form the image. The most relevant ones to polymer studies are low-energy secondary electrons emitted from the top few nanometers of the specimen, or high energy backscattered electrons. The sample need to be bonded to a small aluminum or brass stub, and if they are of a conductivity that permits the passage of secondary electrons they may need no further treatment.

2.8.2 Spectroscopic Studies

Many polymeric materials such as rubbers, fibers, films often fail to yield useful transmission spectra. However, these materials (particularly polymeric films) can be investigated by the FTIR-ATR (Fourier Transform Infra Red-Attenuated Total Reflection) technique. The spectra obtained by this technique gives useful information on the polymer-penetrant interaction (chemical or physical in nature). This technique was used in the present work to examine the nature and extent of the interaction of the penetrants with the polymeric material.

The principles of the FTIR-ATR method are based on the phenomenon of total internal reflection. In a typical experiment, the sample (refractive index n_2) is brought into direct contact with the reflecting surface of a prism of high refractive index n_1 ($n_1 > n_2$). When the angle of incidence of the light beam at the prism sample interface exceeds the critical angle ϕ_c, total internal reflection takes place. At the critical angle of total internal reflection the following relation should hold (Siesler and Holland-Moritz, 1980):

$$\sin \phi_c = \frac{n_2}{n_1} = n_{21} \tag{2.35}$$

By the superposition of the incident and reflected light beam, a standing wave perpendicular to the totally reflecting interface is established.

The penetration depth d_p for which the electric field component has decreased to 1/e of its value in the interface, is related to other parameters by the following relationship (Siesler and Holland-Moritz, 1980):

$$d_p = \frac{\lambda_1}{2.\pi(sin^2\phi - (n_2/n_1)^2)^{1/2}} \tag{2.36}$$

Here ϕ is the angle of incidence, λ_1 wavelength of radiation in the optical denser medium, and n_1 and n_2 are the refractive indices.

The penetration depth of the radiation into the optical rarer medium (sample) is usually of the order of a few micrometers, which is sufficient to constitute a short absorbing path. Therefore, total internal reflection will be attenuated in the wavelength regions of sample absorption. The spectrum recorded is, thus, similar to the

transmission spectrum of the sample surface with the only difference being the higher intensities of absorption bands at longer wavelengths.

An investigation on chlorine interaction with polyamide reverse osmosis (Du Pont B-9 membrane) was undertaken by Glater and Zachariah (1984). These polyamide membranes are chlorine sensitive.

2.9 Process Parameters Affecting Pervaporation

For a given film, attainment of optimum rate and selectivity is generally dependent on the following process variables:

1. Feed temperature
2. Feed composition
3. Charge pressure: upstream pressure and downstream pressure

2.9.1 Effect of Feed Temperature

When the temperature of tne feed increases, the permeation rate also increases. The relationship generally follows an Arrhenius-type law (Huang and Lin, 1968; Cabasso et al., 1974 A; and Choo, 1962):

$$J = J_0 exp(-\frac{E_p}{RT}) \tag{2.37}$$

where E_p is the overall activation energy for permeation and J_0 is the pre-exponential factor. The activation energy is equal to the combined apparent activation energy for diffusion and heat of sorption. The value of E_p of permeation varies usually in the range 4-15 kcal/mole. The selectivity is also dependent on the temperature. In most cases a small decrease of selectivity is observed with increasing temperature. This decrease in selectivity might be because of an increase in the thermal motion of polymer chains with the increase in temperature, which results in larger diffusional holes (if the separation is supposed to take place by solution-diffusion mechanism).

2.9.2 Effect of Feed Composition

The concentration of feed stream has an effect on permeation rate and selectivity. A marked effect of feed composition on permeation rate and selectivity was demonstrated by Featherstone and Cox (1971). The hydrophobic poly(propylene) was reported to be selective towards acetone in acetone-water system at lower than 75 mole % acetone in the charge, whereas at higher than 80 mole% acetone these membranes were water selective.

2.9.3 Effect of Charge Pressure

The effect of upstream pressure and downstream pressure has been studied by Greenlaw et al. (1977 A), Duggal and Thompson (1986) and Ghosh and Rawat (1966). The permeation rates for hexane through poly(ethylene) film were measured over the range of pressures 1 to 20 atmospheres on the upstream side of the membrane and 133 Pa to 40020 Pa on the downstream side. It was found that the rates varied linearly with upstream pressure when liquid was in contact with the downstream face, but were independent of upstream pressure when vapor was in contact with the downstream face. Some unexpected and intriguing data on the effect of upstream pressure were reported by Aptel et al. (1974 A). The pervaporation of water and N-dimethylformamide mixture was performed using the PTFE-P4VP grafted membrane. The permeation rate decreased with an increase in the upstream pressure. This decrease in permeation rate was attributed to the compaction effect in the membrane.

Kataoka et al. (1991) discussed the effect of the upstream pressure on pervaporation permeation rate and selectivity using a mathematical formulation. The following two cases were studied:

1. Case 1: The pressure inside the membrane is constant and equal to the upstream pressure. In this case the upstream pressure has no effect on the pervaporation rate as the upstream pressure approaches infinity.

2. Case 2: The pressure changes across the membrane from the upstream pressure

to the downstream pressure linearly. In this case the pervaporation permeation rate increases and approaches infinity as the upstream pressure increases towards infinity.

Although their assumptions of the constant total penetrant concentration and the constant diffusion coefficient across the membrane seem unrealistic, their conclusions look quite reasonable.

Chapter 3

Theoretical Development

In the last chapter some of the drawbacks of available transport models were discussed. Solution-diffusion does not consider phase change inside the membrane, while the pore-flow does take account of this phenomenon. Another drawback of solution-diffusion is related to the pressure and penetrant concentration profile. The solution-diffusion model considers the pressure inside the membrane as a constant value and equal to the upstream pressure value. The free volume model developed by Huang and coworkers utilizes the penetrant concentration profile obtained from mathematical formulations and does not utilize an experimental penetrant profile. An insight into the penetrant concentration profile must be sought. In addition, the transport model should be able to generate profiles obtained experimentally and should be able to explain the phenomenon observed. In the present thesis an attempt has been made to develop a new transport model to describe steady-state pervaporation. The features of newly developed transport model are:

- Model considers chemical potential gradient as the driving force for the flow of penetrants.
- Model considers the phase change of penetrant inside the membrane.
- Model considers the pressure profile inside the membrane.

- Model assumes the presence of an imaginary phase (liquid or vapor) in equilibrium with the membrane phase.
- Model utilizes experimental sorption data from liquid and vapor phases.
- Model assumes isothermal condition across the membrane.
- Model considers coupling in the liquid-filled region of the membrane but does not consider coupling in the vapor-filled region of the membrane.

The chemical potential gradient is the driving force for the flow of the penetrant. A membrane is split along the penetrant flow direction into small segments and the presence of an imaginary liquid (or vapor) phase which is in thermodynamic equilibrium with each membrane segment is assumed. A schematic diagram is shown in figure 3.1. The potential gradient established in the imaginary liquid (or vapor) phase is then considered to be the driving force for the penetrant flow.

The derivation of the mathematical equations for pure component permeation is shown in first section of this chapter. The second section of present chapter contains discussions on binary component permeation. The last section of the chapter describes the strategy for calculating the theoretical penetrant concentration profile inside the membrane.

3.1 Single Component System

In the generalized treatments of transport phenomena, it is recognized that the driving force for the movement of one molecular species relative to another is the gradient in chemical potential for that species. As a general expression the penetrant permeation rate at isothermal condition is given by (Katchalsky and Curran, 1965):

$$J = -\frac{c}{f}\frac{d\mu}{dl} \tag{3.1}$$

where c is the concentration of the penetrant in the membrane (mol/m^3), f is a constant (J-sec/m^2), $d\mu$ is the difference in chemical potential on both sides of the

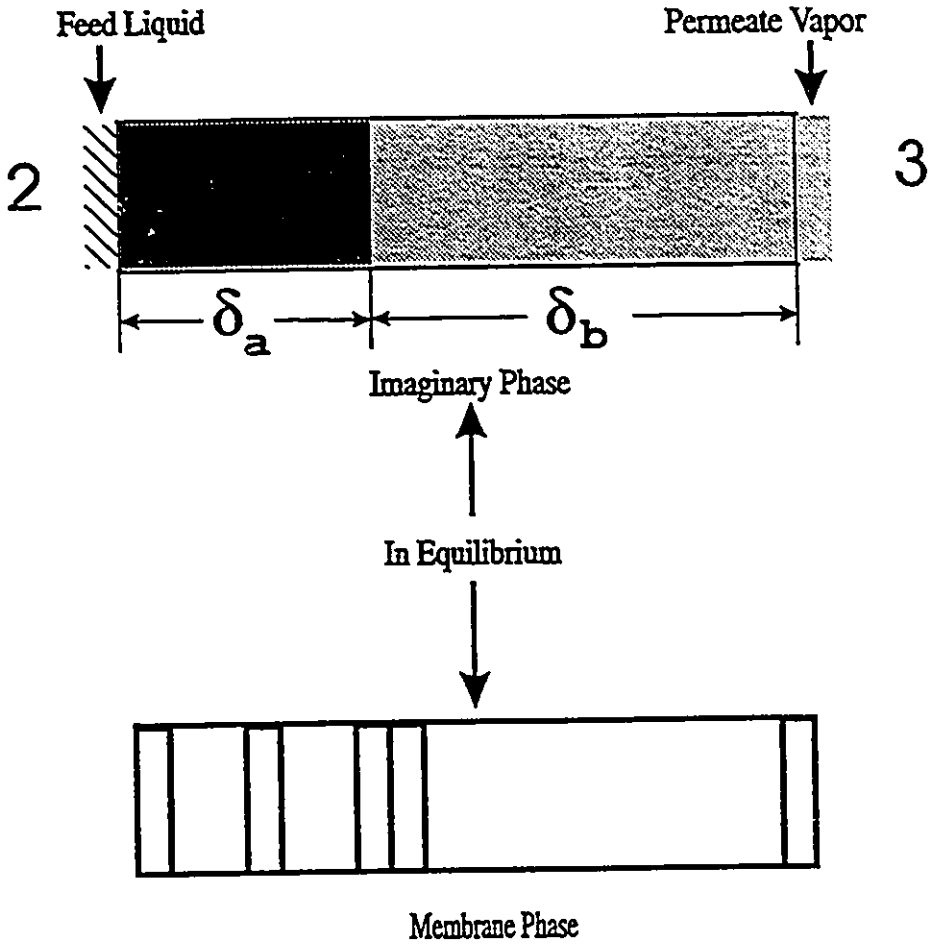

Figure 3.1: A Conceptual Diagram of the Model

membrane segment whose thickness is dl. It should be noted that the chemical potential is that of the imaginary liquid (or vapor) phase that is in equilibrium with the segment of the membrane phase.

In the absence of electric fields and other similar potentials, it is known from equilibrium thermodynamics that the chemical potential of penetrant is a function only of the concentration and the pressure (or state of stress) at constant temperature (isothermal condition). Therefore, inside a membrane, the gradient of chemical potential of the species in a transport situation manifests itself in terms of gradients of concentration and pressure.

Many small segments in the membrane cross-section are assumed. The first membrane segment is in sorption equilibrium with the feed liquid. Similarly, one can assume the presence of an imaginary phase that is in sorption equilibrium with the penetrant in each segment. Obviously, such an imaginary phase should be liquid when the segment number is small. As we move in the direction of penetrant flow, the pressure and the composition of the imaginary liquid phase should change gradually. At a point, where vapor pressure of the imaginary phase is no longer greater than the vapor pressure of the penetrant, the imaginary phase would be the vapor phase. Adsorption equilibrium is established between the imaginary vapor phase and the penetrant in the membrane. As far as the imaginary phase is concerned, therefore, there exists a clear boundary between liquid and vapor phase.

Since the membrane phase is in equilibrium with the imaginary phase:
μ_i(imaginary phase) = μ_i(membrane phase)
and:
a_i(imaginary phase) = a_i(membrane phase)
Thus μ_i (chemical potential of component i) and activity a_i are both standardized on the same basis for both liquid and vapor phases of the system, i.e. $a_i = 1$ for pure liquid penetrant at the temperature and pressure of the system. We are able to write the same mathematical equations as those derived by the pore model. The possible presence of concentration polarization will also be shown for the binary mixture permeation case.

It would be possible to assume the presence of an imaginary liquid phase which

is in equilibrium with the penetrant in the membrane segment when the distance l is not large. At a distance l from the upstream interface, a membrane segment whose thickness is dl is considered. The chemical potential will be calculated in the above mentioned imaginary liquid phase.

The chemical potential can be related to the activity and the pressure gradient by the following equation:

$$d\mu = RTlna + VdP \tag{3.2}$$

The activity of pure liquid is unity. Therefore, in case of the pure liquid transport it is evident from equation 3.2 that the chemical potential change will be caused only by the pressure change. The pressure of the liquid phase changes from P to $P + dP$ as the distance increases from l to $l + dl$. In this case dP should have a negative sign. Since the molar volume of the penetrant is constant, the change in the chemical potential of the penetrant from distance l to $l + dl$ should be:

$$d\mu = VdP \tag{3.3}$$

where V is the molar volume of liquid. Although the above equation was written for the imaginary liquid phase, it should also be applicable to the membrane phase. Combining equations 3.1 and 3.3 yields:

$$J = -\frac{1}{f}cV\frac{dP}{dl} \tag{3.4}$$

When the pressure of the imaginary phase is between the upstream pressure P_2 and the saturation vapor pressure P_s the phase is liquid and both c and V can be regarded as constant. Then, integrating equation 3.4 from $l = 0$ to $l = \delta_a$ and $P = P_2$ to $P = P_s$ we obtain:

$$J = \frac{1}{f}cV\frac{P_2 - P_s}{\delta_a} \tag{3.5}$$

where δ_a is the thickness of the imaginary liquid phase. Simplifying equation 3.5:

$$J = \frac{A}{\delta_a}(P_2 - P_s) \tag{3.6}$$

where

$$A = \frac{c.V}{f} \tag{3.7}$$

When the pressure of the imaginary phase is below saturation vapor pressure ($P_\bullet$), the phase is vapor and both c and $d\mu$ are function of pressure p. The chemical potential gradient can be expressed by the following equation for the imaginary vapor phase:

$$d\mu = RT\frac{dP}{P} \tag{3.8}$$

The most widely used theory of physical adsorption is the multilayer theory of Brunauer, Emmett and Teller (1938) or BET theory. The BET theory extends the earlier monolayer theory of Langmuir adsorption isotherm to account for the adsorption of additional layers on the first adsorbed layer. Type II isotherm is very common in the case of physical adsorption and undoubtedly corresponding to multilayer formation. When BET adsorption isotherm is applied for the penetrant adsorption into the polymer matrix case (Gregg and Sing, 1967), the equation can be written as following:

$$c = \frac{c_m \frac{P}{P_\bullet}}{(\frac{1}{C_k} + \frac{C_k - 1}{C_k}\frac{P}{P_\bullet})(1 - \frac{P}{P_\bullet})} \tag{3.9}$$

where C_k is a constant and c_m is the concentration corresponding to monolayer coverage. BET equation is not valid in the whole range of the partial pressure. The BET equation was modified in the range $\frac{P}{P_\bullet} \geq 0.7$ as indicated in the Appendix C. Suppose the modified functional form is written as:

$$c = F_1(\frac{P}{P_\bullet}) \tag{3.10}$$

Substituting c and $d\mu$ in equation 3.1 from equation 3.10 and equation 3.8 we obtain:

$$J = \frac{RT}{f}F_1(\frac{P}{P_\bullet})\frac{d(\frac{P}{P_\bullet})}{(\frac{P}{P_\bullet})dl} \tag{3.11}$$

Integrating equation 3.11 from $l = \delta_a$ to $l = \delta_a + \delta_b$ and $P/P_\bullet = 1.00$ to $P/P_\bullet = P_3/P_\bullet$:

$$J.\int_{\delta_a}^{\delta_a+\delta_b} dl = \frac{RT}{f}\int_{1.00}^{\frac{P_3}{P_\bullet}} F_1(\frac{P}{P_\bullet})\frac{d(\frac{P}{P_\bullet})}{(\frac{P}{P_\bullet})} \tag{3.12}$$

The shape of J versus $\frac{P_3}{P_\bullet}$ curve is very similar to that of $1 - (P_3/P_\bullet)^2$ as shown in Appendix C. Therefore, J can be approximated by:

$$J = \frac{B}{\delta_b}(P_\bullet^2 - P_3^2) \tag{3.13}$$

where B is a constant involving several physical quantities.
As total thickness of the membrane is δ, therefore,

$$\delta = \delta_a + \delta_b \tag{3.14}$$

where δ_a and δ_b are the thickness of liquid and vapor regions, respectively. Combining equations 3.6, 3.13 and 3.14, we obtain:

$$J = \frac{A}{\delta}(P_2 - P_*) + \frac{B}{\delta}(P_*^2 - P_3^2) \tag{3.15}$$

This equation is applicable when $P_3 < P_*$. The above equation is the same as the permeation rate of pure liquid derived on the basis of the pore flow model (equation 2.10).

When $P_3 \geq P_*$, the above equation simplifies to the following form:

$$J = \frac{A}{\delta}(P_2 - P_3) \tag{3.16}$$

At this point the difference between the approach taken to develop the present model and the approach taken by Greenlaw et al. (1977 A) should be pointed out. The basic underlying difference is the founding equation on which the models are based upon. Greenlaw et al. (1977 A) derived their equations starting from Fick's first law. On the other hand, in the present case the founding equation is the basic chemical potential equation (equation 3.1). In the case of Fick's first law equation the concentration of the penetrant is the driving force for the flow. In an ideal case and after making some assumptions the Fick's first law equation can be derived from the basic chemical potential equation for the transport. The detailed derivation of this equation is shown in the appendix, section F.

3.2 Binary Component System

For the analysis of binary mixtures the following assumptions are made:

- the two flows are coupled in the liquid part of the membrane.
- the two flows are uncouples in the vapor part of the membrane.

- isothermal condition.

The value of $d\mu$ can be substituted from equation 3.2 into equation 3.1, we obtain:

$$J = -\frac{c_i^l}{f_i^l} RT \frac{lna_i}{dl} - \frac{c_i^l}{f_i^l} V_i^l \frac{dP}{dl} \tag{3.17}$$

for the liquid transport of ith component, when the transport of ith and jth components is totally uncoupled. Superscript l refers to the liquid phase. It should be noted that the second term (pressure term) of equation 3.17 is practically negligible compared to the first term (activity term) since the molar volume, V, of liquid is very small. However, it is known that the pressure effect on the transport is far greater in reality than the theoretical prediction probably due to the presence of convective flow (Adam et al., 1983). Then, the transport of both ith and jth species should be strongly coupled, resulting in a low membrane selectivity. Equation 3.17 is no longer applicable. Instead, the second term of equation 3.17 should be replaced by a term corresponding to convective flow, which yields:

$$J_i = -\frac{c_i^l}{f_i^l} RT \frac{dlna_i}{dl} + X_i c^l v^l \tag{3.18}$$

where X_i is the mole fraction of ith component in the feed mixture, c^l is the total molar concentration of the liquid mixture (mol/m^3) and v^l is the velocity of the feed mixture (m/s) by convective flow.

For the vapor phase an assumption of uncoupled flow can be made, which yields:

$$J_i = -\frac{c_i^v}{f_i^v} RT \frac{dP_i}{P_i} \tag{3.19}$$

where superscript v refers to the vapor phase. Equations similar to equations 3.18 and 3.19 can be written for the jth component:

$$J_j = -\frac{c_j^l}{f_j^l} RT \frac{dlna_j}{dl} + X_j c^l v^l \tag{3.20}$$

$$J_j = -\frac{c_j^v}{f_j^v} RT \frac{dP_j}{P_j} \tag{3.21}$$

If the membrane selectivity is assumed to be caused primarily by the vapor phase transport, which is given by equations 3.19 and 3.21, and also if an assumption is made that a given membrane is preferentially permeable to the jth component:

$$\frac{Y_i}{Y_j} = \frac{J_i}{J_j} < \frac{X_i}{X_j} \tag{3.22}$$

where X and Y represent the mole fraction in the upstream side (liquid) and downstream side (vapor) of the membrane, respectively. The latter assumption can only be satisfied when $\frac{d\ln a_i}{dl} > 0$ and $\frac{d\ln a_j}{dl} < 0$ in equations 3.18 and 3.20. Implications of the above equations are as follows:

- Starting from the side of the membrane that is facing the feed liquid, the activity (or the concentration) of the slower component (ith component in this case) should increase in the direction of the penetrant flow in the liquid that is in equilibrium with the membrane phase. Furthermore, the latter concentration reaches a maximum at the liquid/vapor phase boundary. Then, the concentration of the ith component starts to decrease in the vapor phase. At the other end of the membrane that is facing the vacuum, the concentration of ith component becomes the lowest and it is even lower than that in the feed. The jth component is enriched in the downstream.

- Similarly, the concentration of the ith component in the penetrant mixture that is present in the membrane phase should also show a maximum at the liquid/vapor phase boundary. Thus, the theory predicts the possibility of the presence of concentration polarization inside the membrane.

Generally, in membrane separation processes one component (say component j) of the mixture permeates through the membrane preferentially. The other (component i) component, on the other hand, is left behind on the feed side of the membrane. Component i should diffuse back to the bulk feed solution quickly enough to prevent the build-up of component i near the membrane-feed solution interface. As the flow is generally laminar in the immediate vicinity of the membrane, the back-transfer can only be of a diffusive nature. An increase in concentration of non-preferentially component at the membrane interface is called concentration polarization.

The concept of concentration polarization can easily be understood by assuming two barrier membrane layers connected in series, one that is facing the feed, being swollen with liquid and nonselective, and the other that is facing the downstream vapor, being dry and selective. When a nonselective membrane layer is followed by a selective one in series, concentration polarization occurs inevitably, as many theories on the concentration polarization predict. The phenomena of concentration polarization occurring on the membrane surface (not inside the membrane) is well documented in literature (Rautenbach and Albrecht, 1989) for membrane processes. The most common approach to describe the phenomena of concentration polarization is based on the boundary film theory, in which the presence of a boundary layer is assumed. Generally, concentration polarization leads to:

- decreased flux,
- and decreased selectivity.

The problem of concentration polarization occurring at the membrane surface does not play an important role in majority of pervaporation processes since the permeabilities of membranes are low. A brief introduction to the phenomena of concentration polarization is given in appendix D

3.3 Strategy for Plotting Theoretical Concentration Profiles Inside the Membrane for Binary Mixture Systems

Using the above model the theoretical concentration profile of the slower component (acetic acid in this case) can be plotted by following the method mentioned in this section.

3.3.1 Calculation of Phase Boundary in the Imaginary Phase at 25°C

The vapor permeation rate equations for component i and j can be written as follows:

$$J_i = \frac{B_i}{\delta_b}(P^2_{i,*} - P^2_{i,3}) \tag{3.23}$$

$$J_j = \frac{B_j}{\delta_b}(P^2_{j,*} - P^2_{j,3}) \tag{3.24}$$

The variables used in the above equations are defined in the nomenclature. Subscripts $*$ and 3 refer to the phase boundary and the downstream side, respectively.

Rearranging equations 3.23 and 3.24 yields:

$$J_i = \frac{B_i}{(\delta)(\frac{\delta_b}{\delta})}(P^2_{i,*} - P^2_{i,3}) \tag{3.25}$$

$$J_j = \frac{B_j}{(\delta)(\frac{\delta_b}{\delta})}(P^2_{j,*} - P^2_{j,3}) \tag{3.26}$$

Furthermore, the following equation is valid:

$$\frac{\delta_a}{\delta} + \frac{\delta_b}{\delta} = 1.00 \tag{3.27}$$

Among the variables involved in the above equations, the known variables are:

- $\frac{B_i}{\delta}$ and $\frac{B_j}{\delta}$ at 25°C obtained from the permeation data of pure component for ith and jth component, respectively.
- Quantities J_i, J_j, $P_{i,3}$ and $P_{j,3}$ are available from the pervaporation experiments of binary mixture.

Equations 3.25 to 3.27 are solved by using the vapor-liquid equilibrium data and following the iteration method to calculate the position of the phase boundary ($\frac{\delta_a}{\delta}$ and $\frac{\delta_b}{\delta}$). Iterations are performed by using the values of $P_{i,*}$ and $P_{j,*}$ from vapor-liquid equilibrium data. Here $P_{i,*}$ and $P_{j,*}$ indicate the partial vapor pressures of component i and j, respectively (refer appendix D). Therefore, the values of $\frac{\delta_a}{\delta}$ and $\frac{\delta_b}{\delta}$ and the best fit values of $P_{i,*}$ and $P_{j,*}$ can be obtained using equations 3.25 to 3.27 by iteration

method and using the vapor-liquid equilibrium data. Initial (guess) values of $P_{i,\bullet}$ and $P_{j,\bullet}$ are to be taken from vapor-liquid equilibrium data. Vapor-liquid equilibrium data for acetic acid-water system at different temperatures was taken from the literature. Refer to table E.1, table E.2 and table E.3 in the appendix for the data.

From vapor-liquid equilibrium data of components i and j the following relationships can be written:

$$P_{i,\bullet} + P_{j,\bullet} = P_{\bullet} \tag{3.28}$$

where $P_{\bullet}$ is total vapor pressure.

$$Y_{i,\bullet} = \frac{P_{i,\bullet}}{P_{\bullet}} \tag{3.29}$$

$$Y_{i,\bullet} = f(X_{i,\bullet}) \tag{3.30}$$

where $Y_{i,\bullet}$ and $X_{i,\bullet}$ are the mole fractions of component i at phase boundary in the vapor phase and liquid phase, respectively. Using equations 3.28 to 3.30 the values of $Y_{i,\bullet}$ and $X_{i,\bullet}$ corresponding to the best fit values of $P_{i,\bullet}$ and $P_{j,\bullet}$ can be obtained. These values will be used in the next section to calculate the mass transfer coefficient.

3.3.2 Calculation of Mass Transfer Coefficient

The equation for concentration polarization based on the boundary film theory approach can be written as follows:

$$\frac{X_{i,\bullet} - Y_{i,3}}{X_{i,2} - Y_{i,3}} = exp(v/k) \tag{3.31}$$

where $X_{i,2}$, $X_{i,\bullet}$ and $Y_{i,3}$ are the mole fractions of component i in the liquid feed mixture, at phase boundary and in the downstream, respectively. In equation 3.31 v and k refer to penetrant velocity (m/s) and mass transfer coefficient (m/s), respectively. For the derivation of equation 3.31, refer to appendix D. It is assumed that component i (acetic acid) permeates through the membrane slower than the component j and the position of the highest concentration of the slower component (component i) coincides with the liquid-vapor phase boundary.

Furthermore, the following relationship is valid:

$$v = \frac{J_i.M_i}{\rho_i} + \frac{J_j.M_j}{\rho_j} \tag{3.32}$$

where M_i and M_j are the molecular weights of components i and j, respectively. It is assumed that densities of ith and jth components (ρ_i and ρ_j, respectively) in the mixture are the same as their pure component densities. Quantities J_i and J_j are known from pervaporation data. Therefore, the value of v can be calculated from equation 3.32 by substituting the values of known parameters on the right side.

In equation 3.31 the following quantities are known:

- $X_{i,*}$ value obtained from the calculations performed in section 3.3.1
- Quantities $Y_{i,3}$ and $X_{i,2}$ from pervaporation data.

The value of mass transfer coefficient k can be calculated from equation 3.31 by substituting above known quantities and the value of v obtained from equations 3.32.

3.3.3 Calculation of Phase Boundary and Mass Transfer Coefficient at Different Temperatures

For performing the calculations in section 3.3.1 the values of parameters $\frac{B_i}{\delta}$ and $\frac{B_j}{\delta}$ at 25°C were used. These values were obtained from pure component permeation data at 25°C. In the permeation data of the pure component (water and acetic acid) the permeation rate for each component was recorded against the downstream pressure. Equations 3.15 and 3.16 can be used to calculate these parameters. It should be noted that these parameters will change with temperature. Pure component permeation data is available only at 25°C. These parameters at 35°C and 40°C were obtained in the following manner.

An assumption was made that these parameters change in proportion to concerned penetrant permeation rate for each component. From equation 3.23 the permeation rate equations for component i at 25°C and 35°C can be written as:

$$J_{i,25} = \frac{B_{i,25}}{\delta_{b,25}}(P^2_{i,*,25} - P^2_{i,3,25}) \tag{3.33}$$

and

$$J_{i,35} = \frac{B_{i,35}}{\delta_{b,35}}(P^2_{i,*,35} - P^2_{i,3,35}) \tag{3.34}$$

The first subscript in the sequence of subscripts, i.e. i or j refers to the component i or j. The second subscript $*$ or 3 refers to vapor-liquid equilibrium boundary or to the downstream, respectively. The third subscript 25 or 35 refers to the temperature of the feed mixture in °C. Therefore, in this case $P_{i,*,25}$ indicates the saturation vapor pressure of component i at 25°C and $B_{i,25}$ refers to the parameter B for component i at 25°C. By rearranging equations 3.33 and 3.34, the following equation can be obtained:

$$\frac{B_{i,35}}{\delta_{b,35}} = \frac{B_{i,25}}{\delta_{b,25}} \cdot \frac{J_{i,35}}{J_{i,25}} \cdot \frac{P^2_{i,*,25} - P^2_{i,3,25}}{P^2_{i,*,35} - P^2_{i,3,35}} \tag{3.35}$$

A similar relationship can be obtained for the component j:

$$\frac{B_{j,35}}{\delta_{b,35}} = \frac{B_{j,25}}{\delta_{b,25}} \cdot \frac{J_{j,35}}{J_{j,25}} \cdot \frac{P^2_{j,*,25} - P^2_{j,3,25}}{P^2_{j,*,35} - P^2_{j,3,35}} \tag{3.36}$$

In the above equations the values of quantities $P_{i,*,35}$ and $P_{j,*,35}$ for the desired composition can be obtained from the vapor-liquid equilibrium data. The values of parameters $J_{i,25}$, $J_{j,35}$, $P_{i,3,25}$ and $P_{j,3,35}$ (corresponding to the downstream pressure conditions) can be obtained from the pervaporation data. Thus, the numerical value of the parameter $\frac{B_{i,35}}{\delta_b}$ can be calculated if the value of the parameter $\frac{B_{i,25}}{\delta_b}$ is known with one single pervaporation data at 35°C. Similarly the values of the parameter $\frac{B}{\delta_b}$ at 40°C can also be computed for both components separately.

3.3.4 Penetrant Profile in the Imaginary Phase

The objective now should be to generate penetrant composition profile along the penetrant flow direction in the liquid-filled region and in the vapor-filled region of the membrane. At this point it should be remembered that we are still dealing with the imaginary phase and not the membrane phase. For the case when the imaginary phase is liquid, the following equation can be used to find different $X_{i,l}$ (refers to the value of X_i at any position l) values at different positions (l) in the membrane:

$$\frac{X_{i,l} - Y_{i,3}}{X_{i,2} - Y_{i,3}} = exp(\frac{v}{k} \cdot \frac{l}{\delta_a}) \tag{3.37}$$

This equation can also be derived from the boundary film theory and will give us the values of $X_{i,l}$ at different positions, i.e. $\frac{l}{\delta_a}$. This relative distance should be converted to $\frac{l}{\delta}$ which is relative to the total membrane thickness.

Equations 3.23 and 3.24 can be rewritten in the following manner for calculating the vapor pressure at a position l_x from the phase boundary inside the membrane along the permeant flow direction:

$$J_i = \frac{B_i}{(\delta)(\frac{l_x}{\delta})}(P^2_{i,\bullet} - P^2_{i,l}) \tag{3.38}$$

$$J_j = \frac{B_j}{(\delta)(\frac{l_x}{\delta})}(P^2_{j,\bullet} - P^2_{j,l}) \tag{3.39}$$

A further rearrangement of equations 3.38 and 3.39 leads to the following equations for the calculation of partial vapor pressures of components i and j:

$$P_{i,l} = \sqrt{P^2_{i,\bullet} - J_i \cdot \frac{\frac{l_x}{\delta}}{\frac{B_i}{\delta}}} \tag{3.40}$$

$$P_{j,l} = \sqrt{P^2_{j,\bullet} - J_j \cdot \frac{\frac{l_x}{\delta}}{\frac{B_j}{\delta}}} \tag{3.41}$$

These equation will give the value of $P_{i,l}$ and $P_{j,l}$ and, therefore, the mole fraction can be calculated as follows

$Y_{i,l} = P_{i,l}/(P_{i,l} + P_{j,l})$.

The position $\frac{l_x}{\delta}$ should be converted to relative distance $\frac{l}{\delta}$ measured relative to the membrane-feed mixture interface. By combining the data for the liquid and vapor part we should have data for the composition (mole fraction of acetic acid in this case) of imaginary phase at different positions across the membrane.

3.3.5 Penetrant Profile in the Membrane Phase

To find the amount and the composition of the penetrant in the membrane phase, sorption data are to be used or applied. In other words, the sorption data are applied to find the composition of the penetrant in the membrane phase from that of the imaginary phase. For the liquid part, liquid sorption data will be used. For the

vapor part, vapor sorption data will be used. Thus, corresponding values for the mole fraction of the penetrant in the binary penetrant mixture and the total sorbed amount can be obtained at different relative distances, all across the membrane.

Finally, we should have the values of the mole fraction of the slower component (acetic acid) in the membrane phase versus the relative distance in the membrane. The second data will be the total penetrant (sorbed) amount in the membrane phase versus the relative distance across the membrane. These values can be compared to the experimental penetrant concentration profile obtained.

Assuming convective flow for liquid mixtures in the liquid-filled portion of the membrane, the equation for A_{mixt} for liquid mixture can be written as follows:

$$J_i + J_j = \frac{A_{mixt}}{\delta a}(P_2 - P_*) \tag{3.42}$$

It should be noted that a strong coupling, and no separation, is assumed in the liquid transport, whereas no coupling is considered in vapor transport.

Chapter 4

Experimental Aspects

4.1 Membrane Preparation

The polymer (poly-m-phenylene-iso(70)-co-tere(30)-phthalamide, abbreviated as PA hereafter) was used for membrane making. This polymer was synthesized by Nguyen et al. (1987 A) according to the method reported by Gan et al. (1975) and has 70% of iso-phthaloyl component and 30% of tere-phthaloyl component. It is known that tere-phthaloyl component is highly symmetrical and forms a less amorphous structure, while iso-phthaloyl component is less symmetrical and forms a more amorphous structure (Gan et al., 1975). The polymer has a number average molecular weight of 31,000 daltons. The polymer is a random copolymer having the following structure:

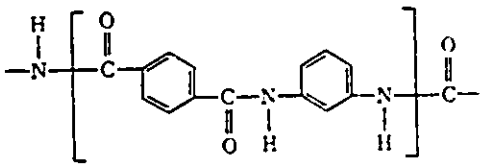

and

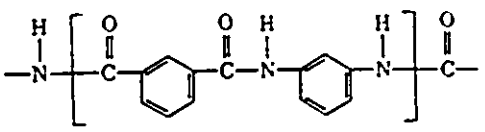

The casting solution was prepared by mixing 10.3 wt% aromatic polyamide (PA) polymer, 3.8 wt% LiCl, and 85.9 wt% dimethyl acetamide (solvent). This casting composition was chosen based on the study done by Nguyen et al. (1987 A). The solution was filtered and kept for 48 hours in order to allow the air bubbles to coalesce. The resulting casting solution was cast onto a glass plate at room temperature. Its casting thickness was adjusted by a casting knife. In the present case the casting thickness was 2 mils=5.08x10^{-5} m. The glass plate with the polymer solution on the top of it was put immediately in the oven and kept at 95°C for two hours. The resulting membrane film together with the glass plate was then put in the gelation bath consisting of cold water. The membrane film peeled off by itself from the glass plate. The resultant membrane was expected to be symmetric.

4.2 Pervaporation Experiments

The first step in evaluating pervaporation performance of a membrane for a given separation (Neel, 1991) is the determination of the feed mixture (upstream)-downstream composition (X-Y) curve. In this diagram the composition of one particular component in the feed mixture is plotted against the composition of the same component in the downstream. This diagram is similar to the well-known vapor-liquid equilibrium diagrams used in distillation processes. Additionally, the permeation rate versus composition curves at the defined process conditions should be determined. These curves, at the present state of the art, cannot be computed apriori. Hence, these curves must be established experimentally.

A schematic diagram of the pervaporation set-up is shown in figure 4.1.

The pervaporation set-up consisted of a static permeation cell (made of stainless steel and with an effective membrane area of 9.6x$10^{-4}m^2$), product collection traps and a vacuum pump. Feed liquid (100 g) was loaded in the cell at the desired temperature. The permeation cell was kept in a water bath to control the temperature. For establishing the feed-downstream composition curve, the temperature was kept at 25°C. The downstream pressure was controlled by introducing nitrogen gas in the system close to the vacuum pump. Nitrogen gas had to be introduced at the point

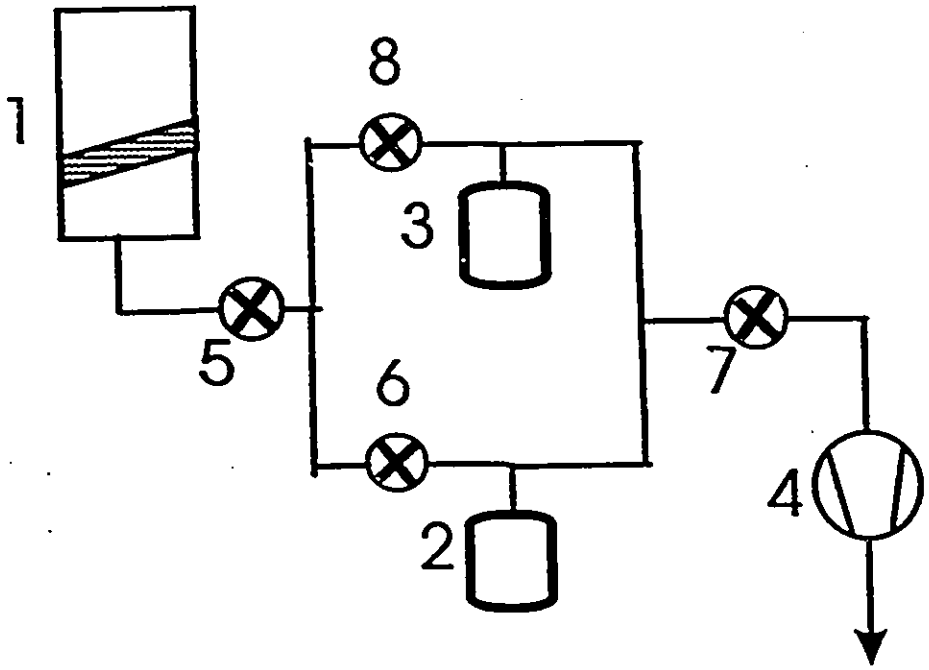

1 - Permeation Cell
2, 3- Cold Traps Immersed in Liquid Nitrogen Container
4 - Vacuum Pump
5, 6, 7, 8 - Valves

Figure 4.1: Experimental Set-Up of Pervaporation System Used

where it did not affect the estimation of the actual downstream pressure, i.e. total vapor pressure of the permeating vapors had to be measured correctly.

In the first set of experiments the downstream pressure was kept at 467 Pa by a vacuum pump. This downstream was achieved even without introducing nitrogen gas. Experiments were performed using pure acetic acid, distilled water and different binary compositions of acetic acid-water mixture. Permeating vapor was condensed in the product collection trap cooled by liquid nitrogen. In the experimental set-up it was possible to accommodate two traps. These traps were arranged in such a way as to enable one trap to be removed with the collected product while the other was being used at the same time. Thus, samples could be withdrawn at any time without interrupting the permeation run. Liquid nitrogen was used because it solidifies the permeating vapors immediately, thus reducing errors that could be caused by evaporation in the collecting traps.

For performing the first set of experiments, the membrane film to be tested was first placed in the cell. A filter paper was generally used under the membrane to prevent any damage to the membrane surface from the porous plate of the cell. The cell was bolted together and was connected to the vacuum system. Now, the system was evacuated. The system was tested for leaks before connecting the cell to the system. The cell was immersed in a constant temperature water bath. The constant temperature bath was filled with water and maintained at a desired temperature. The liquid mixture to be separated was introduced into the top half of the cell, and the traps placed in a Dewar flask containing liquid nitrogen. Vacuum was applied to the system. Steady state of permeation was monitored by measuring permeation rates every 30 minutes. Steady state permeation rates were reached in all cases after 120 minutes of experimental runs. Permeation rates were measured by weighing the cold traps filled with products. For each experimental run a new membrane was assembled in the cell. Once the run was complete, the water bath was emptied and the cell was dismantled. Product samples were analyzed using a Gas Chromatograph: SHIMAZU GC-8A equipped with a thermal conductivity detector having a 1.80 meter long columns packed with Chrom-P 80/100 mesh. The calibration curve used for the analysis is shown in the appendix I.1.

A second set of experiments was performed to establish the penetrant profile inside the membrane. In these experiments, a stack of identical membranes (typically 9 membranes) was used for concentration profile studies. It is assumed that the stack of identical membranes is a good model for a single membrane of the same thickness. These experiments were performed at a controlled temperature and with controlled downstream pressure. When steady state pervaporation was reached, the permeation rates were measured by weighing the product. After measuring the permeation rate, the cell was disconnected from the vacuum line and the stack of membranes was dismantled. The stack was then blotted free of surface fluid and the stack was rapidly separated into substacks (typically three membranes in each substack). Each substack was weighed quickly. The position of the sub-stack was noted properly and the substacks were numbered for convenience. Penetrant present in the polymeric membrane was collected into another cold trap, for each substack. The collected product was weighed and analyzed by a Gas Chromatographic technique.

Concentration profile studies were performed for pure water at room temperature but at different downstream pressures to study the effect of downstream pressure on the shape of concentration profile. The profile experiments were also performed with a binary mixture of acetic acid-water at different temperatures and downstream pressures.

To examine the error in determining the weight of a substack, control experiments were carried out. In these experiments the weight decrease was measured as a function of time. With a time lapse of 2 minute while putting the substack of membranes in the weighing trap the error was estimated to be ± 4 %. Each experiment was repeated to check the reproducibility, and the average value of the two is reported in the present work.

4.3 Liquid Sorption Studies

Membrane samples were dried for performing liquid sorption studies. The samples were dried by putting them in the dessicator and applying a gentle vacuum. Constant weights of dried samples were reached in about 48 hours. These dried membrane

samples (typically having a dry weight of 0.30 g) were allowed to equilibrate in the mixture of a known composition contained in a beaker at a set temperature for 48 hours. The temperature was controlled by putting the beaker into a water bath. The sample was taken out of the bath, blotted free of surface liquid, weighed and placed in a dry container. The container was then connected to the vacuum line and to another trap cooled by liquid nitrogen, where the liquid sorbed by the polymer was collected. The collected amount of penetrants was weighed and analyzed by using a Gas Chromatographic technique. The liquid sorption data is plotted in the following manner. The mole fraction of one component (acetic acid in this case) in the feed is plotted against the mole fraction of the same component in the sorbed mixture. The mole fraction of acetic acid in the feed is also plotted against the total sorbed amount of the penetrants.

4.4 Vapor Sorption Studies

The membrane samples were dried using the same method as for liquid sorption studies. These dried samples of membrane were used for vapor sorption studies. Vapor sorption apparatus includes Cahn microbalance and a vapor sorption chamber. The Cahn automatic recording electromicrobalance Model RG was used in the experiments. A schematic diagram of the vapor sorption setup is shown in figure 4.2.

For starting a vapor sorption experiment, membrane samples were placed inside the sorption chamber on a hook specially fabricated for this purpose. The liquid chamber was filled with a liquid mixture of known binary composition. For the time being this part was isolated from the vacuum system. Now the system was evacuated and the weight of the sample was recorded. The Cahn balance was connected to a computer monitor (PC). The weight of the sample was recorded continuously. Once the weight of the sample became constant, the liquid system was connected to the vacuum system. This caused the vapors to be released from the liquid mixture. The composition of the vapors can be obtained from vapor-liquid equilibrium data of the binary system. The membrane sample was allowed to equilibrate with the vapors for 48 hours or until the final weight of the sample became constant. In brief, the

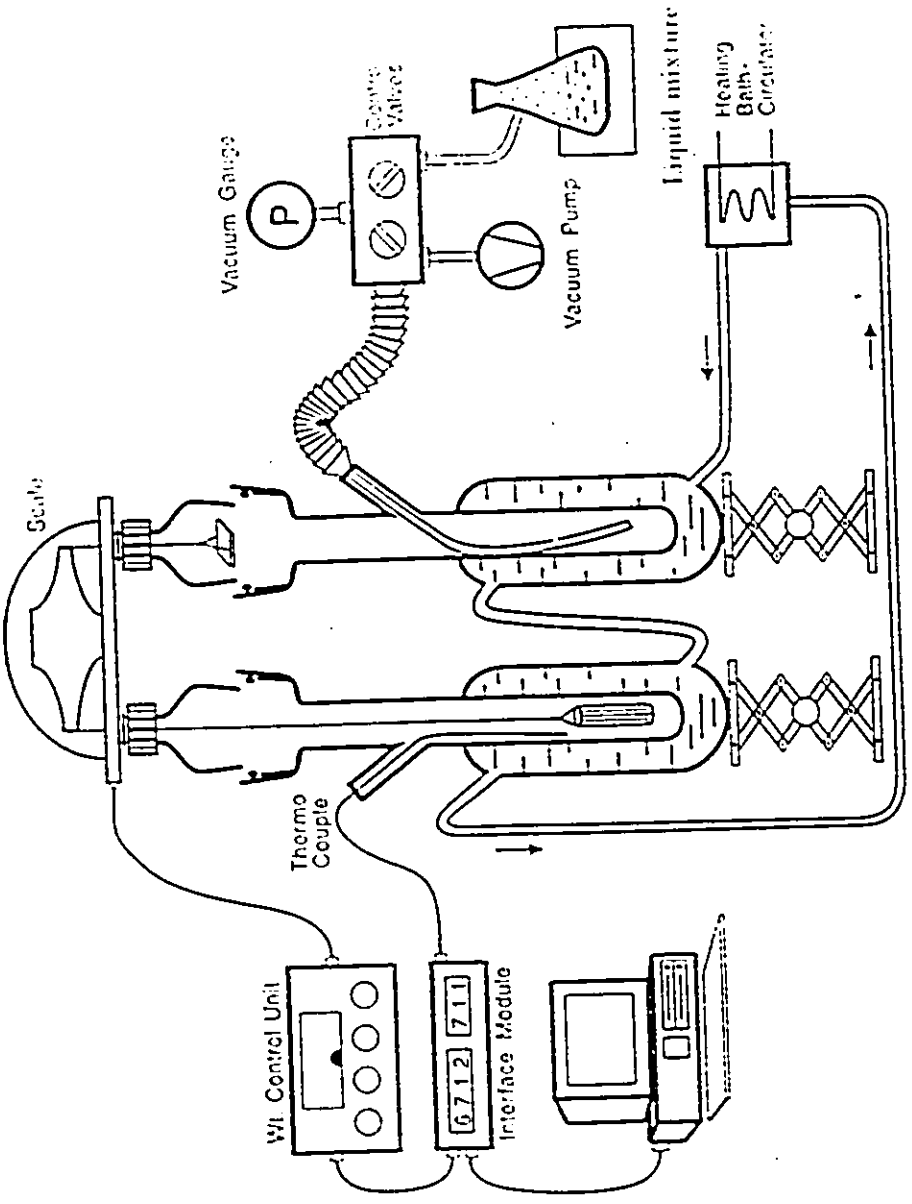

Figure 4.2: A Schematic Diagram of Vapor Sorption Apparatus

Figure 4.2: A Schematic Diagram of Vapor Sorption Apparatus

dry membrane samples were exposed to a defined binary vapor phase, which was in equilibrium with a liquid mixture of known composition. Now the sample was taken out of the sorption chamber and put into another dry container. The weight fraction of penetrant sorbed by the membrane was determined by weighing the membrane samples for different penetrant activities. The membrane sample was desorbed using the concept mentioned above and sample collected in the cold trap was analyzed by a Gas Chromatographic technique. Vapor sorption studies were performed at 25°C, 35°C and 40°C.

4.5 State of Permeant Studies Using Calorimetry

Preliminary studies on the state of permeant in the membrane were carried out by thermal analysis. The thermal analysis was performed with a calorimeter. To perform the thermal analysis a membrane sample of known weight was allowed to soak in pure water or acetic acid bath for 48 hours. The sample was then taken out and blotted free of any surface liquid. The sample was weighed again and put into the sample pan provided in the calorimeter. Separate runs were made for membrane sample soaked in water and acetic acid, respectively. The calorimeter used is Model BT built by Setaram of Lyon, France. It is a twin cell Tian-Calvet heat-flow calorimeter.

The heart of the calorimeter is a massive aluminum block with two identical cylindrical cavities located symmetrically about the center. A thermopile surrounds each cavity. The two thermopiles are identical and are connected in opposition to give the differential thermopile output. A matched pair of stainless-steel cylindrical cells each with a capacity of $13 \times 10^{-6} m^3$, can be lowered into the two cavities. One of these cells is termed as the reference cell and the other one is termed as the measurement cell, the choice being arbitrary. Two platinum sensors are provided for temperature measurement. Each sensor has four leads connected to it, thereby enabling 4-wire resistance measurements. A heater wound on outside of the block provides the thermal energy required for temperature control. The operating range of the calorimeter is 73 to 473 K. It takes around 8 hours to cool the calorimeter from 300 to 78 K using liquid nitrogen. Dry helium is used as the exchange gas

during cooling and dry N_2 during measurements. The control and operation of the calorimeter has been automated by interfacing it with a computer and some auxiliary equipment. The controller used is a Hewlett-Packard desk-top computer HP9836.

4.6 Microscopic and Spectroscopic Studies

4.6.1 Microscopic Studies

Air dried membrane samples were used for SEM studies. Small strips of membrane were cut from the sample. Then these pieces were immersed in liquid nitrogen and fractured. The strip was stuck on 45° angle brass stubs on carbon tape. The sample was sputter coated with a thin layer of gold in a Pokaron SC 502 sputter coater. The coated sample was looked at in a JSM 5300 scanning electron microscope. Non-conducting samples need the deposition of a thin layer of carbon, gold or gold-palladium to provide a conducting surface, unless the use of a very low accelerating voltage is acceptable.

4.6.2 Spectroscopic Studies

The sample of the polymeric membrane for performing spectroscopic studies was prepared in the following manner. The cast membrane film (aromatic polyamide) was dried in a dessicator for 24 hours by applying a gentle vacuum. This dry membrane film was dipped in the liquid mixture of acetic acid or water. The membrane film was taken out once the film was saturated with the liquid solution. For this purpose the film was kept in the liquid for 48 hours. Once the film was taken out, the surface liquid was taken away using a filter paper. Then this saturated polymeric film was immediately placed in the FTIR-ATR instrument for the spectroscopic studies.

Chapter 5

Results and Discussion

5.1 Microscopic Studies for Polyamide Membrane

Aromatic polyamide membranes of a casting thickness of 2 mils = 50.8 μm were prepared using the method described in the experimental part of this work. Many layers of these membranes were to be laminated to perform the pervaporation experiments. In this case the assumption was that the thick membrane (typically 9 membranes laminated) can be a model for the single membrane. Therefore, each of these membranes should be a symmetric membrane. To check the validity of this assumption the micrographs of the resultant membranes were taken using a SEM technique. Two micrographs taken from a scanning electron microscope are shown in figure 5.1. These two micrographs show the two sides of the same membrane. It is evident from the micrographs that the two sides of the membranes were similar. No obvious structure was detected in the micrographs, which means that the membrane was dense. The attached micrographs show a 3 to 4 μm thick dry membrane with few features. It should be recalled that the casting thickness of the membrane was 50.8 μm (2 mils). Both surfaces of the membrane looked smooth under electron microscope. The cross-section showed no visible pores or change in structure from one side to the other side.

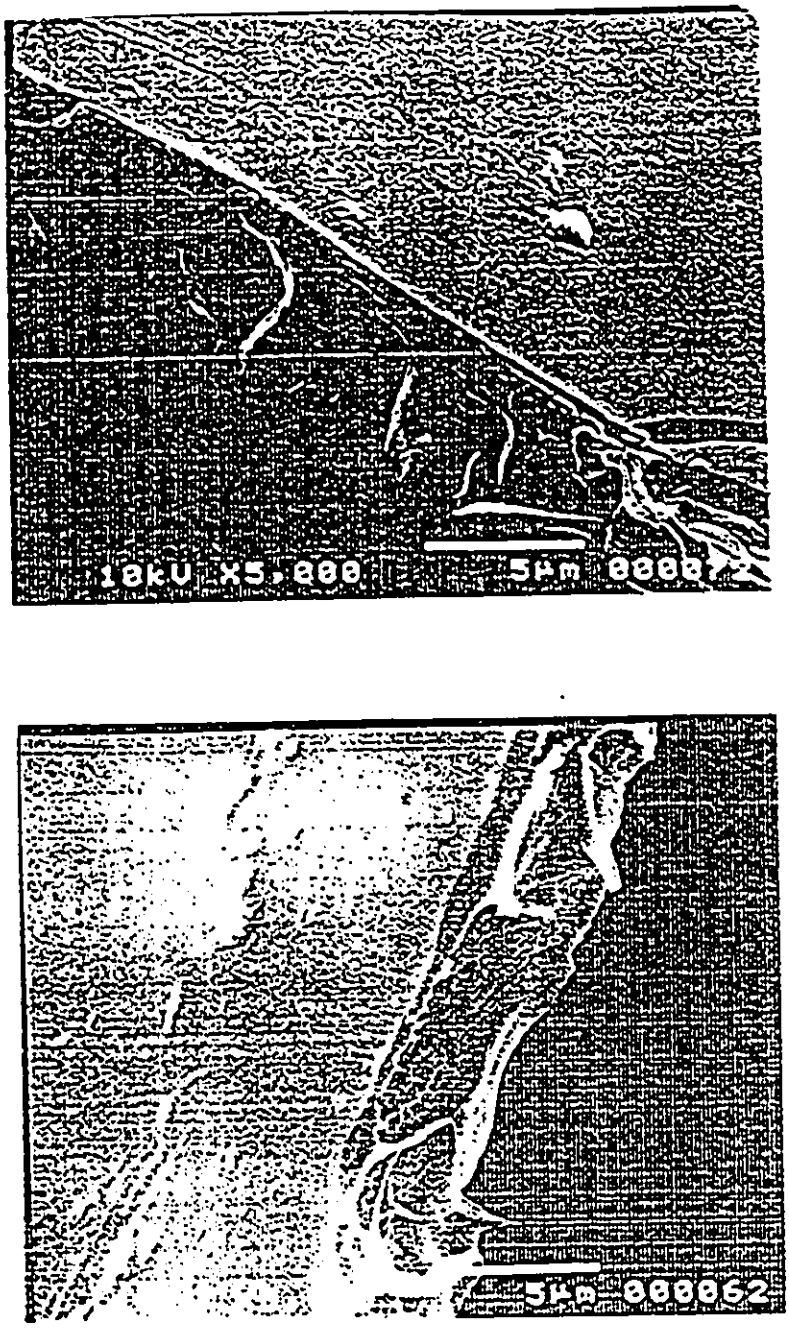

Figure 5.1: Scanning Electron Micrographs of the Symmetric Polyamide Membrane

5.2 Pervaporation of Acetic Acid-Water Binary Mixture

Steady state pervaporation experiments were performed by using a single layer of symmetric aromatic polyamide membrane. Figure 5.2 shows the results of the pervaporation experiments for the binary mixture of acetic acid and water at 25°C. Pervaporation data for the binary mixture is given in a tabular form in appendix G. The cast thickness of the membrane was 50.8 μm (2 mils). The temperature throughout these experiments was maintained at 25°C and downstream pressure was kept at 467 Pa (3.5 mm Hg). In this figure the mole fraction of acetic acid in the feed is plotted against the mole fraction of acetic acid in the downstream. This figure also shows the permeation rate (mol/s-m^2) at a constant temperature and at constant downstream pressure as a function of the mole fraction of acetic acid in the feed solution. The whole range of the binary mixture composition was covered.

From the steady state pervaporation experiments of the binary mixture of acetic acid/water it is evident that the mole fraction of acetic acid in the downstream was always lower than that in the feed. In other words these results clearly indicate that aromatic polyamide membranes are preferentially permeable to water. The total permeation rate decreased in a nonlinear manner with an increase of the mole fraction of acetic acid in the feed solution. The permeation rate of pure water was almost eight times that of pure acetic acid. The permeation rate decreased from 3.67×10^{-3} mol/s-m^2 to 0.46×10^{-3} mol/s-m^2 while going from pure water to pure acetic acid.

Each experiment was repeated to check the reproducibility. Average values are reported and the error is estimated to be $\pm$ 2.5 % in all cases of permeation measurements and $\pm$ 1.0 % for mole fraction measurements.

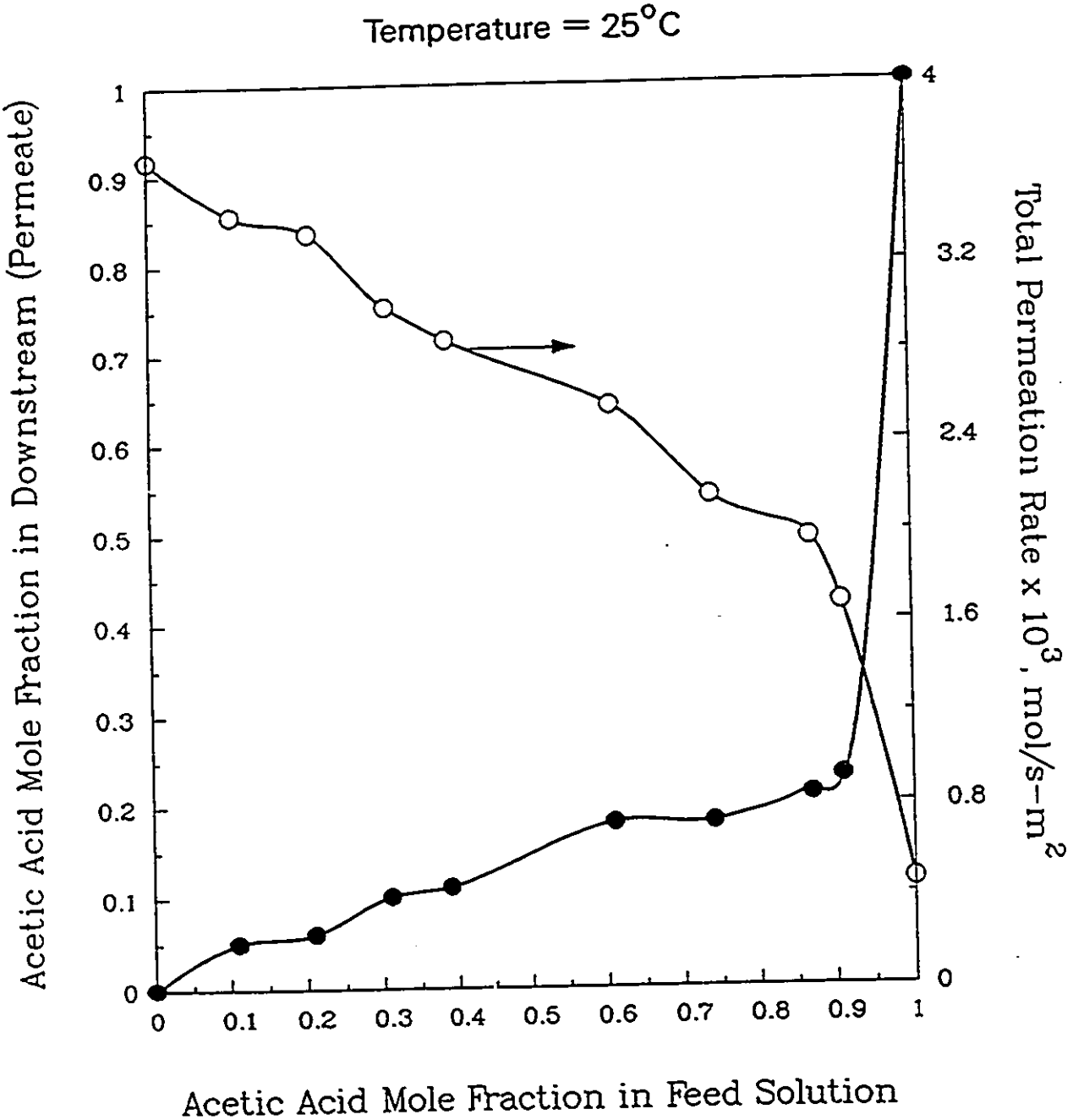

Figure 5.2: Pervaporation Data for Acetic Acid/Water System for Aromatic Polyamide Membrane

Table 5.1: Pervaporation Data for Single Polyamide Membrane at 25°C and at the Downstream Pressure of 467 Pa

S. No.	The Mole Fraction of Acetic Acid in the Feed	Separation factor α	β
1	0.115	2.46	1.20
2	0.21	4.16	1.56
3	0.31	4.04	1.83
4	0.39	5.45	2.22
5	0.61	7.12	3.62
6	0.74	12.96	5.8
7	0.87	25.17	13.25
8	0.91	33.85	15.67

The separation factors at different binary compositions are shown in table 5.1. The separation factor $\alpha_{i,j}$ and enrichment factor β are defined by equations 2.2 and 2.3, respectively. The separation factor α is dependent on the feed composition, as is evident from the table 5.1. The separation factor varies from 2.4 to 33.8. The highest separation factor was obtained at the lowest water concentration in the feed. This shows that pervaporation is much more selective at lower concentrations of the preferentially permeating component.

5.3 Pure Component Pervaporation

Figures 5.3 and 5.4 show the results of the pervaporation experiments of pure component (acetic acid and water respectively) using a single layer of aromatic polyamide membrane (casting thickness: 2 mils) at different downstream pressures. The temperature of the feed mixture was kept constant at 25°C and the downstream pressure was varied in these pervaporation experiments. The range of downstream pressure covered by these experiments was from 467 Pa to 13355 Pa.

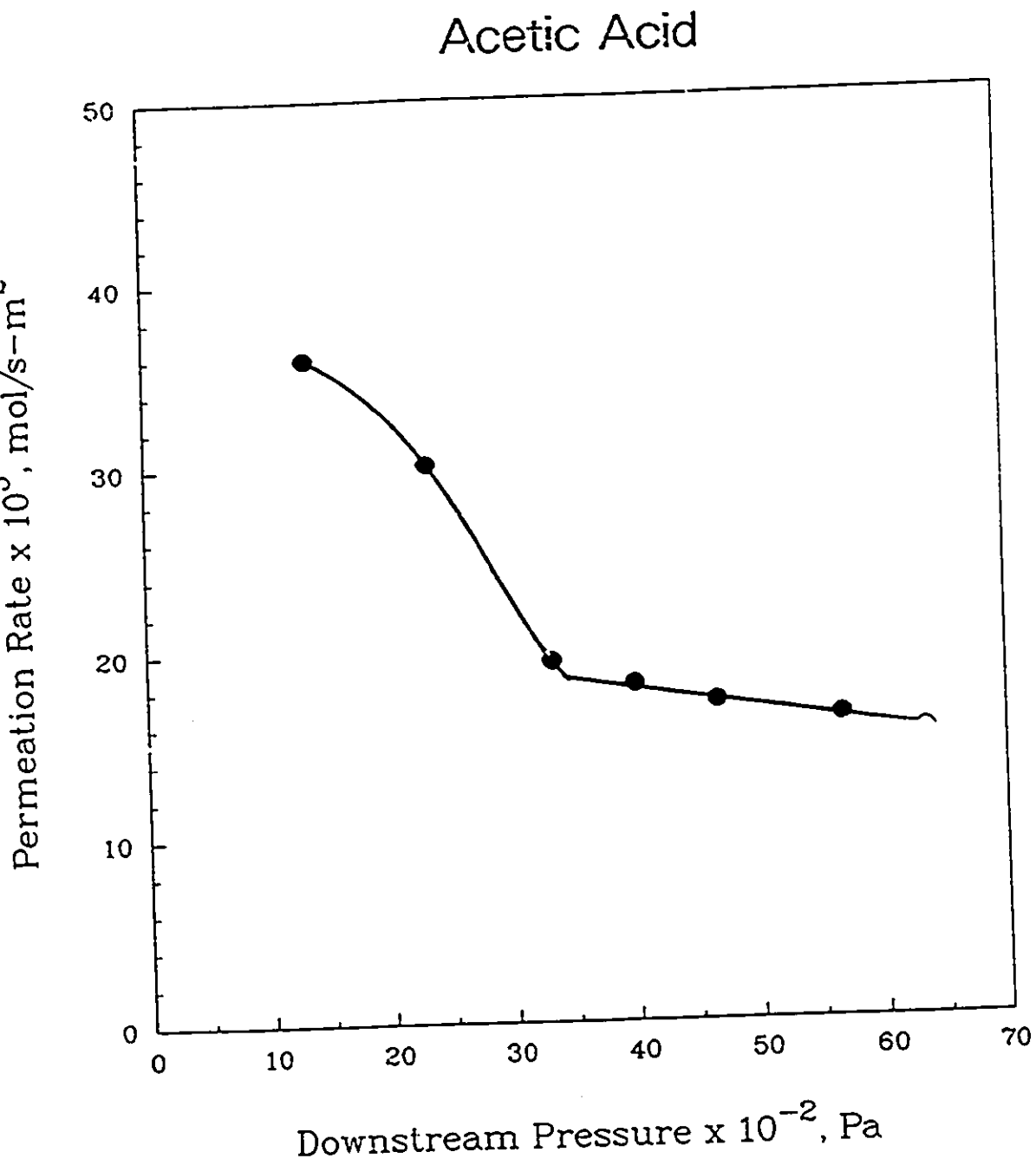

Figure 5.3: Effect of Downstream Pressure on the Pure Acetic Acid Permeation Rate at 25°C

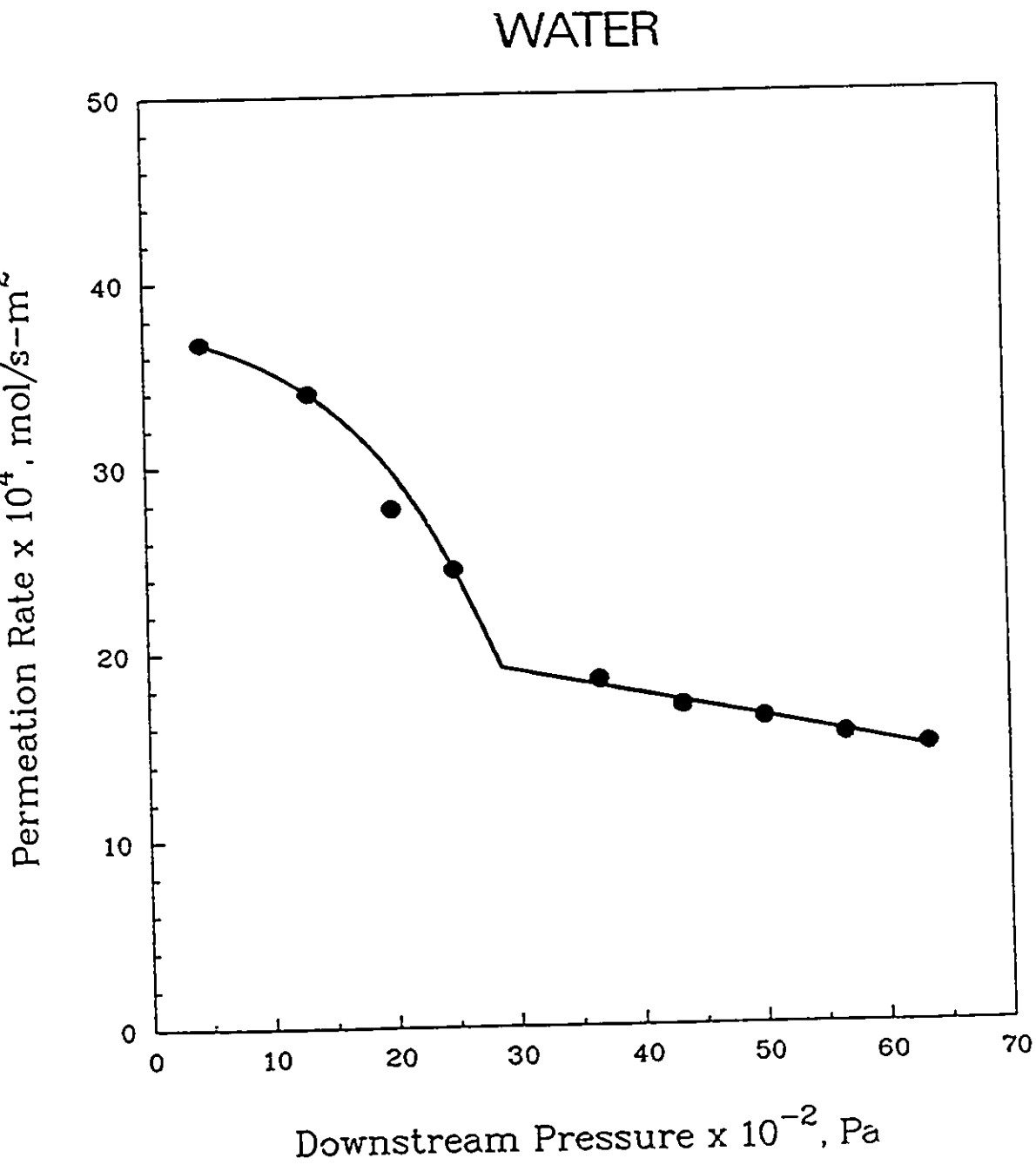

Figure 5.4: Effect of Downstream Pressure on the Pure Water Permeation Rate at 25°C

In these figures the downstream pressure is plotted on x axis and the permeation rate is plotted on the y axis. For any given downstream pressure the pervaporation permeation rate for water was roughly an order of magnitude higher than that of acetic acid. The data in tabular form are given in the appendix H.1 and in H.2. The error in the estimation of permeation rate is estimated to be $\pm$ 2.5 %. These results combined with the pervaporation data for binary acetic acid-water system clearly reaffirm that aromatic polyamide membranes are preferentially permeable to water. The shape of the permeation curve is also important. At lower downstream pressure the shape of the curve is parabolic, whereas for higher downstream pressure the shape is linear. An explanation was sought for this particular nature of the curve.

Let us examine the nature of the mathematical formulations derived for the pure component permeation (equation 3.15). The equation has two terms. The first term with the constant $\frac{A}{\delta}$ has a linear pressure term, i.e. $(P_2 - P_*)$. On the other hand the pressure term with the $\frac{B}{\delta}$ represents a parabolic shape, i.e. $(P_*^2 - P_3^2)$. The implications of this equation are as follows. At a downstream pressure (P_3) greater than the saturation vapor pressure (P_*) of the component, the second term in the equation will vanish and there will be only the linear relationship of permeation rate with pressure differential (equation 3.16). On the other hand if the downstream pressure is lower than the saturation vapor pressure, both terms will be there (equation 3.15). Thus, the shape of the curve showing permeation rate versus downstream pressure should be a combination of a linear and a parabolic function. The inflection point of this curve should correspond to the saturation vapor pressure of the component. However, there is no guarantee that this value of saturation vapor pressure will be the same as the literature value of the saturation vapor pressure for the same component.

5.3.1 Calculations Using the Newly Developed Transport Model

Using the transport model the values of the parameters $\frac{A}{\delta}$ and $\frac{B}{\delta}$ have been calculated. The values are:

- For Acetic Acid:
  $\frac{A_i}{\delta} = 1.79\text{x}10^{-6} mol/s - m^2 - Pa$
  $\frac{B_i}{\delta} = 1.76\text{x}10^{-8} mol/s - m^2 - Pa^2$

- For Water:
  $\frac{A_i}{\delta} = 1.66\text{x}10^{-5} mol/s - m^2 - Pa$
  $\frac{B_i}{\delta} = 1.68\text{x}10^{-7} mol/s - m^2 - Pa^2$

The above numerical values were obtained by a best fit of the parameters involved in the transport equations (equations 3.16 and 3.15) to the experimental values of permeation rates illustrated in figures 5.4 and 5.3.

The values of saturation vapor pressures obtained from the curves for water and acetic acid were 2900 Pa (21.75 mm Hg) and 3550 Pa (26.62 mm Hg), respectively. However, literature values for the saturation vapor pressures for water and acetic acid at the same temperature are 3188 Pa (23.9 mm Hg) and 2093 Pa (15.7 mm Hg), respectively. The value of saturation vapor pressure for water obtained from the permeation curve was close to the literature value of the saturation vapor pressure of the water (2900 Pa and 3188 Pa, respectively). On the other hand, the value of saturation vapor pressure for acetic acid obtained from the permeation curve was significantly higher than the literature value (3550 Pa as compared to 2093 Pa). The difference in the value of the saturation vapor pressure is probably due to a stronger interaction between acetic acid and polyamide as compared to the one between water and polyamide membrane. The state of water inside the membrane during steady-state pervaporation was much more closer to the free water. However, for acetic acid the case was different. Acetic acid was present in the bound state inside the polymer.

To obtain a better understanding of the above mentioned anomalous behavior of acetic acid in the polymeric membrane, some studies were performed using differential scanning calorimeter. These studies were carried out based on the presumption that the state of permeant inside the membrane might be different than the bulk state. The results obtained from these studies are discussed in a later section of this chapter.

5.4 Liquid Sorption Studies from Binary Mixture of Acetic Acid and Water

Figure 5.5 shows the liquid sorption data for the binary mixture of acetic acid and water at 25°C. In this figure the mole fraction of acetic acid in the bulk solution is plotted against the mole fraction of acetic acid in the sorbed phase. The mole fraction of acetic acid in the bulk liquid mixture is also plotted against the total sorbed amount per unit weight of the dry aromatic polymeric membrane (kg/kg of dry polymer). From this figure it is evident that aromatic polyamide membranes preferentially sorb water from water-acetic acid mixture. The sorbed amount of pure water was much greater as compared to that from pure acetic acid from the liquid phase. The values of sorbed amount from pure water and pure acetic acid are 0.62 kg/kg of dry polymer and 0.11 kg/kg dry polymer, respectively. The error in the estimation is estimated to be $\pm$ 3 % for the sorbed amount and $\pm$ 2 % for the mole fraction estimation. It should be noted that the shape of the curve representing the mole fraction of acetic acid in the sorbed phase against the mole fraction in the feed mixture is very similar to the pervaporation curve showing the relationship between the mole fraction of acetic acid in the feed versus the mole fraction of acetic acid in the downstream (figure 5.2).

Figures 5.6 and 5.7 show the liquid sorption data for acetic acid-water mixture at 35°C and 40°C, respectively. The sorbed amount was significantly higher as compared to that at 25°C. There was an interesting feature for the total sorbed amount at 35°C and 40°C. The total sorbed amount of the mixture showed a different behavior from that observed at 25°C. A maximum in the total sorbed amount was observed close to 50 mole % of acetic acid. This indicates that the total sorbed amount from pure water was lower than the total sorbed amount from the binary mixture of acetic acid/water at certain intermediate composition. An explanation was sought for this behavior.

The phenomenon can be explained in terms of the plasticizing effects of the penetrants and the interactions between penetrants and polymer. Stronger interactions

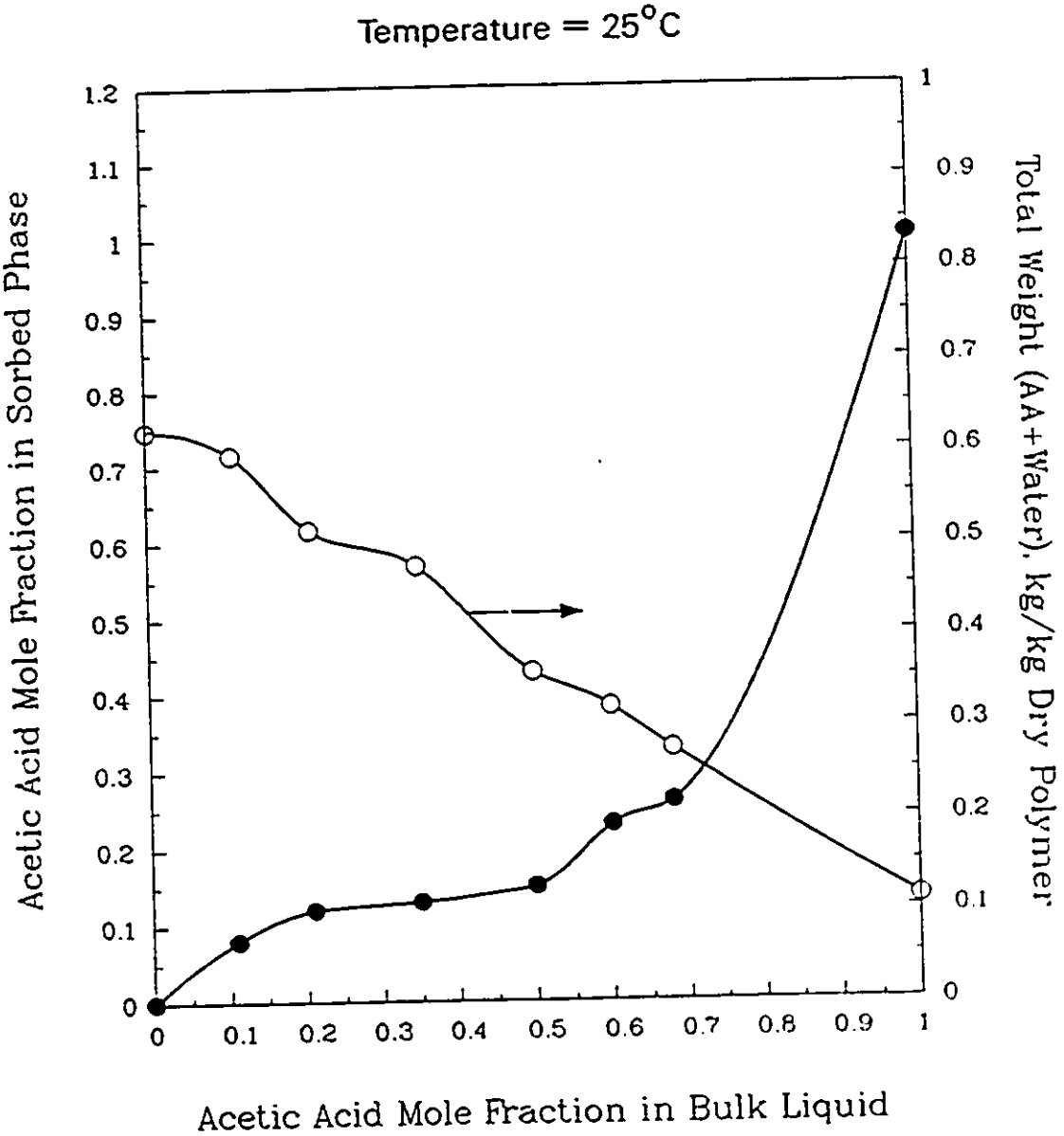

Figure 5.5: Liquid Sorption Data for Acetic Acid/Water System for Aromatic Polyamide Membrane

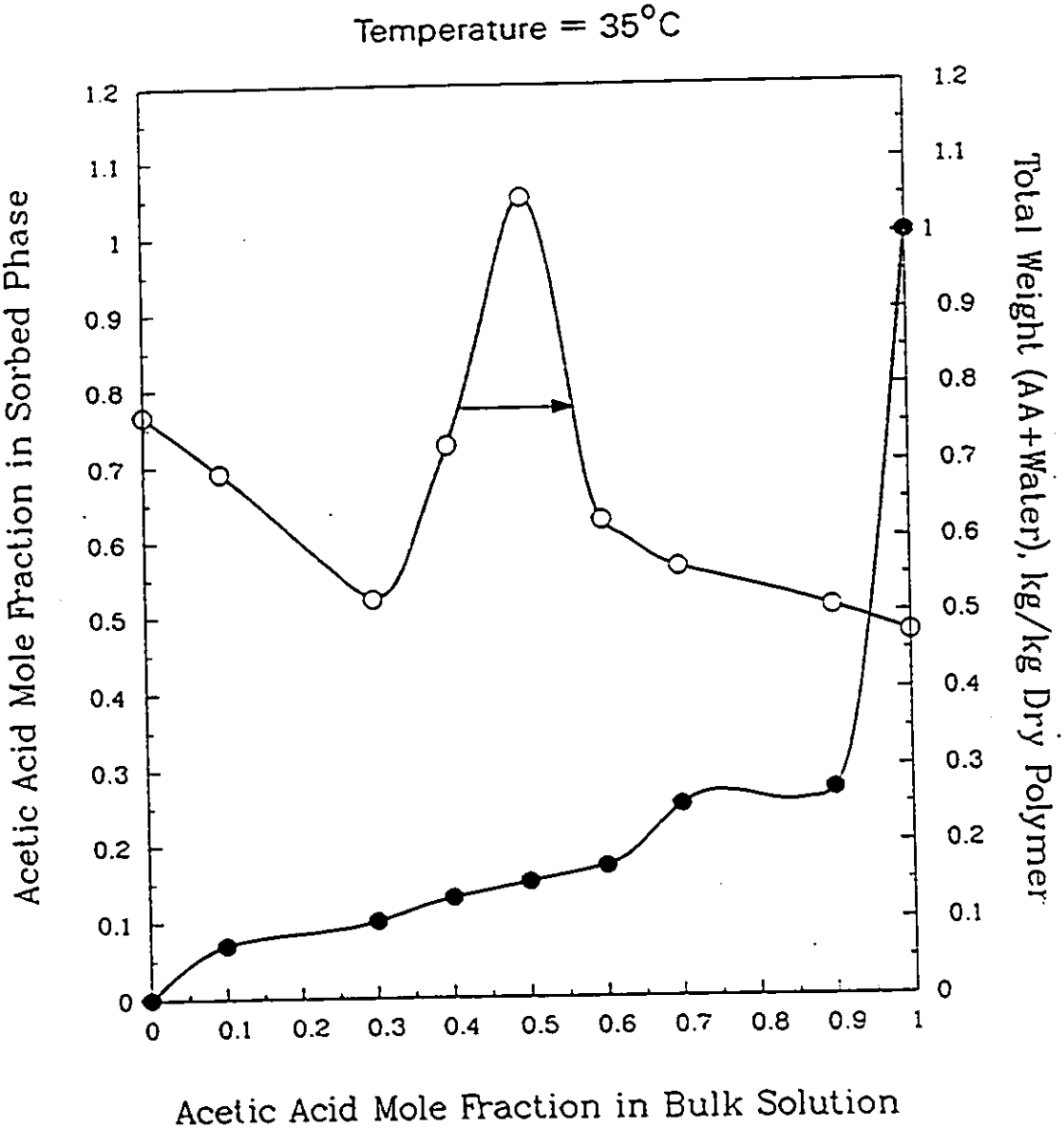

Figure 5.6: Liquid Sorption Data for Acetic Acid/Water System for Aromatic Polyamide Membrane

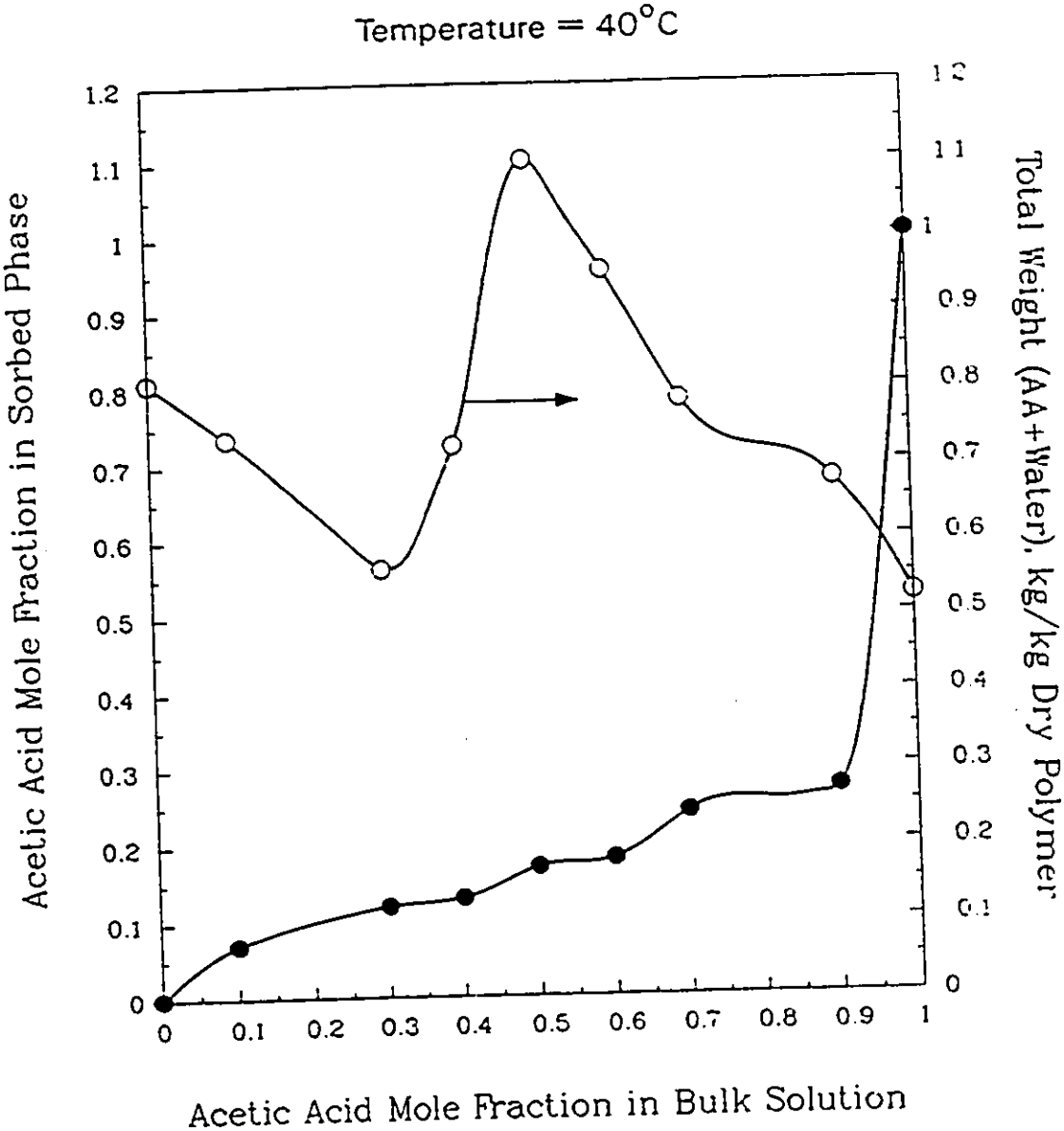

Figure 5.7: Liquid Sorption Data for Acetic Acid/Water System for Aromatic Polyamide Membrane

can be formed (Huang and Yeom, 1991) at low temperatures and reduce the plasticizing effect. However, as the temperature increases the interaction becomes weaker, so that the plasticizing effect can be recovered. The effect of temperature on the water cluster formation in the polymeric membrane should also be taken into account while explaining these data. The possibility of water association with acetic acid also changes at different temperature. All these effects combined make the sorption data at a particular temperature a unique data for a particular membrane-penetrants system.

Both acetic acid and water swell the polymer membrane to different extents. In this case one liquid in a mixture "sees" a different polymer structure because of the swelling effect of the other liquid. When two penetrants are present in the film together, they exert a mutual diluting effect on each other which enhances their individual activity coefficients and, thus, their plasticizing capability. Apart from liquid-liquid interactions, the reason for peaking (at 35°C and 40°C) of the sorption curve may be in the difference between the plasticizing action of the two liquids. As water swells the polyamide polymer more than acetic acid does, the acetic acid molecule "sees" a looser polymer structure in the presence of water than in its absence.

Interestingly, a maximum in the permeation rates was reported at a concentration of 10 wt% and at 75°C by Huang and Yeom (1991). This observation indicated that the mixture permeated through the membrane faster than either of the pure components.

The sorption selectivity from the liquid phase was compared to the pervaporation selectivity. Table 5.2 gives the pervaporation selectivity at 25°C and liquid sorption selectivity at the same temperature. The comparative data of liquid sorption and pervaporation show that in this case the preferentially sorbed component was also preferentially permeated through the polymeric membrane. However, this conclusion should not be generalized.

A comparative liquid sorption data at different temperatures is shown in table 5.3. The mass of membrane to liquid volume was identical for all of these experiments.

Table 5.2: Comparison of Pervaporation Selectivity to the Liquid Sorption Selectivity

Mole Fraction of Acetic Acid in Bulk Solution	Pervaporation at 25°C β	Sorption at 25°C β
0.10	1.20	1.1
0.30	1.83	1.67
0.40	2.22	2.03
0.60	3.62	3.12
0.70	5.40	4.03
0.90	15.67	12.5

Table 5.3: Liquid Sorption Data at Different Temperatures

Mole Fraction of AA in Bulk Solution	Mole Fraction of AA in Sorbed Phase at 25°C	Mole Fraction of AA in Sorbed Phase at 35°C	Mole Fraction of AA in Sorbed Phase at 40°C
0.10	0.08	0.07	0.10
0.30	0.13	0.10	0.12
0.40	0.14	0.13	0.13
0.50	0.15	0.15	0.17
0.60	0.23	0.17	0.18
0.70	0.26	0.25	0.24
0.90	0.30	0.27	0.27

5.5 Vapor Sorption Studies for Polyamide-Acetic Acid-Water

Sorption isotherms have been determined for the binary vapor mixture of acetic acid and water vapor at 25°C, 35°C and 40°C. These sorption isotherms are shown in figures 5.8, 5.9 and 5.10, respectively. In these figures the ratio of partial pressure to the saturation vapor pressure for each component is plotted on the x axis. The sorbed amount for each component (acetic acid and water) is plotted on the y axis.

The amount of water vapor sorbed in the polymer was almost one order of magnitude higher than that of acetic acid. The amount of any component sorbed from the saturated vapor phase was much lower than that from the liquid phase. Thermodynamically, the amount sorbed from the vapor phase should be equal to the one from liquid phase at the saturation vapor pressure. But these data show that this was not the case for this system. For example, at 25°C the amount sorbed from pure water vapor was 0.10 kg/kg of dry polymer, whereas from the pure liquid water the amount was 0.623 kg/kg dry polymer. Similarly, from pure acetic acid vapor the sorbed amount was 0.023 kg/kg of dry polymer as compared to 0.111 kg/kg of dry polymer from the liquid phase. The error in the estimation is $\pm$ 3 % for the sorbed weight measurements and $\pm$ 1.5 % for the mole fraction estimations.

From the thermodynamical standpoint, it is hardly conceivable that the swelling of the membrane polymer can be noticeably different when the material is contacted, at the same temperature, with a pure liquid and its saturated vapor. In both cases, indeed, the activity of the penetrant is the same and equilibrium sorption uptakes should, therefore, be the same. The activity of a component is, however, the product of the activity coefficient and the concentration of the component. Thus, equal activity in two cases may not necessarily mean that the concentration of the penetrant must also be the same. The activity coefficient still can have different values in two cases. One may also conceive that the sorption taking place at the upstream surface of the membrane could be slower from a saturated vapor than from a liquid phase. Another explanation may be provided by the fact that the presence of small amounts

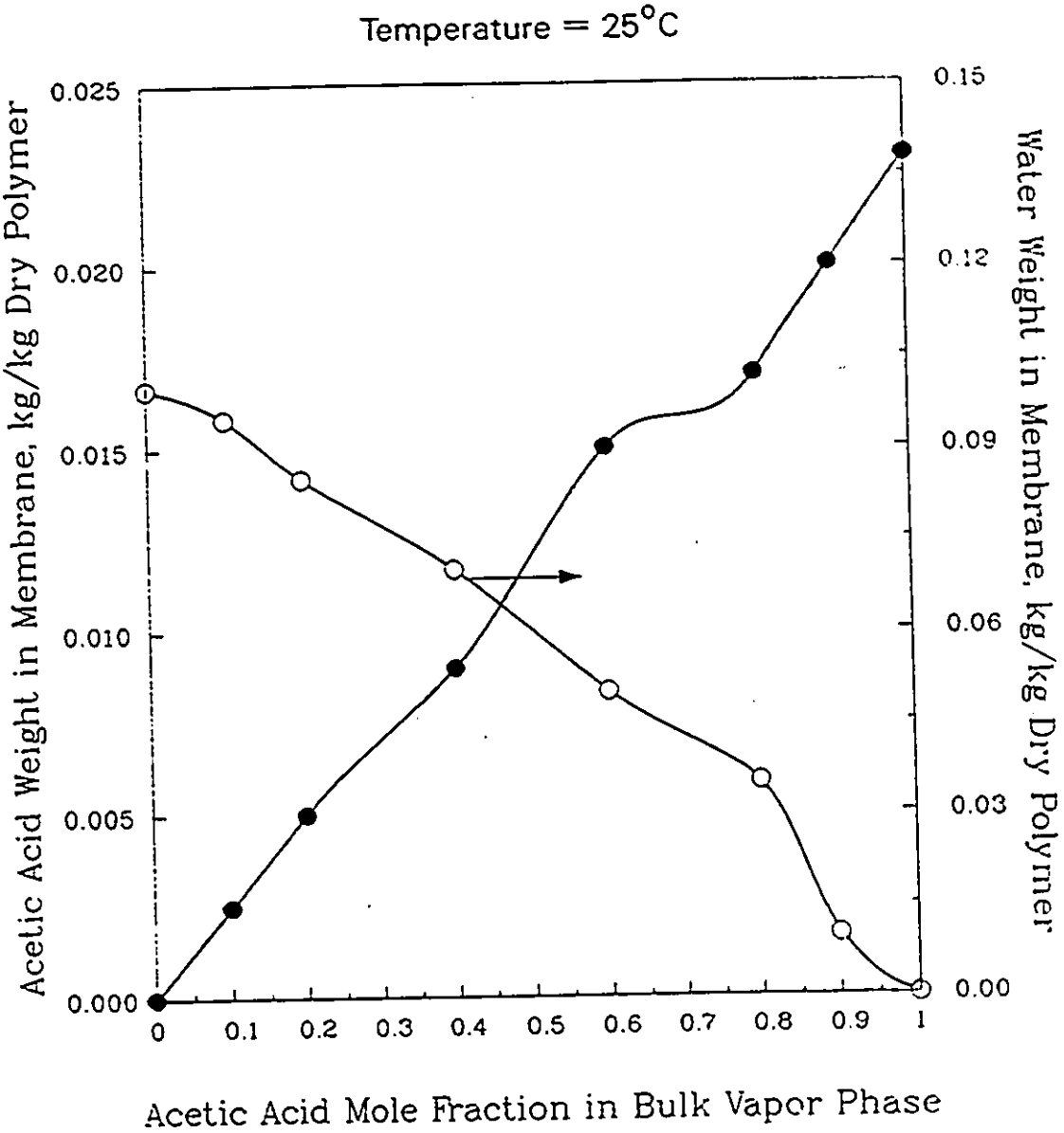

Figure 5.8: Vapor Sorption Data for Acetic Acid/Water System for Aromatic Polyamide Membrane

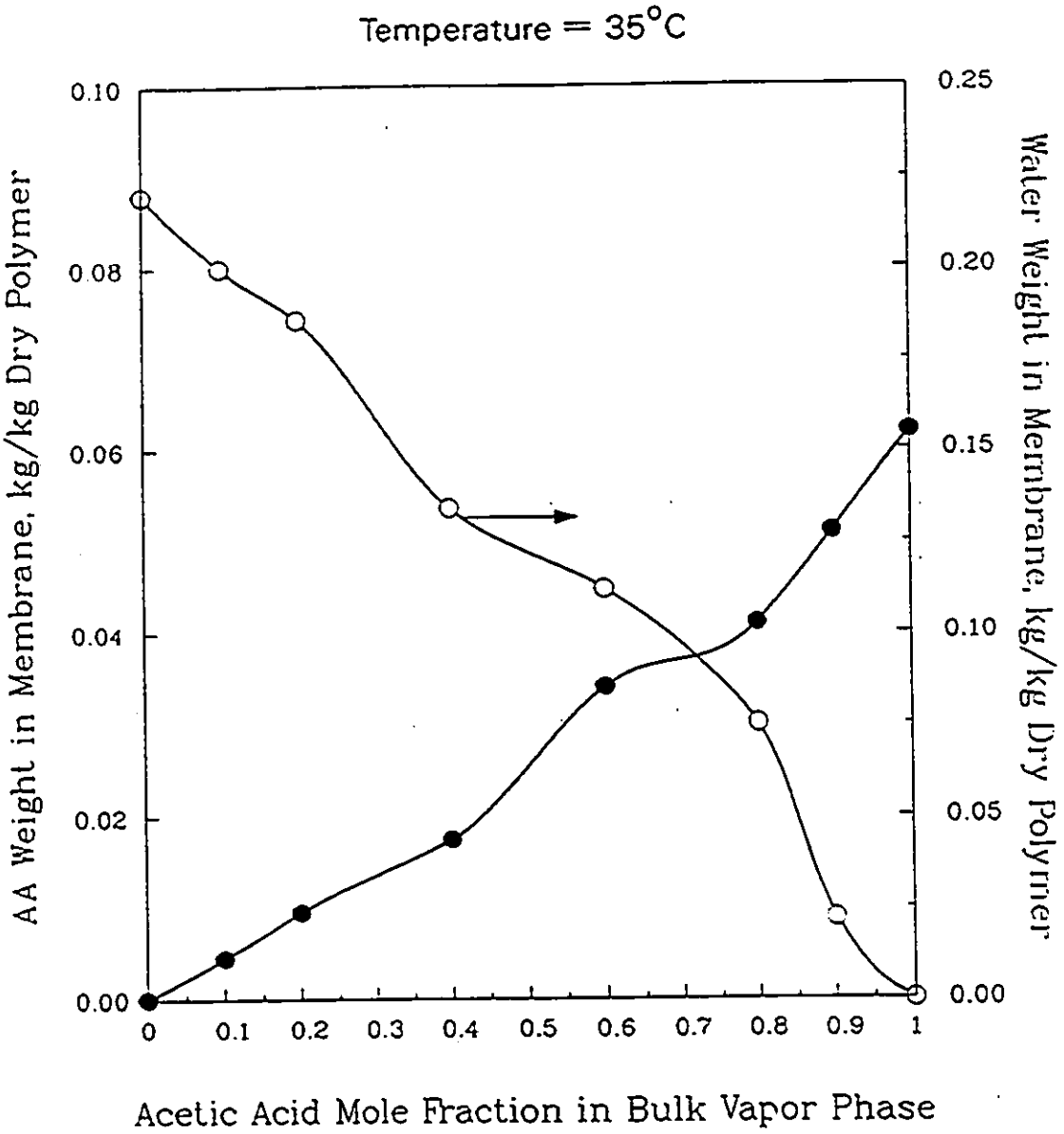

Figure 5.9: Vapor Sorption Data for Acetic Acid/Water System for Aromatic Polyamide Membrane

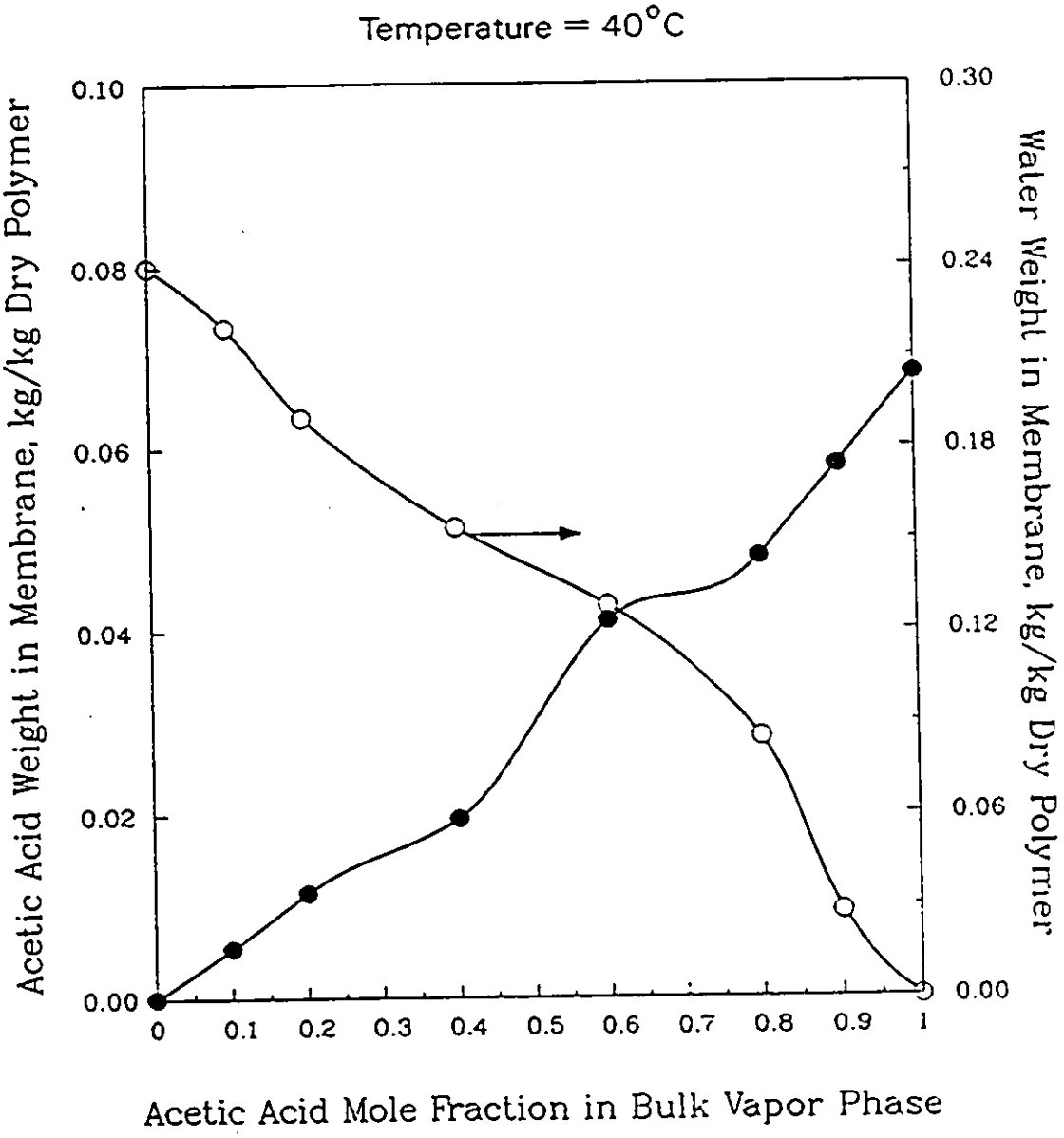

Figure 5.10: Vapor Sorption Data for Acetic Acid/Water System for Aromatic Polyamide Membrane

of air or other permanent gases drastically reduces the rate at which a polymer film absorbs a saturated vapor emanating from a liquid surface situated at some distance from the film.

5.6 Pure Penetrant Concentration Profile Inside the Membrane During Steady State Pervaporation

Pervaporation experiments were carried out by a stack of membranes using pure water as a penetrant. The effect of the downstream pressure on the penetrant concentration profile across the membrane was studied. Figure 5.11 illustrates the profile of the water content across the membrane at different downstream pressures. The water content in the three sections of the membrane is given in the figure. The sections are numbered as 1, 2 and 3 starting from the one closest to the liquid/membrane interface. The water content decreased from section 1 to 3 when the downstream pressure was sufficiently low. Only when the downstream pressure was high, i.e. 13332 Pa (100 mm Hg), the water content was practically equal at each section. At the downstream pressure of 467 Pa (3.5 mm Hg), the water content in section 1 was 0.72 kg/kg dry membrane. It should be noted that the water content was 0.623 kg/kg dry membrane when the membrane was in sorption equilibrium with liquid water (from the liquid sorption data at the same temperature). Estimated errors in sorbed amount measurements is $\pm$ 3 % for sections 1 and 2, and $\pm$ 5 % for section 3.

The water content in section 1 decreased with an increase in the downstream pressure, and at 13332 Pa (100 mm Hg) the water content became nearly one half of the equilibrium value. In section 3, the water content was 0.1 kg/kg dry membrane for any downstream pressure equal to or less than 4000 Pa (30 mm Hg), but it went up to 0.3 kg/kg dry membrane at 13332 Pa (100 mm Hg).

The implications of the above experimental data are quite important. Together with the pure water permeation rate data given in figure 5.4, the data in figure 5.11 shows that the amount of water drawn into section 1 of the membrane was more than

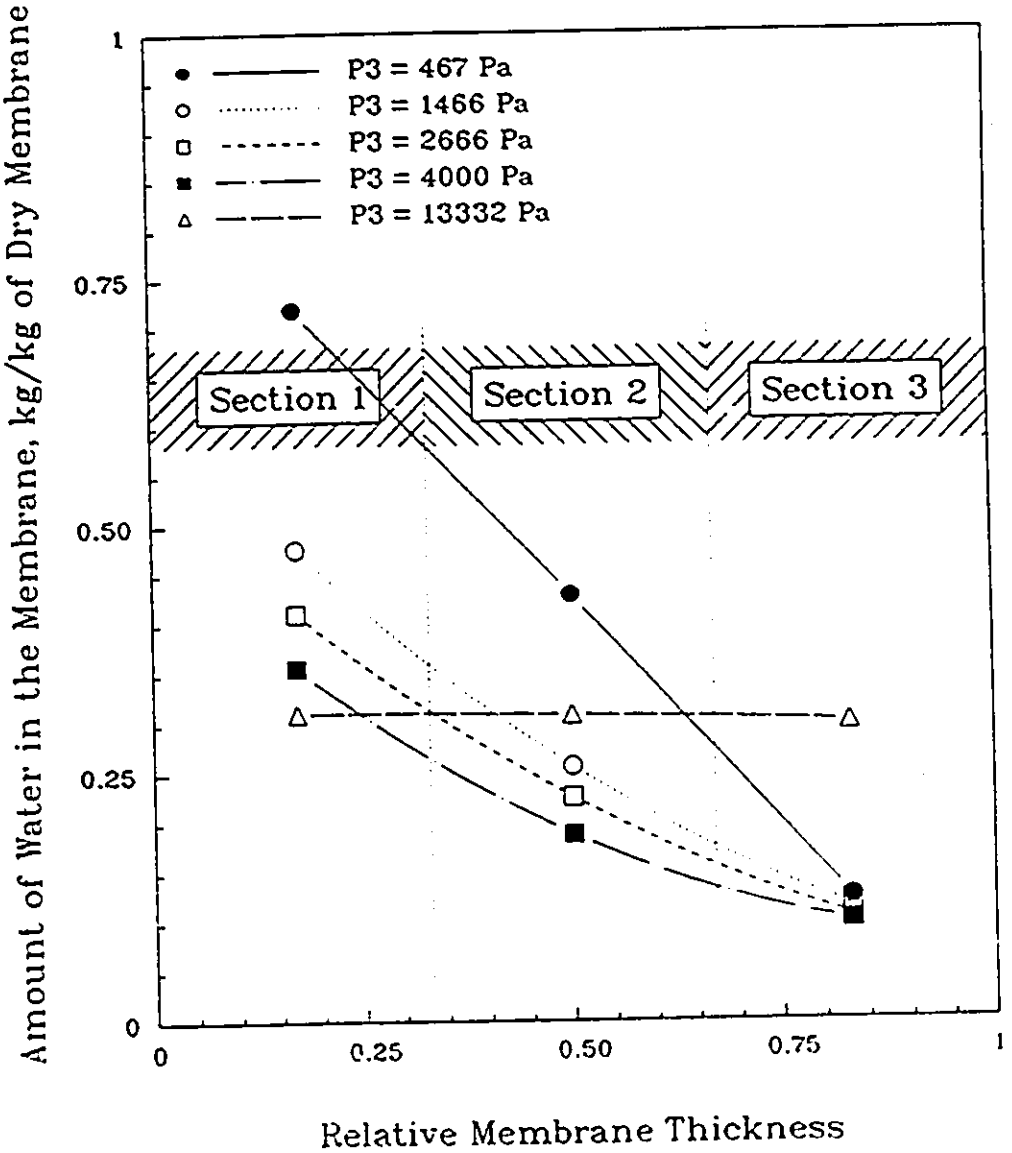

Figure 5.11: Effect of Downstream Pressure on the Pure Water Concentration Profile Inside the Membrane at 25°C

the equilibrium value when high vacuum was applied on the downstream side and water permeation rate was high. Discrepancies exist between the experimental water content and the equilibrium sorption value and were reported by different authors (Tock et al., 1974; Mulder et al., 1985; and Kim and Kammermeyer, 1970). The above results lead to two questions:

1. Is the polymer structure during steady-state pervaporation different from the one in thermodynamic equilibrium ?

2. Is thermodynamic sorption equilibrium established at the feed/membrane interface ?

The interpretation of the above observation is as follows. When high vacuum is applied on the downstream side, vacuum tends to draw water from feed liquid into the section 1 of the membrane. As a result, the space between the polymer segments is forced to open to accommodate more water molecules and the membrane swells to a degree higher than that corresponding to the sorption equilibrium.

Going back to figure 5.11, at a downstream pressure higher than 467 Pa (3.5 mm Hg), the water content in section 1 was higher than the value at the sorption equilibrium. The water content decreased as the downstream pressure increased. At the downstream pressure of 13332 Pa (100 mm Hg), the amount of penetrant was 0.3 kg/kg dry polymer, which is approximately one half of the water content at the sorption equilibrium. These results indicate that the intersegmental opening decreased with an increase in the downstream pressure as did the degree of swelling. The most interesting results were the water contents corresponding to the downstream pressure of 13332 Pa (100 mm Hg). They are almost constant from section 1 to 3. This is natural since both ends of the membrane are in contact with liquid. However, the water content was only one half of the one at the sorption equilibrium. These data lead to the conclusion that the dynamic equilibrium achieved during pervaporation is different from the static equilibrium achieved during the sorption equilibrium. In the dynamic equilibrium the penetrant (water) enters the membrane from one side and water leaves the membrane from the other side. The penetrant concentration in the membrane is different in the two cases.

Table 5.4: Results of the Calculations Based on the Solution-Diffusion Model for Pure Water Permeation at Different Downstream Pressures for Polyamide Membrane at 25°C

Parameter	P_3	P_3	P_3	P_3
-	467 Pa	1466 Pa	2666 Pa	4000 Pa
-	(3.5 mm Hg)	(11.00 mm Hg)	(20 mm Hg)	(30 mm Hg)
C_0	0.882	0.615	0.521	0.42
N	0.169	0.148	0.134	0.119

5.6.1 Calculations Using the Solution-Diffusion Model

First the calculations were performed using the solution-diffusion model for the pure component permeation with a concentration dependent diffusivity. For a detailed calculation procedure, refer to appendix N. The concentration dependence of the diffusivity assumed is as follows:

$$D_c = D_0(1 + c^N) \tag{5.1}$$

An analysis of the data of pure water permeation during pervaporation has been performed for calculating the diffusion coefficient for the polymer at zero concentration of the penetrant. The numerical value for the diffusion coefficient at zero concentration of the penetrant obtained from the calculation is $D_0 = 7.6\text{x}10^{-12} m^2/\text{s}$. The values of the parameter N and the concentration at the liquid-membrane interface, C_0, are given in table 5.4.

The results presented in table 5.4 is explained as follows. As the downstream pressure increases, the penetrant concentration inside the membrane decreases. This is evident from the experimental data. The value of the parameter N decreases with increasing downstream pressure.

The calculation can also be performed for the binary mixture of water-acetic acid assuming no coupling. The permeation rate of binary mixture can be split into two sets of pure component permeation data assuming no coupling.

5.7 Effect of Process Variables on Penetrant Concentration Profiles

Effect of following three variables was studied on the penetrant concentration profiles. The variables were:

- downstream pressure,
- feed mixture temperature, and
- feed composition.

Figure 5.12 shows the penetrant concentration profile inside the membrane for binary mixture of acetic acid-water system. The relative distance inside the membrane is plotted on the x axis. This figure shows the effect of downstream pressure on the penetrant concentration profile and on the total sorbed amount. The mole fraction of acetic acid in the feed mixture was kept constant at 0.50 in all these experiments and the experiments were performed at 25°C. The membrane was divided into three sections, namely, section 1, 2 and 3. The downstream pressure was kept at 467 Pa (3.5 mm Hg), 1200 Pa (9.0 mm Hg) and 2666 Pa (20.00 mm Hg), respectively.

First let us examine the mole fraction of acetic acid in the membrane. The results corresponding to the downstream pressure of 467 Pa (3.5 mm Hg) and 2666 Pa (20 mm Hg) are first examined. At section 1, the acetic acid mole fraction for 467 Pa (3.5 mm Hg) was higher, whereas the acetic acid mole fraction for 2666 Pa (20 mm Hg) was lower than the value corresponding to the sorption equilibrium. The equilibrium sorption value corresponding to the mole fraction of acetic acid of 0.5 at 25°C is approximately 0.17. The mole fraction of acetic acid decreased gradually from section 1 to 3 corresponding to both downstream pressures of 467 Pa (3.5 mm Hg) and 2666 Pa (20 mm Hg). In the downstream vapor, the mole fraction of acetic acid at 467 Pa (3.5 mm Hg) was lower than that corresponding to 2666 Pa (20 mm Hg). These results reflect the degree of swelling of polymer at section 1 and dryness at section 3, respectively. At the downstream pressure of 467 Pa (3.5 mm Hg) the feed solution was strongly drawn into section 1 of the membrane, intensifying the

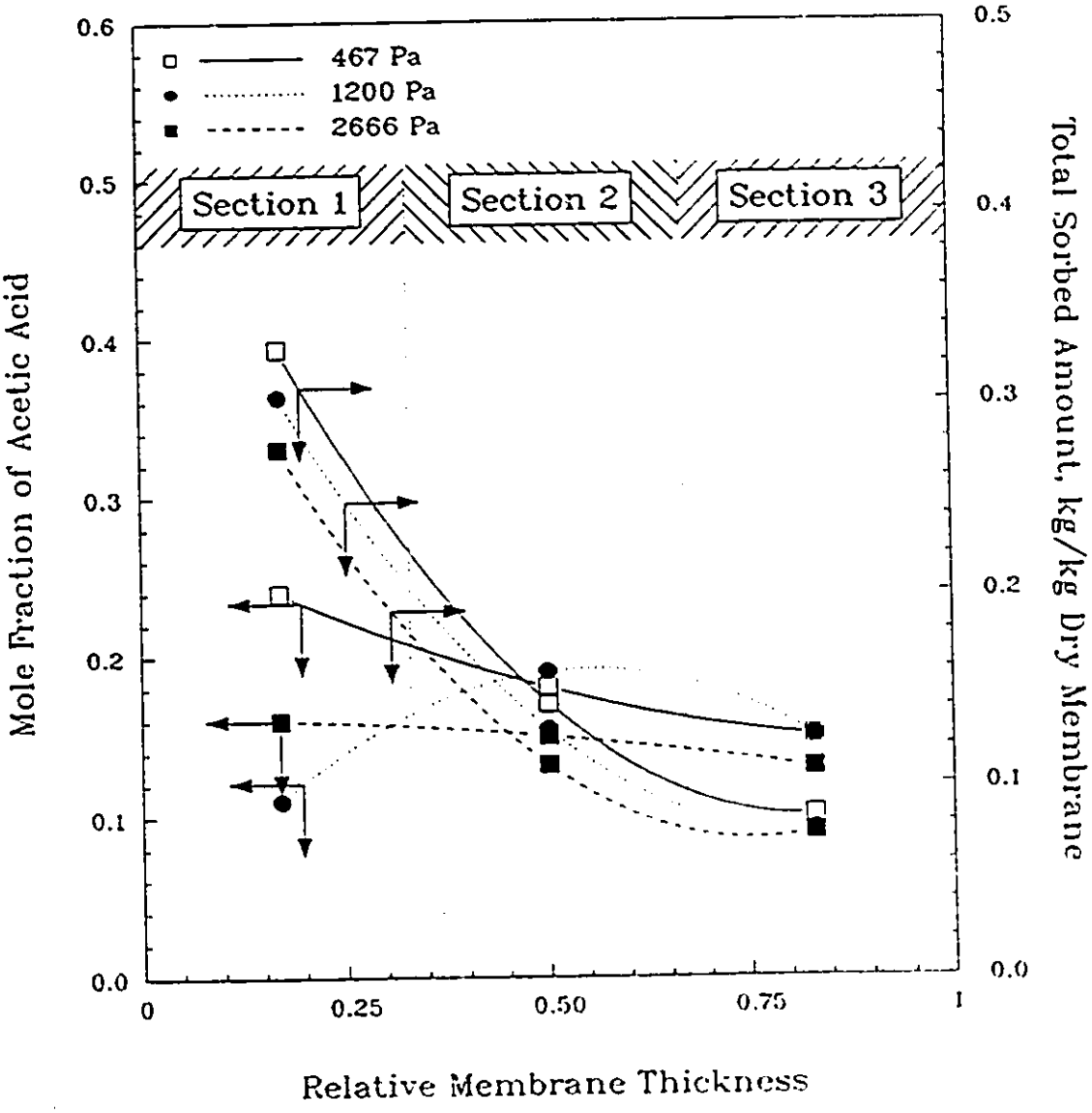

Figure 5.12: Effect of Downstream Pressure on Penetrant Profile Across the Membrane for Acetic Acid/Water at 25°C

swelling of polymer. As a result, the acetic acid mole fraction was closer to the one in the feed and higher than the sorption equilibrium value. On the downstream side, however, the membrane was the most dry at 467 Pa (3.5 mm Hg) and the selectivity of the membrane was the highest. As a result, the acetic acid mole fraction at the downstream face was lower than that corresponding to 2666 Pa (20 mm Hg). The trend was exactly the opposite at the downstream pressure of 2660 Pa (20 mm Hg). The profile corresponding to the downstream pressure of 1200 Pa (9.0 mm Hg) was the most spectacular. It shows a maximum of the acetic acid mole fraction at section 2. The presence of the maximum in the acetic acid mole fraction was reported in an earlier paper (Tyagi and Matsuura, 1991) and was attributed to concentration polarization that may arise when a swollen nonselective layer is followed by a dry selective layer in the direction of the penetrant flow. When the downstream pressure was 1200 Pa (9.0 mm Hg), the selectivity of the dry layer was sufficiently high while the diffusivity of the swollen layer was sufficiently low, and combination of those two factors led to concentration polarization. When the downstream pressure was either higher or lower than 1200 Pa (9.0 mm Hg), concentration polarization did not occur because neither one of those two requirements was satisfied.

At this point, one important point should be made about the way points were joined. The point at the membrane-liquid feed interface is the crucial one. If we assume sorption equilibrium at the membrane-feed interface, the point just inside the membrane should be the one corresponding to the sorption equilibrium. In the above cases, if we put this point at the membrane-feed interface, in almost all studies the phenomena of concentration polarization would be observed. However, in spite of the absence of the sorption equilibrium data point, only the experimental data points show this phenomenon.

In figure 5.12 now let us analyze the total sorbed amount (kg/kg of dry polymeric membrane) by the membrane in different sections. At all three different downstream pressures the total sorbed amount showed a definite trend. It was the highest in section 1 and the lowest in section 3 at any downstream pressure. The total sorbed amount of the penetrant in the membrane decreased at higher downstream pressure, i.e. the sorbed amount is higher at 467 Pa (3.5 mm Hg) as compared to 1200 Pa

(9.00 mm Hg). Moreover, the amount in section 3 of the membrane for all three cases was significantly lower than that in other sections. The sorbed amount in section 1 was of the same order of magnitude as from liquid sorption at the same temperature, whereas the sorbed amount in section 3 of the membrane was comparable to the amount sorbed from the vapor phase at the same temperature. This observation leads to the conclusion that indeed the top part of the membrane is swollen and the bottom part is dry.

Figure 5.13 shows the total penetrant content and the acetic acid mole fraction in each membrane section for different operating temperatures. The notation used in this figure is the same as that in figure 5.12. The feed acetic acid mole fraction and the downstream pressure were maintained at 0.50 and 467 Pa (3.5 mm Hg), respectively. The patterns observed for 40°C, 35°C and 25°C were very similar to those observed for 467 Pa (3.5 mm Hg), 1200 Pa (9.0 mm Hg) and 2666 Pa (20 mm Hg), respectively, except for high total penetrant contents corresponding to 35°C and 40°C. The mole fraction of acetic acid corresponding to 35°C shows a peak, indicating the concentration polarization phenomenon occurring inside the membrane. However, for higher and lower temperatures this phenomenon was not observed.

Figure 5.14 shows the effect of acetic acid mole fraction in the feed mixture on the penetrant concentration profile inside the membrane. These pervaporation experiments were also conducted with a stack of aromatic polyamide membranes at 25°C and at the downstream pressure of 467 Pa (3.5 mm Hg). The experiments were performed at mole fractions of acetic acid of 0.13, 0.25, 0.37, 0.50 and 0.65, respectively, however, figure 5.14 shows only data corresponding to acetic acid mole fraction of 0.13, 0.25 and 0.50, respectively. Data corresponding to other feed compositions are shown in appendix M. The acetic acid mole fraction corresponding to 0.25 mole fraction in the feed shows a peak. Others do not.

Each experiment reported above was repeated to check the reprodicibility. Average values are reported in the present thesis. Estimated errors are:

- $\pm$ 2.5 % for permeation rate estimation,
- $\pm$ 2.0 % for mole fraction fraction measurements in sections 1 and 2.
- $\pm$ 3.0 % for sorbed amount measurements in sections 1 and 2.
- $\pm$ 5.0 % for sorbed amount and mole fraction measurements in section 3.

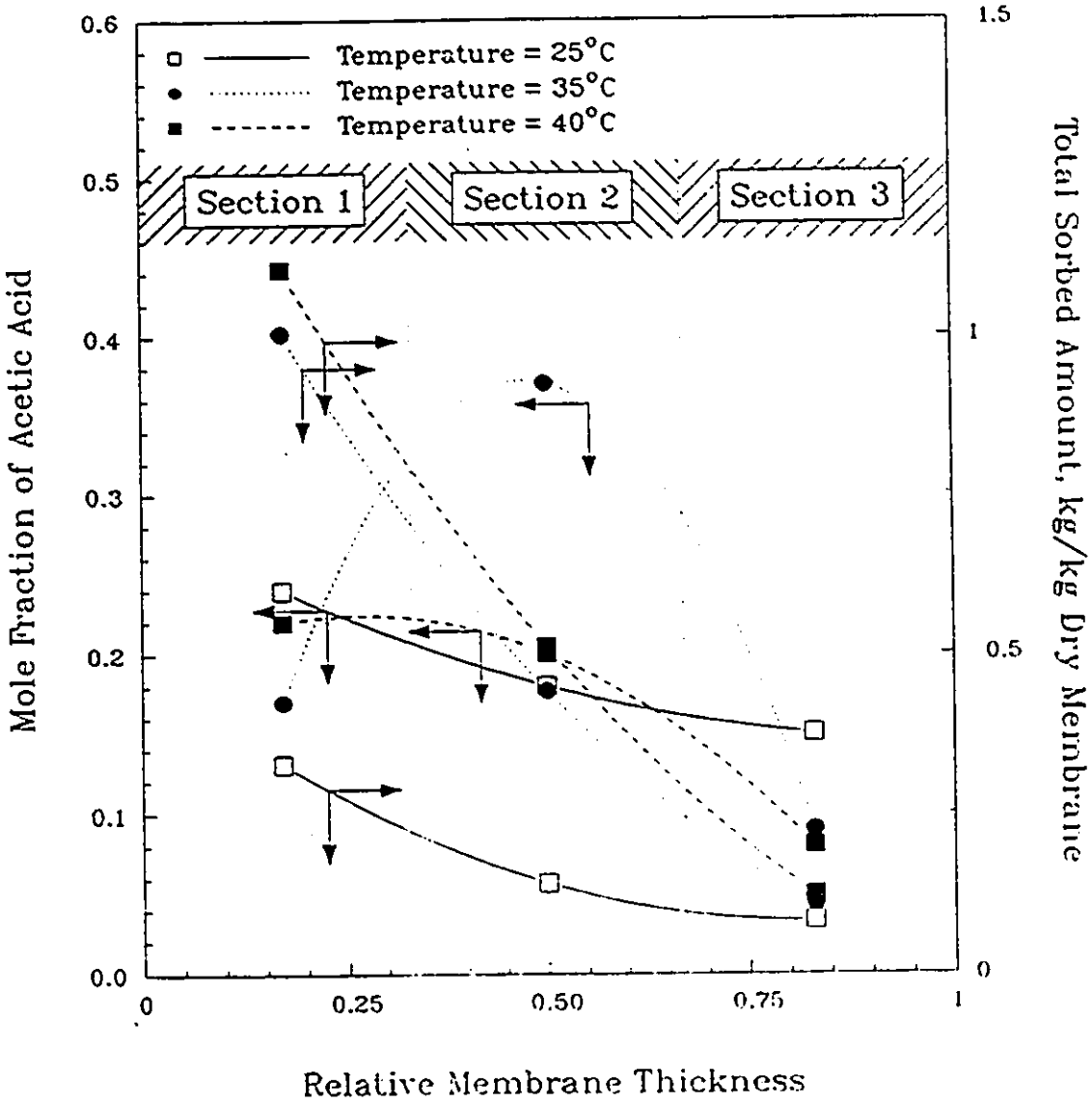

Figure 5.13: Effect of Feed Temperature on Penetrant Profile Across the Membrane for Acetic Acid/Water Mixture

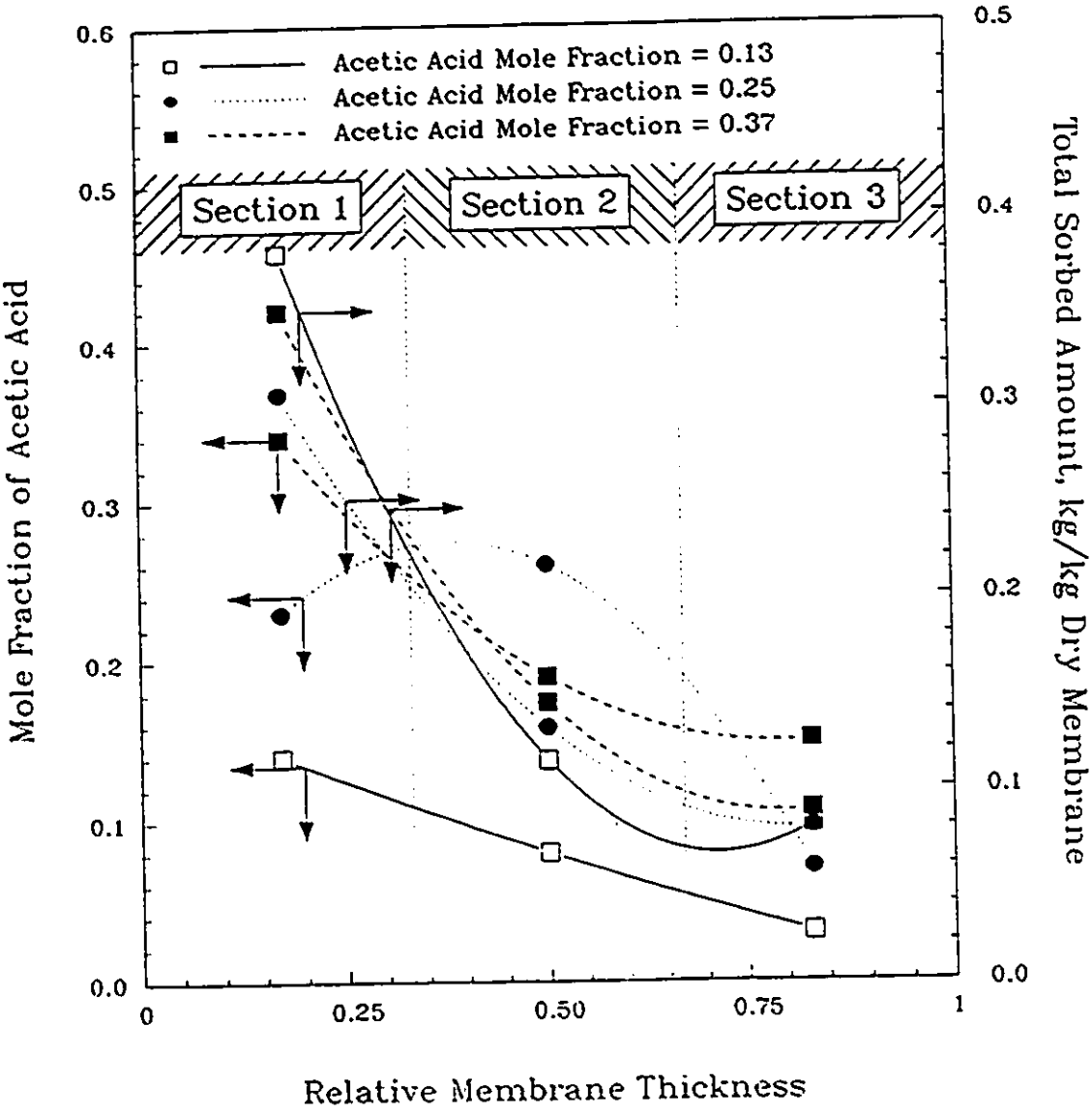

Figure 5.14: Effect of Feed Composition on Penetrant Profile Across the Membrane for Acetic Acid/Water Mixture at 25°C

Table 5.5: Effect of Downstream Pressure on Permeation Characteristics at 25°C and at 0.50 Acetic Acid Mole Fraction in the Feed

Downstream Pressure Pa (mm Hg)	Mole Fraction of Acetic Acid in Downstream	Total Molar Permeation Rate $x10^3$, mol/s-m^2
467 (3.5)	0.07	0.41
1200 (9.0)	0.10	0.18
2666 (20.0)	0.12	0.13

Table 5.5 shows the effect of downstream pressure on the total permeation rate and mole fraction of acetic acid in downstream. As the downstream pressure was increased, the total permeation rate decreased and mole fraction of acetic acid increased (separation decreased). Therefore, for higher permeation rate and higher selectivity lower downstream pressure should be used. Table 5.6 shows the effect of temperature on selectivity and the total permeation rate. With an increase of temperature the total permeation rate increased while selectivity remained constant. An increase of permeation rate with temperature is expected if the system follows an Arrhenius relationship. Table 5.7 shows the effect of feed composition on total permeation rate and selectivity. As acetic acid mole fraction was increased in the feed mixture the total permeation rate decreased.

Table 5.6: Effect of Feed Temperature on Permeation Characteristics at the Downstream Pressure of 467 Pa (3.5 mm Hg) and at 0.50 Acetic Acid Mole Fraction in the Feed

Feed Temperature - °C	Mole Fraction of Acetic Acid in Downstream	Total Molar Permeation Rate x10^3, mol/s-m^2
25	0.07	0.41
35	0.08	0.51
40	0.07	0.56

Table 5.7: Effect of Feed Composition on Permeation Characteristics at 25°C and at the Downstream Pressure of 467 Pa (3.5 mm Hg)

Acetic Acid Mole Fraction in the Feed -	Mole Fraction of Acetic Acid in Downstream	Total Molar Permeation Rate x10^3, mol/s-m^2
0.13	0.03	0.98
0.25	0.05	0.79
0.37	0.05	0.73
0.50	0.07	0.41
0.65	0.16	0.34

5.8 Testing the Transport Models

The newly developed transport model was used to calculate the theoretical penetrant concentration profile curves. The following data is needed to generate these curves:

- Vapor-liquid equilibrium data for acetic acid-water system at 25°C, 35°C and 40°C.
- Pure component permeation data at different downstream pressures to obtain $\frac{B_i}{\delta}$ and $\frac{B_j}{\delta}$ parameters. These parameters were calculated using the pure component permeation data of individual component at a fixed temperature (details in section 3.3).
- Liquid sorption and the vapor sorption data for the binary system for the same polymeric membrane at 25°C, 35°C and at 40°C. The sorption data are necessary to find the sorbed amount and the mole fraction of each component in the membrane phase in equilibrium with the imaginary phase.

The newly developed transport model was used to compare the predicted penetrant profile with the experimental one. The calculation for the phase boundary between liquid and vapor phase inside the membrane was also performed using the transport model.

5.8.1 Effect of Process Variables on the Phase Boundary

The effect of different process variables on the phase boundary was calculated using the newly developed transport model. The detailed procedure for the calculation is described in chapter 3, section 3.3. A computer program used to perform the calculations and a sample output are attached in appendix Q. The summary of calculation results are shown in tables 5.8, 5.9 and 5.10.

First let us examine the effect of downstream pressure on the liquid-vapor phase boundary shown in table 5.8. The table shows the results for the phase boundary calculations at feed temperature of 25°C and acetic acid feed mole fraction of 0.50. For the downstream pressure of 467 Pa (3.5 mm Hg) the vapor-filled region has the

Table 5.8: Effect of Downstream Pressure on the Phase Boundary

Downstream Pressure Pa (mm Hg)	$\frac{\delta_a}{\delta}$ Relative Liquid-Filled Region	$\frac{\delta_b}{\delta}$ Relative Vapor-Filled Region
467 (3.5)	0.15	0.85
1200 (9.0)	0.22	0.78
2666 (20.0)	0.74	0.26

highest value. As the downstream pressure increases from 467 Pa (3.5 mm Hg) to 2666 Pa (20 mm Hg) the proportion of vapor-filled region decreases from 0.85 to 0.26. As the vapor-filled region is the part where selectivity takes place, the decrease in the vapor-filled portion shows the decrease in selectivity. This observation is in agreement with the pervaporation data at these downstream pressures. In the pervaporation experiments the lowest selectivity was observed for the highest downstream pressure. At the downstream pressure of 2666 Pa (20.00 mm Hg), the membrane was almost totally filled with the liquid. The relative liquid-filled region was 0.74 in this case. As the total saturation vapor pressure of the mixture is very close to 2666 Pa (20.00 mm Hg) at this temperature, it is quite reasonable to expect that the phase was mostly liquid. This is similar to the case in reverse osmosis, where both feed and downstream are in liquid phase. Thus, the transport model can describe the experimental data very well.

The effect of the feed composition on the vapor-liquid phase boundary is shown in table 5.9. These data correspond to the downstream pressure of 467 Pa (3.5 mm Hg) and the feed temperature of 25°C. A definite trend in the value of the relative vapor-filled portion can be noticed when the acetic acid mole fraction is increased from 0.13 to 0.50. The relative vapor-filled portion increased from 0.51 to 0.85. In other words, the membrane selectivity should increase as the mole fraction of acetic acid is increased or the water mole fraction is decreased. Referring back to the pervaporation

Table 5.9: Effect of Feed Composition on the Phase Boundary

Mole Fraction of Acetic Acid in Feed	$\frac{\delta_w}{\delta}$ Relative Liquid-Filled Region	$\frac{\delta_h}{\delta}$ Relative Vapor-Filled Region
0.13	0.49	0.51
0.25	0.48	0.52
0.37	0.44	0.56
0.50	0.15	0.85
0.65	0.28	0.72

data of the binary mixture at the same process conditions, it is evident that lower mole fraction of water in the binary mixture led to higher separation factors (refer to table 5.1). Therefore, the observed trend of the pervaporation data is in agreement with the prediction using the transport model. However, once the feed concentration of acetic acid increases further, the relative vapor-filled region diminishes to 0.72.

The effect of temperature on the phase boundary is shown in table 5.10. These data correspond to a downstream pressure of 467 Pa (3.5 mm Hg) and acetic acid mole fraction in feed of 0.50. From the table it is evident that the relative vapor-filled portions corresponding to the feed temperature of 25°C and 40°C are close, 0.85 and 0.86, respectively. But, at the feed temperature of 35°C, the vapor-filled portion was the least, i.e. 0.79. It should be recalled that the phenomenon of concentration polarization occurring inside the membrane was observed only at 35°C. Thus, a moderate selectivity occurring inside the membrane was attributed to one of the factors leading to the phenomenon of concentration polarization. During the steady state pervaporation experiments, the selectivity at 25°C and 40°C was the same, which can be explained by the same phase boundary position in the two cases.

The table 5.11 shows the summary of the calculated data using the transport model. The table shows the acetic acid mole fraction at different positions inside

Table 5.10: Effect of Temperature on the Phase Boundary

Feed Temperature °C - -	$\frac{\delta_a}{\delta}$ Relative Liquid-Filled Region	$\frac{\delta_b}{\delta}$ Relative Vapor-Filled Region
25	0.15	0.85
35	0.21	0.79
40	0.14	0.86

the membrane. Relative mass transfer coefficients are also presented in table 5.11 taking the mass transfer coefficient at the downstream pressure of 467 Pa (3.5 mm Hg), feed temperature 25°C and at the acetic acid mole fraction of 0.5 to be the basis. The absolute value of the mass transfer coefficient corresponding to the above process conditions is 6.24×10^{-8} m/s. The mass transfer coefficient at the downstream pressure of 2666 Pa (20.00 mm Hg) is close to zero. This pressure is close to the total saturation vapor pressure of the feed mixture at these conditions.

The penetrant concentration profile inside the membrane was predicted using the newly-developed transport model. The prediction was made using the vapor-liquid equilibrium data, pure component permeation data, liquid sorption data, vapor sorption data and the pervaporation data. The prediction using the transport model was compared to the experimental penetrant concentration profile. Six representative figures are shown in this section of this chapter. Other figures are attached in the Appendix P. Both experimental and the predicted penetrant concentration profiles corresponding to the same process conditions are plotted on the same figure. Figures 5.15, 5.16 and 5.17 show the total sorbed amount of the penetrants in the membrane phase plotted against the relative distance inside the membrane. Figure 5.15 corresponds to the downstream pressure of 467 Pa (3.5 mm Hg), feed temperature of 25°C and acetic acid mole fraction of 0.5 in the feed mixture. Figure 5.16 shows the results at the downstream pressure of 467 Pa (3.5 mm Hg), feed temperature of 25°C and

Table 5.11: Summary of Calculation Data Showing Acid Mole Fraction in the Membrane Phase at Different Positions

Down-stream Pressure Pa -	Tempe-rature °C -	Mole Fraction of AA in Bulk Solution -	Mole Fraction of AA at Feed-Liquid-Membrane Interface -	Mole Fraction of AA at Liquid-Vapor Boundary: Liquid-Filled Region -	Mole Fraction of AA at Liquid-Vapor Boundary: Vapor-Filled Regio -	Mole Fraction of AA in Down-stream -	Relative Mass Transfer Coeffi cient
467	25	0.50	0.16	0.19	0.05	0.07	1.00
1200	25	0.50	0.16	0.17	0.04	0.10	1.39
2666	25	0.50	0.16	0.16	0.03	0.12	
467	25	0.13	0.09	0.15	0.03	0.07	0.22
467	25	0.25	0.12	0.17	0.04	0.07	0.30
467	25	0.37	0.14	0.17	0.04	0.07	0.65
467	25	0.65	0.24	0.27	0.06	0.07	1.49
467	35	0.50	0.16	0.17	0.04	0.07	1.58
467	40	0.50	0.17	0.17	0.05	0.07	3.62

acetic acid mole fraction of 0.25 in the feed mixture. Figure 5.17 shows similar data at 35°C (downstream pressure of 467 Pa and acetic acid mole fraction in feed solution 0.50). From these figures it is evident that the agreement between the predicted values and the experimental values is reasonable in all three cases.

The calculated values of the total penetrant in the membrane shows a steep decline at the phase boundary. This steep decline reflects the large difference in the sorbed amount depending on whether the sorption was from the liquid or the vapor phase. The amount sorbed from the liquid phase was an order of magnitude higher than that from the vapor phase.

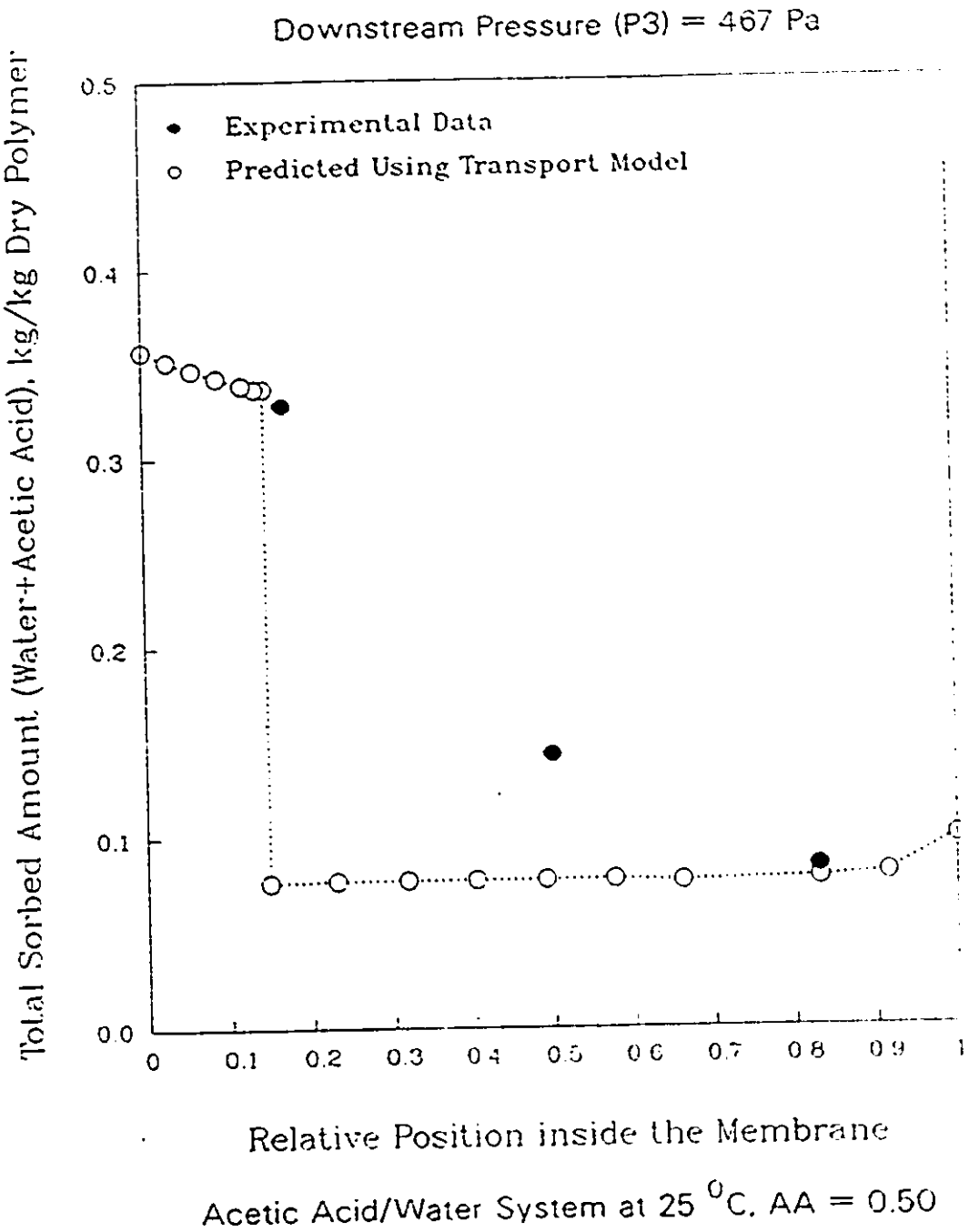

Figure 5.15: Calculated Penetrant Profile Compared with the Experimental Data

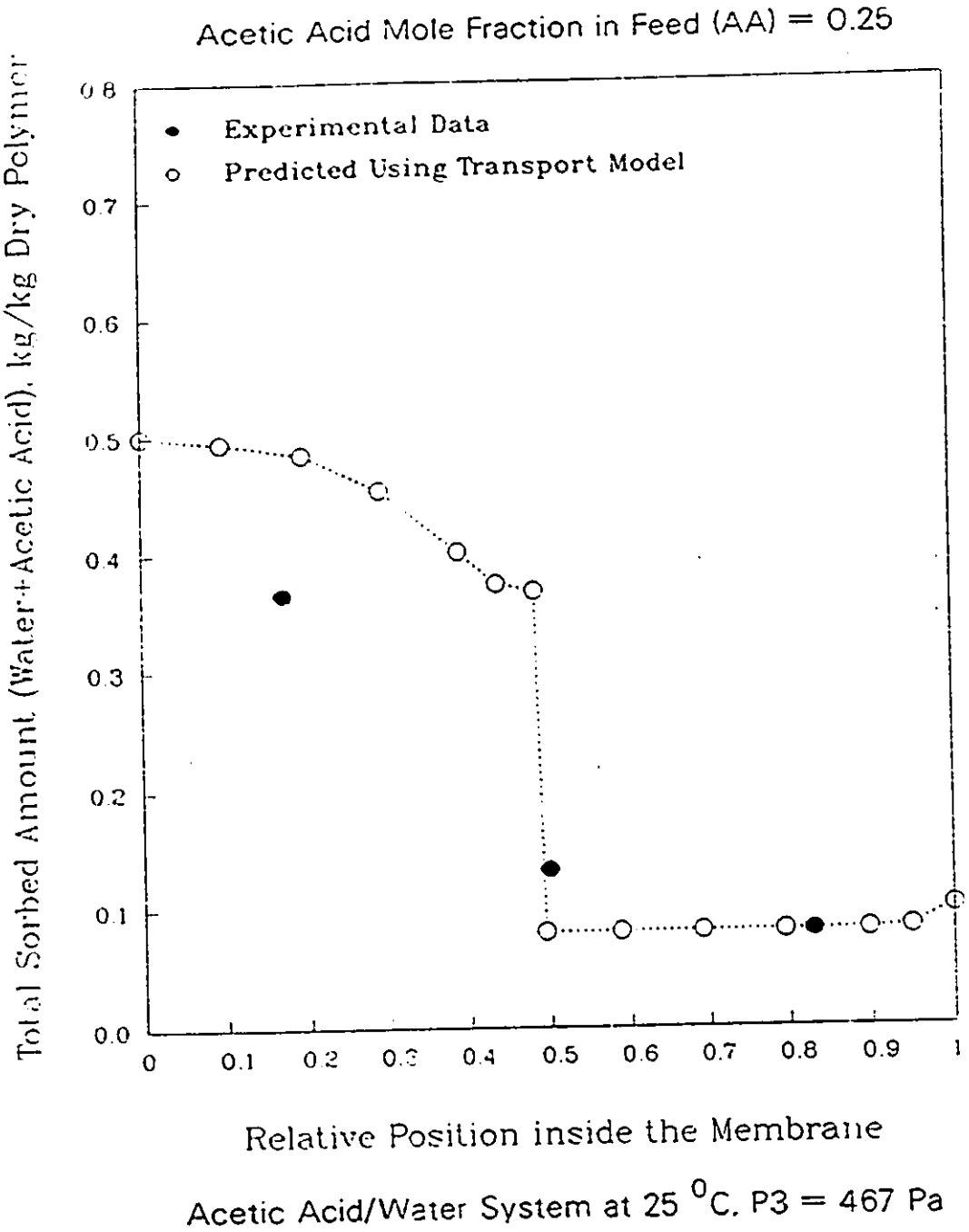

Figure 5.16: Calculated Penetrant Profile Compared with the Experimental Data

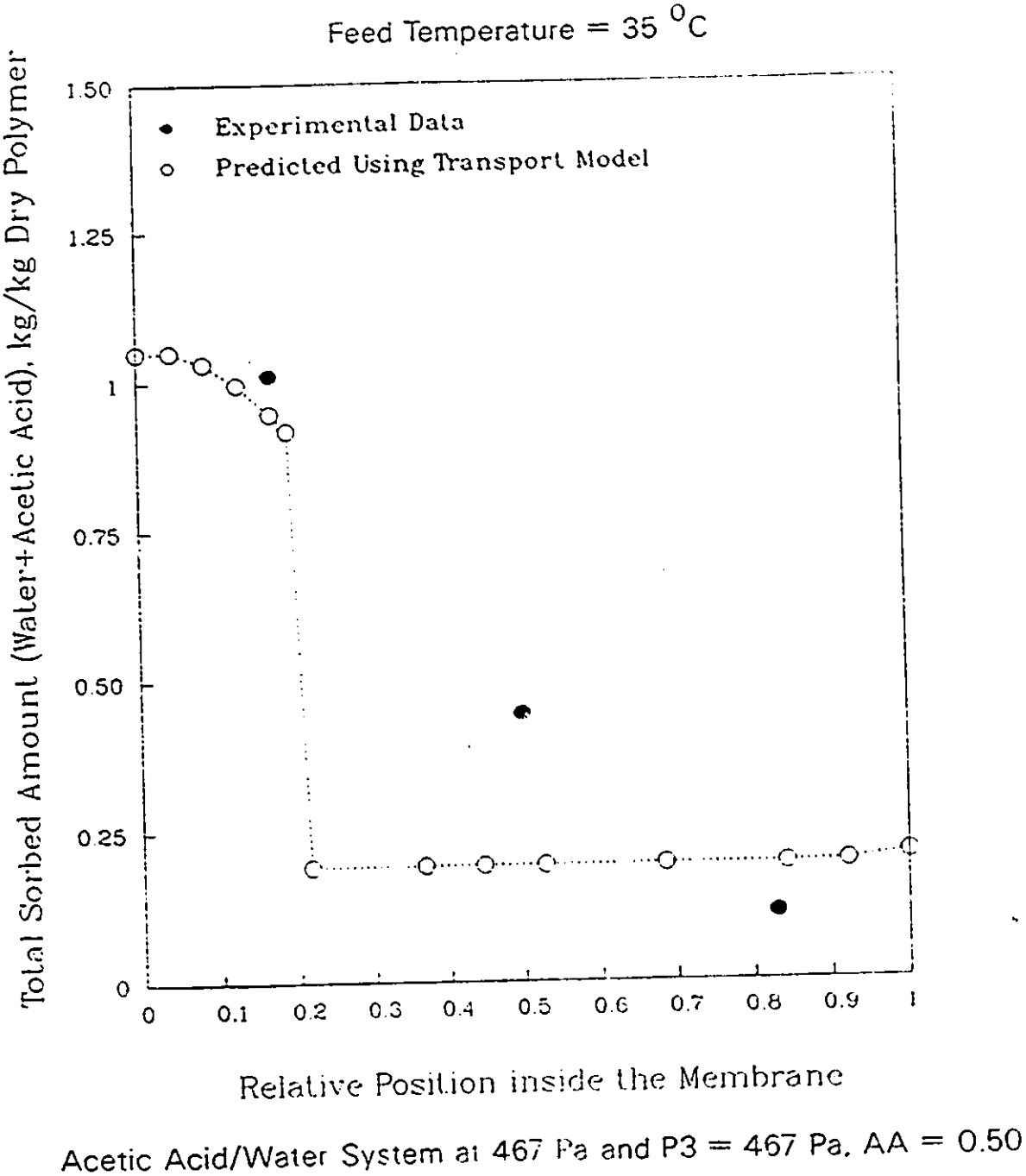

Figure 5.17: Calculated Penetrant Profile Compared with the Experimental Data

Figures 5.18, 5.19 and 5.20 show the calculated results for acetic acid mole fraction profile compared with the experimental one. The mole fraction is plotted against the relative distance inside the membrane in these figures. There are only three experimental points available. Therefore, the prediction of the position of the phase boundary inside the membrane depends very much upon the manner in which these points are joined together. An additional data point can be obtained at the membrane-feed liquid interface from equilibrium liquid sorption experiments. However the point at the membrane-feed solution interface is not plotted in these figures. Figure 5.18 shows the data at the downstream pressure of 467 Pa (3.5 mm Hg) and at the feed temperature of 25°C. In the experimental data the relative position of the maximum for acetic acid mole fraction inside the membrane corresponds to the liquid-vapor phase boundary. The relative position obtained from the experimental data was 0.18. The predicted value for the relative position of the maximum using the newly developed transport model was 0.15. In figure 5.19 the experimental data shows that the relative position of the maximum in the mole fraction of acetic acid was 0.45 (roughly, depending how three points are joined together). The predicted value for the relative position was 0.48, which is in good agreement with the experimental data. Similarly, in figure 5.20 the relative position of the maximum from the experimental data was 0.16 as compared to the 0.14 obtained from the calculation using the transport model. The position of the maximum indicates the relative liquid-filled portion of the membrane. Other figures are presented in the appendix P. Therefore, the transport model is able to describe the qualitative behavior of experimental data quite well.

It should be recalled that the coupling between the flow of two penetrants (acetic acid and water in this case) was considered in the liquid-filled section of the membrane. The coupling was not considered in the vapor-filled section of the membrane. If the coupling phenomenon in the vapor-filled region is also quantified and incorporated into the transport model, the agreement with the experimental data would be even better. On the other hand, the transport model would become more complex as compared to the present simple and easy-to-use model.

It should also be pointed out that the phenomenon of concentration polarization

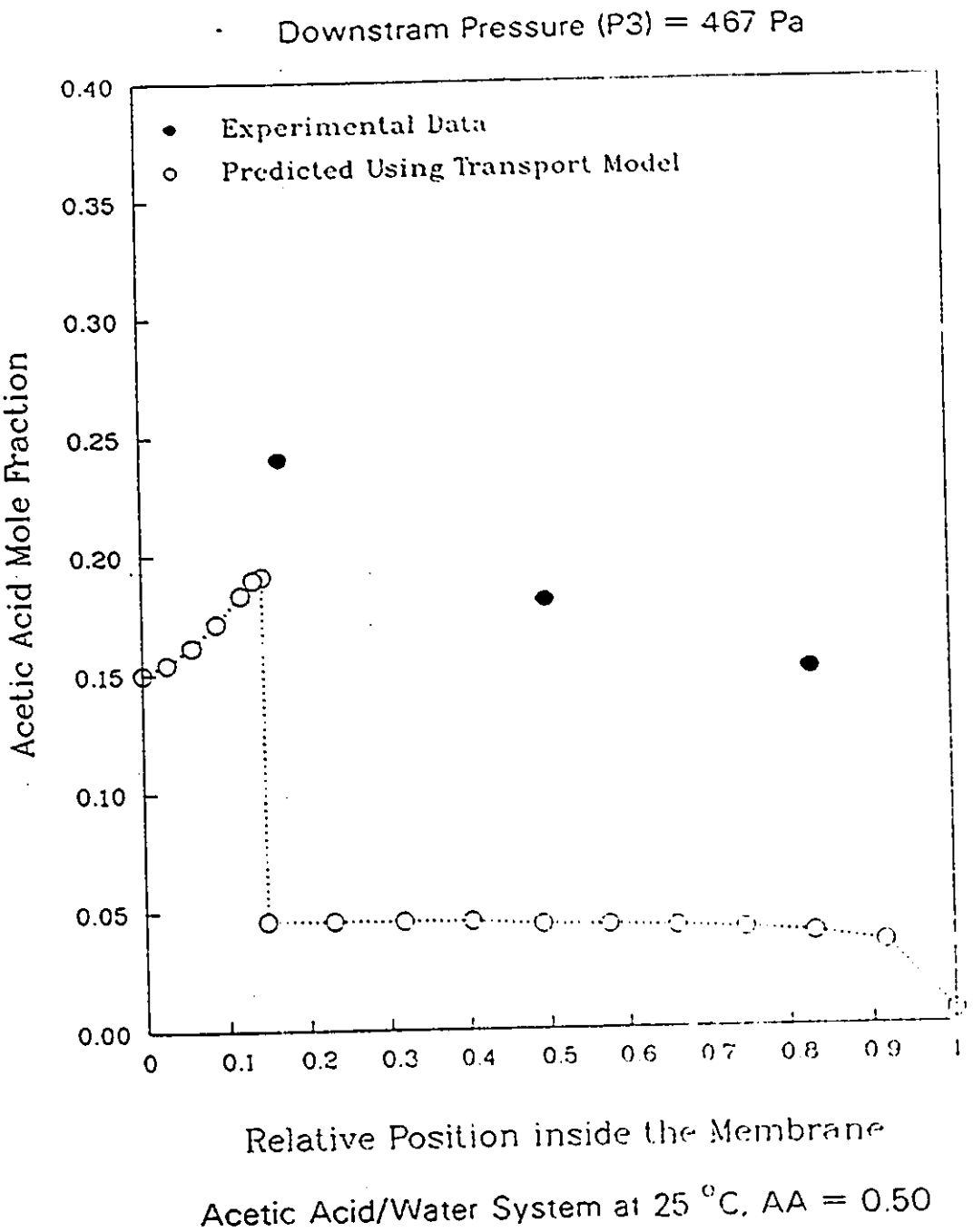

Figure 5.18: Calculated Penetrant Profile Compared with the Experimental Data

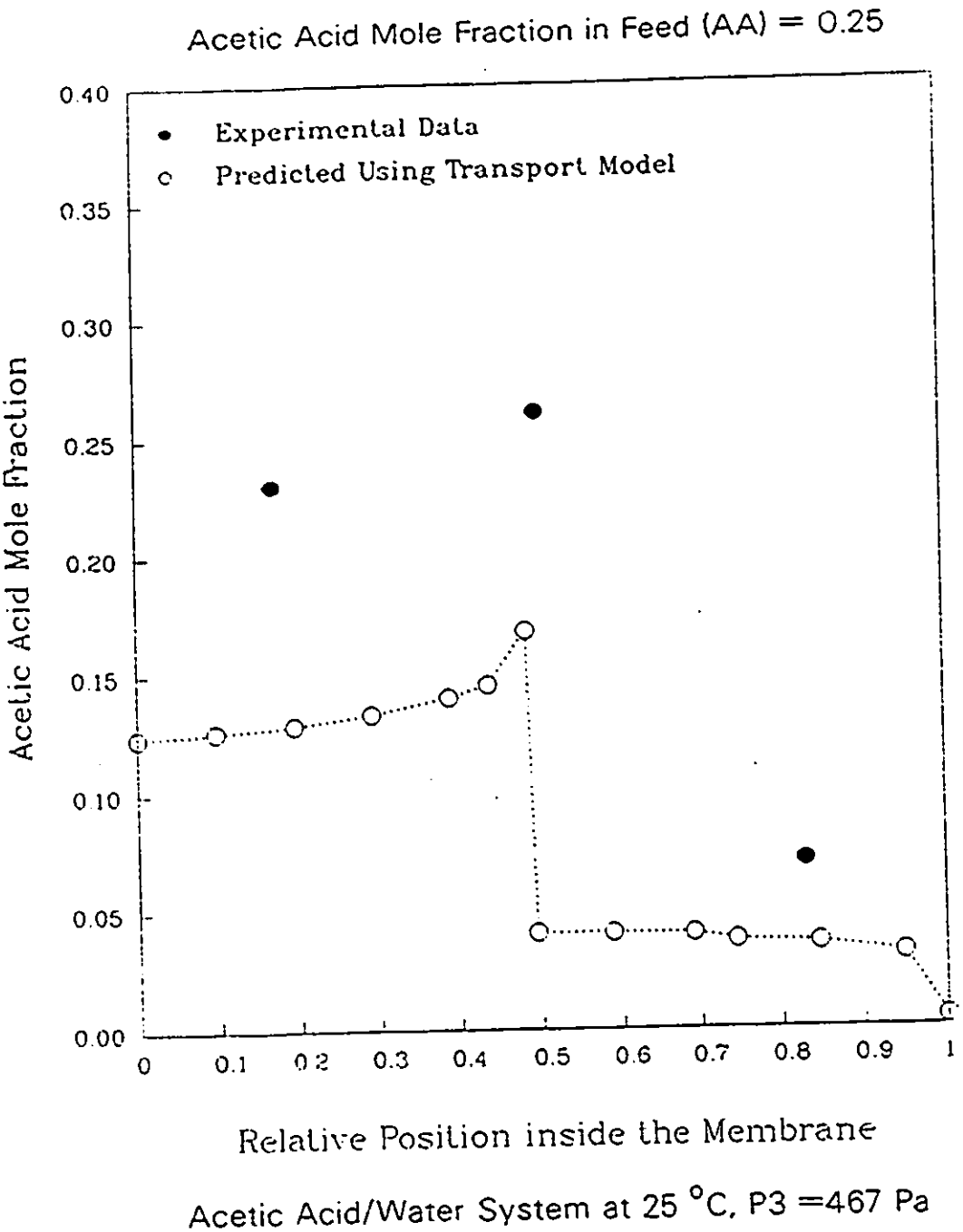

Figure 5.19: Calculated Penetrant Profile Compared with the Experimental Data

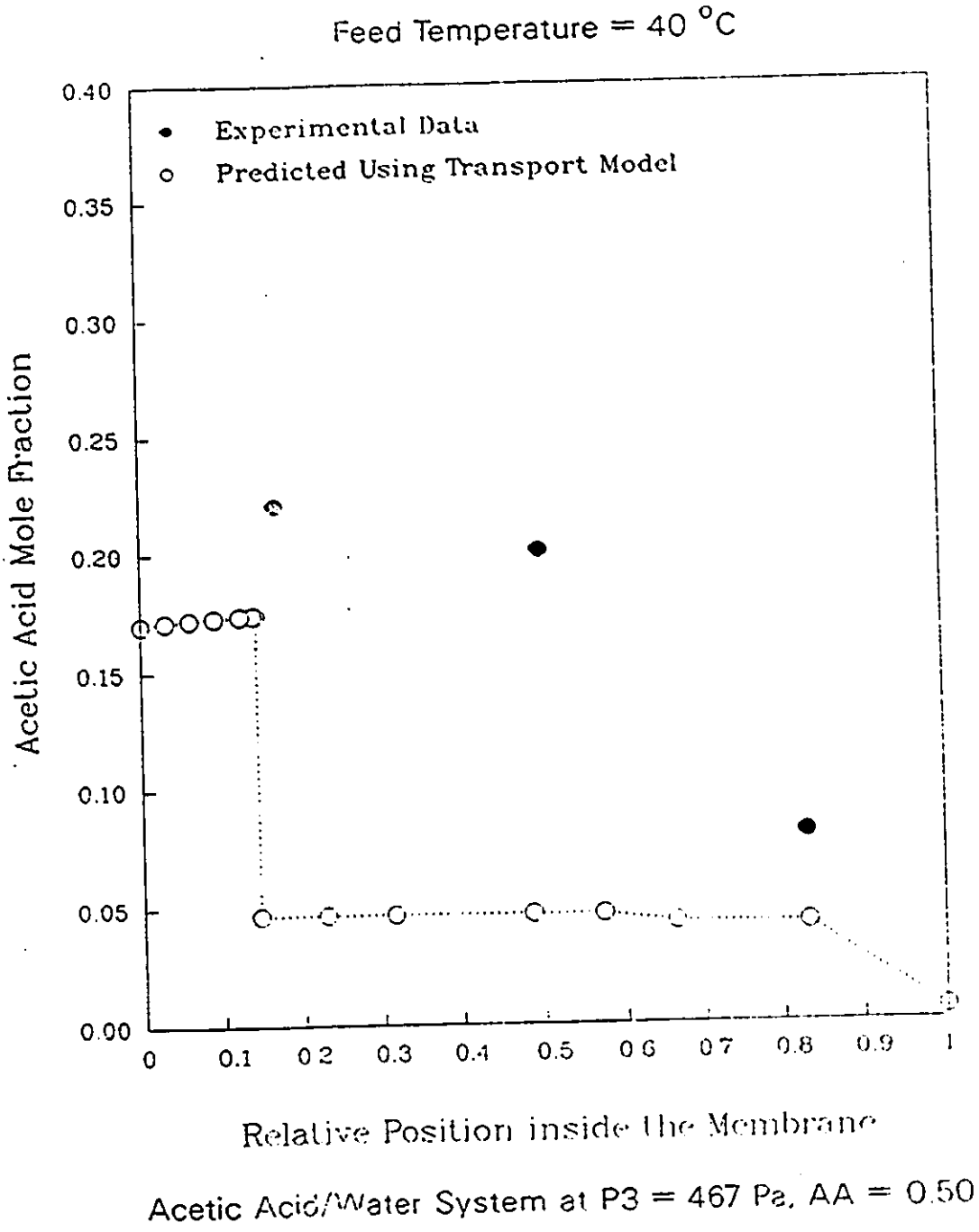

Figure 5.20: Calculated Penetrant Profile Compared with the Experimental Data

occurring inside the membrane was first reported in the present work. Other transport models available in the literature fail to predict this phenomenon. Therefore, the present work is the first theoretical work that can reconstruct the penetrant concentration profiles inside the membrane showing concentration polarization. The present work is also the first attempt to examine the predictability of the newly-developed transport model.

5.9 Calorimetric Studies for the State of Permeant

The system polyamide membrane-water-acetic acid was investigated by calorimetry. Measurements were made with a Setaram heat-flow calorimeter. Scans were made at the heating rate of 10 Kh^{-1}. The scans were made for the membrane sample alone, aromatic polyamide membrane-acetic acid and membrane-water system. The precision of calorimeter calibration was ± 1 % in the range 85 to 100 K and ± 0.5 % over the rest of the temperature range.

Figure 5.21 shows the scan on a 0.942 g sample of polyamide membrane. There is a broad endothermic transition starting at about 310 K. On completion of the latter transition, the sample was cooled back to room temperature and weighed. The sample lost 13.9% of its mass. On second heating, no mass loss was observed.

The results obtained for the membrane-acetic acid system were the most interesting. Figure 5.22 shows the scan on a 1.104 g sample of membrane (aromatic polyamide) containing acetic acid from the liquid phase. The amount of acetic acid present represented full saturation of the membrane with liquid phase at 25°C which is 0.111 kg/kg of dry polymer. The experimentally measurable parameters by DSC are the depression in freezing and melting points, and heats of solidification and melting. Melting point of acetic acid is 290 K. However, as seen in figure 5.22, no phase transition corresponding to melting of acetic acid in the membrane was observed. It means that acetic acid present inside the membrane did not melt as we would expect when acetic acid melts in a bulk form. At this point the data of saturation vapor pressure of acetic acid calculated based on the permeation data should be recalled (figure 5.3). This value was higher than the literature value of the saturation vapor pressure. Now, from DSC studies we conclude that acetic acid present inside the membrane does not show a melting peak at all. Based on these two results it can be concluded that acetic acid in the membrane is present only in the non-freezable bound state.

The total amount of acetic acid present in the membrane was 0.154 g. Melting of

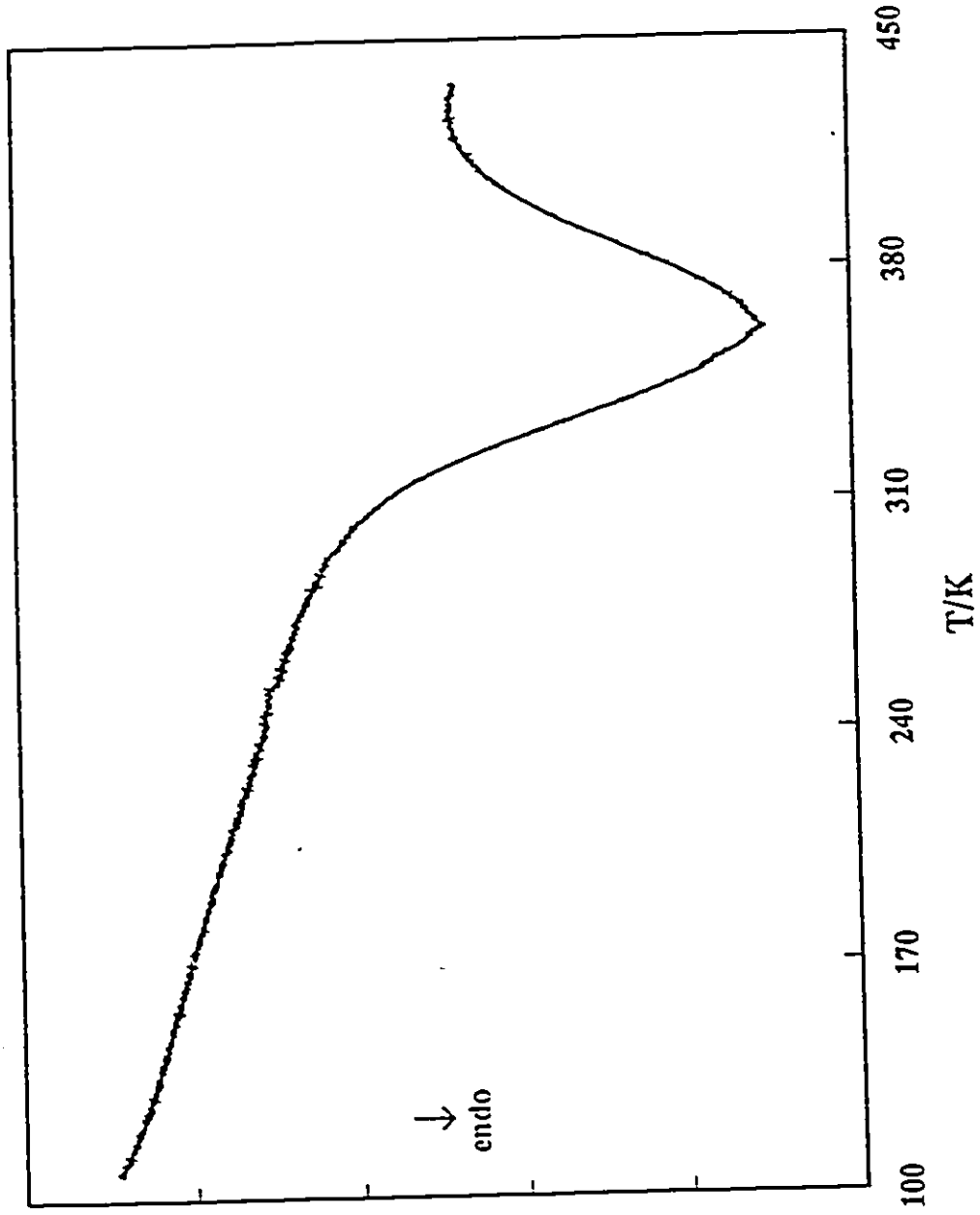

Figure 5.21: Calorimetric Analysis of Polyamide Membrane

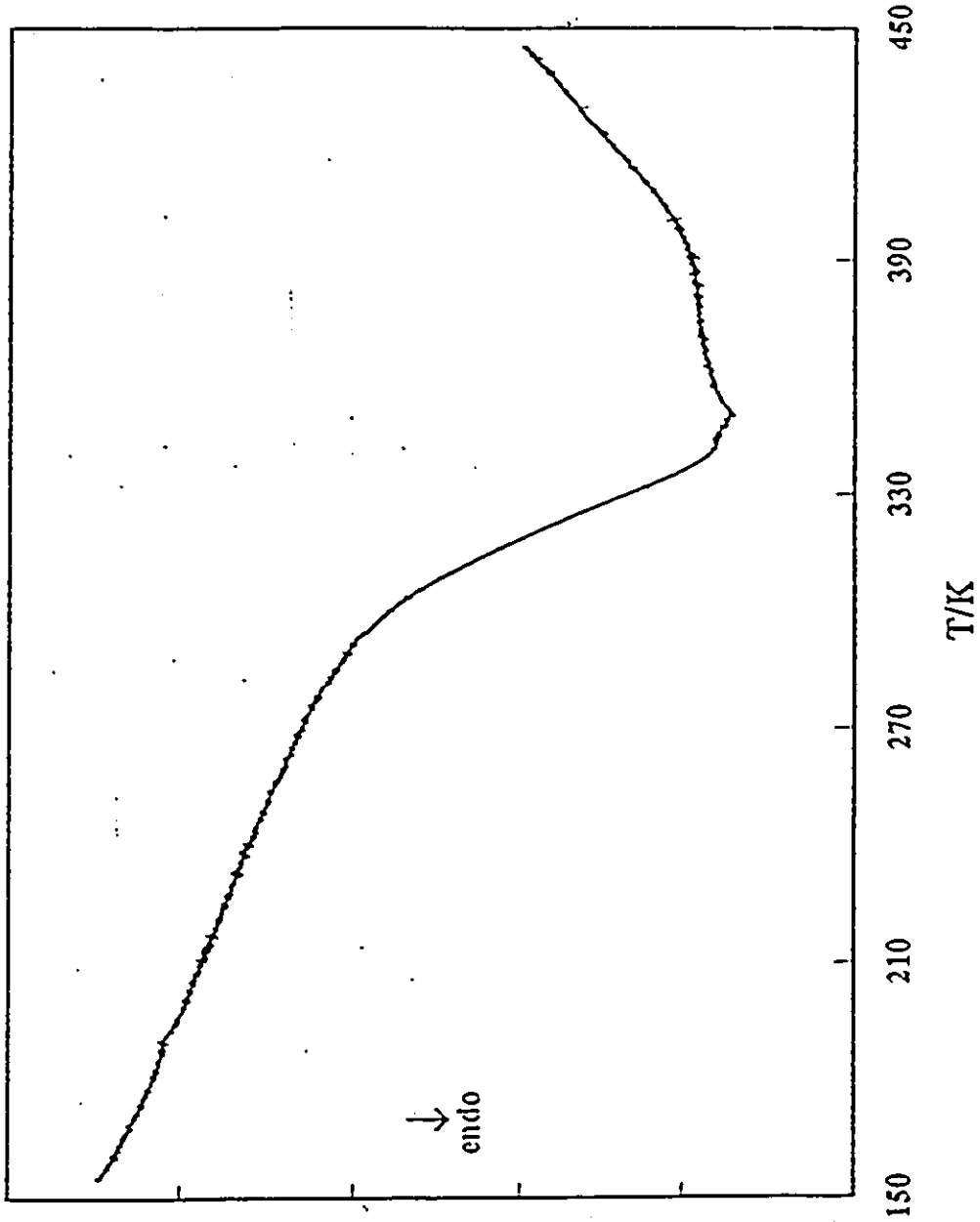

Figure 5.22: Calorimetric Analysis of Polyamide-Acetic Acid System

0.154 g of acetic acid requires 30 J which should give a large calorimetric signal. For comparison, 0.154 g of acetic acid was placed in the calorimeter cell, frozen, and then scanned at the rate of 10 Kh^{-1}. The calorimeter showed a sharp peak. The acetic acid used in this work (Anachemia, Reagent Grade) melted at 289.2 K and the heat of melting was determined to be 185.6 Jg^{-1} (literature value being 195.3 Jg^{-1}). This discrepancy is attributed to some impurity in the the sample. Figure 5.22 indicates no melting peak (transition) for acetic acid, therefore, it appears that all the acetic acid in the membrane is present in the non-freezable bound state.

Another sample of 0.265 g dry polymeric membrane containing 0.154 g water (58 % by mass) sorbed from the liquid phase was also studied. The water concentration represents saturation solubility at room temperature. The results are shown in figure 5.23. The interesting result in figure 5.23 is that, unlike acetic acid, water did undergo melting transition at 273.2 K. The heat of melting was determined to be 201.2 Jg^{-1}. Heat of melting of bulk ice is 333.5 Jg^{-1}. Thus there is a depression in heat of melting of water in the membrane. To determine the relative amounts of bound and bulk-like water scans on a number of membrane samples containing varying levels of water will be required. However, for the present work, this work was deemed to be sufficient. The depressed heat of melting indicated that though water could undergo bulk-like freezing transition, it was present in confined geometries provided by the pores in the membrane or the spacing between the junction points of the polymer.

The transport of the bound penetrant is expected to be slower than that of the bulk fluid, the friction experienced by the penetrant being dependent on the strength of the polymer-penetrant interaction. From the DSC data described above we are able to conclude that water should transport faster through the polyamide membrane than acetic acid. This result is in accordance with the data obtained in our pervaporation studies.

At this point the data obtained for saturation vapor of acetic acid from the pure component permeation should be recalled. A higher value than that found in the literature was obtained for acetic acid. The anomaly in the saturation vapor pressure can be explained based on thermodynamic arguments. The experimental saturation vapor pressure found to be higher than the literature value can be explained if we

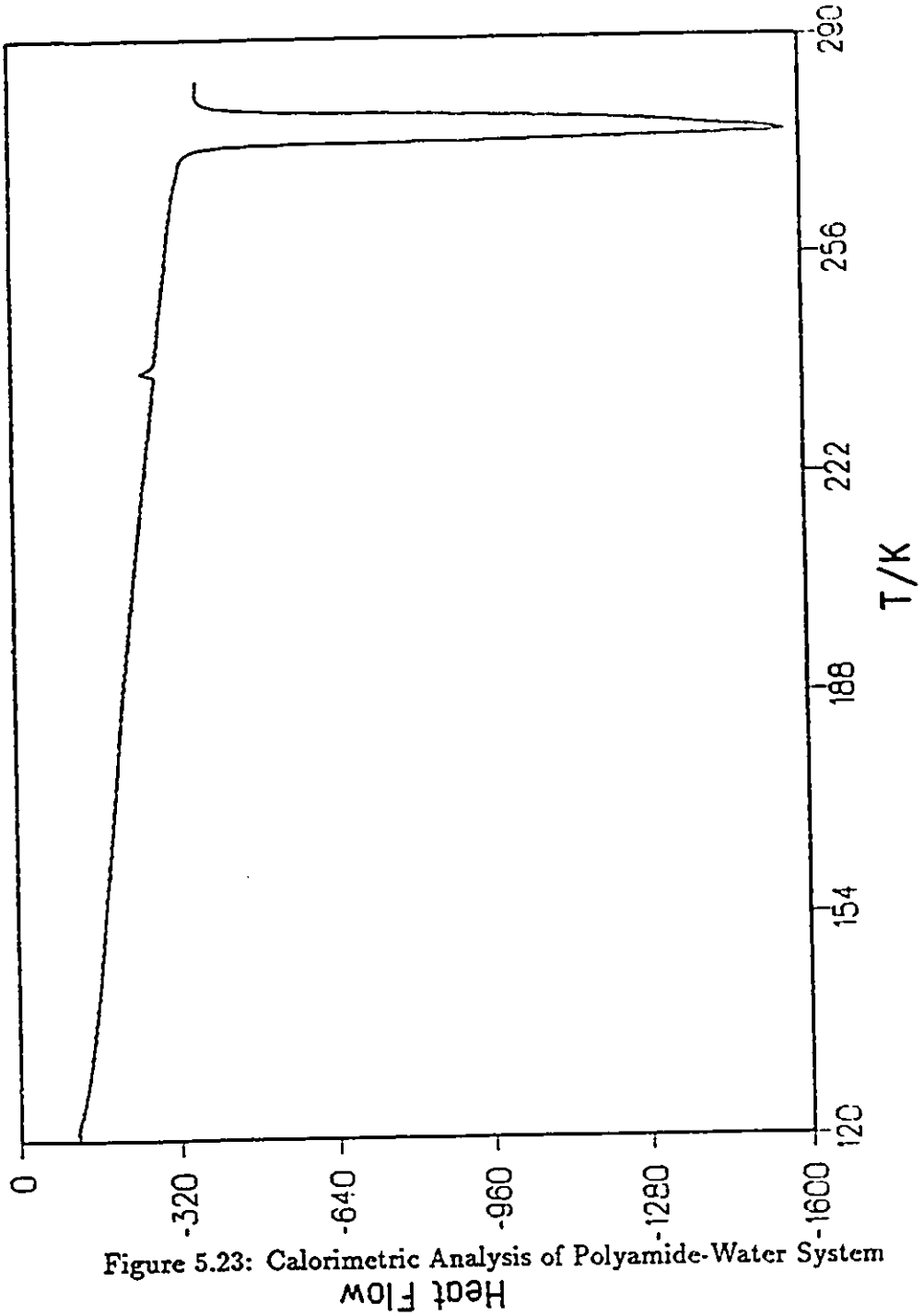

Figure 5.23: Calorimetric Analysis of Polyamide-Water System

consider the supersaturation in the membrane.

5.10 Spectroscopic Studies

Spectroscopic studies were also performed for acetic acid-water and polyamide system. Spectrographs were obtained for dry polyamide membrane and for the membrane soaked in acetic acid. The objective of these studies was to investigate the type of interaction acetic acid has with the polyamide membrane.

Figures O.1 and O.2 are shown in the appendix O. Figure O.1 shows the IR spectra for the polyamide control membrane. Figure O.2 shows the IR spectra for the polyamide membrane soaked in acetic acid. These spectra are the same from the qualitative point of view, indicating that there was no chemical change in the polymer after being soaked in acetic acid. However, the characteristic peaks of acetic acid which should be observed at 1710 wavenumbers shifted to 1708 wavenumbers. These spectrograms indicate that there is a strong physical interaction between acetic acid and aromatic polyamide polymer.

5.11 Implications of the Experimental Data for the Membrane Design

In the present study a transport model was used which considers both phases (liquid and vapor) inside the membrane. It was assumed that the part filled with liquid is nonselective and the part filled with vapor is selective. Based on these assumptions an analysis of the binary mixture permeation led to the possibility of the concentration polarization occurring inside the membrane. This theoretical prediction was substantiated with the help of experimental data obtained. The phenomenon of concentration polarization occurred in some specific cases but not in all cases.

Another important finding from the experimental data was that the amount of the sorbed species inside the membrane was higher than that of the equilibrium sorption value in some cases. This phenomenon can be termed as supersaturation. Based on this phenomenon it was concluded that the polymer structures during steady-state pervaporation and equilibrium sorption are different. During steady-state pervaporation a dynamic equilibrium is established which is different from the static equilibrium established during equilibrium sorption experiments. In view of these two important observations, some questions arise:

1. Is the concentration polarization inside the membrane favorable for the system performance?

2. Is the supersaturation favorable for the pervaporation permeation rate and selectivity?

The typical concentration polarization equation involves the term $exp(v/k)$, which represents concentration polarization modulus. This term should be minimized in order to minimize the concentration polarization phenomenon. In the above expression v is defined by equation 3.32 and is the penetrant permeation velocity. The mass transfer coefficient, which is the ratio of diffusion coefficient and the thickness of the boundary layer adjacent to the membrane ($\frac{D}{\delta_a}$), is denoted by k (refer to equation D.9). Here D represents the diffusion coefficient of penetrant in the liquid-filled region and δ is the interfacial boundary layer thickness.

There are two possibilities to minimize this term. The first one is to lower v, which is impractical since an increase in v is normally desirable. The other possibility is to maximize k, i.e. maximize the mass transfer coefficient. Mass transfer can be maximized either by:

- reducing the thickness of the interfacial layer,
- or by increasing the value of the diffusion coefficient D.

In the present case, the interfacial layer represents the liquid-filled region of the pore or the layer where liquid transport takes place. For pervaporation, the diffusivity of the penetrant inside the membrane is a function of the penetrant concentration in the membrane. A high concentration of the penetrant inside the membrane results in a greater value of diffusivity.

From all the pervaporation data obtained it was quite clear that the permeation rate was greater when the concentration of the penetrant inside the membrane was greater in the liquid-filled portion of the membrane. For example, for the pure water permeation case, the highest permeation rate (1.62×10^{-3} mol/s-m^2) was observed while the sorbed amount of the penetrant in the liquid-filled region (section 1) was also the highest (0.718 kg/kg of dry polymer). Therefore, higher penetrant concentration in the membrane will lead to greater diffusivity value, greater mass transfer coefficient and, eventually, to greater total permeation rates.

Thus, minimization of concentration polarization is favorable to obtain greater permeation rates and lower concentration polarization modulus. In conclusion, concentration polarization occurring inside the membrane has negative side effects e.g., lower permeation rate and lower selectivity.

From the experimental data of concentration profiles obtained for binary mixture at different downstream pressures, it was evident that at lower downstream pressure the membrane was more swollen on the liquid side. Whereas, at the same downstream pressure the membrane was the most dry on the downstream side, and at this downstream pressure the highest selectivity was obtained. On the other hand the feed temperature did not have any effect on the selectivity of the membrane. Higher

permeation rates were obtained at higher temperatures. Normally, to maximize the driving force for a given feed mixture, an engineer can either raise feed temperature or lower the downstream pressure.

A novel composite pervaporation membrane can be designed based on the above observations. This membrane should utilize a bottom layer for selectivity, hence it should be a dense and selective layer. The top layer should have good interaction with the preferentially permeating component in the downstream. A dense polymeric base film (to achieve high selectivity) should be coated with a thin layer of hydrophilic polymer for the purpose of preferential permeation of water from a water-acetic acid mixture. In order to achieve high permeation rates the base membrane should not be very dense otherwise the permeation rate will be sacrificed. The top layer should also be as thin as possible. The following requirements must be satisfied for the design of composite membranes:

1. The thickness of the layer, where the liquid transport takes place, should be as thin as possible to increase the mass transfer coefficient of the layer.

2. The coated layer should be as highly swollen as possible to increase the penetrant diffusivity.

3. The bottom layer, where the vapor transport takes place, should be dense (but not too thick) so that a high selectivity can be achieved.

In asymmetric membranes, when the depth of the liquid phase exceeds the thickness of the top (skin) layer the phase boundary is located in porous sublayer. Thus, the small pores in the top skin layer, which would be most selective, cannot be effectively utilized for vapor transport. Instead, larger pores at the transition layer are used for vapor transport. As a result the selectivity of the membrane is lowered. If deep liquid penetration can be prevented, so that the small pores of the top skin layer can be utilized for vapor transport alone, the membrane selectivity will increase. One possible method to achieve the above objective would be to coat the top surface of the asymmetric membrane with another membrane. The coating material should have the desired properties mentioned in the above discussion (good solubility to

preferentially permeating component). Note the case when the membrane which was highly swollen in section 1 (liquid part), gave the highest permeation. For example for the separation of water from an aqueous-organic mixture, one could conceive of a hydrogel that could be used to coat an asymmetric membrane.

Chapter 6

Conclusions

Based on the experimental data presented the following conclusions can be drawn:

1. Aromatic polyamide membranes are preferentially permeable to water.

2. The newly established theory, where the chemical potential gradient is considered as the driving force for the flow of the penetrant, leads to the same mathematical relationships as derived by the pore model.

3. Experimental results show the evidence of the presence of concentration polarization occurring inside the membrane which has been theoretically predicted.

4. The concentration polarization occurring in the membrane should be minimized. The minimization of this phenomenon is favorable to obtain greater permeation rates during steady state pervaporation. Concentration polarization modulus can be minimized by:

   - keeping the liquid-filled region $\frac{\delta_A}{\delta}$ as small as possible.
   - keeping penetrant concentration of the preferentially permeating component in the liquid-filled region of the membrane as high as possible.

5. The newly developed transport model can describe the qualitative behavior of the experimental data. Therefore, the present work is the first theoretical work

that can reconstruct penetrant profiles inside the membrane showing concentration polarization.

6. Static equilibrium attained during equilibrium sorption experiments is different from the dynamic equilibrium attained during steady-state pervaporation.

7. All of acetic acid present in the membrane is in the bound state, whereas some water is present in bulk-like state in the polymeric membrane.

8. Higher sorption of penetrant during steady-state pervaporation leads to higher permeation rates.

A novel membrane design for pervaporation separation has been proposed. This membrane is a composite membrane consisting of two distinct layers. The top layer should be as thin as possible. The top part of the polymeric membrane should have strong interaction with the preferentially permeating component of the mixture. The bottom layer should be the selective layer and should be dense.

Chapter 7

Recommendations and Future Directions

- The newly developed transport model is a useful working tool for correlating and predicting binary mixture separations. However, it would be even more useful if thermal effects associated with the latent heats of evaporation were included in the model. Depending on permeation rate, such effects can invalidate the assumption of isothermal operation.

- The coupling was considered in liquid-filled region of the membrane but was not considered in the vapor-filled region of the membrane. The phenomenon of coupling should be quantified and incorporated in the vapor-filled region of the membrane also.

- The parameters $\frac{A}{\delta}$ and $\frac{B}{\delta}$ used in the transport model are lumped parameters. These parameters should be split into various parameters related to different physico-chemical phenomena to properly reflect the effect of the physico-chemical interaction between the penetrant and the membrane.

- The penetrant concentration profiles should be established for a polymeric membrane of graded morphology. This membrane will model an asymmetric membrane. For example, a stack of 9 membranes having 3 symmetric membranes of

small pore size and 6 membranes of larger pore size can be used for this purpose.

- The effect of membrane morphology (pore size and pore size distribution) on pure component permeation should be studied. This study will give an insight into the effect of morphology on the interaction of penetrant(s) with the polymeric membrane. For example, in the present study the saturation vapor pressure obtained from the experimental pervaporation data of pure component permeation was higher than the literature value. Studies should be carried out for the same polymeric membrane having a different morphology. These studies will help to tailor our membrane design for pervaporation separation.

References

- Aptel, P., N. Challard, J. Cuny and J. Neel, "Application of the Pervaporation Process to Separate Azeotropic Mixtures," J. Membrane Sci. 1, 271-287 (1976)

- Aptel, P., J. Cuny, J. Jozefonvicz, G. Morel and J. Neel, "Liquid Transport Through Membranes Prepared by Grafting of Polar Monomers Onto Poly(tetrafluoroethylene) Films. II. Some Factors Determining Pervaporation Rate and Selectivity," J. Appl. Poly. Sci. 18, 351-364 (1974 A)

- Aptel, P., J. Cuny, J. Jozefonvicz, G. Morel and J. Neel, "Liquid Transport Through Membranes Prepared by Grafting of Polar Monomers Onto Poly(tetrafluoroethylene) Films. III. Steady-State Distribution in Membrane During Pervaporation," J. Appl. Poly. Sci. 18, 365-378 (1974 B)

- Ballweg, A. H., H. E. A. Brüschke, W. H. Schneider, G. F. Tusel, K. W. Böddeker and A. Wenzlaff, "Pervaporation Membranes: An Economic Method to Replace Conventional Dehydration and Rectification Columns in Ethanol Distillaries," Proc. Fifth Int. Symp. on Alcohol Fuel Technology, Auckland, New Zealand, May 13-18, 1982

- Bartels-Caspers, C., Tusel-Langer and R. N. Lichtenthaler, "Sorption Isotherm of Alcohols in Zeolite-Filled Silicone Rubber and in PVA-Composite Membranes," J. Membrane sci. 70, 75-82 (1992)

- Bell, C. M., F. J. Gerner and H. Strathmann, "Selection of Polymers for Pervaporation Membranes," J. Membrane Sci. 36, 315-329 (1988)

- Best, M. E. and C. R. Moylan, "Diffusion of Water into a Photopolymer Film," J. Appl. Poly. Sci. **45**, 17-23 (1992)
- Binning, R. C., R. J. Lee, J. F. Jennings and E. C. Martin, "Separation of Liquid Mixtures by Permeation," Ind. Eng. Chem. **53**, 45-50 (1961)
- Bitter, J. G. A., "Transport Mechanism in Membrane Separation Processes," Koninklijke SHELL Laboratorium Amsterdam, 1990
- Blackadder, D. A. and J. S. Keniry, "The Measurements of the Permeability of Polymer Membranes to Solvating Molecules," J. Appl. Poly. Sci. **16**, 2141-2152 (1972)
- Blais, P., in "Reverse Osmosis and Synthetic Membranes," S. Sourirajan, Ed., National Research Council Canada, Ottawa, Chapter 9, 1977
- Bŏddeker, K. W., "Terminology in Pervaporation," J. Membrane Sci. **51**, 259-272 (1990 A)
- Bŏddeker, K. W. and G. Bengtson, "Pervaporation of Low Volatility Aromatics from Water," J. Membrane Sci. **53**, 143-158 (1990 B)
- Bŏddeker, K. W., G. Bengtson and H. Pingel, "Pervaporation of Isomeric Butanols," J. Membrane Sci. **54**, 1-12 (1990 C)
- Bŏddeker, K. W. and A. Wenzlaff, "Pervaporation With Ion Exchange Membranes," Proc. 1st Int. Conf. on Pervaporation Processes in the Chemical Industry, R. Bakish Ed., Bakish Materials Corp., Englewood N. J., pp. 96-110, 1986
- Bontoux, L. G. and D. S. Soane, "Sequential Vapor Sorption of Additional Penetrants in Preswollen Polymers," J . Appl. Poly. Sci. **38**, 915-922 (1989)
- Brun, J. P., C. Larchet, R. Melet and G. Bulvestre, "Modelling of Pervaporation of Dilute Aqueous Solutions of Organic Compounds Through Polymer Membranes," J. Membrane Sci. **23**, 257-283 (1985)

- Brunauer, S., P. H. Emmett and E. Teller, "Adsorption of Gases in Multimolecular Layers," J. Amer. Chem. Soc. **60**, 309-319 (1938)
- Brüschke, H. E. A., "State-of-the-Art of Pervaporation," Proc. 3rd Int. Conf. on Pervaporation Processes in Chemical Industry, R. Bakish Ed., Bakish Materials Corp., Englewood N. J., pp. 2-11, 1988
- Cabasso, I., J. Jagur-Grodzinsky and D. Vofsi, "Polymeric Alloys of Polyphosphonates and Acetyl Cellulose I. Sorption and Diffusion of Benzene and Cyclohexane," J. Appl. Poly. Sci. **18**, 2117-2136 (1974 A)
- Cabasso, I., J. Jagur-Grodzinsky and D. Vofsi, "A Study of Permeation of Organic Solvent Through Polymeric Membranes Based on Polymeric Alloys of Polyphosphonates and Acetyl Cellulose. II Separation of Benzene, Cyclohexene and Cyclohexane," J. Appl Poly. Sci. **18**, 2137-2147 (1974 B)
- Cabasso, I. and Z. Z. Liu, "The Permseiectivity of Ion-Exchange Membranes for Non-Electrolyte Liquid Mixtures, I. Separation of Alcohol/Water Mixtures with Nafion Hollow Fibers," J. Membrane Sci. **24**, 101-119 (1985)
- Carter, J. W. and B. Jagannadhaswamy, "Separation of Organic Liquids by Selective Permeation Through Polymeric Films," Brit. Chem. Eng. **9**, 523-526 (1964)
- Chen M. S. K., G. S. Markiewicz and K. G. Venugopal, "Development of Membrane Pervaporation TRIM^{TM} Process for Methanol Recovery from CH_3OH /MTBE /C4 Mixtures," AIChE Symp. Ser. No. 272, Vol. 85, 82-88 (1989)
- Choo C. Y., "Membrane Permeation," Adv. Petrol. Chem. **6**, 73-117 (1962)
- Cohen, M. H. and D. Turnbull, "Molecular Transport in Liquids and Glasses," J. Chem. Phys. **31**, 1164-1169 (1959)

- Deng, S. and S. Sourirajan, "Separation of Acetic Acid/Water by Pervaporation Using Laminated Hydrophobic and Hydrophilic Membranes," Proc. 4th Int. Conf. on Pervaporation Processes in Chemical Industry, R. Bakish Ed., Bakish Materials Corp., Englewood N. J., pp. 84-92, 1989

- Deng, S., S. Sourirajan and T. Matsuura, "A Study of Laminated Membranes for Separation of Acetic Acid/Water Mixtures by Pervaporation Process," Internal Report, IMRI, Dept. of Chem. Eng., Univ. of Ottawa, 1990

- Duggal, A. and E. V. Thompson, "Dependence of Diffusive Permeation Rates and Selectivities on Upstream and Downstream Pressures. VI. Experimental Results for the Water/Ethanol System", J. Membrane Sci. 27, 13-30 (1986)

- Farber, L., "Applications of Pervaporation," Science 82, 158 (1935)

- Fels, M. and R. Y. M. Huang, "Diffusion Coefficients of Liquids in Polymer Membranes by a Desorption Method," J. Appl. Poly. Sci. 14, 523-536 (1970)

- Fels, M. and R. Y. M. Huang, "Theoretical Interpretation of the Effect of Mixture Composition on Separation of Liquids in Polymer," J. Macromol. Sci. Phys. B 5, 89-110 (1971)

- Featherstone, W. and T. Cox, "Separation of Aqueous-Organic Mixtures by Pervaporation," Ind. Eng. Chem., Proc. Des. Dev. 16, 817-819 (1971)

- Flemming, H. L. and C. S. Slater, "Pervaporation," Part III in "Membrane Handbook," Ho, W. S. W. and K. K. Sirkar Ed., Van Nostrand Reinhold, N. Y., pp 103-132, 1992

- Fujita, H., "Diffusion in Polymer-Diluent Systems," Adv. Poly. Sci. 3, 1-47 (1961)

- Gan, L. H., P. Blais, D. J. Carlsson, J. Sprunchuk and D. M. Wiles, "Physicochemical Characterization of Some Fully Aromatic Polyamides," J. Appl. Poly. Sci. 9, 69-82 (1975)

- Ghosh, S. K. and B. S. Rawat, "Effect of Permeate Pressure in Liquid Permeation Process," Indian J. Technol. 4, 62-64 (1966)
- Gilliland, E. R., R. F. Baddour and J. L. Russell, "Rates of Flow Through Microporous Solids," AIChE Journal 4, 90-96 (1958)
- Glater, J. and M. R. Zachariah, "A Mechanistic Study of Halogen Interaction with Polyamide Reverse-Osmosis Membranes," in "Reverse Osmosis and Ultrafiltration," A. C. S. Symp. Ser. 281, S. Sourirajan and T. Matsuura, Ed., pp. 346-358, 1984
- Gmehling, J., U. Onken and W. Arlt, "Vapor-Liquid Equilibrium Data Collection: Aqueous-Organic Systems (Supplement 1), Chemistry Data Series, Vol. I, Part 1a," DECHEMA, Frankfurt, 1981
- Greenlaw, F. W., W. D. Prince, R. A. Shelden and E. V. Thompson, "Dependence of Diffusive Permeation Rates on Upstream and Downstream Pressures: I. Single Component Permeant," J. Membrane Sci. 2, 141-151 (1977 A)
- Greenlaw, F. W., R. A. Shelden and E. V. Thompson, "Dependence of Diffusive Permeation Rates on Upstream and Downstream Pressures: II. Two Component Permeant," J. Membrane Sci. 2, 333-348 (1977 B)
- Gregg, S. J. and K. S. W. Sing, "Adsorption Surface Area and Porosity," Academic Press Inc., New York, Chapter 2, 1967
- Harrison, B. and A. Asfour, "A Computer-Aided Experimental Setup for Studying Sorption Kinetics," J. Appl. Poly. Sci. 44, 181-184 (1992)
- Hansen, C. M., "The Universality of the Solubility Parameter," Ind. Eng. Chem. Prod. Res. Dev. 8, 2-11 (1969)
- Heisler, E. G., A. S. Hunter, J. Siciliano and R. H. Treadway, "Solute and Temperature Effects in the Pervaporation of Aqueous Alcoholic Solutions," Science 124, 77-78 (1956)

- Hennepe, H. J., C., D. Bargeman, M. H. V. Mulder and C. A. Smolders, "Zeolite-Filled Silicone Rubber Membrane. Part 1. Membrane Preparation and Pervaporation Results," J. Membrane Sci. **35**, 39-55 (1987)

- Hernandez, R. J., J. R. Giacin and E. A. Grulke, "The Sorption of Water Vapor by an Amorphous Polyamide," J. Membrane Sci. **65**, 187-199 (1992)

- Hickey, P. J., F. P. Juricic and C. S. Slater, "The Effect of Process Parameters on the Pervaporation of Alcohols through Organophilic Membranes," Sep. Sci. & Tech. **27**, 843-861 (1992)

- Hirai, Y. and T. Nakajima, "Sorption Behaviour of Water Vapor into Polyelectrolyte Complex of Poly(Acrylic Acid)/ Poly(4-Vinylpyridine)," J. Appl. Poly. Sci. **37**, 2275-2281 (1989)

- Huang, R. Y. M., M. Balakrishnan and J. W. Rhim, "Pervaporation Separation of Pentane-Alcohol Mixtures Using Nylon 6-Polyacrylic Acid (PAA) Ionically Crosslinked Membranes. II. Experimental Data and Theoretical Interpretation," J. Appl. Poly. Sci. **46**, 109-118 (1992)

- Huang, R. Y. M. and X. Feng, "Pervaporation of Water/Ethanol Mixtures by an Aromatic Polyetherimide Membrane," Sep. Sci. & Tech. **27**, 1583-1597 (1992)

- Huang, R. Y. M. and V. J. C. Lin, "Separation of Liquid Mixtures by Using Polymer Membranes, I. Permeation of Binary Organic Liquid Mixtures through Polyethylene," J. Appl. Poly. Sci. **12**, 2615-2631 (1968)

- Huang, R. Y. M., A. Moreira, R. Notarfonzo and X. F. Xu, "Pervaporation Separation of Acetic Acid-Water Mixtures Using Modified Membranes I. Blended Polyacrylic Acid (PAA)-Nylon Membranes," J. Appl. Poly. Sci. **35**, 1191-1200 (1988)

- Huang, R. Y. M. and J. W. Rhim, "Prediction of Pervaporation Separation Characteristics for the Methanol-Pentane-Nylon 6 Poly(Acrylic Acid) Blended

Membrane System," J. Membrane Sci. 71, 211-220 (1992)

- Huang, R. Y. M., Y. Xu, Y. Jin and C. Lipski, "Novel Blended Nylon Membranes for the Pervaporation Separation of Acetic Acid-Water and Ethanol-Water Liquid Mixture Systems," Proc. 2nd Int. Conf. on Pervaporation Processes in the Chemical Industry, R. Bakish Ed., Bakish Materials Corp., Englewood N. J., pp. 225-239, 1987

- Huang, R. Y. M. and C. K. Yeom, "Pervaporation Separation of Aqueous Mixtures Using Crosslinked Polyvinyl Alcohol Membranes. III. Permeation of Acetic Acid-Water Mixtures," J. Membrane Sci. 58, 33-47 (1991)

- Hwang, S. T. and K. Kammermeyer, "Pervaporation," in "Membranes in Separations," Techniques of Chemistry, Vol. VII, John Wiley and Sons, New York, pp. 99-123, Chapter VII, 1975

- Inaba, T., M. Kondo, H. Izaba, Y. Nagase and K. Sugimoto, "Pervaporation of Ethanol-Water Mixture with Modified Substituted-Polyacetylene," Proc. 4th Int. Conf. on Pervaporation Processes in Chemical Industry, R. Bakish Ed., Bakish Materials Corp., Englewood N. J., pp. 28-39, 1990

- Iwatsubo, T., T. Yamanaka, S. Yamamoto, K. Mizoguchi and Y. Suda, "Concentration Profiles of Permeant in Membranes Under Pervaporation-A Proposal of a New Method to Determine the Profiles," Sen-I Gakkaishi 44, 367-373 (1988)

- Kataoka, T., T. Tsuru, S. Nakao and S Kimura, "Membrane Transport Properties of Pervaporation and Vapor Permeation in Ethanol-Water System Using Polyacrylonitrile and Cellulose Acetate Membranes," J. Chem. Eng. Jpn 24, 334-339 (1991)

- Katchalsky, A. and P. E. Curran, "Nonequilibrium Thermodynamics in Biophysics," Harvard Univ. Press, Cambridge, Mass., Chapter 10, 1965

- Kesting, R. E., "Synthetic Polymeric Membranes," 2nd Ed., John Wiley & Sons, New York, Chapter 2, 1985

- Kim, S. N. and K. Kammermeyer, "Actual Concentration Profiles in Membrane Permeation," Sep. Sci. 5, 679-697 (1970)
- Kimura, S. and T. Nomura, "Pervaporation of Alcohol-Water Mixtures with Silicone Rubber Membrane," Membrane 7, 353-354 (1983)
- King, C. J., "Separation Processes," 2nd Ed., McGraw Hill Book Company, New York, pp. 762-763, 1980
- Kober, P. A., "Pervaporation, Perstillation and Percrystallization," J. Am. Chem. Soc. 39, 944-948 (1917)
- Kucharski, M. and J. Stelmaszek, "Separation of Liquid Mixtures by Permeation," Int. Chem. Eng. 7, 618-622 (1967)
- Laatikainen, M. and M. Lindstrom, "Measurements of Sorption in Polymer Membranes with a Quartz Crystal Microbalance," J. Membrane Sci. 29, 127-141 (1986)
- Larchet, C., G. Bulvestre and M. Guillou, "Separation of Benzene-n Heptane Mixtures by Pervaporation with Elastomeric Membranes. II. Contribution of Sorption to the Separation Mechanism," J. Membrane Sci. 17, 263-274 (1984)
- Lee, C. H., "Theory of Reverse Osmosis and Some Other Membrane Permeation Operations," J. Appl. Poly. Sci. 19, 83-95 (1975)
- Lee, Y. M., D. Bourgeois and G. Belfort, "Selection of Polymer Membrane for Pervaporation," Proc. 2nd Int. Conf. on Pervaporation Processes in the Chemical Industry, R. Bakish Ed., Bakish Materials Corp., Englewood N. J., pp. 249-265, 1987
- Long, R. B., "Liquid Permeation Through Plastic Films," Ind. Eng. Chem. Fund. 4, 445-451 (1965)
- Maeda, Y., M. Tsuyumoto, H. Karakane and H. Tsugaya, "Separation of Water-Acetic Acid Mixture by Pervaporation Through Aromatic Polymer Membranes,"

Proc. 5th Int. Conf. on Pervaporation Processes in the Chemical Industry, R. Bakish Ed., Bakish Materials Corp., Englewood N. J., pp. 31-44, 1991

- McCandless, F. P., "Separation of Aromatics and Naphthenes by Permeation Through Modified Vinylidene Fluoride Films," Ind. Eng. Chem. Prod. Res. Dev. **12**, 354-359 (1973)

- McCandless, F. P. and W. B. Downs, "Separation of C_8 Aromatics Isomers by Pervaporation through Commercial Polymer Films," J. Membrane Sci. **30**, 111-116 (1987)

- Masuda, T., B. Z. Tang and T. Higashimura, "Ethanol-Water Separation by Pervaporation through Substituted Polyacetylene Membrane," Poly. J. **18**, 565-567 (1986)

- Matsumoto, Y. and M. Kondo, "Transport Model in PEBA Membrane," Presented at 6th Int. Conf. on Pervaporation Processes in Chemical Process Industries, held in Ottawa, Sept. 28-30, 1992

- Michaels, A. S., R. F. Baddour, H. J. Bixler and C. Y. Choo, "Conditioned Polyethylene as a Permselective Membrane," Ind. Eng. Chem. Proc. Des. Dev. **1**, 14-25 (1962)

- Mochizuki, A., Y. Sato and H. Ogawara, "The Behaviour of Bi-active Layer Membrane in Pervaporation," Membrane 9, 279-280 (1984)

- Mulder, M, "Basic Principles of Membrane Technology," Kluwer Academic Publishers, Dordrecht, Chapter 1, 1991

- Mulder, M. H. V., A. C. M. Franken and C. A. Smolders, "On the Mechanism of Separation of Ethanol-Water Mixtures by Pervaporation II. Experimental Concentration Profiles," J. Membrane Sci. **23**, 41-58 (1985)

- Mulder, M. H. V., J. O. Hendrikman, H. Hegeman and C. A. Smolders, "Ethanol-Water Separation by Pervaporation," J. Membrane Sci. **16**, 269-284 (1983)

- Mulder, M. H. V. and C. A. Smolders, "On the Mechanism of Separation of Ethanol/Water Mixtures by Pervaporation I. Calculations of Concentration Profiles," J. Membrane Sci. **17**, 289-307 (1984)
- Mulder, M. H. V. and C. A. Smolders, "Pervaporation, Solubility Aspects of the Solution Diffusion Model," Sep. & Purifi. Methods **15**, 1-19 (1986)
- Nagy, E., O. Borlai and A. Ujhidy, "Membrane Permeation of Water-Alcohol Binary Mixtures," J. Membrane Sci. **7**, 109-118 (1980)
- J. Neel, "Introduction to Pervaporation," in "Pervaporation Membrane Separation Processes," R. Y. M. Huang Ed., Elsevier Science Publishers, New York, pp 1-100, Chapter 1, 1991
- Neel, J., Q. T. Nguyen, R. Clement and R. Francois, "Separation of Water-Organic Mixtures by Pervaporation. An Insight Into The Mechanism of The Process," Proc. 2nd Int. Conf. On Pervaporation Processes in The Chemical Industry, R. Bakish Ed., Bakish Materials Corp., Englewood N. J., pp. 35-48, 1987
- Neel, J., Q. T. Nguyen, R. Clement and L. Leblanc, "Fractionation of Binary Liquid Mixtures by Continuous Pervaporation," J. Membrane Sci. **15**, 43-62 (1983)
- Nguyen, T. D., T. Matsuura and S. Sourirajan, "Effect of Nonsolvent Additives on the Pore Size and the Pore Size Distribution of Aromatic Polyamide RO Membranes," Chem. Eng. Comm. **54**, 17-36 (1987 A)
- Nguyen, T. Q., A. Essamri, R. Clement and J. Neel, "Synthesis of Membranes for the Dehydration of Water-Acetic Acid Mixtures by Pervaporation, 1. Polymer Material Selection," Makromol. Chem. **188**, 1973-1984 (1987 B)
- Nguyen, T. Q. and K. Nobe, "Extraction of Organic Contaminants in Aqueous Solutions by Pervaporation," J. Membrane Sci. **30**, 11-22 (1987)

- Okada, T. and Matsuura T., "A Study on the Pervaporation of Ethyl Alcohol/Heptane Mixtures by Porous Cellulose Membranes," Proc. 3rd Int. Conf. on Pervaporation Processes in the Chemical Industry, R. Bakish Ed., Bakish Materials Corp., Englewood N. J., pp. 224-230, 1988
- Okada, T. and T. Matsuura, "A New Transport Model For Pervaporation," J. Membrane Sci. **59**, 133-150 (1991)
- Okada, T., M. Yoshikawa and T. Matsuura, "A Study on the Pervaporation of Ethanol/Water Mixtures on the Basis of Pore Flow Model," J. Membrane Sci. **59**, 151-168 (1991)
- Osada, Y. and T. Nakagawa, Ed., "Membrane Science and Technology," Marcel Dekker Inc., New York, Chapter 1, 1992
- Paul, D. R. and O. M. Ebra-Lima, "The Mechanism of Liquid Transport Through Polymer Membranes," J. Appl. Poly. Sci. **15**, 2199-2210 (1971)
- Pearce, G. K., "Pervaporation vs Distillation: A Comparative Costing for Alcohol Dehydration," Proc. 4th Int. Conf. on Pervaporation Processes in the Chemical Industry, R. Bakish Ed., Bakish Materials Corp., Englewood N. J., pp. 278-296, 1991
- Rautenbach, R. and R. Albrecht, "On the Behaviour of Asymmetric Membranes in Pervaporation," J. Membrane Sci. **19**, 1-22 (1984)
- Rautenbach, R. and R. Albrecht, "The Separation Potential of Pervaporation. Part 1. Discussion of Transport Equations and Comparison with Reverse Osmosis," J. Membrane Sci. **25**, 1-23 (1985)
- Rautenbach, R. and R. Albrecht, "Membrane Processes" John Wiley & Sons, New York, pp 363-421, Chapter 12, 1989
- Reineke, C. E., J. A. Jagodzinski and K. R. Denslow, "Highly Water Selective Cellulosic Polyelectrolyte Membranes for the Pervaporation of Alcohol-Water Mixtures," J. Membrane Sci. **32**, 207-221 (1987)

- Rhim, J. W. and R. Y. M. Huang, "On the Prediction of Separation Factors and Permeabilities for the Separation of Binary Mixtures by Pervaporation," J. Membrane Sci. 46, 335-348 (1989)

- Rhim, J. W. and R. Y. M. Huang, "Prediction of Pervaporation Separation Characteristics for the Ethanol-Water-Nylon 4 Membrane System," J. Membrane Sci. 70, 105-118 (1992)

- Richman, D. and F. A. Long, "Measurement of Concentration Gradients for Diffusion of Vapors in Polymers," J. Am. Chem. Soc. 82, 509-513 (1960)

- Schwarz, H. H., K. Richau and D. Paul, "Symplex Membranes for Pervaporation," Proc. 5th Int. Conf. on Pervaporation Processes in the Chemical Industry, R. Bakish Ed., Bakish Materials Corp., Englewood N. J., pp. 79-87, 1991 A

- Schwarz, H. H., K. Richau and D. Paul, "Membranes from Polyelectrolyte Complexes," Polymer Bulletin 25, 95-100 (1991 B)

- Shimidzu, T. and H. Okushita, "Selective Separation of Cyclohexane-Cyclohexanone-Cyclohexanol Mixtures through Poly(N-Vinylpyrrolidone-co-acrylonitrile) Membrane," J. Membrane Sci. 39, 113-123 (1988)

- Siegel, R. D. and R. W. Coughlin, "Enhancing the Permeation Characteristics of Polyethylene by Membrane Irradiation in the Fully Swollen State," J. Appl. Poly. Sci. 14, 2431-2439 (1970)

- Siesler, H. W. and K. Holland-Moritz, Infrared and Raman Spectroscopy of Polymer, Marcel Dekker, Inc., New York, Chapter 3, 1980

- Sikonia, J. G. and F. P. McCandless, "Separation of Isomeric Xylenes by Permeation through Modified Plastic Films," J. Membrane Sci. 4, 333-348 (1977)

- Sourirajan, S., S. Bao and T. Matsuura, "An Approach to Membrane Separation by Pervaporation," Proc. 2nd Int. Conf. on Pervaporation Processes in the

Chemical Industry, R. Bakish Ed., Bakish Materials Corp., Englewood N. J., pp. 9-12, 1987

- Sourirajan, S. and T. Matsuura, "Reverse Osmosis and Ultrafiltration: Process Principles," National Research Council of Canada, Ottawa, Chapter 1, 1985
- Spitzen, J. W. F., E. Ellinghorst, M. H. V. Mulder and C. A. Smolders, "Solution-Diffusion Aspects in the Separation of Ethanol/Water Mixture with PVA Membranes," Proc. 2nd Int. Conf. on Pervaporation Processes in the Chemical Industry, R. Bakish Ed., Bakish Materials Corp., Englewood N. J., pp. 209-224, 1987
- Sweeny, R. F. and A. Rose, "Factors Determining Rates and Separation in Barrier Membrane Permeation," Ind. Eng. Chem. Prod. Res. Dev 4, 248-251 (1965)
- Tealdo, G., G. Castello and G. D'Amato, "Water-Glycerol Permeation through Styrene-Grafted and Sulphonated PTFE Membrane," J. Membrane Sci. 11, 3-9 (1982)
- Thomas, M., M. Escoubes, P. Esnault and M Pineri, "Determination of the Permeant Concentration Profile in a Membrane During Gas Permeation" J. Membrane Sci. 46, 57-65 (1989)
- Tock, R. W. M., J. Y. Cheung and R. L. Cook, "Dioxane-Water Transport Through Nylon-6 Membranes," Sep. Sci. 9, 361-379 (1974)
- Tyagi, R. K. and T. Matsuura, "Possibility of Concentration Polarization Inside the Membrane During Steady State Pervaporation," Proc. 5th Int. Conf. on Pervaporation Processes in the Chemical Industry, R. Bakish Ed., Bakish Materials Corp., Englewood, N. J., pp. 460-474, 1991
- Vrentas, J. S. and J. L. Duda, "Molecular Diffusion in Polymer Solutions," AIChE Journal 25, 1-24 (1979)

- Wesslein, M., A. Heintz, G. A. Reinhardt and R. N. Lichtenthaler, "Pervaporation of Binary and Multicomponent Mixtures Using PVA Membranes: Experimental and Model Calculations," Proc. 3rd Int. Conf. on Pervaporation Processes in the Chemical Industry, R. Bakish Ed., Bakish Materials Corp., Englewood, N. J., pp. 172-180, 1988

- Xu, Y. F. and R. Y. M. Huang, "Pervaporation Separation of Acetic Acid-Water Mixture Using Modified Membranes. Part I. Ionically Crosslinked Polyacrylic Acid (PAA)-Nylon 6 Membranes, J. Appl. Poly. Sci. **36**, 1121-1128 (1988)

- Yamada, S., " Evaluation of Pervaporation Membrane for Separation of Liquid-Liquid Mixture," Membrane **6**, 168-184 (1981)

- Yamada, S. and T. Hamaya, "Liquid Permeation and Separation by Surface-Modified Polyethylene Membranes," J. Membrane Sci. **17**, 125-138 (1984)

- Yeom, C. K. and R. Y. M. Huang, "Modelling of the Pervaporation Separation of Ethanol-Water Mixtures Through Crosslinked Polyvinyl Alcohol Membrane," J. Membrane Sci. **67**, 39-55 (1992 A)

- Yeom, C. K. and R. Y. M. Huang, "A New Method of Determining the Diffusion Coefficients of Penetrants Through Polymeric Membranes From Steady State Pervaporation Experiments," J. Membrane Sci. **68**, 11-20 (1992 B)

- Yoshikawa, M., Y. P. Handa, D. Coony and T. Matsuura, "Anomalous Physicochemical Properties of Ethanol in a Polymeric Membrane," Makromol. Chem., Rapid Commun. **11**, 387-391 (1990)

- Yoshikawa, M., S. Ochiai, M. Tanigaki and W. Eguchi, "Application and Development of Synthetic Polymer Membranes III. Separation of Water-Ethanol Mixture through Synthetic Polymer Membranes Containing Ammonium Moieties," J. Poly. Sci. Poly. Lett. Ed. **26**, 263-268 (1988)

- Yoshikawa, M., N. Ogata and T. Shimizu, "Polymer Membrane as a Reaction Field. III. Effect of Membrane Polarity on Selective Separation of a Water-Ethanol Binary Mixture Through Synthetic Polymer Membranes," J. Membrane Sci. **26**, 107-114 (1986 A)

- Yoshikawa, M., T. Yukoshi, K. Sanui and N. Ogata, "Selective Separation of Water-Ethanol Mixture through Synthetic Polymer Membranes Having Carboxylic Acid as a Functional Group," J. Poly. Sci., Part A, Poly. Chem. **24**, 1585-1597 (1986 B)

- Yoshikawa, M., T. Yukoshi, K. Sanui and N. Ogata, "Separation of Water-Acetic Acid Mixtures by Pervaporation through Synthetic Polymer Membranes Containing Pendant Carboxylic Acid," Membrane, **10**, 247-253 (1985)

Appendix A

Some Azeotropic Distillation Processes

Table A.1: Some Azeotropic Distillation Processes

Azeotrope	Entrainer
Ethanol/Water	Benzene or Trichlorethylene
Isopropylalcohol/Water	Benzene or Hexane
Acetic Acid/Water	Ethylenedichloride or Butylacetate or Propylacetate
Ethyl benzene/p-xylene	2-Methyl butanol
Heptane/Toluene	MEK-water azeotrope
Benzene, paraffins, cycloparaffins	Acetone or other ketones

Appendix B

Membranes Used in Pervaporation Processes

Table B.1: Polymeric Materials Used in Pervaporation

Mixture	Membrane	Reference
water/ethanol	Poly(vinylalcohol) (GFT)	Wesslein et al., 1988
water/ethanol	Cellulose Acetate	Binning et al., 1961
water/ethanol	PVP grafted-PTFE	Aptel et al., 1976
water/ethanol	Nylon 6	Nagy et al., 1980
water/ethanol	Cellulose derivatives, Poly(acrylonitrile)	Mulder et al., 1983
water/ethanol	Poly(dimethylsiloxane), Poly(sulphone) and	Mulder et al., 1983
water/ethanol	Poly(vinylidenefluoride)	Mulder et al., 1983
water/ethanol	Silicon Rubber(SR)	Kimura and Nomura, 1983
water/ethanol	Poly(1-[trimethylsilyl]-1-propyne)	Masuda et al., 1986
water/ethanol	Zeolite-filled SR	Hennepe et al., 1987
water/ethanol	Cellulosic Polyelectrolytes	Reineke et al., 1987
water/ethanol	Aromatic Polyetherimide	Huang and Feng, 1992
water/ethanol	Polyvinylalcohol	Yeom and Huang, 1992 A
water/alcohol	Nafion^R	Cabasso and Liu, 1985
water/glycerol	Modified PTFE	Tealdo et al., 1982

Table B.2: Polymeric Materials Used in Pervaporation

Mixture	Membrane	Reference
water/2-propanol	Modified CA	Carter and
-	-	Jagannadhaswamy, 1964
water/2-propanol	Sulphonated-	
	Poly(ethylene)	Cabasso and Liu, 1985
water/2-propanol	Nylon-6, Cellophane	Nagy et al., 1980
	Cellulose Acetate	Nagy et al., 1980
water/acetone	Poly(propylene)	Featherstone and Cox, 1971
	PTFE-PVP	Aptel et al., 1976
water/dioxane	Nylon 6	Tock et al., 1974
water/dioxane	PVP grafted PTFE	Neel et al., 1983
water/tetrahydrofuran	PVP grafted PTFE	Neel et al., 1983
water/halogenated-	Silicone	Nguyen and Nobe, 1987
hydrocarbons		
water/phenol	Polyether-block-	Böddeker and
	polyamide(PEBA)	Bengtson, 1990 B
water/phenol	PEBA	Matsumoto and Kondo, 1992

Table B.3: Polymeric Materials Used in Pervaporation

Mixture	Membrane	Reference
hydrocarbons		
isomers	Poly(ethylene)/PVF	Michaels et al., 1962
o, m, p-xylenes	Commercial	McCandless and Downs, 1987
m and p-xylenes	Modified PVDF	Sikonia and
-	-	McCandless, 1977
isomeric butanols	Polyether-block-Polyamide	Böddeker et al., 1990 C
benzene/n-heptane	Poly(butadiene-acrylonitrile)(NBR)	Larchet et al., 1984
benzene/cyclo-	Poly(ethylene)	Huang and Lin, 1968
hexane	Poly(propylene)	Kucharski and
		Stelmaszek, 1967
	Modified Vinylidene	McCandless, 1973
	Fluoride Films	Cabasso et al., 1974 A
	Polymeric Alloys	Cabasso et al., 1974 B
	Oriented	Kucharski and
	Poly(isoprene)	Stelmaszek, 1967
benzene/aniline	Modified PE	Yamada and Hamaya, 1984
benzene/phenol	Irradiated PE	Yamada, 1981
benzene/benzyl-alcohol	Irradiated PE	Yamada, 1981
hexane/heptane	Poly(ethylene)	Greenlaw et al., 1977 A
toluene/heptane	Poly(ethylene)	Fels and Huang, 1970
Ternary Mixtures		
cyclohexane-	Poly(N-vinyl-	Shimidzu and
cyclohexanone-	pyrrolidone-co-	Okushita, 1988
cyclohexanol	Acrylonitrile)	-

Appendix C

BET Approximation

The BET equation is written as follows:

$$F_1(\frac{P}{P_s}) = \frac{c_m \frac{P}{P_s}}{(\frac{1}{C_k} + \frac{C_k - 1}{C_k}\frac{P}{P_s})(1 - \frac{P}{P_s})} \tag{C.1}$$

Then, permeation flux equation can be written as:

$$J = \frac{RT}{f} c_m G_1(\frac{P}{P_s}) \frac{d(\frac{P}{P_s})}{dl} \tag{C.2}$$

where,

$$G_1(\frac{P}{P_s}) = \frac{1}{(\frac{1}{C_k} + \frac{C_k - 1}{C_k}\frac{P}{P_s})(1 - \frac{P}{P_s})} \tag{C.3}$$

1. BET equation is valid only when $\frac{P}{P_s} < 0.7$ (Bartels-Caspers et al. 1992).

2. For $0.7 \leq \frac{P}{P_s} \leq 1.0$, a linear extrapolation of the function $G_1(\frac{P}{P_s})$ is used.

3. A function $F_2(\frac{P}{P_s})$ is defined as:

   - $$F_2(\frac{P}{P_s}) = G_1(\frac{P}{P_s}) \ \textit{when}\ 0 \leq \frac{P}{P_s} < 0.7 \tag{C.4}$$

   - $$= G_1(0.7) + G_1'(0.7)(\frac{P}{P_s} - 0.7) \ \textit{when}\ 0.7 \leq \frac{P}{P_s} \leq 1.0 \tag{C.5}$$

Table C.1: Comparison of Function $1-(\frac{P_3}{P_\circ})^2$ and $F_2(\frac{P_3}{P_\circ})$

$\frac{P_3}{P_\circ}$	$F_2(\frac{P_3}{P_\circ})$	$3.49[1-(\frac{P_3}{P_\circ})^2]$	Error %
0.0	3.49	3.49	0
0.08	3.47	3.33	3.96
0..64	2.06	1.98	4.0
0.80	1.26	1.30	-3.7
1.00	0.0	0.0	0.0

It should be noted that functions $F_1(\frac{P}{P_\circ})$ defined by equation C.1 and $F_2(\frac{P}{P_\circ})$ defined on the previous page are related to each other by:

$$\frac{F_1(\frac{P}{P_\circ})}{\frac{P}{P_\circ}} = c_m F_2(\frac{P}{P_\circ}) \tag{C.6}$$

Therefore, equation C.2 becomes:

$$J\int_{\delta_\circ}^{\delta_\circ+\delta_h} dl = \frac{RT}{f} c_m \int_{1.00}^{\frac{P_3}{P_\circ}} F_2(\frac{P}{P_\circ}) d(\frac{P}{P_\circ}) \tag{C.7}$$

Since J (permeation rate) depends on $\frac{P_3}{P_\circ}$ only through a function:

$$F_3(\frac{P_3}{P_\circ}) = \int_{1.00}^{\frac{P_3}{P_\circ}} F_2(\frac{P}{P_\circ}) d(\frac{P}{P_\circ}) \tag{C.8}$$

F_3 was evaluated numerically as a function of $\frac{P_3}{P_\circ}$ and compared with $3.49[1-(\frac{P_3}{P_\circ})^2]$ in order to confirm that the above two functions are similar in shape. Table C.1 shows that the two functions agree within $\pm$ 4 % range when $C_k = 2$, which corresponds to BET (Type II) adsorption isotherm.

Appendix D

Concentration Polarization

D.1 A General Concept of Concentration Polarization

Generally, in membrane separation processes one component (say component j) of the mixture permeates through the membrane preferentially. The other component (component i), on the other hand, is left behind on the feed side (upstream) of the membrane. Component i should diffuse back to the bulk feed solution quickly enough to prevent the build-up of component i near the membrane-feed solution interface. This phenomenon of the build-up of slower component at the interface is called concentration polarization. Generally, concentration polarization leads to decreased flux and decreased selectivity.

D.2 Concentration Polarization Defined Inside the Membrane

Concentration polarization inside the membrane is defined in the present section. Mathematical equations are derived to describe the phenomenon of concentration polarization occurring inside the membrane. It should be recalled that the membrane

has two distinct regions, namely; liquid-filled region and vapor-filled region. The liquid-filled region is nonselective and the vapor region is the selective one. At steady state, the net flow rate of the component i in the liquid-filled region is the sum of the diffusive flow and the convective flow and should be equal to the permeation rate of the component i through the membrane. In the present case the thickness of the liquid-filled region is equal to the thickness of the boundary layer. Therefore:

$$-D\frac{dX_i}{dl} + vX_i = vY_{i,3} \tag{D.1}$$

where D is the diffusion coefficient in the boundary layer, X_i the mole fraction of component i as function of distance l, v is the velocity and $Y_{i,3}$ is the mole fraction of component i in the downstream. Rearrangement of equation D.1 yields:

$$\frac{dX_i}{dl} = \frac{v}{D}(X_i - Y_{i,3}) \tag{D.2}$$

and

$$\frac{dX_i}{X_i - Y_{i,3}} = \frac{v}{D}dl \tag{D.3}$$

On integration of equation D.3, we obtain:

$$ln(X_i - Y_{i,3}) = \frac{v}{D}l + C \tag{D.4}$$

where C is an integration constant. The boundary conditions are:
Boundary Condition 1: $X_i = X_{i,2}$ at $l = 0$ and
Boundary Condition 2: $X_i = X_{i,*}$ at $l = \delta_a$ (at the liquid vapor phase boundary)
The integration constant can be calculated using the first boundary condition:

$$ln(X_{i,2} - Y_{i,3}) = C \tag{D.5}$$

Substituting the value of C from equation D.5 into equation D.4:

$$ln(\frac{X_i - Y_{i,3}}{X_{i,2} - Y_{i,3}}) = \frac{v}{D}l \tag{D.6}$$

Using the second boundary condition we obtain:

$$ln(\frac{X_{i,*} - Y_{i,3}}{X_{i,2} - Y_{i,3}}) = \frac{v}{D}\delta_a \tag{D.7}$$

or

$$\frac{X_{i,*} - Y_{i,3}}{X_{i,2} - Y_{i,3}} = exp(\frac{v}{D})\delta_a \tag{D.8}$$

The mass transfer coefficient k can be defined as the ratio of diffusivity and the thickness of the boundary layer (thickness of the liquid-filled region):

$$k = \frac{D}{\delta_a} \tag{D.9}$$

Hence equation D.8 can be rewritten as follows:

$$\frac{X_{i,*} - Y_{i,3}}{X_{i,2} - Y_{i,3}} = exp(\frac{v}{k}) \tag{D.10}$$

Equation D.10 is the same as used in the analysis, i.e. equation 3.31.

The left-hand side of equation D.10 is called "concentration polarization modulus" (CPM). The concentration polarization modulus increases with:

- decrease of mass transfer coefficient (k).
- increase of permeation flux or penetrant velocity (v).
- increase of selectivity.
- decrease of concentration of the preferentially permeating component in the feed mixture.

Appendix E

Vapor-Liquid Equilibrium Data

Table E.1: Vapor-Liquid Equilibrium Data for Acetic Acid/Water System at 25°C
Source: Gmehling et al. (1981) pp 89-109

Mole Fraction of Acetic Acid in the Liquid $X_{i,\bullet}$	Mole Fraction of Acetic Acid in the Vapor $Y_{i,\bullet}$	Total Vapor Pressure Pa (mm Hg) $P_\bullet$
0.000	0.000	3180 (23.86)
0.044	0.029	3173 (23.80)
0.068	0.046	3146 (23.60)
0.084	0.059	3133 (23.50)
0.189	0.147	3026 (22.70)
0.279	0.221	2920 (21.90)
0.413	0.327	2826 (21.20)
0.754	0.619	2573 (19.30)
0.876	0.774	2413 (18.10)
1.000	1.000	2093 (15.70)

Table E.2: Vapor-Liquid Equilibrium Data for Acetic Acid/Water System at 35°C
Source: Gmehling et al. (1981) pp 89-109

Mole Fraction of Acetic Acid in the Liquid $X_{i,\bullet}$	Mole Fraction of Acetic Acid in the Vapor $Y_{i,\bullet}$	Total Vapor Pressure Pa (mm Hg) $P_\bullet$
0.000	0.000	5647 (42.36)
0.100	0.072	5519 (41.40)
0.200	0.178	5394 (40.46)
0.308	0.270	5295 (39.72)
0.402	0.347	5150 (38.63)
0.524	0.442	4998 (37.49)
0.612	0.504	4862 (36.47)
0.711	0.601	4730 (35.48)
0.800	0.700	4538 (34.04)
0.901	0.830	4236 (31.77)
1.000	1.000	3580 (26.85)

Table E.3: Vapor-Liquid Equilibrium Data for Acetic Acid/Water System at 40°C
Source: Gmehling et al. (1981) pp 89-109

Mole Fraction of Acetic Acid in the Liquid $X_{i,\bullet}$	Mole Fraction of Acetic Acid in the Vapor $Y_{i,\bullet}$	Total Vapor Pressure Pa (mm Hg) $P_\bullet$
0.000	0.000	7375 (55.32)
0.043	0.026	7322 (54.92)
0.082	0.053	7279 (54.60)
0.142	0.099	7181 (53.86)
0.211	0.155	7354 (52.91)
0.300	0.235	6909 (51.82)
0.347	0.284	6825 (51.19)
0.454	0.379	6627 (49.71)
0.582	0.491	6375 (47.82)
0.700	0.610	6081 (45.61)
0.743	0.659	5929 (44.47)
0.912	0.855	5207 (39.06)
1.000	1.000	4690 (35.18)

Appendix F

Derivation of Fick's First Law Equation

This section shows the derivation of Fick's first law equation from the chemical potential equation. For the pure component permeation, the permeation rate can be related to the chemical potential by the following equation:

$$J = -\frac{c}{f}\frac{d\mu}{dl} \tag{F.1}$$

The chemical potential is related to the activity and the pressure gradient by the following equation:

$$d\mu = RTdlna + Vdp \tag{F.2}$$

Substituting the value of the chemical potential from equation F.2 to equation F.1, we obtain:

$$J = -\frac{c}{f}\frac{RTdlna + Vdp}{dl} \tag{F.3}$$

If the second term in the above equation (equation F.3) is neglected, the equation becomes:

$$J = -\frac{c}{f}\frac{RTdlna}{dl} \tag{F.4}$$

Assuming a constant activity coefficient, the activity term in equation F.4 can be related to the concentration, and the equation can be rearranged in the following

manner:

$$J = -\frac{RT}{f} c \frac{dc}{c} \frac{1}{dl} \tag{F.5}$$

The ratio $\frac{RT}{f}$ can be written as the diffusion coefficient D, and the concentration c is cancelled out. The final equation becomes:

$$J = -D\frac{dc}{dl} \tag{F.6}$$

Equation F.6 is the Fick's first law equation. This derivation shows that by neglecting the pressure term $V dp$, the chemical potential equation yields the Fick's first law equation.

Appendix G

Pervaporation Data for Binary Mixture

Table G.1: Pervaporation Data for a Single Polyamide Membrane at 25°C and at the Downstream Pressure of 467 Pa (3.5 mm Hg) for Binary Mixture of Acetic Acid/Water

S. No. - -	Mole Fraction of Acetic Acid in the Feed	Mole Fraction of Acetic Acid in the Downstream	Permeation Rate x 10^3, mol/s-m^2
1	0.0	0.0	3.67
2	0.115	0.05	3.42
3	0.21	0.06	3.34
4	0.31	0.10	3.01
5	0.39	0.105	2.86
6	0.61	0.18	2.56
7	0.74	0.18	2.16
8	0.87	0.21	1.97
9	0.91	0.23	1.68
10	1.0	1.00	0.46

Appendix H

Pervaporation Data for Pure Component

Table H.1: Pervaporation Data for Pure Water with a Single Polyamide Membrane at 25°C and at Different Downstream Pressures

S. No. -	Downstream Pressure Pa (mm Hg)	Permeation Rate of Pure Water x 10^3, mol/s-m^2
1	467 (3.5)	3.67
2	1333 (10.0)	3.39
3	2000 (15.0)	2.97
4	2506 (18.8)	2.44
5	3666 (27.5)	1.84
6	4333 (32.5)	1.70
7	5000 (37.5)	1.63
8	5666 (42.5)	1.54
9	6333 (47.5)	1.48

Table H.2: Pervaporation Data for Pure Acetic Acid with a Single Polyamide Membrane at 25°C and at Different Downstream Pressures

S. No.	Downstream Pressure Pa (mm Hg)	Permeation Rate of Pure Acetic Acid x 10^4, mol/s-m^2
1	1333 (10.0)	3.59
2	2333 (17.5)	3.01
3	3333 (25.0)	1.94
4	4000 (30.0)	1.81
5	4666 (35.0)	1.71
6	5666 (42.5)	1.62
7	6333 (47.5)	1.53

Appendix I

Calibration Curve Used for the Analysis

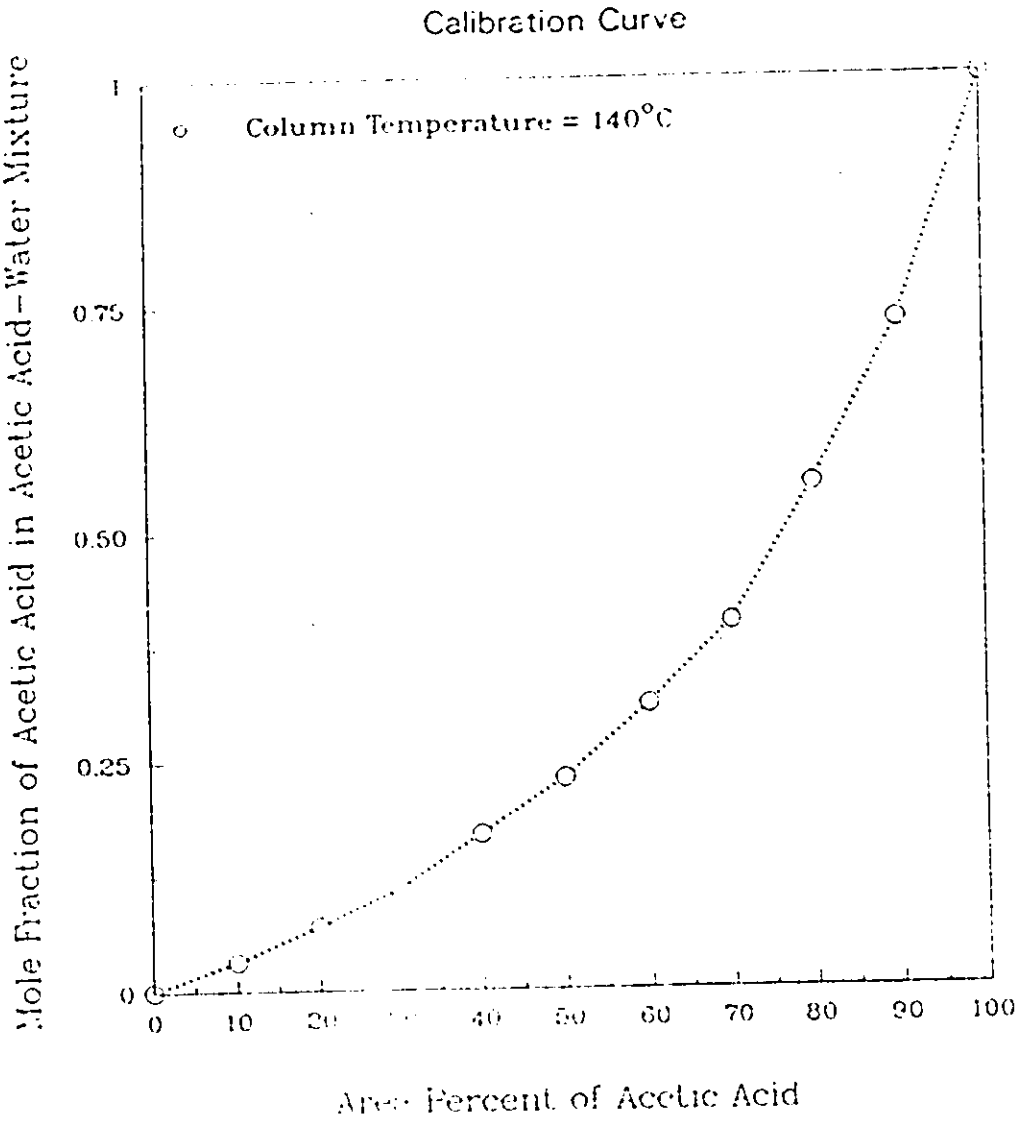

Figure I.1: Calibration Curve for the Gas Chromatographic Analysis of Acetic Acid-Water Mixture

Appendix J

Liquid Sorption Data

Table J.1: Liquid Sorption Data for Polyamide-Acetic Acid/Water System at 25°C

S. No. - - -	Mole Fraction of Acetic Acid in Liquid	Mole Fraction of Acetic Acid in Sorbed Mixture	Total Sorbed Amount kg/kg of Dry Polymer
1	0.00	0.0	0.623
2	0.11	0.08	0.59
3	0.21	0.12	0.51
4	0.30	0.13	0.463
5	0.39	0.14	0.385
6	0.50	0.15	0.357
7	0.60	0.23	0.319
8	0.68	0.26	0.273
9	0.85	0.28	0.182
10	1.00	1.0	0.111

Table J.2: Liquid Sorption Data for Polyamide-Acetic Acid/Water System at 35°C

S. No. - - -	Mole Fraction of Acetic Acid in Liquid	Mole Fraction of Acetic Acid in Sorbed Mixture	Total Sorbed Amount kg/kg of Dry Polymer
1	0.00	0.00	0.766
2	0.10	0.07	0.691
3	0.30	0.10	0.522
4	0.40	0.13	0.724
5	0.50	0.15	1.050
6	0.60	0.17	0.625
7	0.70	0.25	0.562
8	0.90	0.27	0.508
9	1.00	1.00	0.473

Table J.3: Liquid Sorption Data for Polyamide-Acetic Acid/Water System at 40°C

S. No. - - -	Mole Fraction of Acetic Acid in Liquid	Mole Fraction of Acetic Acid in Sorbed Mixture	Total Sorbed Amount kg/kg of Dry Polymer
1	0.00	0.00	0.810
2	0.10	0.07	0.736
3	0.30	0.12	0.562
4	0.40	0.13	0.724
5	0.50	0.17	1.100
6	0.60	0.18	0.953
7	0.70	0.24	0.782
8	0.90	0.27	0.675
9	1.00	1.00	0.522

Appendix K

Vapor Sorption Data

Table K.1: Vapor Sorption Data for Polyamide-Acetic Acid/Water System at 25°C

Ratio of Partial Pressure to Saturation Vapor Pressure (Acetic Acid or Water) -	Sorbed Amount for Acetic Acid - kg/kg of Dry Polymer	Sorbed Amount for Water - kg/kg of Dry Polymer
0.10	0.0025	0.010
0.20	0.0050	0.035
0.40	0.0090	0.050
0.60	0.0150	0.070
0.80	0.0170	0.085
0.90	0.020	0.095
1.00	0.023	0.100

Table K.2: Vapor Sorption Data for Polyamide-Acetic Acid/Water System at 35°C

Ratio of Partial Pressure to Saturation Vapor Pressure (Acetic Acid or Water) -	Sorbed Amount for Acetic Acid - kg/kg of Dry Polymer	Sorbed Amount for Water - kg/kg of Dry Polymer
0.10	0.0045	0.022
0.20	0.0095	0.075
0.40	0.0175	0.112
0.60	0.0340	0.134
0.80	0.0410	0.180
0.90	0.0510	0.200
1.00	0.0620	0.220

Table K.3: Vapor Sorption Data for Polyamide-Acetic Acid/Water System at 40°C

Ratio of Partial Pressure to Saturation Vapor Pressure (Acetic Acid or Water) -	Sorbed Amount for Acetic Acid - kg/kg of Dry Polymer	Sorbed Amount for Water - kg/kg of Dry Polymer
0.10	0.0055	0.028
0.20	0.0115	0.085
0.40	0.0195	0.128
0.60	0.0410	0.154
0.80	0.0480	0.190
0.90	0.0580	0.220
1.00	0.0680	0.240

Appendix L

Pure Penetrant Profile Data

Table L.1: Data for the Profile of Pure Water Content and Permeation Rate at Downstream Pressure of 467 Pa

Designated Stream -	Sorbed Amount of Penetrant kg/kg of Dry Polymer
Section 1	0.718
Section 2	0.428
Section 3	0.125
Permeation Rate	$x10^3$, mol/s-m^2 1.62

Table L.2: Data for the Profile of Pure Water Content and Permeation Rate at Downstream Pressure of 1466 Pa

Designated Stream -	Sorbed Amount of Penetrant kg/kg of Dry Polymer
Section 1	0.476
Section 2	0.256
Section 3	0.116
Permeation Rate	$x10^3$, mol/s-m^2 1.20

Table L.3: Data for the Profile of Pure Water Content and Permeation Rate Downstream Pressure of 2666 Pa

Designated Stream -	Sorbed Amount of Penetrant kg/kg of Dry Polymer
Section 1	0.410
Section 2	0.225
Section 3	0.105
Permeation Rate	$x10^3$, mol/s-m^2 0.98

Table L.4: Data for Permeation Rate at Downstream Pressure of 4000 Pa

Designated Stream -	Sorbed Amount of Penetrant kg/kg of Dry Polymer
Section 1	0.356
Section 2	0.188
Section 3	0.100
Permeation Rate	$x10^3$, mol/s-m^2 0.71

Table L.5: Data for the Profile of Pure Water Content and Permeation Rate at Downstream Pressure of 13332 Pa

Designated Stream -	Sorbed Amount of Penetrant kg/kg of Dry Polymer
Section 1	0.310
Section 2	0.308
Section 3	0.300
Permeation Rate	$x10^3$, mol/s-m^2 0.15

Appendix M

Binary Penetrant Profile Data

Table M.1: Data for the Concentration Profile and Pervaporation of Binary Mixture at 25°C and at the Downstream Pressure of 467 Pa

Designated Stream	Mole Fraction of Acetic Acid	Total Sorbed Amount
-	-	kg/kg of Dry Polymer
Section 1	0.14	0.381
Section 2	0.08	0.115
Section 3	0.03	0.08
Pervaporation Data	-	
AA Mole Fraction in Feed	AA Mole Fraction in Downstream	Total Permeation Rate
-	-	$x10^3$, mol/s-m^2
0.13	0.03	0.98

Table M.2: Data for the Concentration Profile and Pervaporation of Binary Mixture at 25°C and at the Downstream Pressure of 467 Pa

Designated Stream -	Mole Fraction of Acetic Acid	Total Sorbed Amount kg/kg of Dry Polymer
Section 1	0.23	0.365
Section 2	0.26	0.132
Section 3	0.07	0.08
Pervaporation Data	-	
AA Mole Fraction in Feed -	AA Mole Fraction in Downstream -	Total Permeation Rate $x10^3$, mol/s-m^2
0.25	0.05	0.79

Table M.3: Data for the Concentration Profile and Pervaporation of Binary Mixture at 25°C and at the Downstream Pressure of 467 Pa

Designated Stream -	Mole Fraction of Acetic Acid	Total Sorbed Amount kg/kg of Dry Polymer
Section 1	0.34	0.347
Section 2	0.19	0.145
Section 3	0.15	0.09
Pervaporation Data	-	
AA Mole Fraction in Feed -	AA Mole Fraction in Downstream -	Total Permeation Rate $x10^3$, mol/s-m^2
0.37	0.05	0.73

Table M.4: Data for the Concentration Profile and Pervaporation of Binary Mixture at 25°C and at the Downstream Pressure of 467 Pa

Designated Stream	Mole Fraction of Acetic Acid	Total Sorbed Amount kg/kg of Dry Polymer
Section 1	0.24	0.328
Section 2	0.18	0.143
Section 3	0.15	0.084
Pervaporation Data	-	
AA Mole Fraction in Feed	AA Mole Fraction in Downstream	Total Permeation Rate $x10^3$, mol/s-m^2
-	-	
0.50	0.07	0.41

Table M.5: Data for the Concentration Profile and Pervaporation of Binary Mixture at 25°C and at the Downstream Pressure of 467 Pa

Designated Stream -	Mole Fraction of Acetic Acid	Total Sorbed Amount kg/kg of Dry Polymer
Section 1	0.51	0.09
Section 2	0.27	0.086
Section 3	0.13	0.08
Pervaporation Data	-	
AA Mole Fraction in Feed -	AA Mole Fraction in Downstream -	Total Permeation Rate $x10^3$, mol/s-m^2
0.65	0.16	0.34

Table M.6: Data for the Concentration Profile and Pervaporation of Binary Mixture at 35°C and at the Downstream Pressure of 467 Pa

Designated Stream -	Mole Fraction of Acetic Acid	Total Sorbed Amount kg/kg of Dry Polymer
Section 1	0.17	1.01
Section 2	0.37	0.442
Section 3	0.09	0.111
Pervaporation Data	-	
AA Mole Fraction in Feed -	AA Mole Fraction in Downstream -	Total Permeation Rate $x10^3$, mol/s-m^2
0.50	0.07	0.51

Table M.7: Data for the Concentration Profile and Pervaporation of Binary Mixture at 40°C and at the Downstream Pressure of 467 Pa

Designated Stream -	Mole Fraction of Acetic Acid	Total Sorbed Amount kg/kg of Dry Polymer
Section 1	0.22	1.11
Section 2	0.20	0.51
Section 3	0.08	0.12
Pervaporation Data	-	
AA Mole Fraction in Feed -	AA Mole Fraction in Downstream -	Total Permeation Rate $x10^3$, mol/s-m^2
0.50	0.07	0.56

Table M.8: Data for the Concentration Profile and Pervaporation of Binary Mixture at the Downstream Pressure of 1200 Pa and 25°C

Designated Stream -	Mole Fraction of Acetic Acid	Total Sorbed Amount kg/kg of Dry Polymer
Section 1	0.11	0.303
Section 2	0.19	0.129
Section 3	0.15	0.076
Pervaporation Data	-	
AA Mole Fraction in Feed -	AA Mole Fraction in Downstream -	Total Permeation Rate $x10^3$, mol/s-m^2
0.50	0.10	0.18

Table M.9: Data for the Concentration Profile and Pervaporation of Binary Mixture at the Downstream Pressure of 2666 Pa and 25°C

Designated Stream -	Mole Fraction of Acetic Acid	Total Sorbed Amount kg/kg of Dry Polymer
Section 1	0.16	0.27
Section 2	0.15	0.11
Section 3	0.13	0.07
Pervaporation Data	-	
AA Mole Fraction in Feed -	AA Mole Fraction in Downstream -	Total Permeation Rate $x10^3$, mol/s-m^2
0.50	0.12	0.13

Appendix N

Calculations Using Solution-Diffusion Model

This section shows the calculation procedure used to analyze the pure penetrant profile data at different process conditions using the solution-diffusion model. In the present case the penetrant is water and the polymer is aromatic polyamide. The available data is the pure penetrant profile in the polymeric membrane at different downstream pressure and at 25°C. The stepwise procedure of calculation is described below.

- Step 1: The equation of Fick's first law is written as follows:

$$J = -D(c)\frac{dc}{dl} \tag{N.1}$$

where $D(c)$ is the concentration dependent diffusion coefficient and dl is the incremental length. The dependence of diffusion coefficient on the penetrant concentration can take different forms. The following equation was used for the calculations:

$$D(c) = D_0(1 + c^N) \tag{N.2}$$

where c is the penetrant concentration and N is a plasticization parameter; D_0 denotes the diffusion coefficient at zero penetrant concentration and $D(c)$ denotes the diffusion coefficient at the concentration c. Substitution of equation

N.2 into equation N.1 and integration from position $l = 0$ to $l = l$ leads to the following equation:

$$Jl = D_0(c_0 - c) + \frac{D_0}{N+1}(c_0^{N+1} - c^{N+1}) \qquad \text{(N.3)}$$

In equation N.3, c_0 denotes the concentration at distance zero or $l = 0$ and c denotes the concentration at distance l. This equation was used for the calculations.

- Step 2: The known parameters in the equation are J (permeation rate), distance and the concentration c. There are three sets of distance versus concentration data available for a particular downstream pressure. There are three equations and three unknowns (D_0, c_0 and N). The same data is available at four different downstream pressures (467 Pa, 1466 Pa, 2666 Pa and 4000 Pa).

- Step 3: At first, three equations corresponding to the downstream pressure of 467 Pa (3.5 mm Hg) are solved to get the three unknown parameters. The same procedure is followed to calculate the parameters at other downstream pressures.

- Step 4: The diffusion coefficient at zero concentration D_0 should be a constant for a particular system. The average of the values calculated at different downstream pressures is taken, and the values of the parameters c_0 and N are calculated again. The final results of the calculated values are given in table 5.4.

Appendix O

Results of FTIR-ATR Study

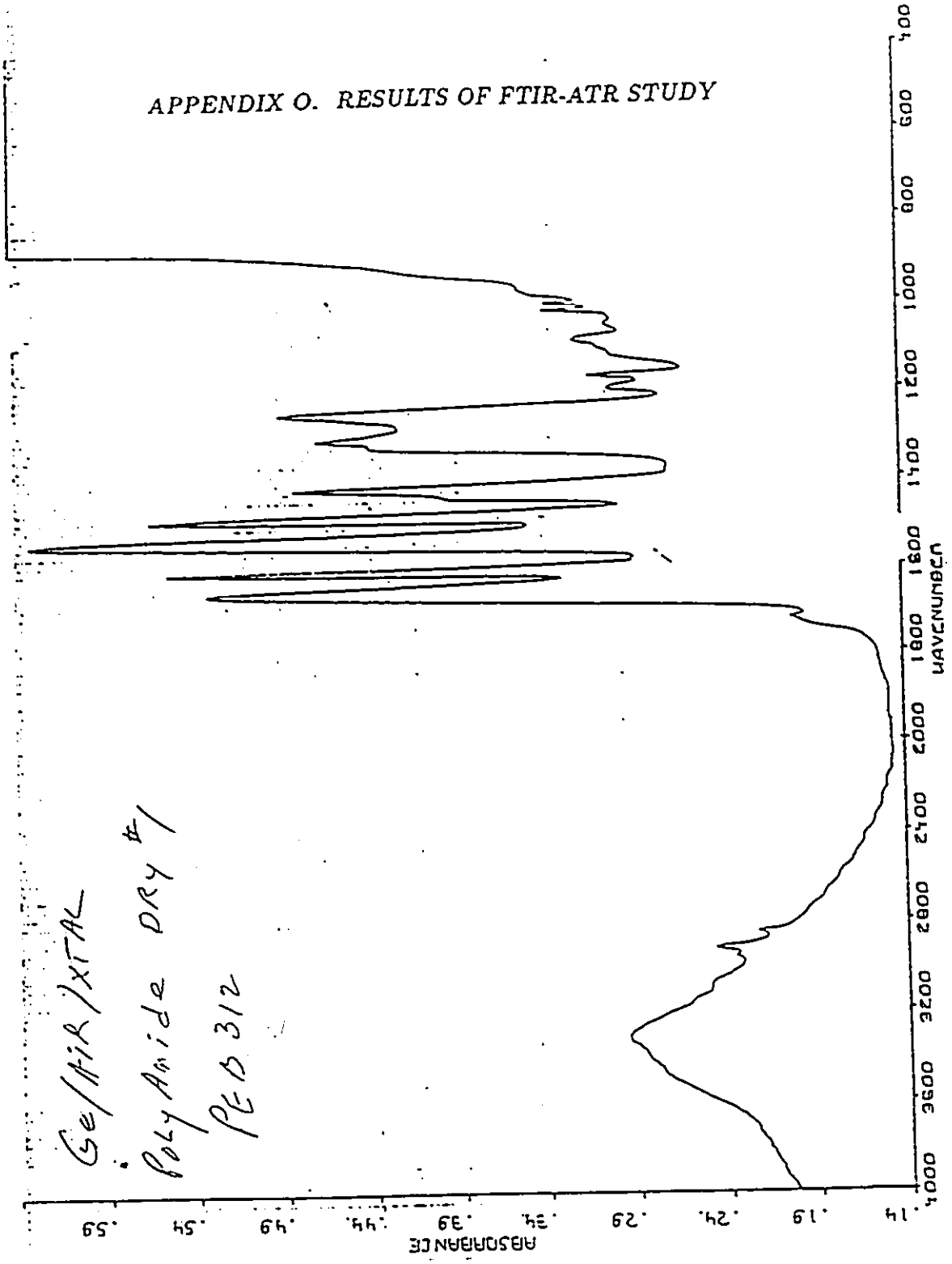

Figure O.1: Infrared Spectra of Dry Polyamide Membrane

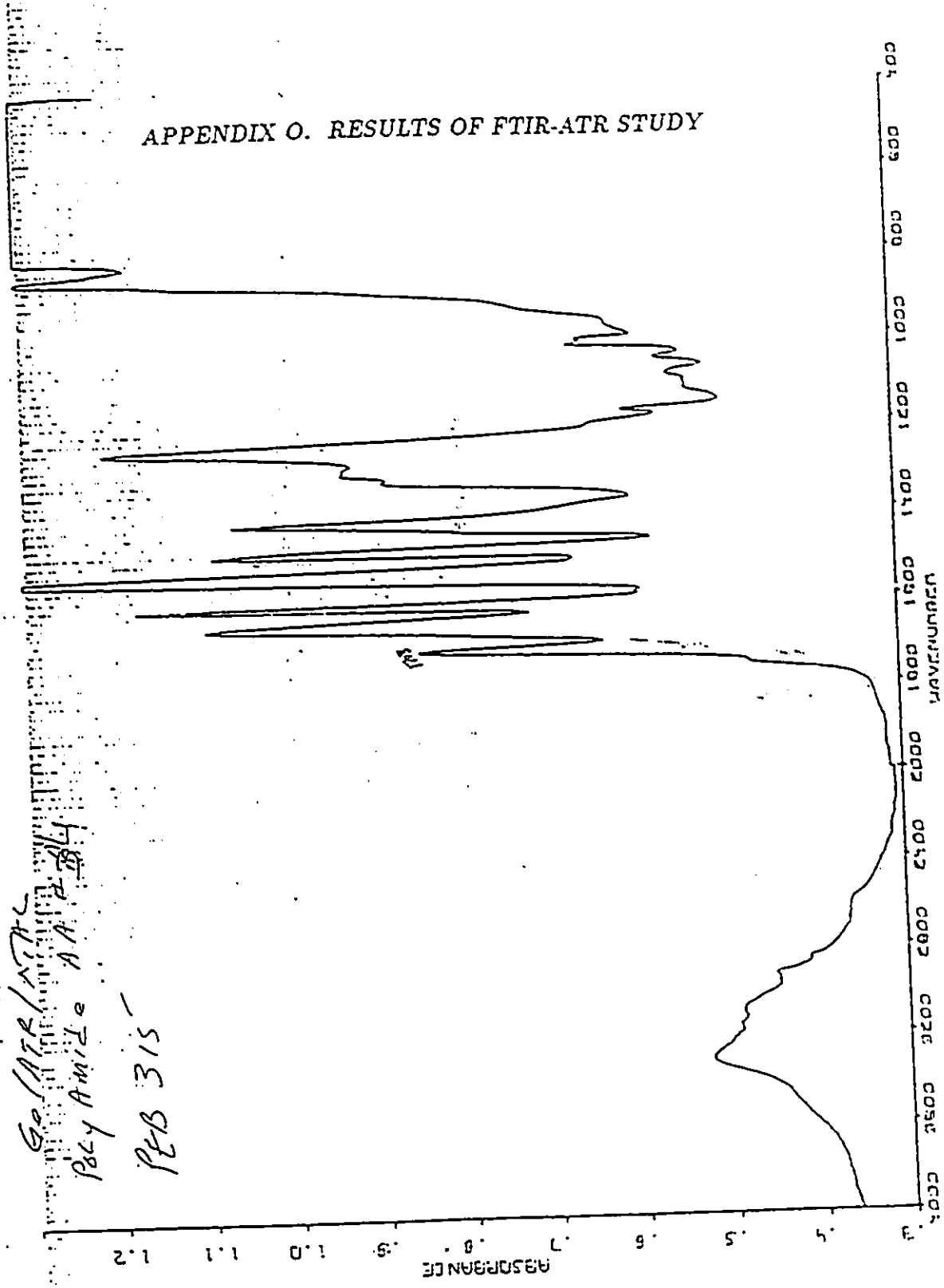

Figure O.2: Infrared Spectra of Polyamide Membrane Soaked in Acetic Acid

Appendix P

Calculation Results Using the Model

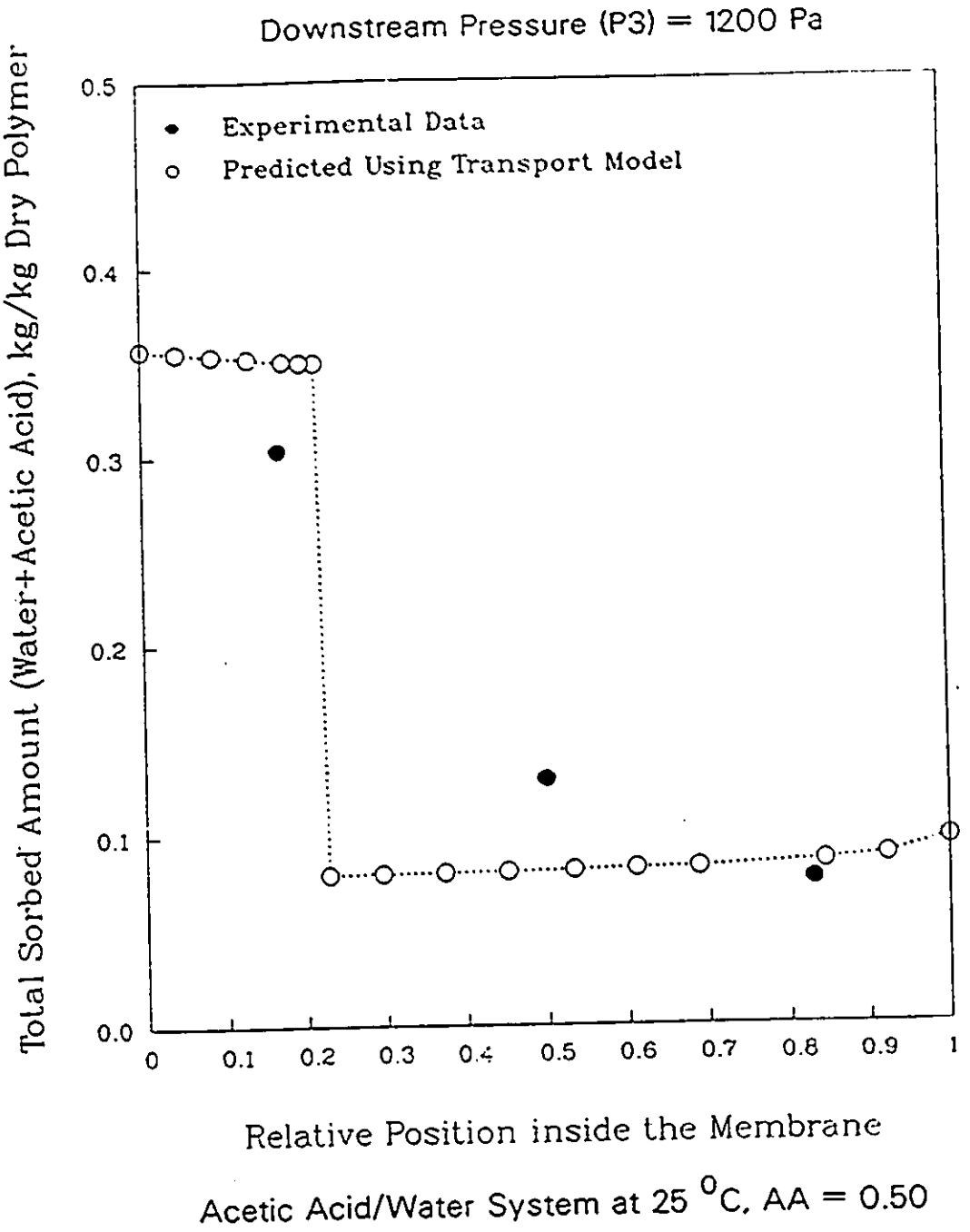

Figure P.1: Calculated Penetrant Concentration Profile Compared with the Experimental Profiles

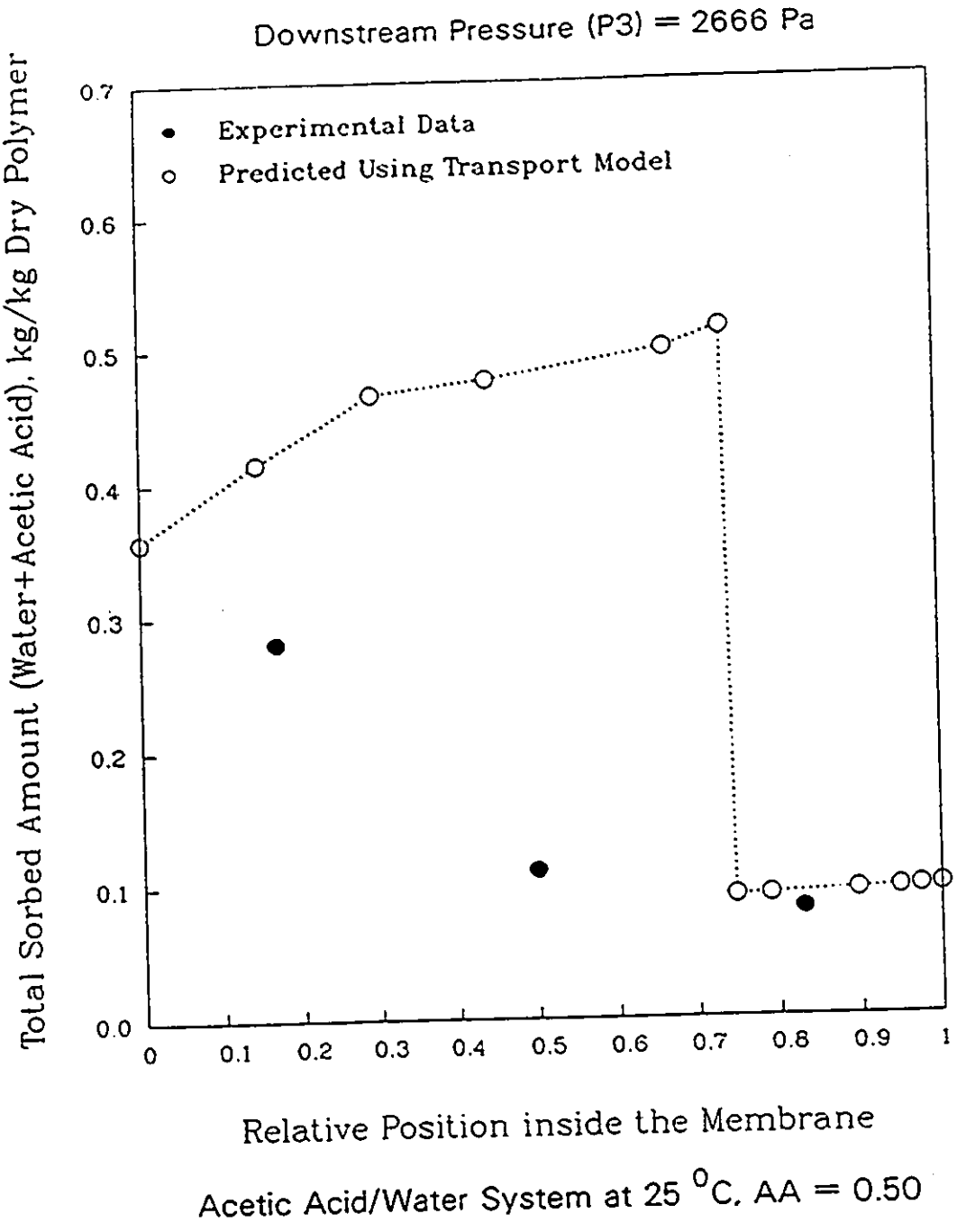

Figure P.2: Calculated Penetrant Concentration Profile Compared with the Experimental Profiles

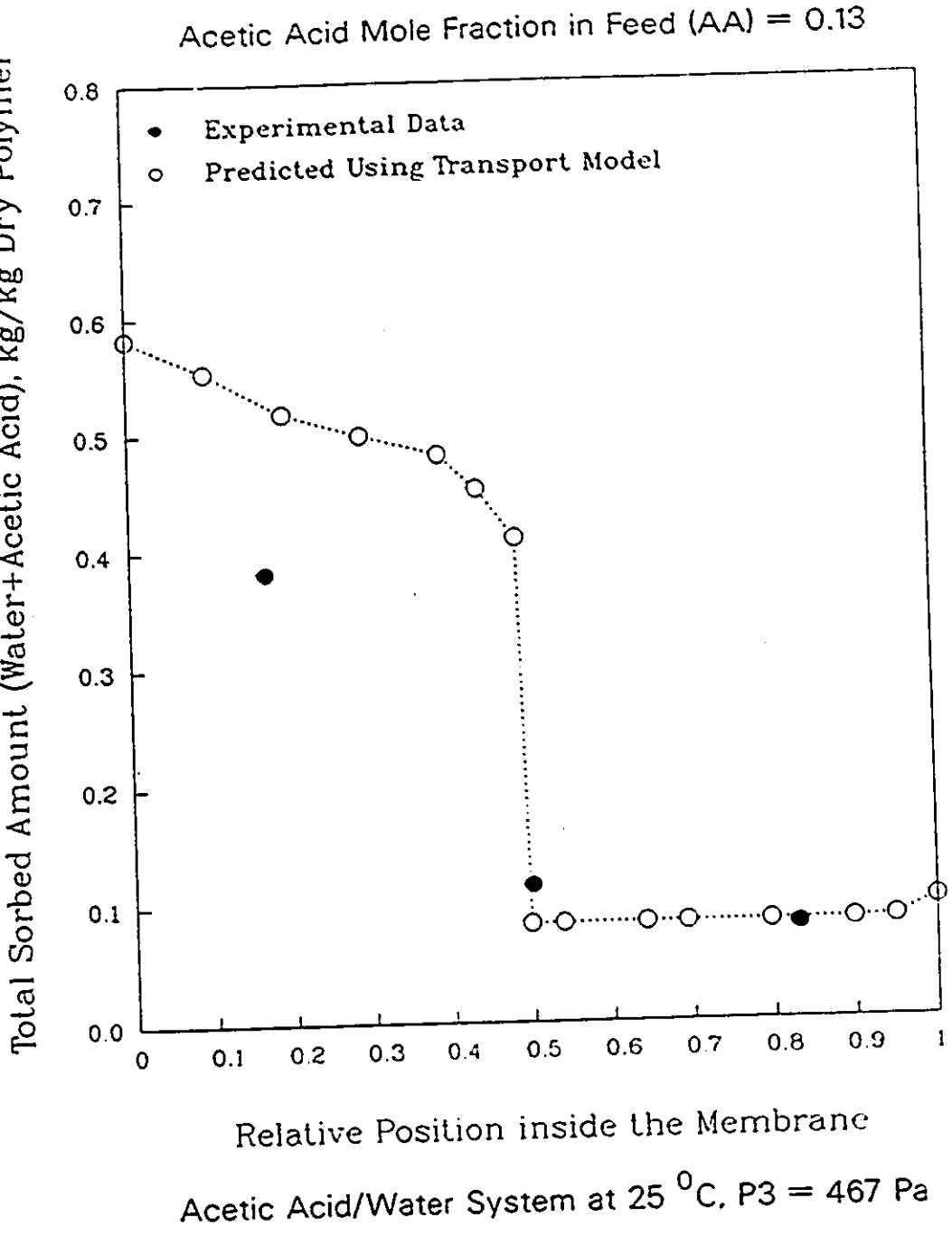

Figure P.3: Calculated Penetrant Concentration Profile Compared with the Experimental Profiles

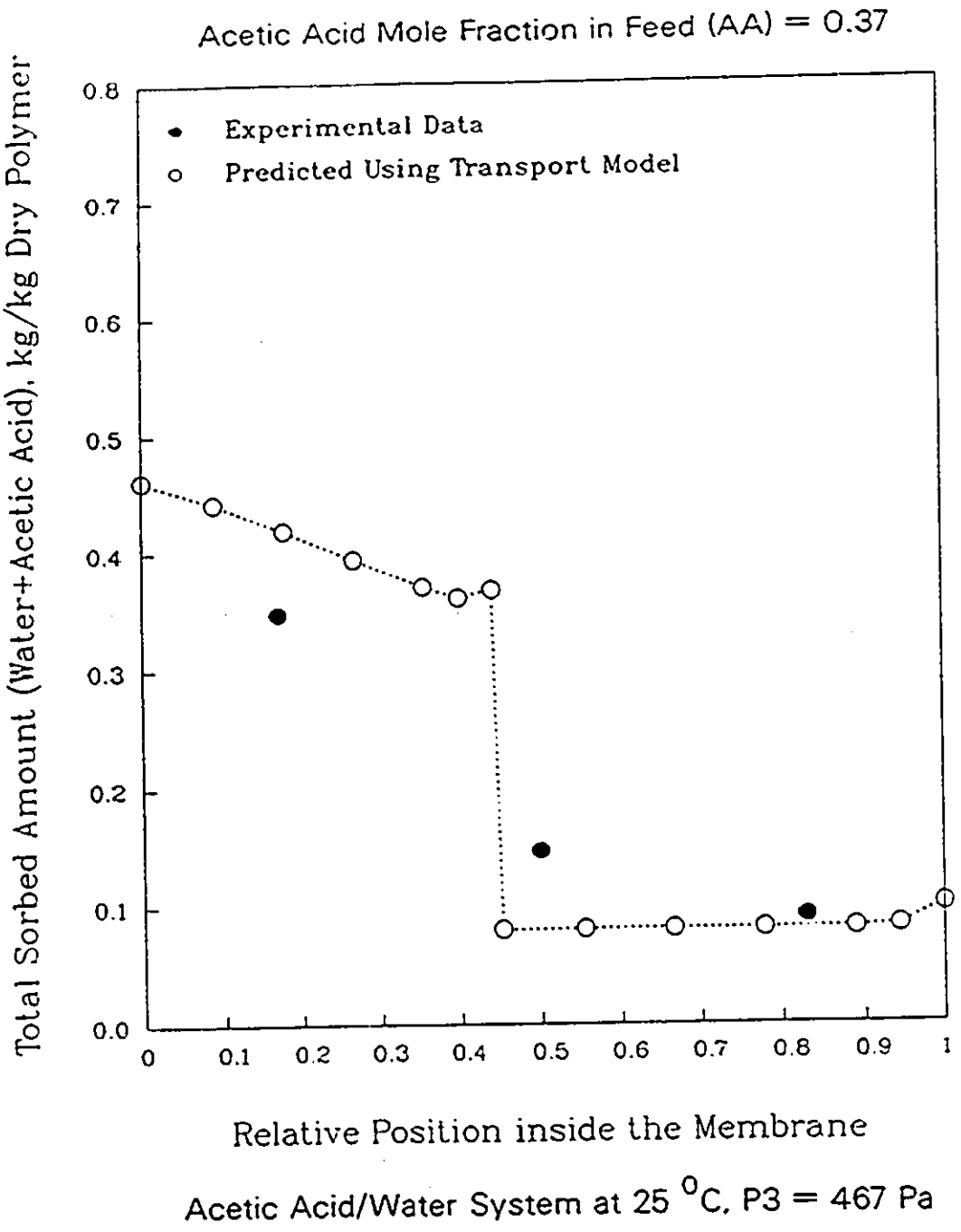

Figure P.4: Calculated Penetrant Concentration Profile Compared with the Experimental Profiles

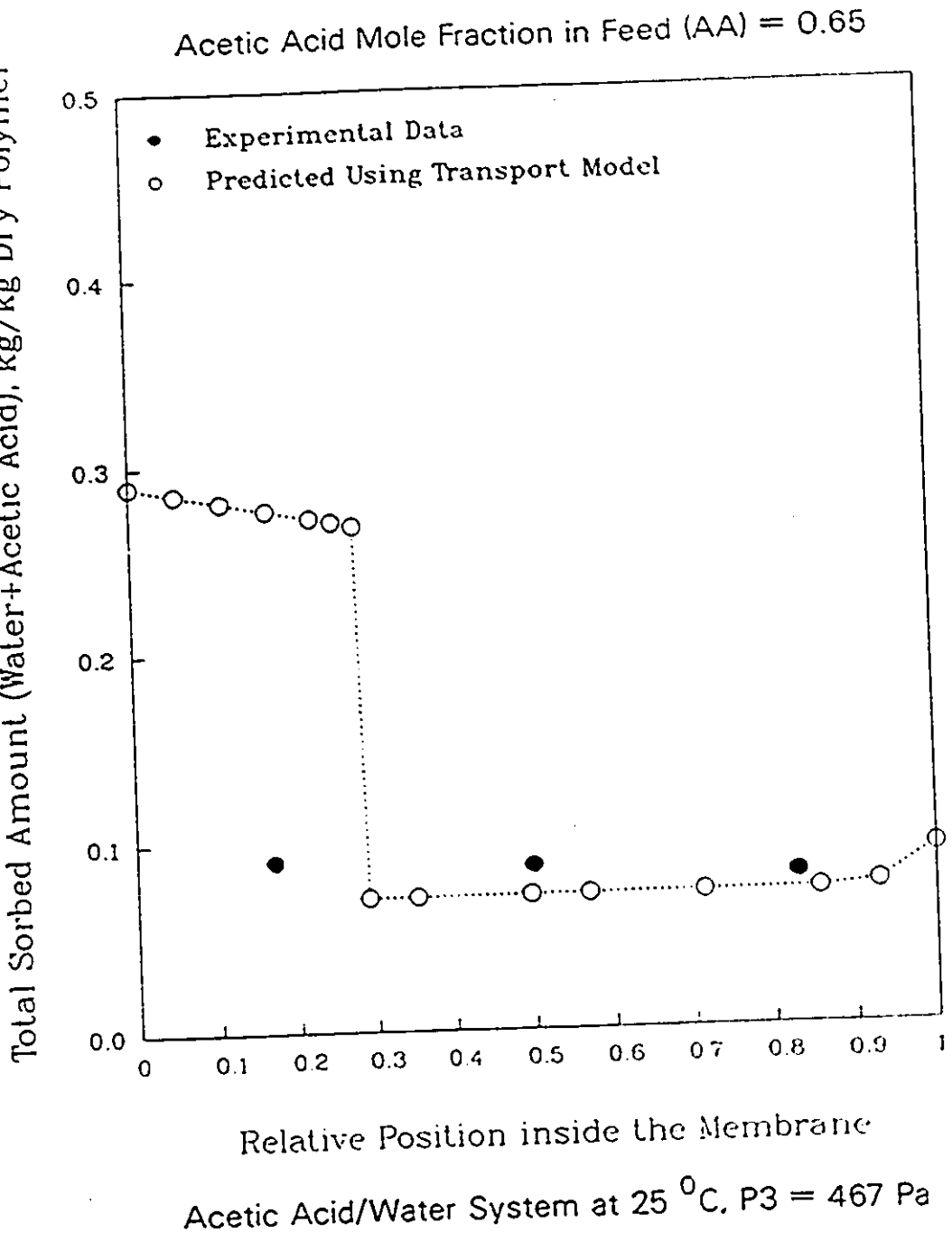

Figure P.5: Calculated Penetrant Concentration Profile Compared with the Experimental Profiles

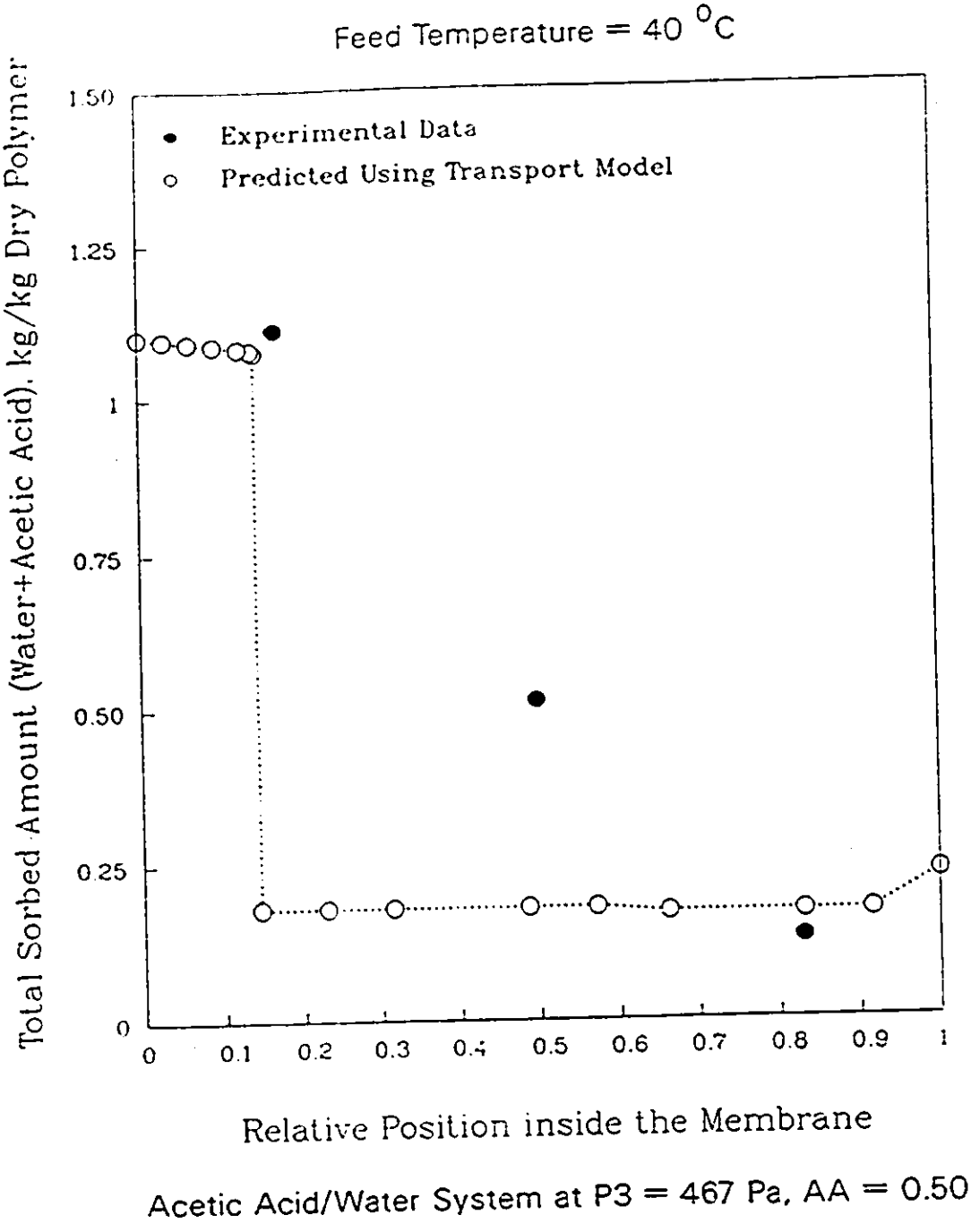

Figure P.6: Calculated Penetrant Concentration Profile Compared with the Experimental Profiles

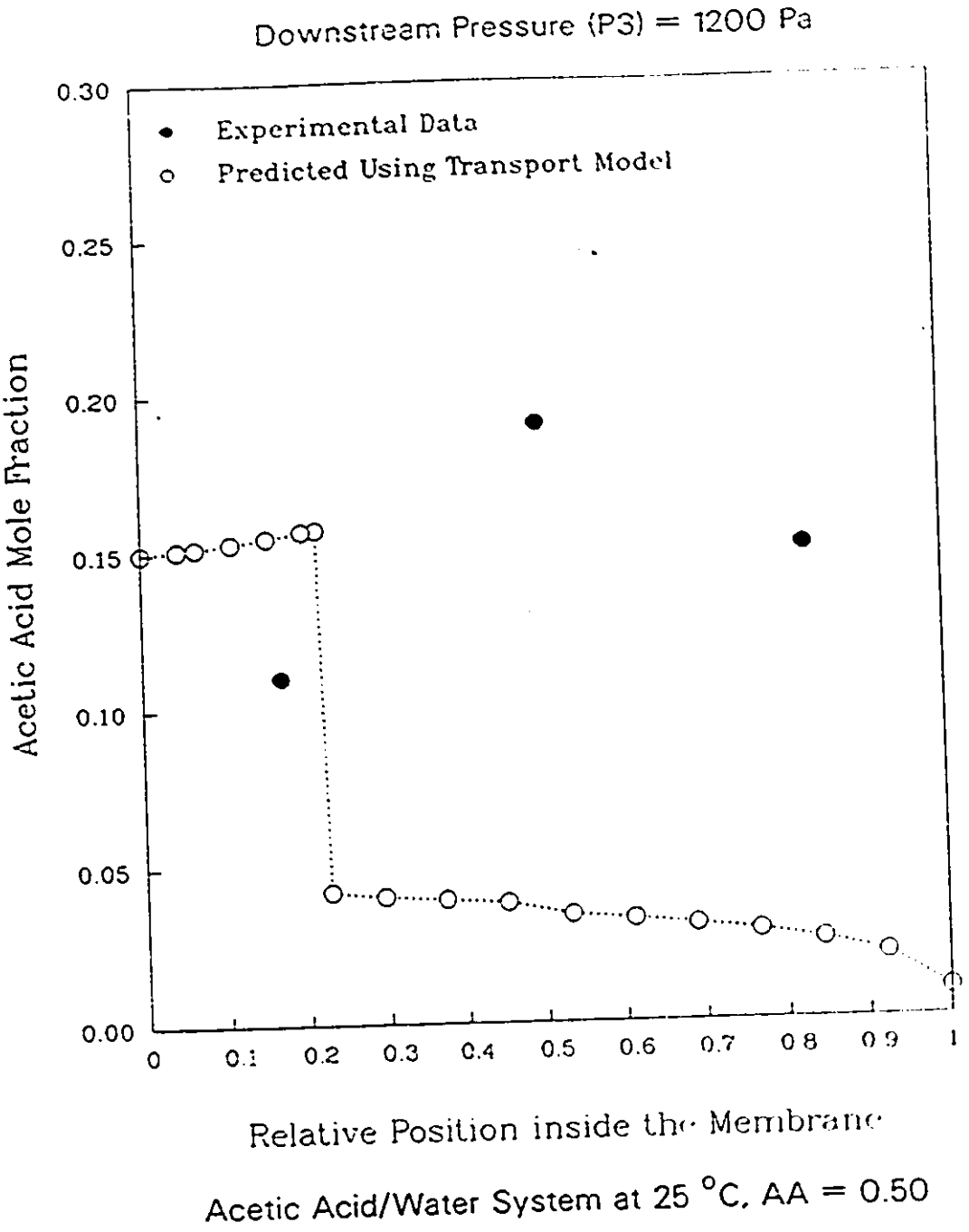

Figure P.7: Calculated Penetrant Concentration Profile Compared with the Experimental Profiles

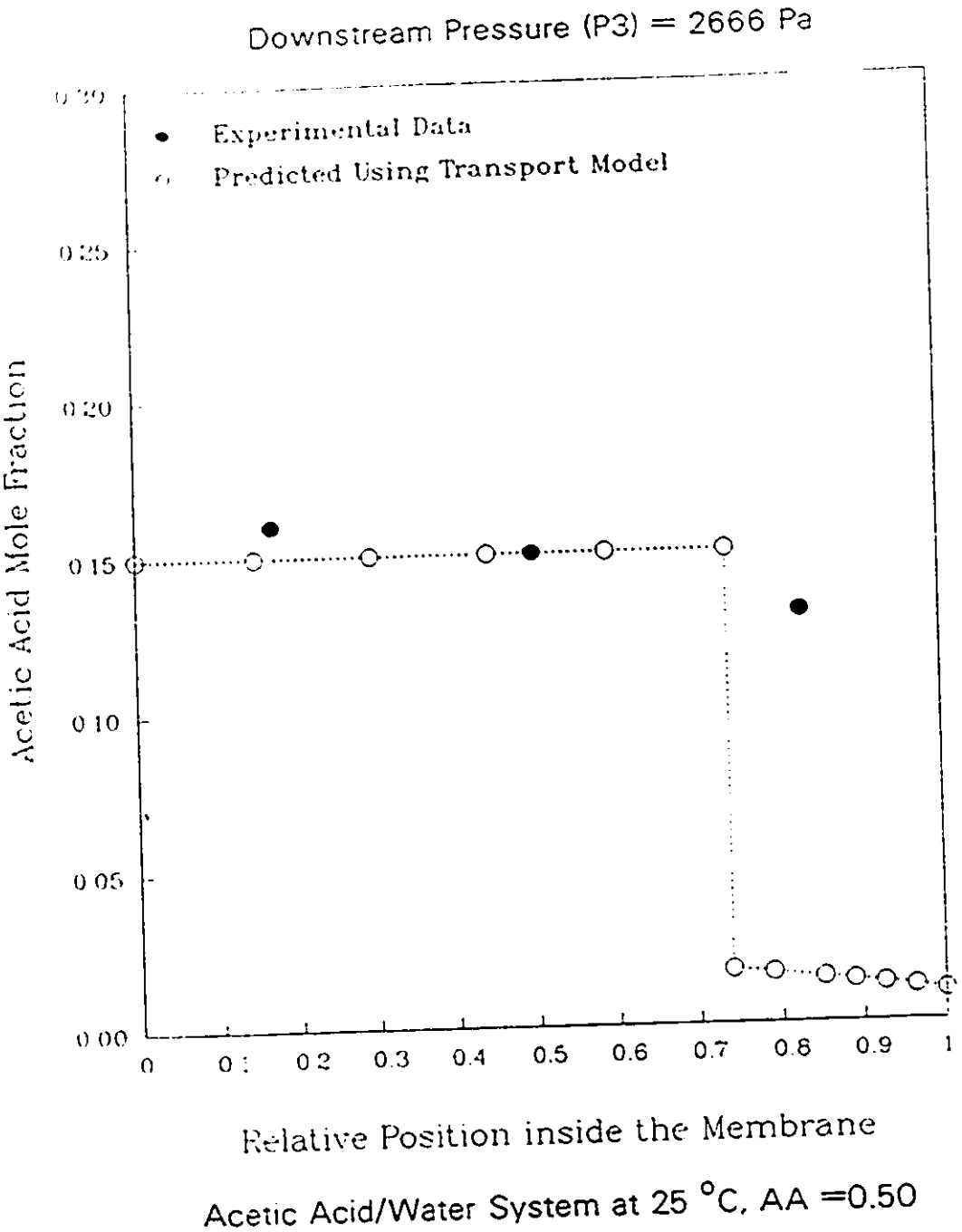

Figure P.8: Calculated Penetrant Concentration Profile Compared with the Experimental Profiles

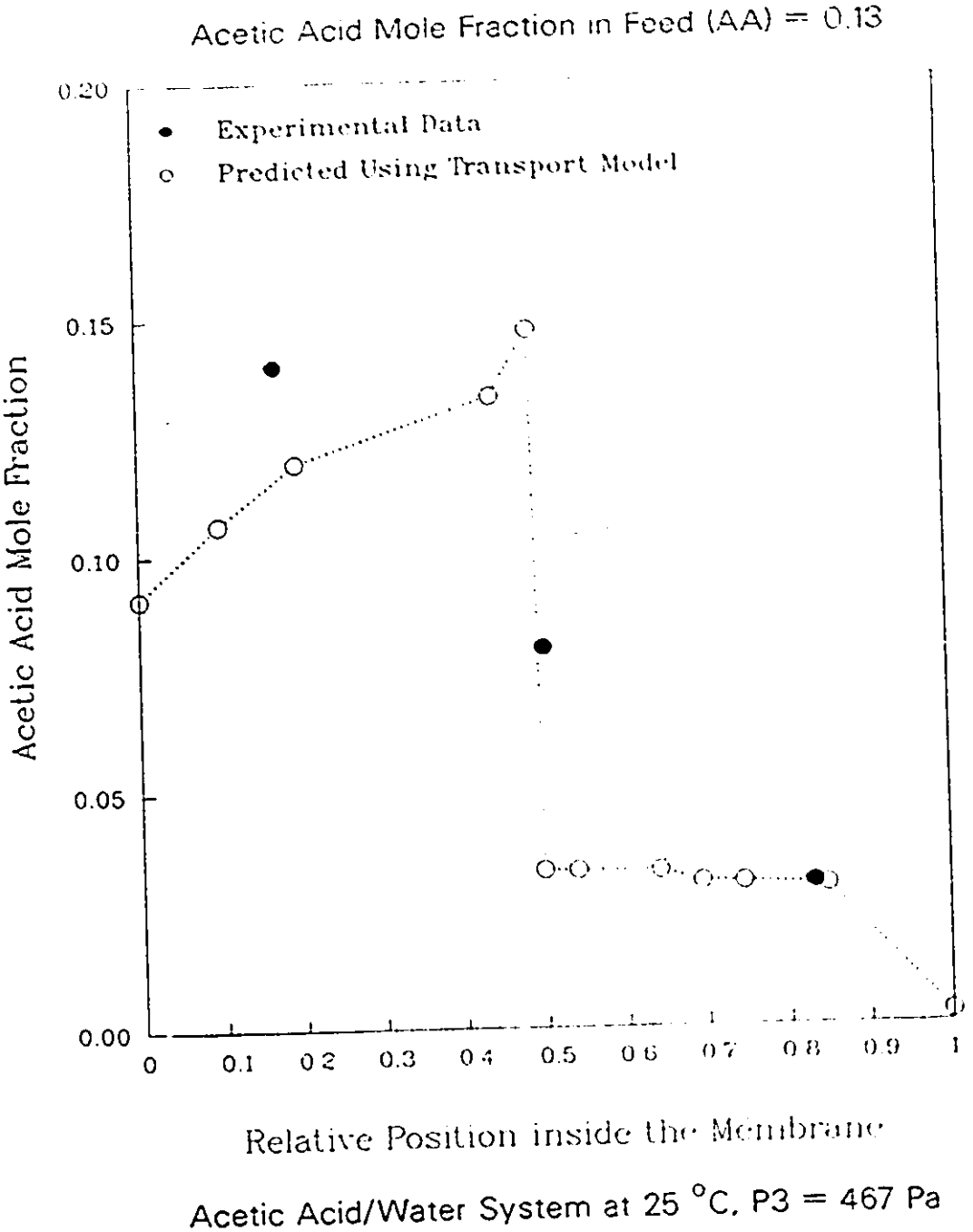

Figure P.9: Calculated Penetrant Concentration Profile Compared with the Experimental Profiles

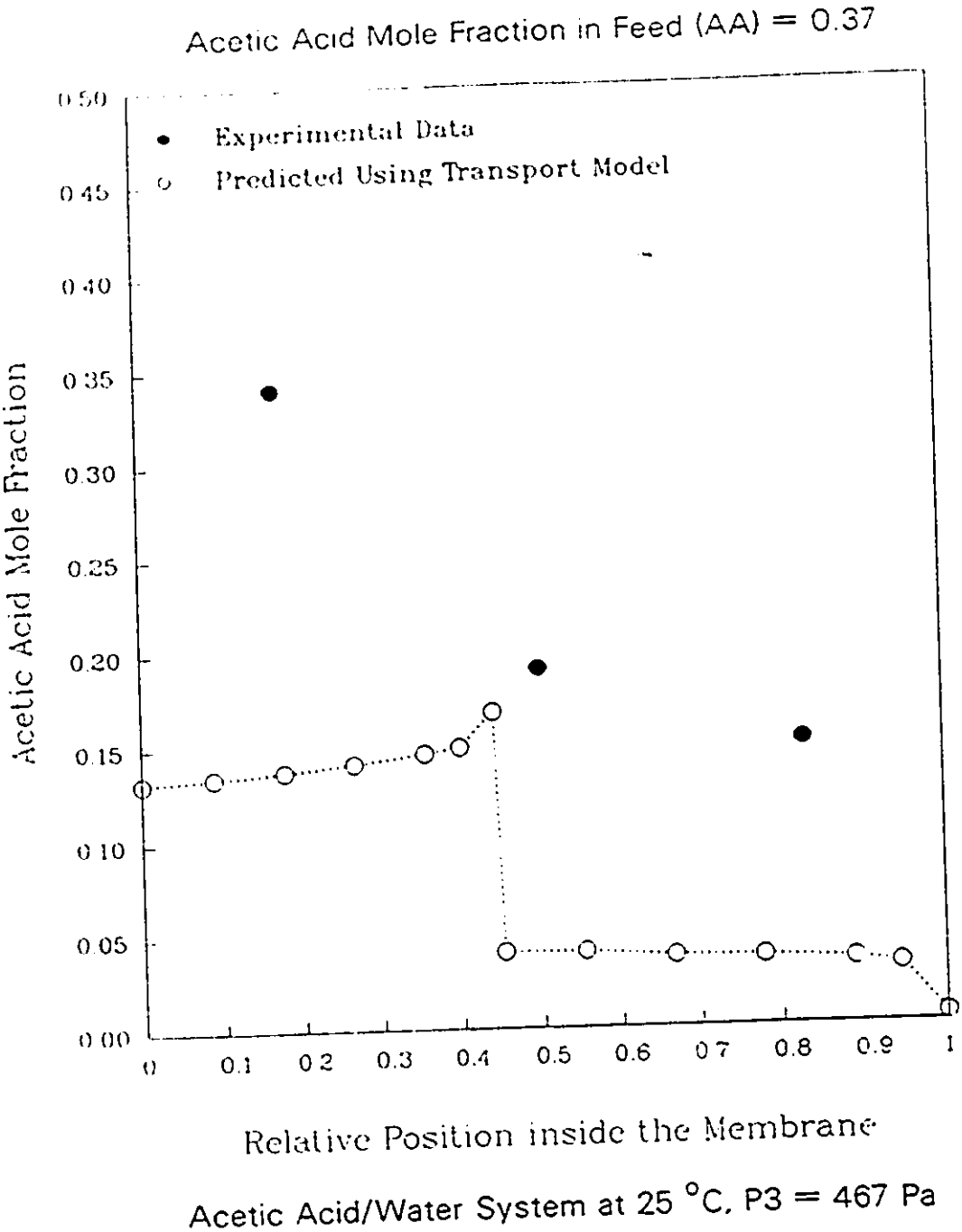

Figure P.10: Calculated Penetrant Concentration Profile Compared with the Experimental Profiles

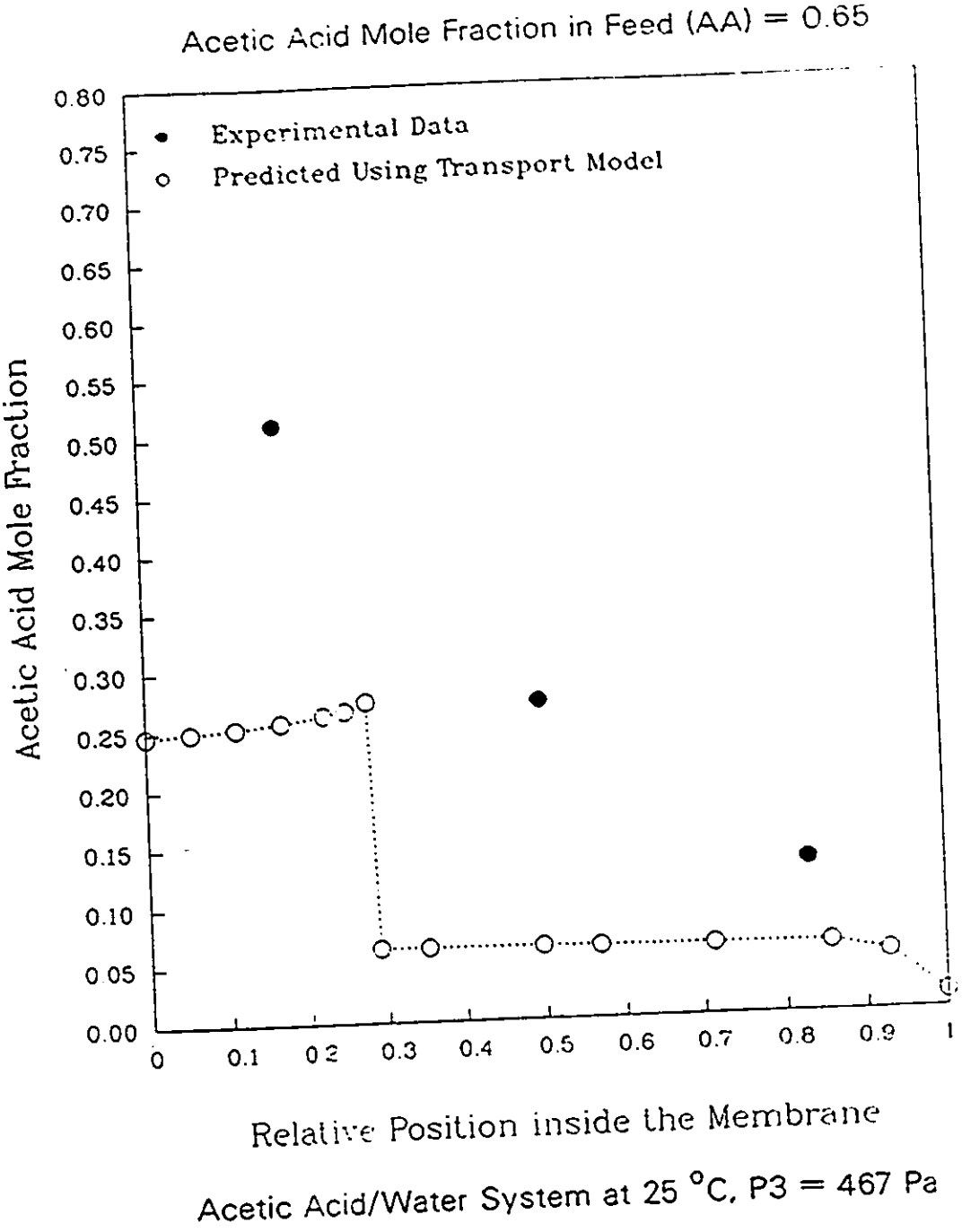

Figure P.11: Calculated Penetrant Concentration Profile Compared with the Experimental Profiles

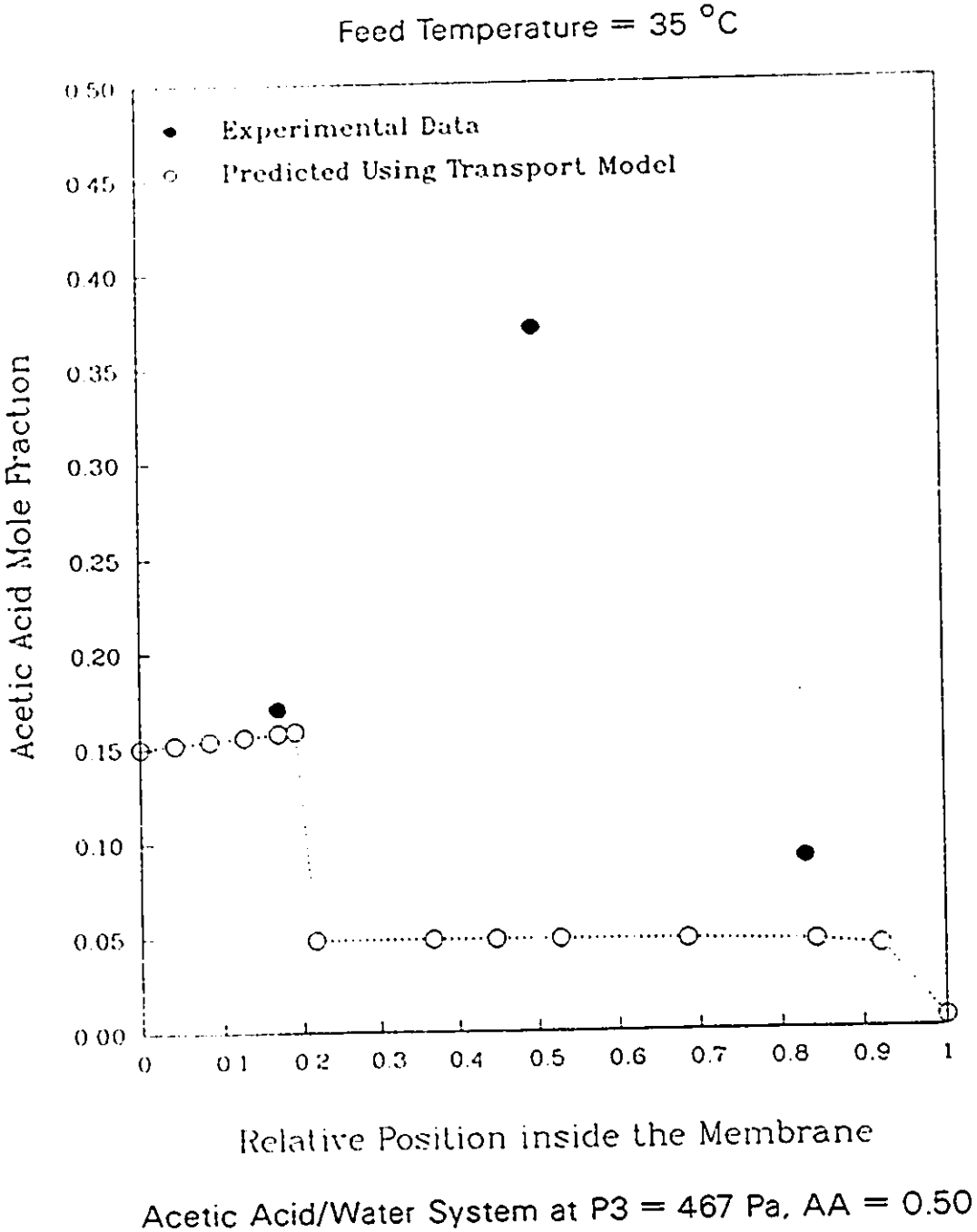

Figure P.12: Calculated Penetrant Concentration Profile Compared with the Experimental Profiles

Appendix Q

Computer Program and Sample Output

```
C     Program Name is :- pervap1
C                        *******
C
C     To calculate the concentration Profile for the pervaporation
C     Data required:
C     1. pure permeation data  (BI/BJ) RATIO
C     2. liquid sorption, vapor sorption data
C     3. pervaporation data
C     4. vapor-liquid equilibrium data
C     process of acetic acid / water system
C     ------------------------------------------------------------
      IMPLICIT REAL*8 (A-H,O-Z)
      REAL*8 MWI,MWJ,KZ
      INTEGER II
      DIMENSION PII(200),PPI(200),PPJ(200),XII(200),YII(200),
     1          YJ(200),PPT(200),AMTD(200),XXA(200),PXX(200),XI(200),
     2          YI(200),WI(200),PPII(200),XXI(200),XMI(200),WW(200),
     3          P1I(200),P2J(200),P3T(200),Y(200),Z(200),WT(200),
     4          XX(100),XEXP(200),YEXP(200),PPTEXP(200),WTEXP(200),
     5          C1(100),PPEXP(200),WIEXP(200),WWEXP(200),XIIEXP(200),
     6          XMIEXP(200),CVLEXI(4),CVLEPJ(4),CLSXMI(4),CLSWT1(4),
     7          CLSWT2(4),CVSWI(4),CVSWW(4),PIEXP(200),PJEXP(200),
     8          XIEXP(200),POSA(200),POSDAA(200),POSDBB(200),
     9          POSABS(200),YMI(200),WMTOT(200)
      DIMENSION X(3),FVEC(3),DIAG(3),FJAC(3,3),R(45),QTF(3),WA1(3),
     *          WA2(3),WA3(3),WA4(3),XGUESS(3),WK(200)
      INTEGER   N,MAXFEV
      CHARACTER*75 TITLE1,TITLE2,TITLE3,STITLE,VLETITLE,LSTITLE,
     *             IDVAR,VSTITLE,SEPMARK
      CHARACTER*40 NAME1,NAME2,NAME3,NAME4,NAME5,NAME6,NAME7
      EXTERNAL     FCN,JAC,DN2QNJ,UMACH
      DATA         NEQN / 2 /
      DATA        MWI,MWJ,WTFLUX,P3,YI3,XI2,PISO,PJSO,AREA/
     1            60.05,18.016,0.0283,3.5,0.07,0.5,15.7,23.8,9.60/
      DATA        BIDELTA,BJDELTA/
     1            0.1115927E-06,0.10786E-05/
C     ------------------------------------------------------------
      COMMON/ONE/ BIJ,QIJ, P3I,P3J,CVLEPJ
C     ------------------------------------------------------------
      WRITE (6,100)
      READ  (5,101) NAME1,NAME2,NAME3,NAME4,NAME5,NAME6,NAME7
      READ  (5,*) XGUESS(1),XGUESS(2)
      OPEN(UNIT=1,NAME=NAME1,TYPE='OLD')
      OPEN(UNIT=2,NAME=NAME2,TYPE='OLD')
      OPEN(UNIT=3,NAME=NAME3,TYPE='UNKNOWN')
      OPEN(UNIT=4,NAME=NAME4,TYPE='UNKNOWN')
      OPEN(UNIT=7,NAME=NAME5,TYPE='UNKNOWN')
      OPEN(UNIT=8,NAME=NAME6,TYPE='UNKNOWN')
      OPEN(UNIT=9,NAME=NAME7,TYPE='UNKNOWN')
C     ------------------------------------------------------------
      WRITE (4,4444)
    1 READ (1,102,END=99) SEPMARK
      READ (1,*   ) NGROUPS
      READ (1,103,END=99) VLETITLE,IDVAR
      READ (1,*   ) (CVLEPJ(I),I=1,4)  , (CVLEXI(I),I=1,4)
      READ (1,*   )  NVLE,(PIEXP(I),PJEXP(I),XIEXP(I),I=1, NVLE)
      READ (1,103) LSTITLE,IDVAR
      READ (1,*   ) (CLSXMI(I),I=1,4),(CLSWT1(I),I=1,4),
     1              (CLSWT2(I),I=1,4)
      READ (1,*   ) NLS,(XIIEXP(I), XMIEXP(I), WTEXP(I), I=1,NLS)
      READ (1,103) VSTITLE,IDVAR
```

```
      READ (1,*   ) (CVSWI(I),I=1,4)   ,  (CVSWW(I),I=1,4)
      READ (1,*   ) NVS,(PPEXP(I), WIEXP(I), WWEXP(I),I=1,NVS)
C     ------------------------------------------------------------------
 4444 FORMAT (T2,'TEMP',T9,'XI2',T16,'XIEQ',T25,'YIEQ',T37,'BIDELTA',
     1 T49,'BJDELTA',T61,'BIJ',T71,'DB11'/T2,75('-'))
      DO 9100 NTEMP = 1,NGROUPS
      READ (2,555,END=99) SEPMARK,TITLE1,TITLE2,TITLE3
      READ (2,*) NSUBGROUP
      DO 9000 NSETS = 1, NSUBGROUP
      READ (2,556) STITLE
      READ (2,*  ) MWI,MWJ,WTFLUX,TEMP,P3,YI3,XI2,PISO,PJSO,AREA,
     1             BIDELTA,BJDELTA
C     ------------------------------------------------------------------
C     Calculation of different parameters
C     ===================================
C      BJDELTA = BIDELTA / BIJ
      BIJ = BIDELTA / BJDELTA
      QT  = WTFLUX/(MWJ*(1.0-YI3) + MWI*YI3)/AREA
      QI  = QT * YI3
      QJ  = QT-QI
      QIJ = QI/QJ
      P3I = P3*YI3
      P3J = P3 - P3I
      WRITE (3,893) TITLE1,TITLE2,TITLE3,STITLE,MWI,MWJ,WTFLUX,TEMP,P3
     1             ,YI3,XI2,PISO,PJSO,AREA,QI,QJ,P3I,P3J,QT,BIJ
C     ------------------------------------------------------------------
C     Calculation of equilibrium XI , YI and PT using subroutine DNSQE
C     ================================================================
C     NOTE:-
C     ****
C     X(1) = PIEQ
C     X(2) = PJEQ
C     ------------------------------------------
      NEQN      = 2
      LDFJAC    = 2
      MAXFEV    = 100
      XTOL      = 1.0D-05
      ERREL     = 1.0D-05
C     ------------------------------------------------------------------
C     SGI subroutine Call
C     *******************
      CALL DNEQNJ (FCN,JAC,ERREL,NEQN,MAXFEV,XGUESS,X,FNORM)
C     ------------------------------------------------------------------
C     Equilibrium Values
C     ==================
      PIEQ      = X(1)
      PJEQ      = X(2)
      PTEQ      = PIEQ + PJEQ
      YIEQ      = PIEQ/PTEQ
      YJEQ      = 1.00 - YIEQ
      XIEQ      = CVLEXI(1)+CVLEXI(2)*PIEQ+CVLEXI(3)*PIEQ*PIEQ+
     1            CVLEXI(4)*PIEQ*PIEQ*PIEQ
C     ------------------------------------------------------------------
C     Calculation of the ratio delta(b)/delta
C     =======================================
      DB11   = BIDELTA * (PIEQ**2.0-P3I**2.0)/QI
      DB22   = BJDELTA * (PJEQ**2.0-P3J**2.0)/QJ
      WRITE (3,33) XIEQ , YIEQ , PTEQ , PIEQ,PJEQ,DB11,DB22
      WRITE (4,3333) TEMP,XI2,XIEQ,YIEQ,BIDELTA,BJDELTA,BIJ,DB11
 3333 FORMAT (T2,F5.2,T9,F5.3,T16,F7.3,T25,F7.4,T37,E12.4,T49,E12.5,
```

```
     1 T61,F7.4,T71,F7.4)
C     ------------------------------------------------------------------
      DAA  =1.000 - DB11
      VK = DLOG ((XIEQ -YI3)/(XI2 - YI3))
      WRITE (3, 290) DB11,DAA,VK,PIEQ, PJEQ,PTEQ,YIEQ,YJEQ, XIEQ
C     ------------------------------------------------------------------
C     Creating many points along DAA
C     ==============================
      NPDAA = 51
      NPINC = 5
      NPDAA2 = (NPDAA-1)/NPINC + 1
      DO 123 JDAA = 1,NPDAA
      POSDAA(JDAA) = DFLOAT(JDAA-1)/DFLOAT(NPDAA-1)
      POSA(JDAA)   = DAA * POSDAA(JDAA)
      XXI(JDAA)=DEXP(VK*POSDAA(JDAA)) * (XI2- YI3) + YI3
      XMI(JDAA)=CLSXMI(1)+CLSXMI(2)*XXI(JDAA)+CLSXMI(3)*XXI(JDAA)**2 +
     1          CLSXMI(4)*XXI(JDAA)**3
      IF(XXI(JDAA).LE.0.500)
     1 WT(JDAA)=CLSWT1(1)+CLSWT1(2)*XXI(JDAA)+CLSWT1(3)*XXI(JDAA)**2 +
     1          CLSWT1(4)*XXI(JDAA)**3
      IF(XXI(JDAA).GT.0.500)
     1 WT(JDAA)=CLSWT2(1)+CLSWT2(2)*XXI(JDAA)+CLSWT2(3)*XXI(JDAA)**2 +
     1          CLSWT2(4)*XXI(JDAA)**3
  123 CONTINUE
C     ------------------------------------------------------------------
      WRITE (3,110) (JDAA,POSDAA(JDAA),POSA(JDAA),XXI(JDAA),
     1      JDAA=1,NPDAA,NPINC)
      WRITE (3,888)
      WRITE (3,310) (JDAA,POSDAA(JDAA),POSA(JDAA),XXI(JDAA),
     1      XMI(JDAA),WT(JDAA),JDAA=1,NPDAA,NPINC)
      WRITE (3,888)
C     ------------------------------------------------------------------
C     Calculation of pressure vs position :
C     ====================================
      NPDBB = 51
      NPINC = 5
      NPDBB2 = (NPDBB-1)/NPINC + 1
      DO 124 JDBB  = 1,NPDBB
      POSDBB(JDBB) = DFLOAT(JDBB-1)*DB11/DFLOAT(NPDBB-1)
      PPI(JDBB)    = DSQRT(PIEQ*PIEQ - (QI/BIDELTA)*POSDBB(JDBB))
      PPJ(JDBB)    = DSQRT(PJEQ*PJEQ - (QJ/BJDELTA)*POSDBB(JDBB))
      YI(JDBB)     = PPI(JDBB)/(PPJ(JDBB)+PPI(JDBB))
      POSABS(JDBB) = POSDBB(JDBB) + DAA
C      PP(JDBB)     = YI(JDBB)
      WI(JDBB)     = CVSWI(1)+CVSWI(2)*YI(JDBB)+CVSWI(3)*
     1               YI(JDBB)**2+CVSWI(4)*YI(JDBB)**3
      WW(JDBB)     = CVSWW(1)+CVSWW(2)*YI(JDBB)+CVSWW(3)*
     1               YI(JDBB)**2+CVSWW(4)*YI(JDBB)**3
      WMTOT(JDBB)  = WI(JDBB) + WW(JDBB)
      YMI(JDBB)    = (WI(JDBB)/MWI)/((WI(JDBB)/MWI)+(WW(JDBB)/MWJ))
  124 CONTINUE
C     ------------------------------------------------------------------
      WRITE (3,111) (JDBB,POSDBB(JDBB),POSABS(JDBB),PPI(JDBB),
     1 PPJ(JDBB),YI(JDBB) ,JDBB=1,NPDBB,NPINC)
      WRITE (3,888)
      WRITE (3,311) (JDBB,POSDBB(JDBB),POSABS(JDBB),PPI(JDBB),
     1 YI(JDBB),YMI(JDBB) ,WMTOT(JDBB),JDBB=1,NPDBB,NPINC)
      WRITE (3,888)
C     ------------------------------------------------------------------
C     Writing to plotting files
```

```
C     ========================
      WRITE (7,210) TITLE1,TITLE2,STITLE
      WRITE (7,225)
      WRITE (7,211) NPDAA,(POSA(JDAA), XXI(JDAA),JDAA=1,NPDAA)
      WRITE (7,225)
      WRITE (7,211) NPDAA2,(POSA(JDAA), XXI(JDAA),JDAA=1,NPDAA,NPINC)
      WRITE (7,228)
      WRITE (7,211) NPDBB,(POSABS(JDBB),YI(JDBB),JDBB=1,NPDBB)
      WRITE (7,228)
      WRITE (7,211) NPDBB2,(POSABS(JDBB),YI(JDBB) ,JDBB=1,NPDBB,NPINC)
C     ------------------------------------------------------------------
      WRITE (8,210) TITLE1,TITLE2,STITLE
      WRITE (8,226)
      WRITE (8,211) NPDAA2,(POSA(JDAA), XMI(JDAA),JDAA=1,NPDAA,NPINC)
      WRITE (8,229)
      WRITE (8,211) NPDBB2,(POSABS(JDBB),YMI(JDBB),JDBB=1,NPDBB,NPINC)
C     ------------------------------------------------------------------
      WRITE (9,210) TITLE1,TITLE2,STITLE
      WRITE (9,227)
      WRITE (9,211) NPDAA2,(POSA(JDAA), WT(JDAA),JDAA=1,NPDAA,NPINC)
      WRITE (9,230)
      WRITE (9,211) NPDBB2,(POSABS(JDBB),WMTOT(JDBB)
     1              ,JDBB=1,NPDBB,NPINC)
C     ------------------------------------------------------------------
 9000 CONTINUE
 9100 CONTINUE
       GO TO 1
C     ------------------------------------------------------------------
  100 FORMAT (T2,'Enter 2 File Names : Input & Output :-')
  101 FORMAT (A40/A40/A40/A40/A40/A40/A40)
  102 FORMAT (A75)
  103 FORMAT (A75/A75)
   33 FORMAT (//T2,'Liquid-Vapor Boundary Results'/T2,30('=')//
     1 T2,'Acetic Acid mole fraction in liquid at boundary'
     2 ,T51,'=',F15.5/ T2,'Acetic Acid mole fraction in vapor at',
     3 ' boundary',T51,'=',F15.5/ T2,'Equilbrium Total Vapor Pressure',
     4 T51,'=',F15.5,2X,'mmHg'/
     5 T2,'Eq. partial pressure for Acetic Acid',T51,'=',
     6 F15.5,2X,'mmHg'/T2,'Eq. partial pressure for Water',T51,'=',
     7 F15.5,2X,'mmHg'/T2,'Ratio delta(b)/delta from acetic acid',T51
     8 ,'=',F15.5/T2,'Ratio delta(b)/delta from water',T51,'=',
     9 F15.5/T2,70('='))
  110 FORMAT (T2,'Liquid Concentration Profile Along DAA'/
     1 T2,50('-')/T2,'No.',T11,'Position',T25,'Position',T40,
     2 'Acetic Acid'/T11,'in delta(a)',T25,'in delta',T40,
     3 'mole fraction'/T40,'XI'/T2,50('-')/
     4 (I5,T11,F8.3,T25,F8.3,T40,F10.5))
  111 FORMAT (T2,'Partial Pressure & Mole Fraction profile along DBB'/
     1 T2,75('-')/T2,'No.',T11,'Position',T21,'Position',T31,
     2 'Acetic Acid',T45,'Water',T60,'MOLE FRACN'/
     2 T11,'delta(b)',T21,'delta',T31,'Partial press.',T45,
     3 'Partial Press'/T31,'mmHg',T45,'mmHg'/T2,75('-')/
     4 (I5,T11,F8.4,T21,F8.4,T31, F10.5,T45,F10.5,T60,F7.3))
  210 FORMAT (T2,70('+')/A75/A75/A75)
  211 FORMAT (I5/(2F10.5))
  225 FORMAT(T2,70('-')/T2,'XXI   vs Position for Liquid Phase')
  228 FORMAT(T2,70('-')/T2,'YI    vs Position for Gas Phase')
  226 FORMAT(T2,70('-')/T2,'XMI   vs Position for Liquid Phase')
  229 FORMAT(T2,70('-')/T2,'YMI   vs Position for Gas Phase')
  227 FORMAT(T2,70('-')/T2,'WT    vs Position for Liquid Phase')
```

```
 230 FORMAT(T2,70('-')/T2,'WMTOT vs Position for Gas Phase')
 290 FORMAT (//T2,'Phase Boundary Data'/T2,20('=')/
    1 T2,'DB11',T51,'=',F15.4/T2,'DAA' ,T51,'=',F15.4/
    2 T2,'VK',T51,'=',F15.4/T2,'Acetic Acid Partial Press at boundary',
    3 T51,'=',F15.4,2X,'mmHg'/T2,'Water Partial Press at boundary',
    4 T51,'=',F15.4,2X,'mmHg'/T2,'Total Vapor Pressure at boundary',
    5 T51,'=',F15.4,2X,'mmHg'/T2,'Acetic Acid vapor mole fraction at',
    6 ' boundary',T51,'=',F15.4/T2,'Water vapor mole fraction at ',
    7 'boundary',T51,'=',F15.4/T2,'Acetic Acid liquid mole fraction ',
    8 'at boundary',T51,'=',F15.4/T2,75('='))
 310 FORMAT (T2,'Liquid Sorption Prediction Along DAA'/
    1 T2,70('-')/T2,'No.',T11,'Position',T25,'Position',T37,
    2 'Acetic Acid',T50,'XMI',T61,'WT'/T11,'in delta(a)',T25,
    3 'in delta',T37,'XI',T50,'  ',T61,'kg/kg'/T2,70('-')/
    4 (I5,T11,F8.3,T25,F8.3,T37,F10.5,T50,F8.3,T61,F8.3))
 311 FORMAT (T2,'Vapor Sorption Prediction Along DBB'/
    1 T2,75('-')/T2,'No.',T11,'Position',T21,'Position',T31,
    2 'Acetic Acid',T42,'PP',T55,'YMI',T65,'WMTOT'/
    2 T11,'delta(b)',T21,'delta',T31,'Partial press.',T42,
    3 ' '/T31,'mmHg',T42,' ',T55,' ',T65,' '/T2,75('-')/
    4 (I5,T11,F8.4,T21,F8.4,T31, F10.5,T42,F7.3,T55,F7.3,T65,F7.3))
 555 FORMAT (A75/A75/A75/A75)
 556 FORMAT (A75)
 888 FORMAT (T2,75('='))
 893 FORMAT ('1',T2,A75/T2,A75/T2,A75/T2,A75//T2,
    * 'Input Parameters for the Permeate'/T2,32('=')/
    * T2,'Acetic Acid Molecular Weight',T41,'=',F15.3/
    * T2,'Water Molecular Weight',T41,'=',F15.3/
    * T2,'Permeate Weight Flux',T41,'=',F15.5,2X,'gm/hr'/
    * T2,'Feed Temperature ',T41,'=',F15.3,2X,'degree C'/
    * T2,'Downstream Pressure ',T41,'=',F15.3,2X,'mmHg'/
    * T2,'Acetic Acid Permeate mole fraction ',T41,'=',F15.3/
    * T2,'Acetic Acid Feed mole fraction ',T41,'=',F15.3/
    * T2,'Acetic Acid Saturation Vapor Pressure',T41,'=',F15.3,2X,
    * 'mmHg'/
    * T2,'Water Saturation Vapor Pressure',T41,'=',F15.3,2X,'mmHg'/
    * T2,'Membrane Area',T41,'=',F15.3,2X,'cm2'/
    * T2,'Acetic Acid molar flux in permeate',T41,'=', E15.5 ,2X,
    * 'mole/hr/cm2'/T2,'Water molar flux in permeate',T41,'=',E15.5,
    * 2X,'mole/hr/cm2'/T2,'Acetic Acid partial press. in permeate',
    * T41,'=',F15.3,2X,'mmHg'/T2,'Water partial press. in permeate',
    * T41,'=',F15.3,2X,'mmHg'/
    * T2,'Total Molar Flux',T41,'=',E15.5,2X,'mol/hr.cm2'/
    * T2,'Ratio of (Bi/Bj)',T41,'=',F15.5/T2,75('='))
C     ------------------------------------------------------------------
   99 STOP
      END
C     ******************************************************************
      SUBROUTINE FCN(X,F,NEQN)
      IMPLICIT REAL*8 (A-H,O-Z)
      DIMENSION X(NEQN),F(NEQN),CVLEPJ(4)
      INTEGER NEQN
      COMMON/ONE/ BIJ,QIJ, P3I,P3J,CVLEPJ
C     ------------------------------------------------------------------
      F(1) = BIJ * (X(1)*X(1) - P3I*P3I) -
     1       QIJ * (X(2)*X(2) - P3J*P3J)
      F(2) = X(2) - (CVLEPJ(1) + CVLEPJ(2)*X(1) + CVLEPJ(3)*X(1)**2 +
     *               CVLEPJ(4)*X(1)**3)
C      PRINT 90,F(1),F(2)
   90 FORMAT (T2,'f(1)=',E14.5,5X,'F(2)=',E14.5)
```

```
      RETURN
      END
C     ***********************************************************************
      SUBROUTINE JAC(NEQN,X,FJAC)
      IMPLICIT REAL*8 (A-H,O-Z)
C      SUBROUTINE JAC(NEQN,X,FVEC,FJAC,LDFJAC,IFLAG)
      INTEGER I,NEQN,IFLAG,K
      DIMENSION X(NEQN),FJAC(NEQN,NEQN),CVLEPJ(4),CVLEPT(4)
      COMMON/ONE/ BIJ,QIJ, P3I,P3J,CVLEPJ
C     ----------------------------------------------------------------
      FJAC(1,1) =  2.0 * BIJ * X(1)
      FJAC(1,2) = -2.0 * QIJ * X(2)
C     ----------------------------------------------------------------
      FJAC(2,1) = - (CVLEPJ(2) + 2.0 * CVLEPJ(3) * X(1) +
     &               CVLEPJ(4) * 3.0 * X(1)**2 )
      FJAC(2,2) = 1.0
C     ----------------------------------------------------------------
      RETURN
      END
```

1 Acetic Acid / Water System at 25 degree C, Feed = 0.50

Effect of downstream pressure

P3 = 3.5 mmHg

Input Parameters for the Permeate

Acetic Acid Molecular Weight	=	60.050	
Water Molecular Weight	=	18.016	
Permeate Weight Flux	=	0.02830	gm/hr
Feed Temperature	=	25.000	degree C
Downstream Pressure	=	3.500	mmHg
Acetic Acid Permeate mole fraction	=	0.070	
Acetic Acid Feed mole fraction	=	0.500	
Water density	=	1.000	g/cm3
Acetic Acid	=	1.049	g/cm3
Acetic Acid Saturation Vapor Pressure	=	15.700	mmHg
Water Saturation Vapor Pressure	=	23.800	mmHg
Membrane Area	=	9.600	cm2
Acetic Acid molar flux in permeate	=	0.98459E-05	mole/hr/cm2
Water molar flux in permeate	=	0.13081E-03	mole/hr/cm2
Acetic Acid partial press. in permeate	=	0.245	mmHg
Water partial press. in permeate	=	3.255	mmHg
Total Molar Flux	=	0.14066E-03	mol/hr.cm2
Ratio of (Bi/Bj)	=	0.10444	

Liquid-Vapor Boundary Results

Acetic Acid mole fraction in liquid at boundary	=	0.55972	
Acetic Acid mole fraction in vapor at boundary	=	0.44844	
Equilbrium Total Vapor Pressure	=	20.42849	mmHg
Eq. partial pressure for Acetic Acid	=	9.16090	mmHg
Eq. partial pressure for Water	=	11.26758	mmHg
Ratio delta(b)/delta from acetic acid	=	0.85273	
Ratio delta(b)/delta from water	=	0.85273	

Phase Boundary Data

DB11 (Relative vapor filled region)	=	0.8527	
DAA (Relative liquid filled region)	=	0.1473	
K (mass transfer coefficient)	=	6.24E-8	m/s
Acetic Acid Partial Press at boundary	=	9.1609	mmHg
Water Partial Press at boundary	=	11.2676	mmHg
Total Vapor Pressure at boundary	=	20.4285	mmHg
Acetic Acid vapor mole fraction at boundary	=	0.4484	
Water vapor mole fraction at boundary	=	0.5516	
Acetic Acid liquid mole fraction at boundary	=	0.5597	

Concentration Profile Along DAA in Liquid Filled Region (Imaginary Phase)

No.	Position in delta(a)	Position in delta	Acetic Acid mole fraction XI
1	0.000	0.000	0.50000

6	0.100	0.015	0.50563
11	0.200	0.029	0.51133
16	0.300	0.044	0.51711
21	0.400	0.059	0.52296
26	0.500	0.074	0.52889
31	0.600	0.088	0.53490
36	0.700	0.103	0.54098
41	0.800	0.118	0.54715
46	0.900	0.133	0.55340
51	1.000	0.147	0.55972

Penetrant Concentration Profile in the Membrane Phase (using Liquid Sorption Data)

No.	Position in delta(a)	Position in delta	Acetic Acid XI	XMI	WT kg/kg
1	0.000	0.000	0.50000	0.164	0.372
6	0.100	0.015	0.50563	0.166	0.369
11	0.200	0.029	0.51133	0.168	0.366
16	0.300	0.044	0.51711	0.170	0.362
21	0.400	0.059	0.52296	0.172	0.359
26	0.500	0.074	0.52889	0.174	0.356
31	0.600	0.088	0.53490	0.177	0.352
36	0.700	0.103	0.54098	0.179	0.349
41	0.800	0.118	0.54715	0.182	0.345
46	0.900	0.133	0.55340	0.185	0.342
51	1.000	0.147	0.55972	0.188	0.338

Partial Pressure & Mole Fraction profile along DBB (Imaginary Vapor Phase)

No.	Position delta(b)	Position delta	Acetic Acid Partial press. mmHg	Water Partial Press mmHg	MOLE FRACN
1	0.0000	0.1473	9.16090	11.26758	0.448
6	0.0853	0.2325	8.69114	10.73881	0.447
11	0.1705	0.3178	8.19449	10.18262	0.446
16	0.2558	0.4031	7.66574	9.59424	0.444
21	0.3411	0.4884	7.09770	8.96733	0.442
26	0.4264	0.5736	6.48005	8.29317	0.439
31	0.5116	0.6589	5.79697	7.55913	0.434
36	0.5969	0.7442	5.02182	6.74567	0.427
41	0.6822	0.8295	4.10274	5.81960	0.413
46	0.7675	0.9147	2.90624	4.71502	0.381
51	0.8527	1.0000	0.24500	3.25500	0.070

Pentrant Concentration Profile in the Membrane Phase (using Vapor Sorption Data)

No.	Position delta(b)	Position delta	Acetic AcidPP Partial pre s. mmHg		YMI	WMTOT
1	0.0000	0.1473	9.16090	0.448	0.046	0.077
6	0.0853	0.2325	8.69114	0.447	0.046	0.077
11	0.1705	0.3178	8.19449	0.446	0.046	0.077
16	0.2558	0.4031	7.66574	0.444	0.045	0.078
21	0.3411	0.4884	7.09770	0.442	0.045	0.078
26	0.4264	0.5736	6.48005	0.439	0.045	0.078